



MOLECULAR ENGINEERING I

Interactions between Molecules and Surfaces

Prepared by: **Molecular Engineering Class of 2020**

René M. Overney, University of Washington

Class: MolENG 510/ChemE554, Spring 2020

Authors:

Molecular Engineering Class Members

Last Name	First Name
Bennett	Nathaniel
Bohmann	Nick
Gokce	Gizem
Hwang	Yeon Mi
James	Ellie
Kiattisewee	Cholpisit Ice
Leung	Philip
Lee	Justin H
Leeds	Bonnielle Kroeker
Liu	Yulai
Mansoor	Sanaa
Meng	Yuhuan
Nguyen	Alexander
Nguyen	Nam Phuong Huynh
Pottenger	Ayumi
Prosswimmer	Tatum Soleil
Shi	Yangwei
Tooley	Marti Rae
Xiang	Xiaofeng

Instructor: René M. Overney

Professor, Department of Chemical Engineering, Molecular Engineering & Sciences Institute, University of Washington, Seattle, WA

Contents

CHAPTER 1: MOLECULAR INTERACTIONS, STATISTICAL DENSITY DISTRIBUTION, AND THERMODYNAMIC PROPERTIES	1
1.1 OVERVIEW	1
1.2 THE MOLECULAR INTERACTION POTENTIAL	2
1.2.1 <i>Self-Energy</i>	2
1.2.2 <i>Radial Density Distribution</i>	4
1.3 CHEMICAL POTENTIAL AND VAN DER WAALS EQUATION OF STATE.....	5
1.3.1 <i>Chemical Potential and Self-Energy</i>	5
1.3.2 <i>Van der Waals Equation of State and Thermodynamic Properties</i>	6
1.3.3 <i>Boltzmann Factor: Gas and Liquid Phase Density</i>	7
1.4 HELMHOLTZ FREE ENERGY OF ATOM PAIR INTERACTION AND PROTEINS	8
1.4.1 <i>Background on Proteins</i>	8
1.4.2 <i>Free Energy and Protein Folding</i>	10
1.5 SUMMARY	12
1.6 REVIEW QUESTIONS.....	13
LITERATURE – SOURCES AND FURTHER READING.....	14
CHAPTER 2: STRONG INTERACTIONS – FROM COVALENT TO IONIC	15
2.1 COVALENT AND METALLIC INTERACTION	15
2.1.1 <i>Covalent Bond Models: Harmonic and Morse</i>	16
2.2 IONIC INTERACTIONS	17
2.2.1 <i>Permittivity and Electric Polarization</i>	18
2.2.2 <i>Coulomb Interactions</i>	20
2.3 ION INTERACTIONS IN DIELECTRIC SOLUTIONS	22
2.3.1 <i>Bjerrum Length</i>	22
2.3.2 <i>Self-Energy and Born Energy of an Ion</i>	24
2.3.3 <i>Ion Solubility – a Stochastic Process</i>	26
2.3.4 <i>Continuum vs. Molecular Approach to Ion-Solvent Effects</i>	27
2.4 ION INTERACTION POTENTIAL (IONIC SOLIDS).....	28
2.4.1 <i>Reference States</i>	31
2.4.2 <i>Range of Electrostatic Forces</i>	32
2.5 SUMMARY	32
LITERATURE – SOURCES AND FURTHER READING.....	35
CHAPTER 3: POLAR INTERACTIONS, HYDROGEN BONDING AND VAN DER WAALS INTERACTION	36
3.1 OVERVIEW	36
3.2 POLAR MOLECULES AND DIPOLE MOMENT	36
3.2.1 <i>Molecular Dipoles</i>	36
3.2.2 <i>Dipole Moment and Dipole Self-Energy</i>	39
3.3 INTERACTIONS INVOLVING STATIC AND ROTATING DIPOLES.....	39
3.3.1 <i>Static Ion-Dipole Interaction</i>	39
3.3.2 <i>Dipole-Dipole Interaction</i>	42
3.3.3 <i>Rotating Dipoles and Angle-Averaged Potentials</i>	43
3.4 DIPOLE INTERACTIONS INVOLVING WATER	47
3.4.1 <i>Dipole Interactions in Water, Solvation and Hydration Forces</i>	47
3.4.2 <i>Hydrogen Bond</i>	47
3.5 SUMMARY	49
3.6 REVIEW	50
LITERATURE – SOURCES AND FURTHER READING.....	53

CHAPTER 4: POLARIZATION AND DISPERSION INTERACTION.....	54
4.1 POLARIZABILITY OF ATOMS AND MOLECULES	54
4.1.1 <i>A Simple Model for Induced Dipoles</i>	54
4.1.1 <i>The Polarizability of Nonpolar Molecules</i>	56
4.1.2 <i>Total Polarizability</i>	58
4.2 ION-SOLVENT MOLECULAR INTERACTIONS	58
4.2.1 <i>Polarization of a Medium</i>	58
4.2.2 <i>Using a Continuum Approach to Calculate Born Energy</i>	59
4.2.3 <i>Using a Molecular Approach to Calculate Born Energy</i>	59
4.3 SOLVENT EFFECTS AND EXCESS POLARIZABILITIES.....	60
4.3.1 <i>Excess Polarizability and Solvent Effect on Interaction Polarity</i>	60
4.4 DIPOLE-INDUCED DIPOLE INTERACTIONS: DEBYE INTERACTION AND POLARIZATION INTERACTIONS.....	62
4.4.1 <i>Relationships between the Polarization of Isolated Molecules and Gas Molecular Properties and Condensed Phase Properties</i>	63
4.4.2 <i>Unified Polarization Equation</i>	66
4.5 VAN DER WAALS-DISPERSION FORCES BETWEEN NON-POLAR MOLECULES	66
4.5.1 <i>Properties of dispersion forces</i>	67
4.5.2 <i>The London Equation</i>	67
4.5.3 <i>Polarization vs. Dispersion Contributions – The Frequency Range</i>	69
4.5.4 <i>Strength of Dispersion Forces in Van der Waals Solids</i>	69
4.5.5 <i>Limitation of the Simple Van der Waals Model</i>	70
4.6 VAN DER WAALS FORCES BETWEEN POLAR MOLECULES	72
4.7 RETARDATION EFFECTS.....	73
4.8 SUMMARY	73
LITERATURE – SOURCES AND FURTHER READING.....	77
CHAPTER 5: MOLECULAR INTERACTIONS IN SOLVENT.....	78
5.1 OVERVIEW	78
5.2 THE GENERAL THEORY OF VAN DER WAALS FORCES BETWEEN MOLECULES AND VAN DER WAALS FORCES IN A MEDIUM	78
5.2.1 <i>General Theory of Van der Waals Interactions: McLachlan Equation</i>	78
5.2.2 <i>McLachlan Equation Expanded with the Excess Polarizability to Solvents</i>	83
5.2.3 <i>Molecular Dispersion Self-Energy</i>	86
5.3 COOPERATIVE INTERACTIONS INVOLVING THE SOLVENT.....	87
5.3.1 <i>The Hydrophobic Effect</i>	88
5.3.2 <i>Hydrophobic Interaction</i>	90
5.3.3 <i>Hydrophilic Interaction</i>	91
5.4 SUMMARY	93
LITERATURE – SOURCES AND FURTHER READING.....	97
CHAPTER 6: VAN DER WAALS FORCES BETWEEN MACROSCOPIC SYSTEMS AND SURFACE	98
6.1 VAN DER WAALS FORCES IN MACROSCOPIC MOLECULAR SYSTEMS.....	98
6.1.1 <i>Pairwise Van der Waals Interaction Potential between Macroscopic Bodies</i>	98
6.1.2 <i>Van der Waals Force-Laws for Bodies of Different Geometries: The Hamaker Constant</i>	99
6.1.3 <i>Hamaker Constants – Combining Relations</i>	102
6.1.4 <i>Derjaguin Approximation</i>	103
6.2 THE LIFSHITZ THEORY OF VAN DER WAALS FORCES	105
6.2.1 <i>Hamaker Constants for Dielectric media</i>	105
6.2.2 <i>Hamaker Constant for Conducting media</i>	108
6.2.3 <i>Theoretical and Experimental Hamaker Constants Comparison</i>	109
6.3 EFFECT OF WETTING FILMS AND DISJOINING FILMS.....	110
6.3.1 <i>Superfluid Helium – A Wetting Film</i>	110

6.4	RETARDATION: SEPARATION EFFECT ON VAN DER WAALS INTERACTION	112
6.4.1	<i>Retardations Considering Two Spheres</i>	113
6.4.2	<i>Metals</i>	113
6.4.3	<i>Hydrocarbons Interacting Across Water</i>	113
6.4.4	<i>Two Surfaces in a Vacuum</i>	114
6.4.5	<i>Casimir Equation</i>	114
6.4.6	<i>Wetting films – Hydrocarbon Films on Water</i>	114
6.5	THE ELECTROLYTE SCREENING EFFECT	114
6.6	WORK OF ADHESION	115
6.6.1	<i>Adhesion Energy Between Two Planar Surfaces</i>	115
6.6.2	<i>Adhesion Energy Between Surfaces with Different Geometries</i>	115
6.6.3	<i>Estimating the Cutoff Distance</i>	116
6.7	INTERFACIAL ENERGY INVOLVING METALS	118
6.7.1	<i>Limitations of Previous Interfacial Energy Equations</i>	118
6.7.2	<i>Metal-Metal Interfacial Energy</i>	118
6.8	SURFACES WITH ADSORBED LAYERS	119
6.9	SUMMARY	121
6.10	REVIEW QUESTIONS	124
	LITERATURE – SOURCES AND FURTHER READING	125
	CHAPTER 7: SELF-ASSEMBLY	126
7.1	OVERVIEW	126
7.2	THERMODYNAMICS OF SELF-ASSEMBLY	128
7.3	Critical Monomer Concentration	130
7.4	OZWALD RIPENING	132
	LITERATURE – SOURCES AND FURTHER READING	132
	CHAPTER 8: STATISTICAL MECHANICS OF PAIR INTERACTIONS IN GASES	133
8.1	OVERVIEW	133
8.2	BOLTZMANN'S LAW, FACTOR AND DISTRIBUTION LAW	134
8.2.1	<i>Multiplicity - Examples</i>	134
8.2.2	<i>Multiplicity and Probability</i>	136
8.2.3	<i>Boltzmann Factor and Boltzmann Distribution Law</i>	137
8.3	PARTITION FUNCTION	138
8.4	INDEPENDENT DISTINGUISHABLE AND INDISTINGUISHABLE PARTICLES	139
8.5	PARTITION FUNCTION AND THERMODYNAMIC PROPERTIES	139
8.5.1	<i>Stirling Approximation</i>	140
8.6	MOLECULAR PARTITION FUNCTION FROM THE STANDARD CHEMICAL POTENTIAL	141
8.7	INTERNAL ENERGY OF A GAS SYSTEM	143
	LITERATURE – SOURCES AND FURTHER READING	144

Chapter 1: Molecular Interactions, Statistical Density Distribution, and Thermodynamic Properties

1.1 Overview

Molecular interactions describe forces between molecules and non-bonded atoms that can be either attractive or repulsive. Fundamentally, they are electrostatic in nature and thus, distinctly different from chemical (covalent) interactions. In contrast to covalent bonds, molecular interactions are affected by many non-chemical processes, such as phase transitions (e.g., melting boiling, sublimations), glass transitions, macromolecular reorganizations and molecular folding (e.g., observed in protein assemblies and for diluted proteins, respectively.), and interfacial collective phenomena (e.g., delamination and wetting). Many science and technological areas depend and utilize molecular interactions. Examples are manifold from

- modern drug designs
- sensor and diagnostic applications
- coating and protection technologies
- material compatibilization and composites,
- energy material, device and conservation applications, to
- nanoscale device technologies

in areas of Bioengineering, Chemical Engineering, Material Sciences and Engineering, Nanoscience/Technology, and Molecular Engineering.

The strength of molecular interactions are on the order of 1-10 kcal/mol (1-50 kJ/mol) and involve more specifically Van der Waals interactions, weak hydrogen bonding and entropic interaction forces. Typically, not considered as molecular interactions are ionic interactions that can reach bond strength of up to 240 kcal/mol as per Table 1.1 below. Ionic interactions involve atomic ions, and thus, represent incomplete molecules with bonding capabilities that are partially covalent.

Table 1.1: Bond interaction comparison

Nature of Bond	Type of Force	Energy (kcal/mol)	Distance
Ionic bond	Coulombic force	180 (NaCl) 240 (LiF)	2.8 Å 2.0 Å
Covalent bond	Electrostatic force (wave function overlap)	170 (Diamond) 283 (SiC)	N/A
Metallic bond	free valency electron sea interaction (sometimes also partially covalent (e.g., Fe and W))	26 (Na) 96 (Fe) 210 (W)	4.3 Å 2.9 Å 3.1 Å
Hydrogen Bond	a strong type of directional dipole-dipole interaction	7 (HF) 50 (ethanamide)	
Van der Waals	(i) dipole-dipole force (ii) dipole-induced dipole force (iii) dispersion forces (charge fluctuation)	2.4 (CH ₄) 22 n-butane	significant in the range of a few Å to hundreds of Å

The most prominent molecular interactions are the Van der Waals (VdW) interactions. Other molecular interactions are: Solvation forces, weak hydrogen bonding, partial-charge interaction, hydrophobic interaction (or more general: entropic interaction), etc.

1.2 The Molecular Interaction Potential

We shall investigate here some of the properties of molecular systems from the perspective of intermolecular interactions. Let us introduce the interaction potential between two molecules in form of a power law model of integer $n > 3$, i.e.

$$w(r) = -\frac{C}{r^n} \quad (1.1)$$

for $r > \sigma$, i.e., valid outside the “hard-sphere diameter” σ . The negative sign of the potential implies that the interaction is attractive. C reflects a positive material specific interaction constant. For $r < \sigma$ the potential shall be infinite repulsive. If we consider now one molecule within an isotropic condensed phase of the “same” (identical) molecules, we can evaluate the interaction energy of a specific molecule i with all its surrounding molecules, as

$$E_i = \int_V w(r)dV = \int_\sigma^L w(r)\rho 4\pi r^2 dr \quad (1.2)$$

where ρ is the particle number density, and, L represents the size of the system. We considered that the number of molecules within the space r and $r+dr$ of an infinitesimal shell thickness of volume $dV = 4\pi r^2 dr$ around molecule i yields an infinitesimal number of molecules $\rho(4\pi r^2 dr)$ that takes part in the interaction. The derived energy E_i represents the cohesive energy. Substituting the potential in Eq. (1.1) into the cohesive energy Eq. (1.2) yields

$$E_i \cong -4\pi C\rho \int_\sigma^{L \rightarrow \infty} \frac{1}{r^{n-2}} dr = -\frac{4\pi C\rho}{(n-3)r^{n-3}}; n > 3 \quad (1.3)$$

whereby, we assumed a large system in comparison to the length scale of the interaction. We shall next introduce the *self-energy* of a molecule, i.e., the energy necessary to bring a molecule in its current position.

1.2.1 Self-Energy

We distinguish molecules in the gas phase from molecules in the liquid or solid condensed phase. While molecules in the condensed phase have nearest neighbors with very small free volumes, molecules in gases do not have neighbors but a lot of free volume between them. The contact closeness of molecules in liquids imposes a structural entropic energy that gas molecules lack.

If we introduce a new molecule i into the gas phase of similar molecules under constant pressure and temperature conditions, the cohesive energy E_i (see Eq. (1.3)) describes the energy necessary to introduce the molecule into the gas phase. This so-called molecular *self-energy*, dubbed μ_{gas}^i for the gas phase, matches the cohesive energy, i.e.,

$$\mu_{gas}^i = E_i \cong -\frac{4\pi C\rho}{(n-3)r^{n-3}} \quad (1.4)$$

Different is the situation, if we introduce the new molecule i into a condensed phase of similar molecules. In condensed phases each molecule can have up to 12 nearest

neighbors that can be considered to be in “contact” with it. For simplicity (i.e., perfect isotropy), we will assume a liquid phase, and thus, consider a *closed packed system*, Fig. 1.1, with 12 nearest neighbors. Introducing a molecule from the vapor phase into the liquid phase requires empty space in the liquid. To provide the space, 12 liquid molecules have to separate, which is equivalent to breaking six bonds (not 12, as we do not count bonds with the empty space that we generate). In energetic terms it involves an energy cost of $-6w(\sigma)$ to form a cavity the size of a molecule], whereby $r = \sigma$ reflects the molecular interaction distance, measured from the center of each molecule. Introducing now the new molecule, 12 new bonds are formed that account for an energy of $+12w(\sigma)$, yielding a net energy change of $+6w(\sigma)$. Thus, while for the gas phase the self-energy amounts to $+12w(\sigma)$, in the liquid phase the self-energy reduces by one half, , i.e.,

$$\mu_{liq}^i = \frac{\mu_{gas}^i}{2} = 6w(\sigma) \cong -\frac{2\pi C\rho}{(n-3)\sigma^{n-3}} \quad (1.5)$$

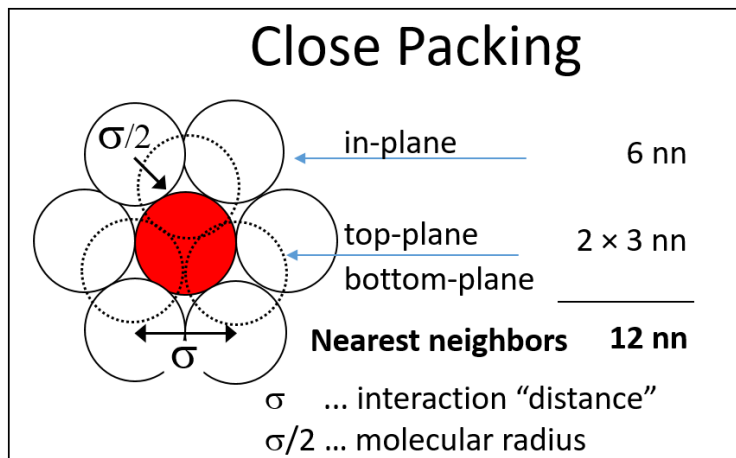


Figure 1.1: Ordered closed packed system. Every reference molecule (highlighted in red) has 12 nearest neighbors (nn).

Considering that the number density ρ of a closed packed system is equivalent to the reciprocal molecular volume v_m , i.e., $\rho = 1/v_m$ with $v_m = (4\pi/3)(\sigma/2)^3$ with the molecular radius $\sigma/2$, the self-energy of a molecule in a liquid can be expressed as

$$\mu_{liq}^i|_{r=\sigma} \cong -\frac{2\pi C\rho}{(n-3)\sigma^{n-3}} = -\frac{12C}{(n-3)\sigma^n} = \frac{12}{(n-3)}w(\sigma). \quad (1.6)$$

As we will see later, for the most prominent molecular interaction, namely the *Van der Waals interaction*, the power law exponent n is 6, which, if substituted into Eq. (1.6) yields,

$$\mu_{liq,VdW}^i \cong 4w(\sigma). \quad (1.7a)$$

Assuming a molar system with $N_A = 6.02 \times 10^{23}$ molecular bonds (Avogadro’s number), the molar cohesive energy (internal energy, $U = -N_A\mu^i$) involving liquids is given by

$$U = -N_A\mu_{liq}^i \cong \frac{12N_A}{(n-3)}w(\sigma) \quad (1.7b)$$

or for $n = 6$, the Van der Waals cohesive energy is

$$U_{VdW} \cong -4N_A w(\sigma). \quad (1.8)$$

Notice the sign convention: While the self-energy expresses the energy stored in the system, the molar cohesive energy expresses the energy released by the system, if dismantled into its components. As a rule of thumb from empirical observations is that in a pure liquid or solid, the Van der Waals cohesive energy is between 4 to 6 times the pair energy.

1.2.2 Radial Density Distribution

In our estimate of the stored cohesive energy we assumed an equidistant isotropic closed packed distribution of the molecules. In reality, we can expect distance fluctuations, and hence, consider a probabilistic density distribution. As per Boltzmann's relation for dilute systems (e.g., gases), the *radial density distribution function* $g(r)$ can be described as

$$g(r) = \frac{\rho(r)}{\rho_0} = \exp\left(\frac{-w(r)}{kT}\right), \quad (1.9)$$

where $\rho(r)$ is the local density at distance r from a reference molecule, $w(r)$ is the pair potential, $k \equiv k_B = 1.38 \times 10^{-23}$ J/K is the Boltzmann constant, and, T is the absolute temperature. $\rho_0 = N/V$ expresses the global (averaged) number density (N is the number of particles in the system of volume V), which can be expressed for a spherical system of radius R as

$$\rho_0 = \frac{\int_0^R \rho(r) dr}{\int_0^R 4\pi r^2 dr} = \frac{3}{4\pi R^3} \int_0^R \rho(r) dr. \quad (1.10)$$

For large distances r , $\rho(r)/\rho_0 \rightarrow 1$ indicating no large scale structure.

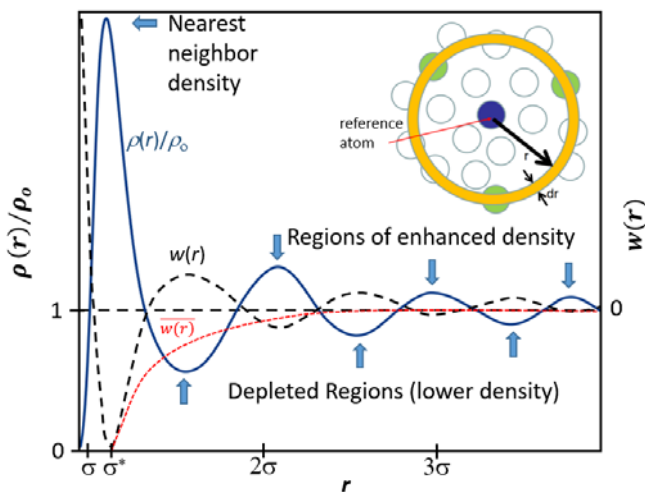


Figure 1.2: Radial density distribution function $\rho(r)/\rho_0$ and pair interaction $w(r)$ for a liquid relative to a reference molecule. $r = \sigma^* > \sigma$ represents a slightly larger (~ 5%) near contact distance, as found for an ordered closed packed solid system, and thus, providing “free volume” that allows the phase to behave liquid-like. $\overline{w(r)}$ is the averaged attractive pair interaction potential from a continuum theoretical perspective. *Inset:* Molecules in the vicinity of a reference molecule. Highlighted is a shell of thickness dr at distance r .

For liquids, at close intermolecular distances, the density distribution function is oscillatory, as depicted in Fig. 1.2. At $r = \sigma^*$, where the mean pair potential $w(r)$ has a minimum (maximum attraction), $\rho(r)$ is maximum exceeding any density value in the liquid. This first and highest peak in the density distribution is to different degree, depending on the liquid, responsible for near distance order in the liquid phase, and thus, responsible for *structural or cooperative entropy*. In the case of liquid argon, $\sigma^* \approx 3.7 \text{ \AA}$

(about 5 % exceeding σ found for closed packed systems) with a $g(r) = \rho(r)/\rho_o$ value of about 3, implying that it is three times more likely that two molecules would be found at this separation compared to the average distance in the unstructured bulk system. The first minimum is found for liquid argon around $r \approx 5.4 \text{ \AA}$, a molecule depleted distance from the reference molecule. Thus, $g(r)$ expresses the bulk relative probability of finding a molecule at distance r from a reference molecule. The total number of molecules in a given infinitesimal shell as depicted in the inset of Fig. 1.2, is given by the product of the shell volume $dV = 4\pi r^2 dr$ and the local density $\rho(r)$, i.e.,

$$dN = 4\pi\rho(r)r^2 dr = 4\pi\rho_o g(r)r^2 dr. \quad (1.11)$$

1.3 Chemical Potential and Van der Waals Equation of State

With the radial distribution function, we can determine the thermodynamic properties of materials. For instance, if we consider an isotropic gas system with molecular pair potential $w(r)$, the total potential energy of a gas system of radius R and N particles can be obtained with Eq. (1.11) from

$$E_{pot} = \frac{1}{2}N \int w(r)dN = 2\pi N\rho_o \int_0^R r^2 g(r)w(r)dr. \quad (1.12)$$

(The factor $\frac{1}{2}$ ensures that each interaction is only counted once.)

1.3.1 Chemical Potential and Self-Energy

As pointed out earlier, we can express statistically the radial distribution function $g(r)$ with Eq. (1.9) in terms of the pair interaction potential as $g(r) = \rho(r)/\rho_o = \exp(-w(r)/kT)$. If we now consider the interaction energy difference per molecule between the structured molecular phase described with the local energy density $\rho(r)$, and, the unstructured molecular phase expressed by ρ_o , each of which described by its self-energy, i.e.,

$$w(r) = \mu_2^i - \mu_1^i, \quad (1.13a)$$

where 1,2 expresses the two phases, then the expression

$$\rho(r) = \rho_o \exp\left(-\frac{\mu_2^i - \mu_1^i}{kT}\right) \quad (1.13b)$$

is equivalent to

$$\mu_1^i + kT \ln \rho(r) = \mu_2^i + kT \ln \rho_o \quad (1.14)$$

More generally, the number densities $\rho(r)$ and ρ_o are replaced by the equilibrium concentrations, X_1 and X_2 , respectively, i.e.,

$$\mu_1^i + kT \ln X_1 = \mu_2^i + kT \ln X_2 \equiv \mu, \quad (1.15)$$

which defines the system chemical potential $\mu = \mu_n^i + kT \ln X_n$ of an ideal system under equilibrium conditions involving all system phases, $n = 1, 2, 3, \dots$. The two components of the chemical potential are the “interaction energies” μ_n^i (*self-energies*, as we restricted ourselves to $w(r)$ interaction) and the thermal components $kT \ln X_n$, for which we have many names, such as, ideal solution entropy, configurational entropy, entropy of dilution, etc. Eq. (1.15) requires that the molecules in the two phases are ideally mixed and dilute. The dimensionless concentration X_n is typically either the mole fraction or volume fraction. For a pure phase we set $X_n = 1$. Returning to the expressions above and considering that

the bulk system, expressed by $X_1 = 1$, is a pure system, the diluted phase concentration X_2 can be expressed as

$$X_2 = \exp\left(-\frac{\Delta\mu}{kT}\right); \Delta\mu \equiv \mu_2^i - \mu_1^i. \quad (1.16)$$

1.3.2 Van der Waals Equation of State and Thermodynamic Properties

Let us next consider a vapor in equilibrium with its condensed liquid phase. The interaction between molecules of radius σ in the gas phase, $w(r) = -C/r^n$, yields the approximate cohesive energy as per Eq. 1.4 of

$$\mu_{gas}^i \approx -\frac{4\pi C\rho}{(n-3)\sigma^{n-3}} \equiv -2a\rho, \quad (1.17)$$

which defines the new parameter a . As we will see, the parameter a represents a measure of the pressure imposed by the molecular interactions on the system, which is in addition to the thermodynamic pressure. As an extension to the ideal gas, we attribute to each particle a non-penetrating interaction volume $B = 4\pi\sigma^3/3$, also dubbed *exclusion volume*. In liquids, the exclusion volume is slightly larger than the actual volume of the molecule. Expressing the concentration X_{gas} in terms of the volume fraction (i.e., $X_2 = 1/v$, where v is the average volume occupied by a molecule, as shown in Fig. 1.3), the concentration (effective density) is

$$X_{gas} = \frac{1}{v - B} = \frac{\rho}{1 - B\rho}. \quad (1.18)$$

if we subtract the exclusion volume from v .

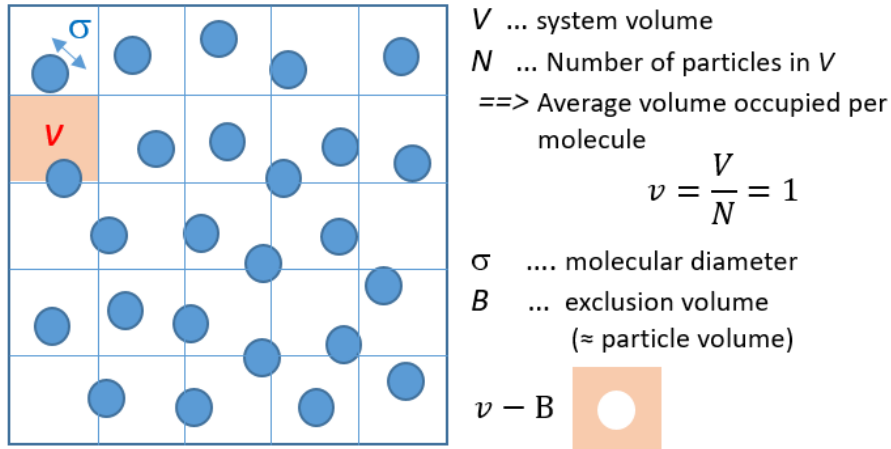


Figure 1.3: Free volume in Van der Waals fluids considering the non-penetrating interaction volume. The volumetric system is here for simplicity in two-dimensions expressed.

Substituting Eqs (1.17) and (1.18) into the chemical potential of a gas, i.e., $\mu = \mu_{gas}^i + kT \ln X_{gas}$ yields

$$\mu = -2a\rho + kT \ln\left(\frac{\rho}{1 - B\rho}\right) \quad (1.19)$$

Next we employ the well-known thermodynamic relation

$$\left(\frac{\partial P}{\partial \rho}\right)_T = \rho \left(\frac{\partial \mu}{\partial \rho}\right)_T ; \rightarrow P = \int_0^\rho \rho' \left(\frac{\partial \mu}{\partial \rho'}\right)_T d\rho' \quad (1.20)$$

which yields for the thermodynamic pressure

$$P = -a\rho^2 - \frac{kT}{B} \ln(1 - B\rho) \approx -a\rho^2 - \frac{kT}{B} \left(\frac{-B}{v - \frac{1}{2}B} \right) = \frac{a}{v^2} + \frac{kT}{\left(v - \frac{1}{2}B\right)} \quad (1.21a)$$

for $B\rho < 1$ using the expansion $\ln(1 - x) = -\sum_{n=1}^{\infty} \left(\frac{1}{n}\right) x^n$. Eq. (1.21) rewritten yields

$$\left(P + \frac{a}{v^2}\right)(v - b) = kT \quad (1.21b)$$

an expression that is known as the *Van der Waals Equation of State (EOS)*. The constants a and $b \equiv \frac{1}{2}B$ can be inferred from the interaction parameter C , the exponent n of the power law, and the minimum interaction distance σ via

$$a = \frac{2\pi C}{(n-3)\sigma^{n-3}} \quad (1.22a)$$

$$b = \frac{2}{3}\pi\sigma^3 \quad (1.22b)$$

For Van der Waals interactions ($n=6$ and $C = C_{vdw}$), it leads to $a = \frac{1}{3}\pi C_{vdw}/\sigma^3$. Finally, the molar representation of the Van der Waals EOS is given by

$$\left(P + a\left(\frac{\bar{n}}{V}\right)^2\right)\left(\frac{V}{\bar{n}} - b\right) = RT \quad (1.23)$$

with the universal gas constant $R = 8.314 \text{ J/mol}\cdot\text{K}$ and the mole number (number of moles) $\bar{n} = N/N_A$.

The Van der Waals EOS allows a comparison of the interaction strength to kT . kT can be thought of as the thermal noise of a system. If the potential energy of a system is exceeding kT by an order of magnitude, the system can be considered to be in a thermodynamic bound state, i.e., liquid state. This shall be illustrated next.

1.3.3 Boltzmann Factor: Gas and Liquid Phase Density

If we consider a vapor to be in equilibrium with its condensed phase, we can equate as per Eq. (1.15) their chemical energies, i.e.,

$$\mu_{gas}^i + kT \ln X_{gas} = \mu_{liq}^i + kT \ln X_{liq} \equiv \mu.$$

Empirically, at standard atmospheric temperature and pressure (STP, $T = 273 \text{ K}$, $P = 1 \text{ atm}$), one mole of gas occupies by about a factor of 1000 times the volume of its liquid condensed state. Considering that $\mu_{gas}^i - \mu_{liq}^i \approx -\mu_{liq}^i$ (the magnitude of μ_{liq}^i dominates μ_{gas}^i), it follows

$$\mu_{liq}^i \approx -(\mu_{gas}^i - \mu_{liq}^i) = -kT \ln \left(\frac{X_{liq}}{X_{gas}} \right) \approx -kT \ln(1000) \approx -7kT \quad (1.24)$$

In other words, the self-energy is strongly attractive, as expected from a liquid phase. As the logarithm is not very sensitive to temperature, it is appropriate to use, the boiling temperature T_B , to estimate the cohesion energy in a liquid, i.e.,

$$\mu_{liq}^i \approx -7kT_B, \text{ or} \quad (1.25a)$$

$$\frac{N_A \mu_{liq}^i}{T_B} \approx -7R \quad (1.25b)$$

With μ_{liq}^i we can determine the energy of vaporization of a mole of substance as

$$U_{vap} = -N_A \mu_{liq}^i = 7RT_B, \quad (1.26)$$

which yields for the latent heat of vaporization (i.e., the enthalpy) $L_{vap} = U + PV$ and $PV = RT_B$ (ideal gas law),

$$\frac{L_{vap}}{T_B} \approx 7R + 1R = 8R \approx 70 \text{ J/K} \cdot \text{mol} \quad (1.27)$$

This rough estimate of the latent heat of vaporization applies to many liquids and is known as Trouton's rule, which states that L_{vap}/T_B is approximately constant of value around 80 J/K·mol or 9 kT (see Table 1.2).

Table 1.2: Boiling Points T_B and Latent Heats of Vaporization for Some Substances

Substance		T_B at 1 atm [K]	L_{vap} [kJ/mol]	T_B / L_{vap} [J/K·mol]	Comments
Neon	Ne	27	1.8	65	
Nitrogen	N ₂	77	5.6	72	
Argon	Ar	88	6.5	74	
Methane	CH ₄	112	8.2	73	
Ammonia	NH ₃	140	23.4	97	
Benzene	C ₆ H ₆	353	20.8	87	
Sodium	Na	1156	91.2	79	metal
Water	H ₂ O	373	40.7	109	high cooperativity

This brings us back to our Boltzmann expression for the density. Eq. 1.13b, which rewritten for this situation reads

$$\rho_{liq} = \rho_{gas} \exp\left(-\frac{\mu_{liq}^i - \mu_{gas}^i}{kT}\right) \approx \rho_{gas} \exp\left(-\frac{\mu_{liq}^i}{kT}\right) \quad (1.28)$$

Eq. (1.28) expresses at which temperature the product of the density of the gas phase with the Boltzmann factor reaches the density of the liquid phase. Thereby, the Boltzmann factor accounts for the temperature and the self-energy of the liquid.

1.4 Helmholtz Free Energy of Atom Pair Interaction and Proteins

1.4.1 Background on Proteins

Protein molecules are heterogeneous unbranched chains composed of a set of only twenty amino acids, Fig. 1.4. Each amino acid has a unique side chain of different chemistry from nonpolar, polar, to positively or negatively charged. Table 1.3 provides a list of amino acids, classified into basic, acidic, polar and non-polar. The amino acid side chains can bond with one another yielding folded protein structures, i.e., conformations. Coiling and folding into three dimensional conformations provides proteins with specific biological functions. *Ionic bonds* are formed between charged amino acid side chains, *hydrogen bonds* are formed between polar side chains, and *Van der Waals interactions* can hold together hydrophobic side chains. A very small amount of bonds are covalent, making noncovalent bonds the most prevalent ones.

Single chain proteins possess *primary*, *secondary* and *tertiary* structures. As depicted in Fig. 1.4., the amino acid sequence, the primary structure, is responsible for the folding

and intramolecular (intra-chain) bonding of the linear amino acid chain that results in the protein's unique three-dimensional shape. Secondary folding patterns known as alpha helices and beta sheets can result from hydrogen bonding between amino groups and carboxyl groups in neighboring regions of the polypeptide chain. The ensemble of formations and folds in a polypeptide constitutes the tertiary structure of a protein as depicted in the inset of Fig. 1.4. Macromolecules comprised of multiple polypeptide chains can form quaternary structures.

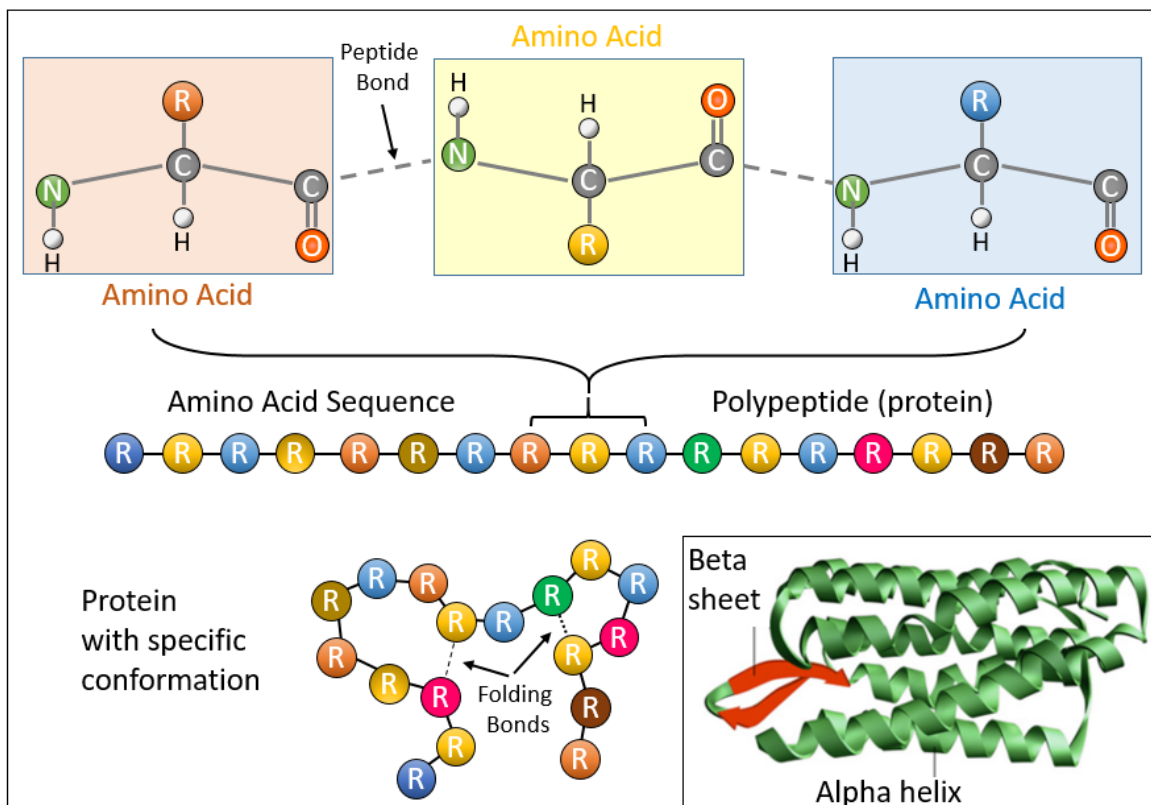
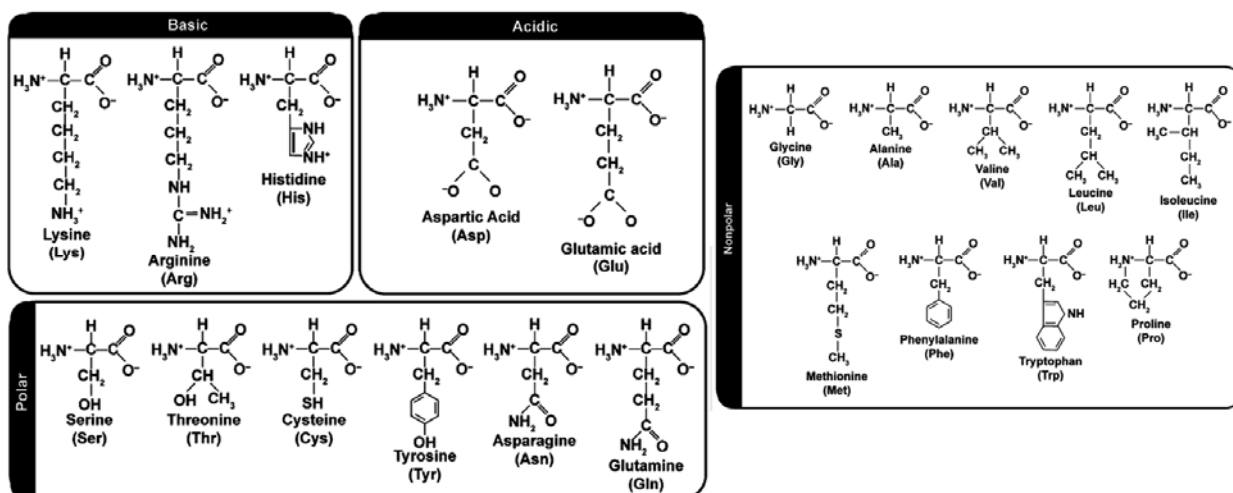


Figure 1.4: Proteins are amino acid sequences that possess specific conformations due to folding caused by intra-chain interactions between amino acid components. Inset: Secondary folding patterns (Source: <https://www.nature.com/scitable/topicpage/protein-structure-14122136/>).

The protein conformation is strongly affected by the environment and history. For instance, the effect of surrounding water, because of its small molecular size but relatively large dipole moment (1.85 D , $1 \text{ D}(\text{ebye}) = 3.335 \times 10^{-30} \text{ Cm}$), can have a profound effect on the conformational states due to the amino acid specific side-groups. Figure 1.4 provides a simple classification into electrically charged amino acids (positive or basic and negative or acidic), polar uncharged amino acid, and, hydrophobic (non-polar) amino acids.

We find that charged side chains often form salt bridges as for Arg, Lys, Asp, and Glu. Polar amino acids such as Gln, Asn, His, Ser, Thr, Tyr, and Cys form hydrogen bonds. Amphipathic amino acids that are often found at the surface of proteins or lipid membranes are sometimes also classified as polar: E.g., Trp, Tyr, and Met. Hydrophobic amino acids are typically found deep buried inside the protein core (Ala, Leu, Met, Phe, Val, Pro and Gly).

Table 1.3: Amino Acids

Tyrosine is sometimes also put to the class of hydrophobic amino acids. Leucine and Isoleucine are often not separately listed, which leads to the count of 20 amino acids. Source: <https://www.researchgate.net/>

1.4.2 Free Energy and Protein Folding

How and why proteins fold to specific conformations and how they maintain their native folds is difficult to answer and often a controversial issue. Generally, we can think of folding to be driven by molecular forces with driving forces based on free energy differences between unfolded and folded states. The folding and unfolding process is cooperative, i.e., the energy has a strong entropic component. Important interactions are besides electrostatic and hydrogen-bonding also hydrophobic effects that involve the solvent (water).

We have introduced with the radial density distribution $g(r)$, Eq. (1.9), an expression for the interaction free energy, or more generally the Helmholtz free energy,

$$w(r) = -kT \ln(g(r)). \quad (1.29)$$

Thereby, $g(r)$ and $w(r)$ represent thermodynamic averages over all possible (micro) states (in our case folding states) at constant density and temperature. Equivalently, $w(r)$ represents the potential of a mean force, or the reversible work of a process, where the relative distances between two system particles are changed.

With the knowledge of $g(r)$ we can determine $w(r)$. $g(r)$ is a superposition of all interatomic distances in the sample and is attained from the structure factor of the liquid solution in question, which is experimentally obtained from diffraction experiments (e.g., X-ray diffraction). The structure factor is the normalized scatter-intensity of a beam of wavelength λ (e.g., X-ray beam) that strikes the liquid solution at a particular angle θ , and is related for liquids to $g(r)$, through

$$S(q) = 1 + \rho_o \int_V d\vec{r} e^{-iqr} g(r), \quad (1.30)$$

where q is the magnitude of the scattering vector obtained from $q = 4\pi \sin(\theta)/\lambda$ for liquids.

So far we assumed that every atom in the polypeptide is considered as scatter center. Imagine now that the beam scatters only on specific atoms, such as peptide N and O atoms (or more generally a and b). In other words, we restrict our sampling to the distances of all atom pairs a and b , and consider the fractional interaction free energy

$w_{ab}(r)$ and fractional radial density function $g_{ab}(r)$. The determination of $g_{ab}(r)$ for hydrogen-bonds, for instance, involving proteins in aqueous solution, requires experimentally that only peptide N and O atoms act as scattering centers.

To achieve this practically, fold libraries are used that provide compiled radial distribution functions of protein structures in solution with known atomic resolution. Summing up all N···O distances in the fold library, we can determine the fractional local number density, as

$$\rho_{ab}(r) = \sum_{pij} \delta_{ab}(r - r_{pij}) \quad (1.30)$$

with each distance represented by the delta function (i.e., $\delta_{ab}(r - r_{pij}) = 0, \infty$ for $r \neq 0$ and $r = r_{pij}$, respectively), ρ representing the protein and i and j the atom pairs. The fractional radial distribution function is then, as per Eq. (1.9), determined from

$$g_{ab}(r) = \frac{\rho_{ab}(r)}{\rho_o}, \quad (1.31)$$

which consequently yields an expression for $w_{ab}(r)$ using Eq. 1.29.

If the fractional radial distribution function is obtained from computational analysis, the global density ρ_o is typically truncated due to computational limitations by a cut-off-distance R , i.e.

$$\rho_o = \frac{\int_o^R \rho_{ab}(r) dr}{\int_o^R 4\pi r^2 dr}. \quad (1.32)$$

Energy differences between two different states and mean forces are simply given by

$$\Delta w_{ab}(r_1, r_2) \quad (1.33a)$$

$$F_{ab}(r) = -\frac{d}{dr} w_{ab}(r). \quad (1.33b)$$

Figure 1.5 provides the interaction free energy $w_{NO}(r)$ of hydrogen bonding as a function of peptide N···O separation distances over the range of 14 Å. The data was compiled from a library of unrelated X-ray structures.

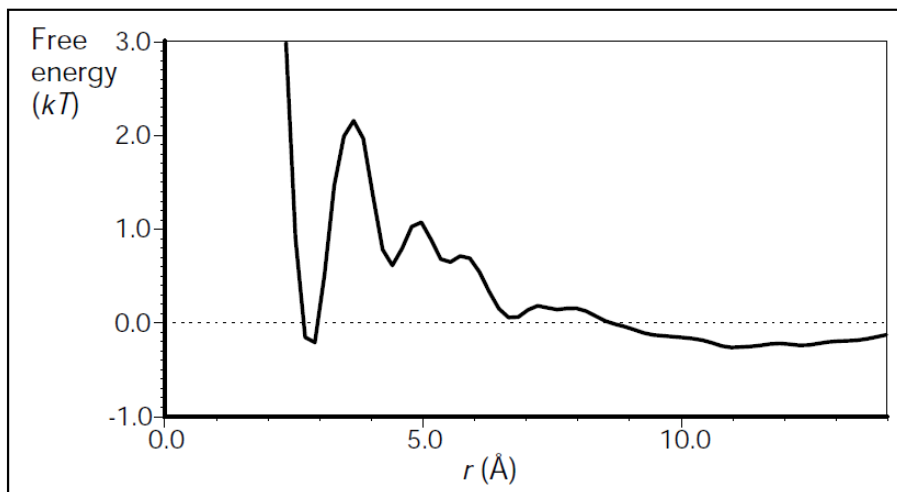


Figure 1.5: Interaction free energy $w_{NO}(r)$ of the N···O hydrogen bond in units of kT of peptides from a fold library of 289 proteins. Source: M.J. Sippl et al., *Folding & Design*, Vol 1(4), 289m, 1996.

1.5 Summary

This overview chapter provides an introduction into *molecular interactions* by initially comparing a variety of bond interactions. Thereby, molecular interactions are found to be the weakest of all with a bond energy on the order of 1 to 10 kcal/mol. They are two orders of magnitude smaller than the strong ionic and covalent interactions (see Table 1.1). Molecular interactions are *electrostatic in nature* and involve “intact” molecules or atoms (this is in contrast to ions that are missing electrons or have too many). The general pair interaction potential is typically expressed in form of a *power law* involving the interaction parameter C and distance r , as

$$w(r) = -\frac{C}{r^n} \quad (1.1)$$

with $n = 6$ for the most prominent of the short ranged molecular interactions, namely the *Van der Waals (VdW) interaction*. Based on this potential the *cohesive energy* within a molecular system of number density ρ , is

$$\mu_{gas}^i = E_i \cong -\frac{4\pi C\rho}{(n-3)r^{n-3}} \quad (1.4)$$

for $n > 3$. The energy here, also called *interaction free energy*, is equivalent to the *self-energy for a gas phase system*. The self-energy reflects the work involved to bring a molecule to a specific place in the system. For the liquid condensed phase of a closed packed system, it is found that the *self-energy* is reduced by one half from the gas phase self-energy, due to the fact that space has to be first generated for the molecule before it can be inserted. The relationship between the *self-energy* of a molecule and its pair interaction free energy with its nearest neighbor is approximately

$$\mu_{liq,vdw}^i \cong 4w(\sigma). \quad (1.8)$$

for closed-packed VdW liquids. Thereby σ reflects the nearest neighbor interaction distance. This finding corresponds well to the empirical observations of self-energies for VdW liquids and solids that were found to vary between 4 to 6 times the pair energy (Rule of Thumb).

After the molecular scale comparison of stored energy and the pair interaction energy for isotopic systems, the discussion switches to density variations on the local scale (typically 2 to 3 σ , for molecular VdW systems). The non-homogenous, fluctuating (oscillating) *density distribution* with distance r from a reference molecule is expressed with *Boltzmann's law* as

$$\rho(r) = \rho_o \exp\left(\frac{-w(r)}{kT}\right), \quad (1.9)$$

where ρ_o is the bulk average density, kT the thermal energy, and k the *Boltzmann constant*. Expression (1.9) relates the local density to the pair interaction, and yields the *chemical potential*, μ , as

$$\mu = \mu_1^i + kT \ln \rho(r) = \mu_2^i + kT \ln \rho_o. \quad (1.14)$$

assuming, we compare two phases (1, local phase and 2, global phase) in equilibrium with each other.

Replacing the densities with species concentrations X_i , the diluted phase concentration of a solution can be expressed in terms of the interaction free energy, as

$$X_2 = \exp\left(-\frac{\Delta\mu}{kT}\right); \Delta\mu \equiv \mu_2^i - \mu_1^i. \quad (1.16)$$

This discussion culminates in a very practical finding, namely, in the determination of the proportionality constant of $\sim 70 \text{ J/K}\cdot\text{mol}$ in the proportional relationship between the molar latent heat of evaporation and the boiling point. In so doing, the simplicity of the molecular model that leads to an accurate verifiable phenomenological number is amazing.

Even more impressive is the derivation that follows from a similar two-phase molecular comparison, namely the *VdW Equation of State* (EOS), i.e.,

$$\left(P + \frac{a}{v^2} \right) (v - b) = kT \quad (1.21b)$$

provided here for a single gas phase molecule that can be simply scaled up to a mole of substance. The VdW EOS resembles the *ideal gas law*, with the difference that (i) the thermodynamic pressure P is corrected by a molecular interaction parameter, expressed by the ratio between VdW parameter $a = 2\pi C/3\sigma^3$ and the square of the average volume v occupied by a molecule in the gas phase, and, (ii) the volume v corrected particle size $b = (2/3\pi\sigma^3)$. $v - b$ is known as *free volume*.

The chapter concludes with a molecular opportune discussion of the pair interactions of folded *proteins*. These heterogeneous unbranched chains of *amino acids* are found to possess multiple structures, classified as *primary, secondary and tertiary structures*. The primary structure, the amino-acid sequence, is responsible for the folding of the chain, the secondary structure involves *hydrogen bonding* and can lead either to *alpha helices* or *beta sheets*, and, the tertiary structure constitutes the ensemble of formations and folds. The protein structure is heavily influenced by the environment (e.g., water, pH) and history (e.g., thermal effects). As the systems above, the *free energy* of a protein fold can be expressed as

$$w(r) = -kT \ln \left(\frac{\rho(r)}{\rho_o} \right) \quad (1.29)$$

in accordance to the Boltzmann density distribution in Eq. (1.9). The local/global density ratio $\rho(r)/\rho_o \equiv g(r)$, known as *radial density distribution function*, is thereby key and determined with the help of *fold libraries*, after which the free energy $w(r)$ is computed as function of the separation distance.

1.6 Review Questions

1. In what regards are molecular interactions different from ionic interactions.
2. Provide three technological examples for which molecular interactions are important
3. $\mu_{gas}^i = E_i \cong -\frac{4\pi C\rho}{(n-3)r^{n-3}}$ describes which energy?
4. Provide a simple relationship (estimate) that relates the self-energy of a molecule in a liquid VdW system to the pair VdW interaction energy.
5. In a thermodynamic equilibrated system how can the density distribution be described formally? What is it related to? What law does it follow?
6. Provide an expression for the chemical potential for each phase (with concentration X_i) of a binary system in equilibrium. What are the two components of the chemical potential?
7. The VdW equation of state differs in what regards from the ideal gas law?
8. What are proteins?

9. What is the primary structure of a protein?
10. Name the two secondary protein structures.
11. How is the interaction free energy potential $w(r)$ determined for a specific intramolecular interaction involving a protein.

Answer Key

1. Molecular interactions are electrostatic interactions that are solely of electrostatic nature involving intact atoms or molecules. Ionic interactions involve atoms or molecules that bear charges.
2. - Modern drug designs
- Sensor and diagnostic applications
- Coating and protection technologies
- Material compatibilization and composites,
- Energy material, device and conservation applications, to
- Nanoscale device technologies
3. Molecular self-energy of the gas phase?
4. $\mu_{liq,VdW}^i \cong 4w(\sigma)$
5. $\rho(r) = \rho_o \exp\left(\frac{-w(r)}{kT}\right)$ as per the Boltzmann Law, the local density is related to the interaction pair potential between the molecules
6. $\mu = \mu_1^i + kTX_1 = \mu_2^i + kTX_2$. The first component in the chemical potential is the self-energy, and the second component is the thermal component that has many names, such as, ideal solution entropy, configurational entropy, and entropy of dilution.
7. The VdW EOS differs from the ideal gas law as follows:
- the thermodynamic pressure P is corrected by a molecular interaction parameter, and,
- the volume v is corrected by the particle size
8. Protein molecules are heterogeneous unbranched chains of a set of only twenty amino acids.
9. The amino acid sequence.
10. Alpha helices and beta sheets.
11. Determine first *radial density distribution function* $g(r) = \rho(r)/\rho_o$ with the help of *fold libraries*, and then calculate the free energy $w(r)$ using the Boltzmann distribution law

$$w(r) = -kT \ln\left(\frac{\rho(r)}{\rho_o}\right)$$

Literature – Sources and Further Reading

1. Intermolecular & Surface Forces, 3rd Ed., J.N. Israelachvili, Academic Press, Boston (2011), Ch. 2 pp 23-43, Ch. 7 pp 147-148, Ch. 15 pp 342-344.
2. Molecular Driving Forces – Statistical Thermodynamics in Chemistry and Biology, Dill and Bromberg, Garland Science, New York (2002), Ch. 6, pp 81-87.

Chapter 2: Strong Interactions – From Covalent to Ionic

In this chapter we will discuss the strong interactions that hold atoms together in molecules. This includes covalent, metallic and ionic interactions. These interactions are termed “strong” in comparison to other interactions, as bond energies of these bonds is on the scale of 10-200 kcal/mol. We first turn our attention to covalent and metallic interactions, in which electrons move between atoms, creating electrostatic forces of attraction.

Table 2.1: Short Range Interactions and Underlying Forces

Nature of Bond	Type of Force	Energy (kcal/mol)	Distance
Ionic bond	Coulombic force	180 (NaCl) 240 (LiF)	2.8 Å 2.0 Å
Covalent bond	Electrostatic force (wave function overlap)	170 (Diamond) 283 (SiC)	N/A
Metallic bond	free valency electron sea interaction (sometimes also partially covalent (e.g., Fe and W))	26 (Na) 96 (Fe) 210 (W)	4.3 Å 2.9 Å 3.1 Å

2.1 Covalent and Metallic Interaction

Within molecules, the interactions between atoms that hold them together are termed covalent bonds, driven by the covalent force. Covalent bonds form through the sharing of electrons between the atoms, as atomic orbitals overlap. Electrons are shared unevenly, depending on the electronegativity of the atoms involved. This uneven distribution of electrons induces partial charges in the atoms. Double and triple covalent bonds can be formed when more than one orbital overlap between atoms, which increase the overall bond strength. Of particular note is the rotational freedom of covalent bonds; while single bonds allow full rotation around the bond axis, double and triple bonds lack this rotational freedom. Covalent bonds also have directionality that determines the bond angle between two atoms, and ultimately the spatial orientation of the resulting molecule. The strength of covalent bonds is on the order of 100 kcal/mol.

Similar to covalent bonds, metallic bonds are the result of electrons being shared between atoms. However, rather than “localized” sharing between two atoms, electrons are “delocalized”, i.e. freely moving around the positively charged metal ion cores. The electron distribution density is uniform throughout the positively charged metal ions, creating a neutral charge in the material. The formation of the so-called electron sea around the metal ion cores causes an overall attractive metallic bond, which is electrostatic in nature. In alkali metals only metallic bonding occurs, with binding energy on the order of 10 kcal/mol. In transition metals, metallic and covalent bonding can occur

simultaneously, raising the binding energy to the order of 100 kcal/mol. The binding energy for metals can be estimated from

$$E = N \left[-\frac{e^2}{4\pi\epsilon_0} \frac{1}{r_0} - \frac{3}{4} \frac{e^2}{4\pi\epsilon_0} k_F + \frac{3}{5} E_F \right] \quad (2.1)$$

wherein N is the number of electrons, e is the elementary charge, ϵ_0 is the permittivity of free space, r_0 is the equilibrium distance between atoms, k_F is the Fermi wave number, and E_F is the Fermi energy.

2.1.1 Covalent Bond Models: Harmonic and Morse

The potential energy of a covalent bond can be approximated using the harmonic oscillator model. The energy of incremental bond stretching around an equilibrium point r_e is given as

$$E = \frac{1}{2} k(r - r_e)^2 \quad (2.2)$$

in which $(r - r_e)$ is the distance from equilibrium, and k is the spring constant of an imaginary spring between the atoms, representing the “stiffness” of the bond in response to stretching. At the equilibrium distance r_e , the potential energy of the system is at a minimum. As the bond shortens, repulsive forces cause the potential energy to rise quickly. In this model, bond lengthening increases the potential energy quickly in response to attractive forces pulling the atoms closer together.

The angular frequency $\omega = 2\pi f$ of bond oscillation, where f represents the frequency of the harmonic oscillation is given by:

$$\omega = \sqrt{k/\mu} \quad (2.3)$$

with μ being the reduced mass of the system. The reduced mass reflects the convoluted mass between the atom pair bound by the covalent bond, i.e.,

$$\mu = \frac{m_1 m_2}{m_1 + m_2} \quad (2.4)$$

While the harmonic potential is a good approximation for the potential energy of covalent bonds involving small bond stretching, it fails in describing high energy displacements of atoms from their equilibrium position. At low energy, bonds will oscillate close to the equilibrium point. However, at higher energies, oscillations will be farther from the equilibrium point, and the harmonic potential does not account for atom dissociation, i.e., bond breaking. A more realistic model for covalent bonds in diatomic molecules (or atoms at interfaces) is the Morse Potential, which does take into account atom dissociation. As the bond length increases, the potential energy increases up to the dissociation energy, leveling off as the bond breaks. This Morse potential is defined as

$$E = D_e (1 - e^{-a(r-r_e)})^2 \quad (2.5)$$

in which D_e is the dissociation energy, and a is the “potential inverse width”, given by

$$a = \sqrt{\frac{k}{2D_e}} = \omega \sqrt{\frac{\mu}{2D_e}} \quad (2.6)$$

The plot below provides a graphical representation of both the harmonic and Morse potential.

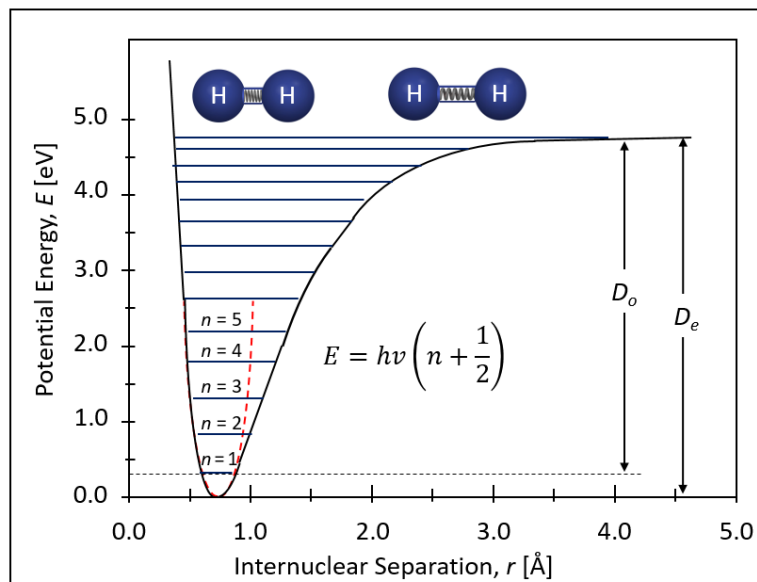


Figure 2.1 Morse Potential for H_2 with quantum vibrational energy states. The red dashed line corresponds to the harmonic oscillator model.

In the Morse Potential model, the quantum vibrational energy states of molecules are denoted by an integer quantum number $n = 0, 1, 2, 3, \dots$. The ground state ($n = 0$), also termed “zero-point energy” reflects the minimum non-zero vibrational energy level of the molecule. As the quantum vibrational energy increases, the bond length will oscillate between the points on the Morse potential corresponding to the potential energy of that state. The vibrational oscillation frequency is determined from the bond stiffness and the reduced mass, as

$$\nu = \frac{1}{2} \sqrt{k/\mu}. \quad (2.7)$$

From this, the vibrational energy of a molecule is given by

$$E = h\nu \left(n + \frac{1}{2} \right) \quad (2.8)$$

where $h = 6.626 \times 10^{-34}$ J/s is the well-known Planck constant. At the zero-point energy ($n = 0$), the vibrational energy is equal to $h\nu/2$, leading to the smallest oscillation around r_e . The non-zero ground state energy brings forward two energy perspectives: (i) the dissociation energy D_e including also the vibrational energy of the ground state, and (ii) the ground-state energy D_o from the non-zero state $n = 1$, as depicted in Fig. 2.1.

2.2 Ionic Interactions

Having discussed covalent interactions and metallic bonding, we turn our attention to the third kind of strong interaction between atomic and molecular particles, the ionic interaction. This interaction is a result of columbic forces between ions of opposite charge, causing attractive force.

2.2.1 Permittivity and Electric Polarization

Given an electric vector field \mathbf{E} , its interaction with a dielectric medium causes charge organization and displacements. On a microscopic scale, dipole moments are created due to electron displacements in atoms and molecules, and, polar molecules are aligned in the electric field, both phenomena resulting in an electric displacement field \mathbf{D} within the dielectric. The situation is different for metals that are impenetrable by the electric field due to the mobility of the freely moving electrons. Figure 2.2 illustrates the difference in behavior of a dielectric and a metal towards an external electric field.

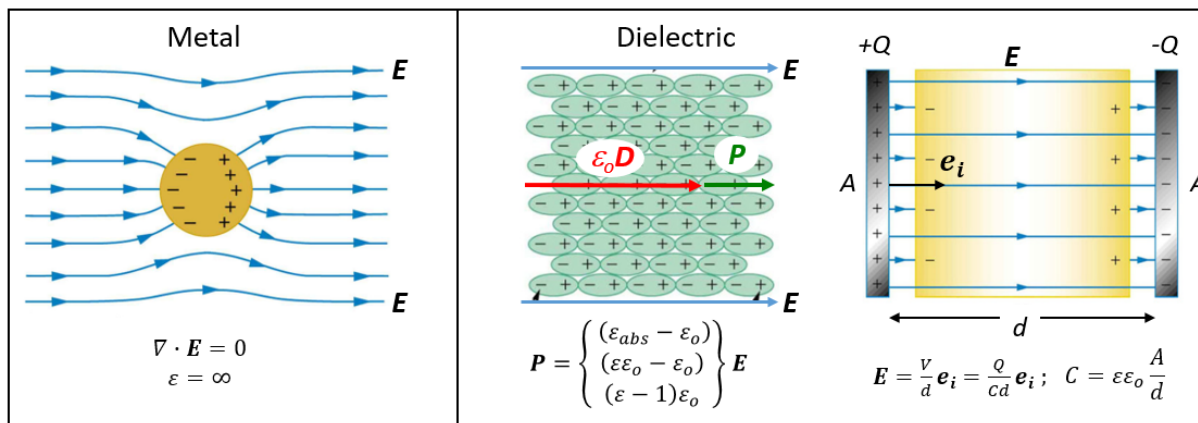


Figure 2.2 (left) Metals oppose the penetration of the electric field \mathbf{E} by forcing with freely moving electrons the electric field lines to align perpendicular to the surface. No net charges are built up within the metal. Consequently, the relative permittivity ϵ is infinite. (right) In dielectric materials, molecules are either polarized and/or aligned to accommodate the external electric field (a concept of energy minimization). Key electrostatic relationships are provided for a capacitor of area dimension A and length dimension d , as depicted, surrounding a dielectric, relating the electric potential $V=Q/C$, the capacitance plate charge and the capacitance C with the medium permittivity and the electric field.

Assuming an instantaneous material response to the external electric field, the displacement field is given by

$$\vec{D} = \epsilon_0 \vec{E} + \vec{P} \quad (2.9)$$

where ϵ_0 is the vacuum permittivity constant, and $\mathbf{P} = (1-\epsilon)\epsilon_0 \mathbf{E}$ is the polarization density that relates the degree of polarization to the relative medium permittivity ϵ and the external electric field. The permittivity ϵ is a material specific property that measures the ability of a material to polarize in response to an electric field. It is in absolute terms expressed with the vacuum permittivity $\epsilon_0 = 8.854 \times 10^{-12} \text{ F/m}$ ($\text{F/m} = \text{C}^2/(\text{Nm}^2)$), as

$$\epsilon_{abs} = \epsilon_0 \epsilon \quad (2.10)$$

and reflects that even vacuum is not “empty”. There exists a non-zero probability that fermion pairs are continuously appearing and disappearing within the vacuum, which are then polarized in an electric field, allowing for permittivity. Mathematically, this can be proven as the vacuum permittivity is inversely proportional to the speed of light and the permeability of a vacuum. As neither of these values is infinite, ϵ_0 cannot be equal to zero. Table 2.2 provides a list of relative permittivities of common materials for reference.

Table 2.2: Relative Static Permittivity of Common Substances

Substance (solid)	ϵ	Substance (liquid)	ϵ	Substance (gas)	ϵ
Electric Insulator					
Alumina	9.3-11.5	Acetone (77° F)	20.7	Air (Dry) (1 bar, 25 °C)	1.0005
Asphalt (25 °C)	2.6	Air, Liquid (-191°C)	1.4	Helium (10 bar, 30 °C)	1.00065
Calcite (25 °C)	8	Alcohol, ethyl (25 °C)		Ethane (3 bar, 20 °C)	1.004
Calcium Carbonate	8.7	Alcohol, methyl (25 °C)	16-31	Propane (2 bar, 20 °C)	1.004
Diamond (25 °C)	5.7-5.9	Aluminum Bromide (AlBr ₃) (100 °C)	3.4	Methane (10 bar, 30 °C)	1.008
Epoxy (25 °C)	3.6	Ammonia (20 °C)	17	Nitrogen (10 bar, 30 °C)	1.005
Glass (25 °C)	4-7	Carbon Disulfide (25 °C)	2.6	CO ₂ (7 bar, 30 °C)	1.0065
Graphite (25 °C)	10-15	Benzene (25 °C)	2.3	Argon (7.5 bar, 30 °C)	1.003
Electric Semiconductor		Glycerol (25 °C)	42.5		
Germanium (25 °C)	16	Hydrofluoric Acid (0 °C)	84.6		
Galium Arsenide (25 °C)	13.1	Kerosene (20 °C)	1.8		
		Methanol (25 °C)	30		
		Water (0 °C)	87.9		
		Water (20 °C)	78		
		Water (40 °C)	73.2		
		Water (60 °C)	66.7		
		Water (80 °C)	60.9		
		Water (100 °C)	55.5		

In the literature, we find another term that relates the material polarization to the electric field, namely, the susceptibility χ , i.e,

$$\mathbf{P} = \epsilon_0 \chi \mathbf{E} \quad (2.11)$$

The electric susceptibility, a dimensionless material constant, provides a measure of the degree of polarization of a dielectric material in response to an applied electric field. Combining this Eq. (2.11) with Eqs. (2.9) and (2.10), one is left with a new expression for the displacement field:

$$\vec{D} = \epsilon_0 (1 + \chi) \vec{E} \quad (2.12)$$

The relative permittivity and electric susceptibility are related as follows:

$$\chi = \epsilon - 1 \quad (2.13)$$

such that in a vacuum, χ is equal to zero. Substituting this relationship into the prior equation for the displacement field, yields

$$\vec{D} = \epsilon_0 \epsilon \vec{E} = \epsilon_{abs} \vec{E} \quad (2.14)$$

This equation is applicable to linear, homogenous, isotropic media, where ϵ_{abs} is constant, and so the displacement field is dependent only on the electric field. One can

further infer from Eq. (2.14) that a material exhibits larger electric field displacements and more dipole polarization for increasing permittivity. This can be exploited in practice, as low permittivity materials can be useful as insulators in electronic applications, such as digital circuits. It is important to note that Eq. (2.14) only holds for instantaneous material response to an electric field, which is practically impossible, as every system has a response time. To account for the response time, Eq. (2.14) is extended to exhibit also time-dependence, i.e.,

$$\vec{D}(\omega) = \epsilon_{abs}(\omega)\vec{E}(\omega) \quad (2.15)$$

leading from a static permittivity ϵ to a dynamic permittivity $\epsilon(\omega)$, where $\omega = 2\pi\nu$ is the electric field frequency. Table 2.1 provides a list of relative permittivities of common substances. A first use of the permittivity is found in our next discussion of the Coulombic interactions between ions. Thereby, the permittivity ϵ represents the medium through which ions are interacting.

2.2.2 Coulomb Interactions

Coulombic or charge-charge (ion-ion) interactions result in one of the strongest physical forces considered in this section. The force between two ions can exceed chemical binding forces, even though it is electrostatic in nature. To introduce Coulomb interactions, we will first examine the electric field that results from an ion. By definition, a positive point charge causes an electric field that radiates from the charge (i.e. the electric field lines denoting the strength of the field point away from the charge). The electric field of a negatively charged point is of equal magnitude and in the opposite direction (i.e. the electric field lines point toward the charge). Figure 2.3a shows the electric field resulting from a positive point charge and Fig. 2.3b shows the electric field of a negative point charge. When a system of point charges is assembled as in Fig. 2.3c, the electric field between the charges is additive.

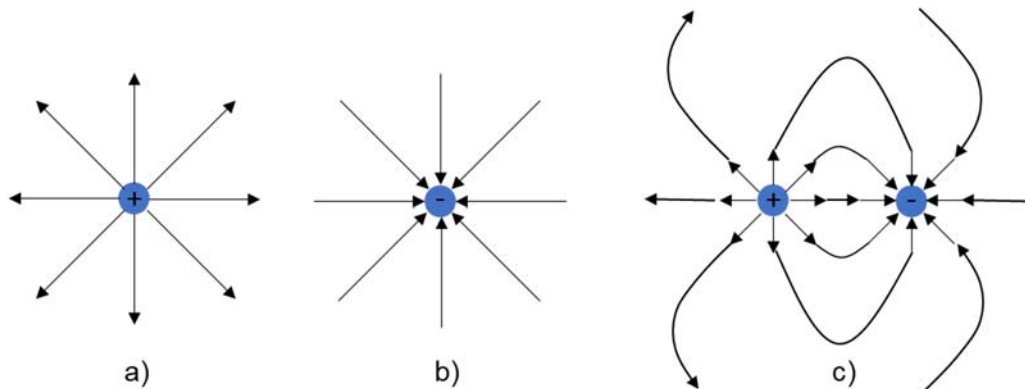


Figure 2.3 (a) The electric field generated by a cation. (b) The electric field generated by an anion. (c) The electric field generated by a cation and anion.

The magnitude of an electric field E_1 at a distance r away from the charge Q_1 generating the field is given by

$$E_1 = \frac{Q_1}{4\pi\epsilon_0\epsilon r^2} \quad (2.16)$$

where ε_0 is the permittivity of free space and ε is the dimensionless relative permittivity of the ion-surrounding medium. The electric field from charge Q_1 Eq. (2.16) acts on a second charge Q_2 at distance r with a force given by

$$F(r) = Q_2 E_1 = \frac{Q_1 Q_2}{4\pi\varepsilon_0 \varepsilon r^2}. \quad (2.17)$$

This force is known as *the Coulomb force* or as Coulomb's law. The factor $\frac{1}{(4\pi\varepsilon_0)} \approx 9 \times 10^9 \text{ Nm}^2/\text{C}^2$ is known as the Coulomb constant k_C . With the force, we can define the interaction potential, i.e.,

$$w(r) = - \int_{\infty}^r F(r') dr' \quad (2.18)$$

as the work required to assemble the ions to distance r from infinite distance, where the interaction free energy is zero. Substituting Eq. (2.17) into Eq. (2.18) yields,

$$w(r) = - \int_{\infty}^r \frac{Q_1 Q_2 dr}{4\pi\varepsilon_0 \varepsilon r^2} = + \left[\frac{Q_1 Q_2}{4\pi\varepsilon_0 \varepsilon r} \right]_{\infty}^r = \frac{Q_1 Q_2}{4\pi\varepsilon_0 \varepsilon r} = \frac{Z_1 Z_2 e^2}{4\pi\varepsilon_0 \varepsilon r} \quad (2.19)$$

where Z and $e = 1.6 \times 10^{-19}$ C correspond to the valency of the ion and the elementary charge, respectively. Note that the Coulomb interaction free energy between ions is inversely proportional to the distance r , indicating a long-range interaction. The interaction energy is weakened by the permittivity of the surrounding with $\varepsilon > 1$ (e.g., for water $\varepsilon = 78$ as per Table 2.2).

The Coulomb interaction is one of the strongest physical forces. As an example, to calculate the Coulomb interaction for Na^+ and Cl^- in contact with one another, r is the sum of the two ionic radii (0.276 nm) and the interaction energy between these two elementary charges in a vacuum (vacuum $\varepsilon = 1$, left out of calculation) is

$$w(r) = \frac{-(1.602 \times 10^{-19} \text{ C})^2}{4\pi \left(8.85 \times 10^{-12} \frac{\text{C}^2}{\text{Nm}^2} \right) (0.276 \times 10^{-9} \text{ m})} = -8.4 \times 10^{-19} \text{ J}. \quad (2.20)$$

This value is approximately 200 kT per ion pair in vacuum, with the thermal energy $kT = (1.38 \times 10^{-23} \text{ J/K})(300 \text{ K}) = 4.1 \times 10^{-21} \text{ J}$ at 300 K. The strength of the Coulomb interaction between Na^+ and Cl^- in this case is similar to the energy of covalent bonds that range from 40–400 kT per bond.

Before moving on and discussing in greater detail the effect of solvent permittivity on Coulombic ion interactions, we close this section by comparing side-by-side the electric field E , the force of moving a charge F , and the work of moving a charge W , with the electrostatic potential V . We simplify the discussion by assuming one-dimensionality in the x -direction. The force of moving a test charge q in an electrical field E is $F = Eq$, which results in the work

$$w(x) = -q \int E(x') dx \quad (2.21)$$

The corresponding electric potential of the test charge is

$$V(x) = \frac{w(x)}{q} = - \int E(x') dx \quad (2.22)$$

and thus, $E = -dV/dx$.

2.3 Ion Interactions in Dielectric Solutions

2.3.1 Bjerrum Length

We return to the example above (Eq. 2.20), when we calculated the Coulomb energy between two ions in contact. We found that the resulting free energy exceeds by two orders of magnitude the thermal noise (kT) in a vacuum ($\varepsilon = 1$) environment. As the Coulomb energy depends on the ion pair distance r , the question arises at which r does the interaction energy balance the thermal noise. We will name that particular distance the Bjerrum length, l_b . As per the worked problem (2.1) below, $l_b = 56 \text{ nm}$ in vacuum.

The Bjerrum length is a length expression for monovalent ion interaction, and most generally expressed for any solvent environment ε , i.e.,

$$l_b \equiv \begin{cases} \frac{e^2}{4\pi\varepsilon_0\varepsilon kT} \\ \frac{e^2}{4\pi\varepsilon_0\varepsilon} \frac{N_A}{RT} \end{cases} \quad (2.23)$$

Eq. (2.23) provides equivalent forms that are either more suitable for single particle systems or molar quantities, with Avogadro's number $N_A = 6.022 \times 10^{23} \text{ mol}^{-1}$ and the universal gas constant $R = 8.314 \text{ J/mol}\cdot\text{K}$. Substituted into Coulomb's law of monovalent ions, it yields

$$w(r) = \frac{e^2}{4\pi\varepsilon_0\varepsilon r} = \begin{cases} \left(\frac{l_b}{r}\right) kT \\ \left(\frac{l_b}{r}\right) \frac{RT}{N_A} \end{cases} \quad (2.24)$$

On closer inspection, the Bjerrum length is the charge distribution distance of monovalent ions in a solvent at which the Coulomb energy of a mole of ion pairs is balanced by the thermal energy RT . This makes the Bjerrum length a very convenient parameter for many calculation purposes, in particular for evaluating critical ion distances in solvents of varying concentration and temperatures (c.f., Table 2.3 for NaCl/water solutions)

Worked problem 2.1

Calculate the Bjerrum length ℓ_b between a Na^+ and Cl^- ion in vacuum at 300 K.

Solution:

For monovalent ions, $Q_1Q_2 = e^2$. At $r = \ell_b$, the Coulomb energy of the interacting ions equals thermal energy.

$$kT = \frac{e^2}{4\pi\varepsilon_0\ell_b} \quad (2.25)$$

Rearrange to solve for ℓ_b .

$$\ell_b = \frac{e^2}{4\pi\epsilon_0 kT} \quad (2.26)$$

Substitute values and solve.

$$\ell_b = \frac{(1.602 \times 10^{-19} \text{ C})^2}{4\pi \left(8.85 \times 10^{-12} \frac{\text{C}^2}{\text{Nm}^2}\right) \left(1.38 \times 10^{-23} \frac{\text{J}}{\text{K}}\right) (300 \text{ K})} = 56 \times 10^{-9} \text{ m.} \quad (2.27)$$

When $r > \ell_b$, thermal energy dominates. When $r < \ell_b$, Coulombic energy dominates. The Bjerrum length can also be substituted into Coulomb's law for monovalent ions to yield

$$w(r) = \frac{e^2}{4\pi\epsilon_0 \epsilon kT} \frac{1}{r} = \frac{\ell_b}{r} \text{ J per ion} \quad (2.28)$$

or

$$w(r) = \frac{e^2 RT}{4\pi\epsilon_0 \epsilon N_A} \frac{1}{r} = \frac{\ell_b}{r} \frac{RT}{N_A} \text{ J per mol} \quad (2.29)$$

which for one mole of substance yields the molar interaction free energy,

$$W(r) = N_A w(r) = \frac{\ell_b}{r} RT \text{ J per mol.} \quad (2.30)$$

With the worked example, we restricted ourselves to vacuum. Let us consider the situation of water as the solvent at room temperature, with $\epsilon \approx 80$. As per Eq. (2.28), the Bjerrum length reduced from 56 nm in vacuum to $56/80 \text{ nm} \approx 0.7 \text{ nm}$, which is about 2-3 times the combined ion distance, or in energetic terms, on the order of RT for monovalent ion salts. It explains the high solubility of monovalent ion salts in water. Thus, because RT is roughly a measure of the thermal noise, the ratio of ℓ_b/r can give us an estimate of the binding stability between ions, or contrarily, the ion dissolution potential in a third media. In a solution of short Bjerrum length compared to the ion crystal spacing a (i.e., $\ell_b \sim a$) the ions are expected to dissolve well. On the other hand, for relatively long Bjerrum lengths (i.e. $\ell_b \gg a$), the media represents a poor solvent for ionic crystal.

As per the equations above, the Bjerrum length depends on the permittivity of the solvent and the absolute temperature. Figure 2.4a below provides the relationship of the Bjerrum length with temperature for water, as well as the functional convoluted relationship between the Bjerrum length (Fig 2.4c and the permittivity of water at specific temperatures (Fig. 2.4b).

Finally, it shall be pointed out that for non-monovalent ions, $Q = Ze$, the expression for the Bjerrum length can be extended to

$$\ell_b = \frac{Z_1 Z_2 e^2}{4\pi\epsilon_0 \epsilon kT} \quad (2.31)$$

and the expression for $w(r)$ can be written as

$$w(r) = \frac{\ell_b}{r} kT(Z_1Z_2). \quad (2.32)$$

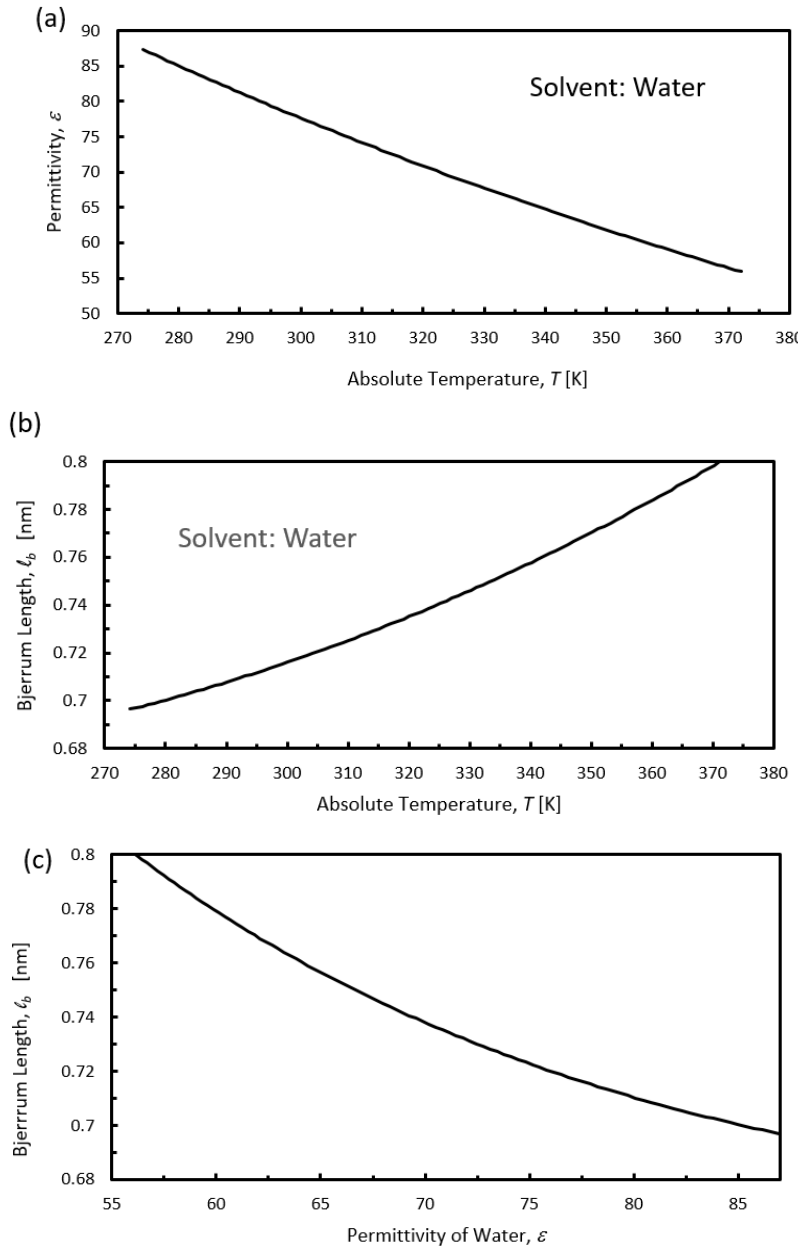


Figure 2.4 (a) Bjerrum length of monovalent ions in water and (b) permittivity of water, both as function of temperature. (c) Convolved relationship of (a) and (b) between the Bjerrum length and the permittivity of water at specific temperatures.

2.3.2 Self-Energy and Born Energy of an Ion

Let us consider an ion within a solvent of permittivity ϵ . As the ion emanates an electric field and polarizes the solvent, the self-energy must reflect the polarization. An elegant way to express the polarization effect of the environment is to assume that at the location

where the ion shall be placed, charges are incrementally building up opposing further charge buildup. This is illustrated in Fig. 2.5 and discussed in the following.

We start with a neutral atom of radius “ a ” at the origin of our coordinate system that we incrementally charge up to the ion charge Q . Because of its interaction neutrality, no energy is needed to place the atom there. Now we bring an incremental charge dq from infinity to the surface of the atom, i.e., from $r = \infty$ to $r = a$. As we only have to consider Coulombic interactions, the process has an incremental energy $dw = 0$. We rename the ionic charge on the atom q at each incremental charging step. In other words, q is a variable. Moving a further charge of same polarity, again of value dq from infinity to the surface, we have to overcome a repulsive Coulombic interaction

$$dw = \frac{qdq}{4\pi\epsilon_0\epsilon a} \quad (2.33)$$

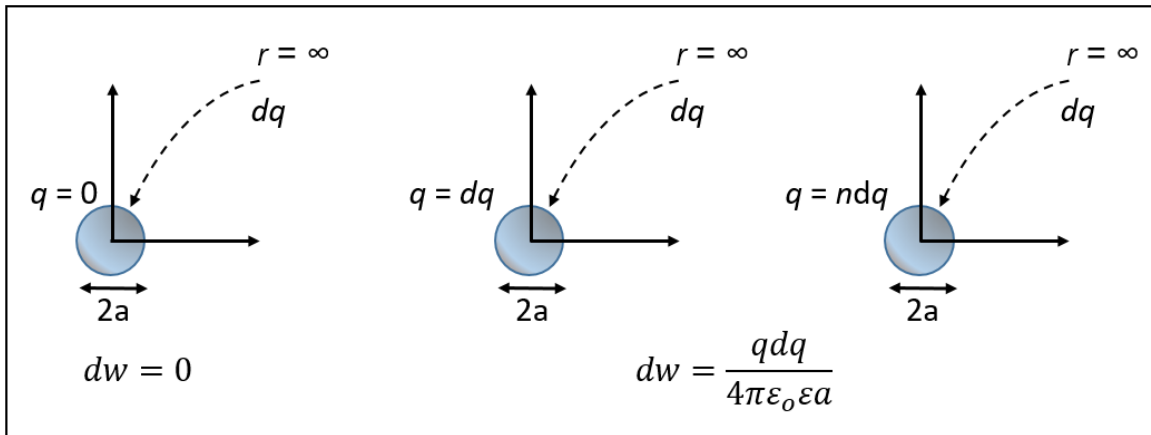


Figure 2.5: Charging a neutral atom of radius a in incremental steps involving the incremental work dw .

If we continue that process, the work done to charge our atom from zero charge to charge Q is

$$\mu^i = \int dw = \int_0^Q \frac{qdq}{4\pi\epsilon_0\epsilon a} = \frac{Q^2}{2(4\pi\epsilon_0\epsilon a)} \quad (2.34)$$

The obtained self-energy of bringing a charge into a solvent is called *Born energy*, which represents the electrostatic free energy of an ion in a medium of constant permittivity ϵ . (An alternative derivation can be found in the specified additional reading by J.N. Israelachvili). We note from the expression above that the Born energy is inversely proportional to the solvent permittivity ϵ .

With the Born energy we can determine the energy involved in transferring an ion of charge Q from one solvent to another. Let us assume the permittivities of the two media are ϵ_1 and ϵ_2 , with media 1 and 2 being the origin and destination of the ion, respectively. Then, the free energy change is given by the difference of the two Born energies, i.e.,

$$\Delta\mu^i \equiv \mu_2^i - \mu_1^i = \frac{Q^2}{2(4\pi\epsilon_0\epsilon)a} \left(\frac{1}{\epsilon_2} - \frac{1}{\epsilon_1} \right) \quad (2.35)$$

For the process to be spontaneous (i.e., run by itself without work), $\Delta\mu^i$ must be negative. In other words,

$$\left(\frac{1}{\varepsilon_2} - \frac{1}{\varepsilon_1}\right) < 0 \quad (2.36)$$

describes a spontaneous ion transfer (dissolution) process from medium 1 to medium 2. If we consider medium 1 to be the gas phase ($\varepsilon_1=1$) and medium 2 water ($\varepsilon_1=78$), the difference in the reciprocal permittivity values is negative, and thus, ions dissolve well in water coming from the gas phase. We can say that ion dissolution is favorable from a medium of lower permittivity to a medium with higher permittivity.

If we consider molar quantities of ions, then the free energy change is given by the Avogadro multiple of the Born energy difference, i.e.,

$$\Delta G = N_A \Delta\mu^i = \frac{N_A Q^2}{2(4\pi\varepsilon_0)a} \left(\frac{1}{\varepsilon_2} - \frac{1}{\varepsilon_1}\right) \approx -\frac{69z^2}{a} \left(\frac{1}{\varepsilon_2} - \frac{1}{\varepsilon_1}\right) \quad (2.37)$$

We thereby replaced the charge Q by its multiple of the elementary charge, i.e., $Q = ze$. For a molar quantity of an ionic system (e.g., NaCl), we have to consider both the anions and cations, and thus, $\Delta G = 2N_A \Delta\mu^i$. If we assume a monovalent ($z = 1$) ionic crystal with $a = 0.14$ nm dissolved in water, the molar free energy is about -1000 kJ/mol.

2.3.3 Ion Solubility – a Stochastic Process

We must consider why ions, that are so stable in a crystalline lattice, spontaneously solubilize. The first explanation that comes to mind is that the increase in ε decreases the energy of an ionic interaction when in solution. The assumptions used in deriving ε , however, breakdown when length scales approach the diameter of a solvent molecule and continuum assumptions are no longer valid. The energy of separating an Na^+ and Cl^- ion in contact with one another is given by

$$\Delta\mu_i = \frac{e^2}{4\pi\varepsilon_0\varepsilon(a_+ + a_-)} \quad (2.38)$$

where a_+ and a_- correspond to the radii of Na^+ and Cl^- , respectively. Plugging this value into the equation for distribution between two phases we get,

$$X_S = e^{-\Delta\mu_i/kT} = \exp\left[-\frac{e^2}{4\pi\varepsilon_0\varepsilon(a_+ + a_-)kT}\right] \quad (2.39)$$

where X_S is the equilibrium mol fraction of ion in solution at saturation. This equation is too simple to compute accurate solubilities, but it does qualitatively predict the effect of the solvent dielectric constant on solute solubility. We see below that a plot of $\log X_S$ versus $1/\varepsilon$ yields a straight line, as predicted by Eq. (2.39).

As predicted by Eq. (2.39), the ion curve passes through the origin since the solute-solvent interaction is purely Coulombic. The curve for glycine does not pass through the origin because there are Van der Waals interactions between glycine and the solvent as well as electrostatic interactions. This interaction is not accounted for in Eq. (2.39). As per our prior discussion, it is notable that the slope of the line in Fig. 2.6 is dependent on $-\Delta\mu_i/kT$ and can be used to back-calculate ion-pair specific quantities such as $a_+ + a_-$.

Many more in-depth approaches exist for predicting the solubility of ions in a solution. In all cases, the solubility is directly related to the difference in free energy between the lattice state and the solubilized state. Accurately predicting this energy difference, however, is nontrivial and often involves using empirically derived correction factors. A more thorough discussion of these corrections is presented in Chapter 3.

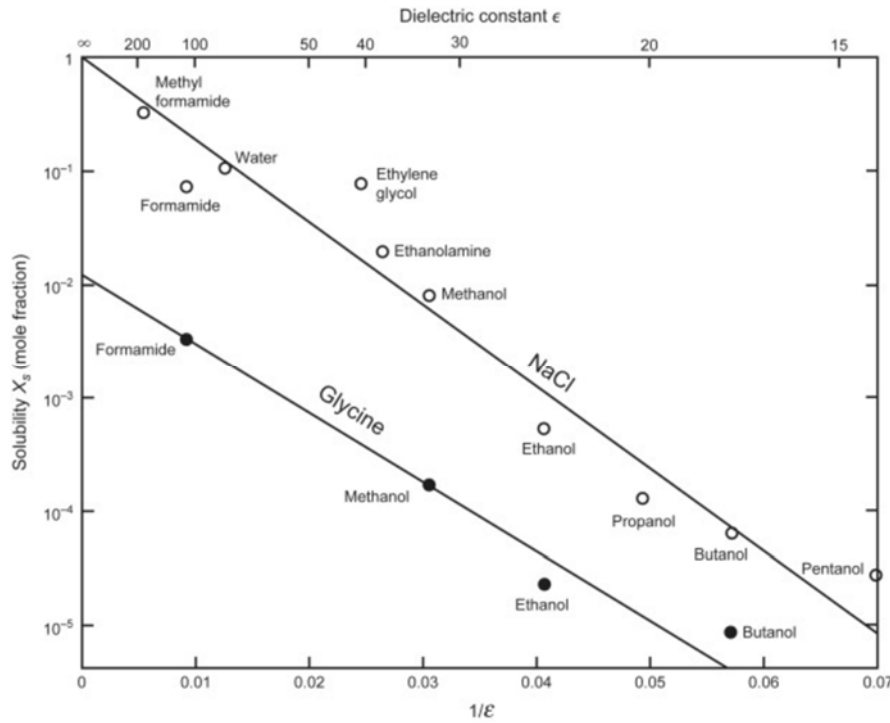


Figure 2.6: Solubility of NaCl and Glycine in a wide variety of solvents at room temperature (Israelachvili, Jacob N. *Intermolecular and Surface Forces*. Elsevier Academic, 2011)

2.3.4 Continuum vs. Molecular Approach to Ion-Solvent Effects

By integrating the Born Energy equation, Eq. (2.40) to an arbitrary radius R we obtain,

$$\mu_i = \frac{Q^2}{8\pi\epsilon_0\epsilon} \left[\frac{1}{a} - \frac{1}{R} \right] \quad (2.40)$$

We see that 50% of the Born energy of an ion of 1 nm radius is contained within 0.1 nm (from the ion surface) and 90% is contained within 1 nm. Because no solvent atom is smaller than 0.1 nm, the local permittivity of solvent can be expected to deviate substantially from the bulk value ϵ . Thus, the continuum approach to calculating the Born energy of an ion breaks down for small ions, such as lithium, or, ions with higher than one valence (charge) numbers. Figure 2.7, compares the Coulomb interaction between monovalent ions in bulk water (more specifically Na^+ and Cl^-) with a molecular dynamic calculation of the pair-potential interaction free energy in water that can change locally the solvent permittivity according to the present ion electric fields and solvent dipole moments. The critical parameters to watch is the width Δr_{max} of the regime between the first two maxima of the oscillatory potential and the size of the solvent molecule σ (in this case water). For NaCl $\Delta r_{max} < \sigma$, which does not provide the necessary space for the water molecules to be aligned as shown in the inset. For the smaller LiCl, the situation is

reversed and strong liquid structuring around the ions, or the binary ion-complex can be expected, which leads to strongly deviating local solvent permittivities. The Born energy would not be appropriate.

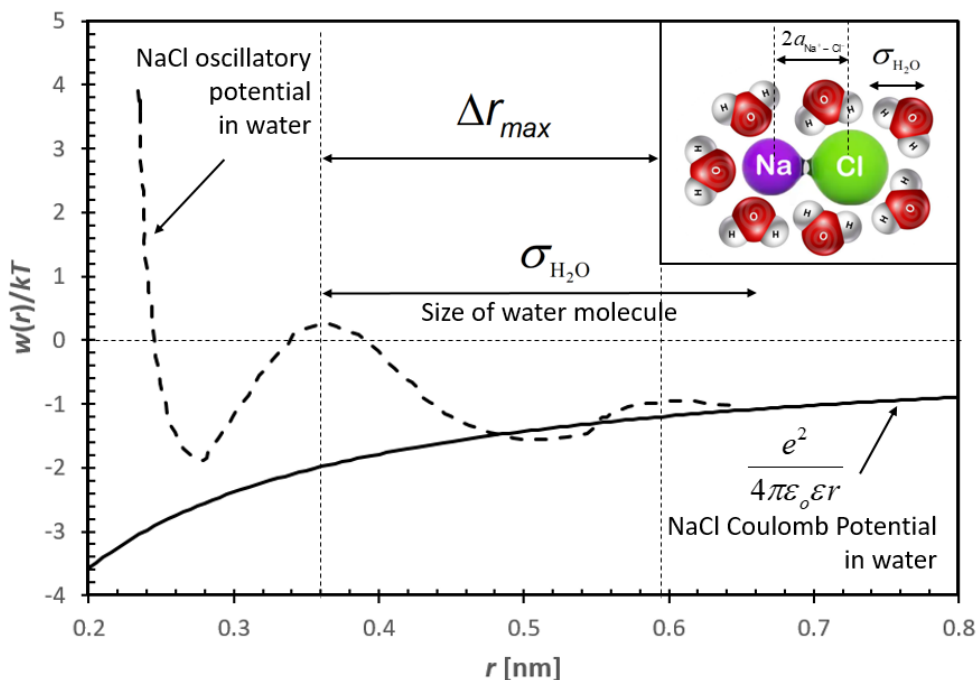


Figure 2.7: Pair-potential of Na^+ and Cl^- in water. Theoretical predictions based on Analytical Integral Equations plotted with coarse dashed line. The continuum prediction is plotted with solid line. The inset illustrates local ordering of the solvent molecules around the ions, which is expected for small ions such as LiCl , but not for NaCl .

2.4 Ion Interaction Potential (Ionic solids)

Having discussed the dissolution of salts in solvents, in this last section, we will discuss the energy that is stored in an ionic crystal. Ionic compounds form crystalline solids with repeating arrangements of anions and cations. The intertwined lattice arrangements of ions, as depicted in Fig. 2.8 for NaCl -type ionic crystals is determined by the charge and valency of the constituent ions. In the case of NaCl , sodium ions and chlorine form two face-centered cubic lattices that are shifted to each other by half the shortest distance between two ions of the same kind. The loosely held valence electrons of the sodium atoms are transferred to the nearby chlorine atoms. The Na^+ and Cl^- ions then organize into an extended crystal array. Each ion is 6-coordinated with octahedral geometry and the crystal structure is face-centered cubic with respect to both sodium and chloride ions.

When considering the Coulombic interaction of the ions in the lattice, one must take into account long-range interactions that are both attractive and repulsive in nature because Coulomb forces are long range (proportional to $1/r$). Each Na^+ ion has 6 nearest-neighbor Cl^- ions at $r = 0.276 \text{ nm}$, 12 next-nearest-neighbor Na^+ ions at $\sqrt{2}r$, 8 additional Cl^- ions at $\sqrt{3}r$, and so on.

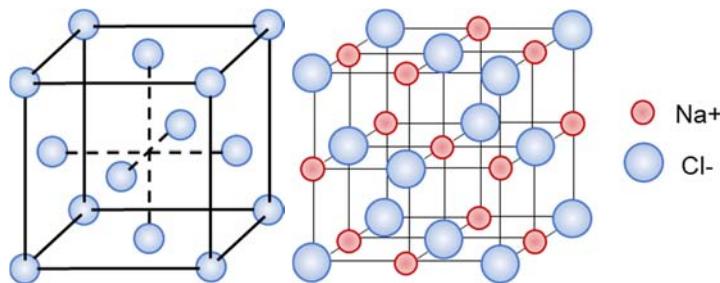


Figure 2.8. (left) Generic face-centered-cubic (FCC) lattice. (right) Crystal structure of NaCl composed of two relatively shifted FCC lattices of Na⁺ and Cl⁻.

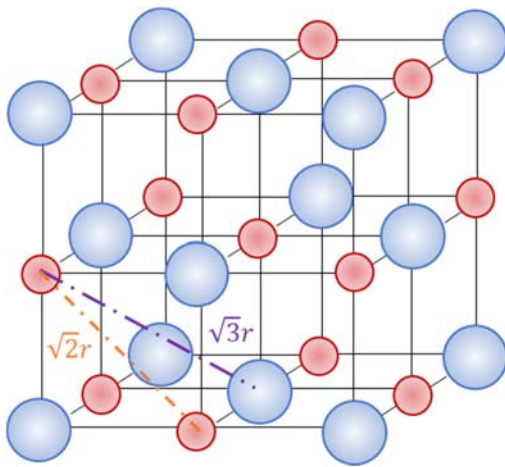


Figure 2.9. Crystal structure of NaCl with distances used for Madelung constant calculation shown.

Each of these neighboring ions contribute to the interaction potential. The total interaction energy for a pair of Na⁺Cl⁻ ions in this lattice is therefore

$$\begin{aligned}\mu^i &= -\frac{e^2}{4\pi\epsilon_0 r} \left[6 - \frac{12}{\sqrt{2}} + \frac{8}{\sqrt{3}} - \frac{6}{2} + \dots \right] \\ &= -\frac{e^2}{4\pi\epsilon_0 r} [6 - 8.485 + 4.619 - 3.00 + \dots] \\ &= -1.748 \frac{e^2}{4\pi\epsilon_0 r} = -1.46 \times 10^{-18} \text{ J.}\end{aligned}\quad (2.41)$$

The constant 1.748 is known as the *Madelung constant*, which is used to determine the electrostatic potential of a single ion in a crystal by approximating the ions as point charges. The value of the Madelung constant depends on the crystal structure and the valency of the ions in the lattice. For other monovalent ionic solids, the Madelung constant ranges between 1.638 and 1.763. For monovalent-divalent pairs (e.g. CaF₂), the value of the Madelung constant can reach 5.

The total interaction energy for the pair of Na⁺Cl⁻ ions in the lattice is negative and approximately the same order of magnitude as for isolated ion pairs in vacuum (see Eq. 2.20). This pair interaction energy can be used to find the *molar lattice energy* or *cohesive energy* (*U*) of an NaCl crystal, the amount of energy required to separate a mole of an

ionic solid into gaseous ions. This is accomplished by multiplying the ion pair interaction energy by Avogadro's number,

$$U = -N_A \mu^i = -\left(6.02 \times 10^{23} \frac{\text{atoms}}{\text{mol}}\right) (1.46 \times 10^{-18} \text{ J}) = -880 \frac{\text{kJ}}{\text{mol}}. \quad (2.42)$$

The value calculated in Eq. (2.42) is about 15% higher than the experimental value of -765 kJ/mol because the previous treatment neglected quantum repulsive forces within the lattice.

The ions in a crystal lattice experience an element of quantum repulsion in addition to the sum of attractive and repulsive Coulombic interactions. As ions approach each other in space, the wavefunctions of their core electrons begin to overlap which results in the formation new energy states for the electrons in the two-nucleus system. At large distances, the electrons of the two ions can have identical quantum numbers, but at small distances as the wavefunctions overlap quantum rules require some electrons to move to a higher energy state. Some of the electrons remain in the original, lower energy states. This increase in energy state requires energy, which gives rise to a repulsive force between the ions preventing them from coming physically closer together. This is known as the *Pauli exclusion principle*. A diagram for the Pauli repulsion term of sodium chloride is shown below.

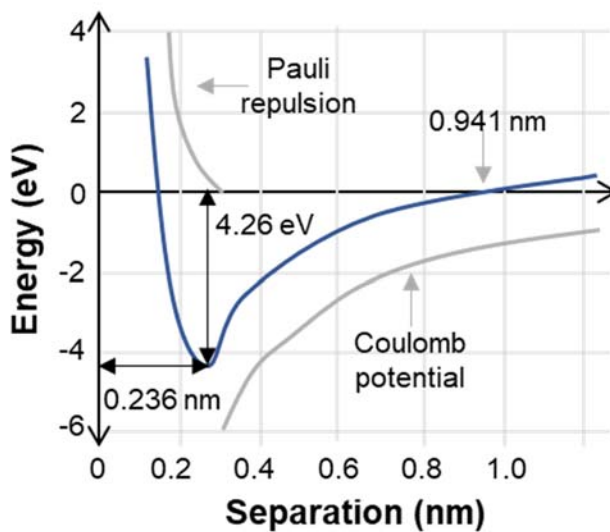


Figure 2.10. Plot of energy versus separation for NaCl showing quantum repulsion and Coulombic attraction. $1 \text{ eV} = 1.602 \times 10^{-19} \text{ J}$.

With this more complete treatment of the forces inside the lattice, the expression for $w(r)$ in vacuum becomes

$$w(r) = \frac{-e^2}{4\pi\epsilon_0 r} + \frac{B}{r^9} \text{ J}, \quad (2.43)$$

where B is a constant and r^9 an empirical observation of ion-ion quantum repulsion. To determine B , minimize $\frac{dw}{dr}$ ($\frac{dw}{dr} = 0$) to find that

$$B = \frac{-e^2 a_0^8}{4\pi\epsilon_0}. \quad (2.44)$$

In this equation, a_0 is the minimum equilibrium spacing between ions in the lattice, which depends on the system. From this more thorough treatment, the total potential energy of one ion in a Na^+Cl^- lattice accounting for both Coulombic interaction and quantum repulsion is

$$w(r) = \left(-1.748 \frac{e^2}{r} + \frac{B}{r^9} \right) \left(\frac{1}{4\pi\epsilon_0} \right) \text{J}. \quad (2.45)$$

Multiplying this equation by N_A gives the total potential energy (U) for a mole of Na^+ and Cl^- ions in a lattice. By minimizing $\frac{dU}{dr}$ ($\frac{dU}{dr} = 0$) and setting $r = a_0$, we can determine equilibrium spacing or equilibrium energy. Skip to Eq. (2.51) to solve for energy; Eqs. (2.46-2.48) are for explanation.

$$\frac{dU}{dr} = 0 = N_A \left(\frac{1.748e^2}{4\pi\epsilon_0 a_0^2} - \frac{9B}{a_0^{10}} \right) \quad (2.46)$$

Solve for B .

$$B = \frac{1.748e^2 a_0^8 N_A}{9} \quad (2.47)$$

Substitute B expression and simplify.

$$U = -\frac{1.748e^2 N_A}{4\pi\epsilon_0 a_0} \left[\frac{a_0}{r} - \frac{1}{9} \left(\frac{a_0}{r} \right)^9 \right] \quad (2.48)$$

With $r = a_0 = 2.82 \text{ \AA}$, the equilibrium spacing of Na^+Cl^- ,

$$\begin{aligned} U_0 &= U = -\frac{1.748e^2 N_A}{4\pi\epsilon_0 a_0} \left[\frac{a_0}{r} - \frac{1}{9} \left(\frac{a_0}{r} \right)^9 \right] \\ &= -\frac{1.748e^2 N_A}{4\pi\epsilon_0 a_0} \left[1 - \frac{1}{9} \right] = -765 \frac{\text{kJ}}{\text{mol}}. \end{aligned} \quad (2.49)$$

This calculated value matches the experimental value mentioned after Eq. (2.42).

The equilibrium potential energy of an ionic solid can be used to calculate the *compression modulus* (K) or *bulk modulus*, a measure of how resistant a substance is to compression. The compression modulus arises from the interatomic potential energy and the volume per ion in the lattice.² Under isotropic pressure,

$$K = -V \frac{dP}{dV} \approx -\frac{U_0}{V} \text{ Pa} \quad (2.50)$$

where V is the volume of the crystal.

2.4.1 Reference States

Having the proper reference state is important for interpreting the meaning of values calculated for energies. As an example, when ions come together to form a condensed phase from the gaseous state, the reference state is at $r = \infty$ and occurs in vacuum ($\epsilon = 1$). This is why Eq. (2.49) for the lattice energy of ionic crystals does not contain the dielectric constant for the medium. However, when two ions interact in a condensed liquid medium, the reference state is also at $r = \infty$, but the dielectric constant of the medium must be considered in calculations because this is the environment the interactions occur within.

2.4.2 Range of Electrostatic Forces

Although Coulombic forces are long-ranged and additive, the net electrostatic interaction on a body is usually complex, difficult to calculate, and of shorter range than expected. In a crystal lattice each positive charge has a negative charge next to it, forming a dipole whose field decays as $1/r^3$ instead of as $1/r^2$ (upcoming in Chapter 3). Each dipole has another dipole as a neighbor, forming a quadrupole whose field decays as $1/r^4$. These contributions decay quickly (exponentially), causing the field observed outside of the ionic lattice to be short-ranged even though it is composed of many long-range interactions. Similarly, a positive ion moving freely in aqueous solution always has a high density of negative ions surrounding it. The positive ion's electric field is *screened* exponentially by these negative ions, and decays more rapidly than would be observed for the isolated positive ion.

2.5 Summary

This overview chapter discusses covalent, metallic, and ionic interactions. These interactions are stronger than most other intermolecular forces, such as hydrogen bonds. Covalent bonds are on the order of 100 kcal/mol, and metallic bonds on the order of 10 kcal/mol. Most intermolecular interactions have a bond strength of around 1 kcal/mol.

Covalent bonds require atoms to share electrons, which result in atomic orbital overlaps. This may lead to an uneven distribution of electrons and partial charges, which confer polarity. Metallic bonds are attractive forces formed from a uniform distribution of electrons that freely move around the positively charged metal ion cores. Since the electrons are evenly distributed, the material has a net neutral charge.

The Morse potential, as described here for a binary atom system,

$$E = D_e (1 - e^{-a(r-r_e)})^2 \quad (2.5)$$

is a convenient interatomic interaction model for the potential energy of a covalent bond. The parameters are the dissociation energy, D_e , the distance of the bond length from equilibrium, $(r - r_e)$, and the “potential inverse width, a . Conversely to a simple harmonic spring potential that does not explain bond breaking, the Morse potential accounts for atom-atom dissociation at a critical distance, where the potential energy matches the dissociation energy.

Ionic bonds are the result of the Coulombic forces between oppositely charged ions, leading to an attractive force. Coulombic interaction is influenced by the environmental permittivity ϵ and the separation distance r between the ions, as shown in Coulomb's force law between the two charges Q_1 and Q_2 :

$$F(r) = Q_2 E_1 = \frac{Q_1 Q_2}{4\pi\epsilon_0 \epsilon r^2} \quad (2.17)$$

Coulomb's force law is the force a charge (Q_2) experiences, if exposed to the electric field $E_1 = Q_1/(4\pi\epsilon_0 \epsilon r^2)$ of an original charge Q_1 . The permittivity (ϵ) reflects the degree of polarizability of the environment in response to an electric field. Coulombic interactions belong to the strongest physical forces, and can be comparable in strength to covalent interactions. The magnitude of the Coulomb interaction free energy, $w_c(r) = - \int F(r) dr = Q_1 Q_2 / (4\pi\epsilon_0 \epsilon r)$ shows a long-range $1/r$ dependence.

As the Coulomb energy depends on the ion pair distance, there should exist a distance where the Coulomb energy between two monovalent ions balances the thermal noise

(kT) . This distance is named Bjerrum length, l_b . It is generally expressed for any solvent environment, as

$$l_b = \frac{Z_1 Z_2 e^2}{4\pi\epsilon_0\epsilon kT} \quad (2.31)$$

The Bjerrum length is very useful in calculating critical ion distances in solvents of varying conditions.

To determine the self-energy of an ion in a solvent of permittivity ϵ , we introduce the concept of the *Born energy*. The Born energy, also known as the *solvation energy*, is the energy needed to bring a charge into existence within a solvent, and can be expressed as,

$$\mu^i = \int dw = \int_0^Q \frac{qdq}{4\pi\epsilon_0\epsilon a} = \frac{Q^2}{2(4\pi\epsilon_0\epsilon)a} \quad (2.34)$$

Using this expression, we can determine the energy required to transfer an ion from one solvent to another. The Born energy can also be used to explain why ions that are stable in a crystalline lattice are soluble in particular solvents. This is because, the strong electrostatic interactions in a crystalline lattice decrease in strength, in a solvent of high ϵ , allowing the ions to spontaneously dissolve into the solution. The mole fraction of ions in solution at the saturation concentration, X_s , can be obtained from

$$X_s = e^{-\Delta\mu_i/kT} = \exp\left[-\frac{e^2}{4\pi\epsilon_0\epsilon(a_+ + a_-)kT}\right] \quad (2.39)$$

where e is the elementary charge, and $(a_+ + a_-)$ reflects the size of a an ion pair (sum of the ion radii of the anion and cation).

Note from Eq. (2.34) that the Born energy was obtained from integrating over the entire space. It turns out, however, that 50% of the ion solvation energy is contained within only 0.1 nm from the ion surface for small ions of 1 nm radius, such as lithium, or ions, with higher than 1 valence numbers. The sodium ion on the other hand is just large enough for the continuum approach to work. Thus for LiCl, we find the local change of the solvent permittivity to have a strong effect on the local permittivity of the solvent, for which the Born energy calculation breaks down. For NaCl, the local change on the solvent permittivity can be neglected, and thus the Born energy calculation is appropriate.

To determine the interaction free energy of ions in a crystal, three forces have to be considered. Two Coulombic interactions, one attractive and one repulsive at a wide variety of distances, and the quantum mechanical Pauli repulsion. The summation of attractive forces and repulsive forces yields a crystal-type dependent prefactor, known as the Madelung constant. For instance, for NaCl-type crystal the Madelung constant, M , is 1.748 and thus, the total Coulombic interaction free energy for a pair of Na^+Cl^- ions in a NaCl lattice is given by

$$\mu^i = -1.748 \frac{e^2}{4\pi\epsilon_0 r} = -1.46 \times 10^{-18} \text{ J} \quad (2.41)$$

If multiplied with Avogadro's number, the molar internal energy exceeds measurements by about 15 %, as we neglected to consider the Pauli repulsion. With the Pauli repulsion, we obey the quantum mechanical rule of quantum states, i.e., two electrons cannot share the same location (i.e., possess the same quantum states). For ion-ion interactions, we include the Pauli repulsion with the semi-empirical equation,

$$w(r) = \frac{-e^2}{4\pi\epsilon_0 r} + \frac{B}{r^9} \text{ J}, \quad (2.43)$$

where B represents the Pauli interaction parameter. This expression yields the correct experimental value of -765 kJ/mol for the internal binding energy of NaCl. In a last illustration, microscopically summed up energies were used to determine phenomenological properties, more specifically, the bulk modulus of NaCl, which was in excellent agreement with experiments.

Review Questions

1. What is the difference between covalent and metallic bonds?
2. How can you approximate the potential energy of a covalent bond using the harmonic oscillator model?
3. In Coulomb interactions, specify the parameters that govern the attractive/repulsive outcome.
4. What is the Bjerrum length?
5. How can we set up the model for deriving the Born energy?
6. Ionic interaction is relatively strong in its solid state. Why is the key factor that some compounds dissolve into water spontaneously?
7. What is the factor that defines the Madelung constant?
8. The calculation of molar lattice energy based on electrostatic interaction usually yields higher than experimental value. Why is that?

Answer Key

1. Covalent bonds exhibit “localized” sharing of electrons. These electrons are shared unevenly, depending on the electronegativities of the atoms in the bond. The uneven sharing of electrons also induces partial charges in the atoms. Metallic bonds are the “delocalized” sharing of electrons where electrons move freely around a metal cation. The electron distribution is uniform, creating an overall neutral charge.
2. Using equation 2.2 from the write-up, the energy (E) around an equilibrium point r_e is

$$E = \frac{1}{2}k(r - r_e)^2$$

Where $(r - r_e)$ is the distance from equilibrium, and k is the spring constant (stiffness of bond) of a spring between the atoms.

3. For coulombic force, $F(r) = Q_2 E_1 = \frac{Q_1 Q_2}{4\pi\epsilon_0 \epsilon r^2}$. The interaction will be attractive if the sign of the vector is negative (moving towards each other). The outcome of the sign depends on the charge of the ions: for an anion/cation pair, the sign will be negative. For other cases, the sign will be positive.
4. The Bjerrum length is a length expression for monovalent ion interaction where the Coulomb energy of an ion pair is balanced by the thermal energy.
5. We can charge a neutral atom of radius a at the origin of the coordinate system in incremental steps.
6. As the environment changes from the vacuum (or low dielectric constant such as air) into water. The strength of electrostatic force decreases due to a higher dielectric constant. However, there is a limit to how much a certain compound dissolve which can be calculated as in Eq. 2.39

7. The Madelung constant depends on the interaction in the crystal lattice, which will be approximate according to that lattice group interaction. For instance, the face-centered-cubic lattice has six ions of different charges surrounding it and those ions will be surrounded by six other ions of the different charges, which fit into cubic orientation.
8. Pauli repulsion occurs when the particles get into very close proximity where electron cloud (wave function) starts to overlap, which forces the electron to move closer to the nucleus, which is its higher energy state. This Pauli repulsion is not included in the electrostatic interaction

Literature – Sources and Further Reading

1. Intermolecular & Surface Forces, 3rd Ed., J.N. Israelachvili, Academic Press, Boston (2011), Ch. 3 p. 61.
2. Molecular Driving Forces – Statistical Thermodynamics in Chemistry and Biology, Dill and Bromberg, Garland Science, New York (2002), Ch. 6, pp 81-87.

Chapter 3: Polar Interactions, Hydrogen Bonding and Van der Waals Interaction

3.1 Overview

In this chapter we will discuss the distinct characteristics of polar molecules and define the dipole moment. We will introduce the dipole self-energy and how this quantity compares to the Born self-energy of an ion. Considering ions and dipoles, we will discuss the variety of electrostatic interactions between them from frozen (static) systems to thermodynamically activated systems, where dipoles are freely rotating. The thermally activated process is attributed to orientational polarization of dipoles in an electric field that can emanate either from a dipole or an ion charge. This is of particular importance, when the two charged objects are further apart, and, at elevated temperatures. We will assess the critical distance at which the transition from static ion-dipole and dipole-dipole interactions to orientational polarized interactions occurs. Our discussion of the orientational polarization interaction will bring forward the first of three Van der Waals interaction terms that follow a $1/r^6$ potential, namely the *Keesom interaction*. We will close this chapter with a discussion of dipole interactions in water, specifically hydrogen bonding, the strongest type of dipole interaction.

3.2 Polar Molecules and Dipole Moment

A polar molecule is a molecule that exhibits an asymmetric electron distribution about its core, and thus, appears upon close inspection to be electrically charged on a local scale. An example is provided in Figure 3.1(a) with the uneven distribution of electrons for water (H_2O) molecules, with (highlighted in red) a heightened resonance time of the electrons around the highly electronegative oxygen atom in H_2O , and (in blue) an electron deprived regime around the hydrogen atoms. This uneven distribution brings forward a partial charge separation that if inspected at greater distance, appears as pair of equal partial charges q with opposite polarity, as depicted in Figure 3.1(b). The two charges with the charge separation l bring forward a dipole moment \vec{u} , pointing in the direction of the charge displacement.

3.2.1 Molecular Dipoles

Molecular dipoles, as illustrated in Figure 3.1(b) are defined by two partial charges each of absolute value q , and, a separation distance l . The magnitude of the dipole moment u is most conveniently defined as

$$u = ql \quad (3.1)$$

which implies the linear dependence on both parameters. The unit of the dipole moment, u , is a Debye (D), where $1\text{D} = 3.336 \times 10^{-30} \text{ C}\cdot\text{m}$. As an example of the dipolar magnitude, consider a partial charge separation over $1 \text{ \AA} = 0.1 \text{ nm}$ of the elementary charge $e = 1.602 \times 10^{-19} \text{ C}$. Eq. (3.1) yields a dipole moment of $1.602 \times 10^{-29} \text{ C}\cdot\text{m}$ or 4.8 D , which is approximately three times the dipole moment of water ($u_{\text{H}_2\text{O}} = 1.85 \text{ D}$, as per Table 3.1).

Table 3.1 below provides a list of dipole moments for selected molecules, bonds, and molecular groups. Figure 3.1(a) shows that the direction of the dipole moment is from the negative charge to the positive charge (as per the physicists, the chemists define it in the

opposite direction). Note from Table 3.1 that permanent dipole moments only occur in asymmetric molecules, e.g., carbon monoxide (CO) but not in symmetric molecules, such as methane (CH_4) or alkanes ($\text{C}_n\text{H}_{2n+2}$). The table lists characteristic dipole moments that can be assigned to each type of covalent bonds. As dipole moments arise from differences in electronegativity (see Figure 3.1) covalent bonds can carry a dipole moment.

Table 3.1: Dipole Moments of Molecules, Bonds and Molecular Groups)
(in Debye Units: $1\text{D} = 3.336 \times 10^{-30} \text{ C m}$)

Molecules				
Alkanes	0^b	H_2O		1.85 ^c
C_6H_6 (benzene)	0^d	$\text{C}_n\text{H}_{2n+1}\text{OH}$ (alcohols)		1.7
CCl_4	0	$\text{C}_6\text{H}_{11}\text{OH}$ (cyclohexanol)		1.7
CO_2	0^e	OMCTS ^f		0.42
CO	0.11	CH_3COOH (acetic acid)		1.7
CHCl_3 (chloroform)	1.06	$\text{C}_2\text{H}_4\text{O}$ (ethylene oxide)		1.9
HCl	1.08	CH_3COCH_3 (acetone)		2.9
HF	1.91 ^c	HCONH_2 (formamide)		3.7 ^c
NH_3	1.47	$\text{C}_6\text{H}_5\text{OH}$ (phenol)		1.5
CH_3Cl	1.87	$\text{C}_6\text{H}_5\text{NH}_2$ (aniline)		1.5
NaCl	8.5	$\text{C}_6\text{H}_5\text{Cl}$ (chlorobenzene)		1.8
CsCl	10.4	$\text{C}_6\text{H}_5\text{NO}_2$ (nitrobenzene)		4.2
Bond Moments				
$\text{C}-\text{H}^+$	0.4	$\text{C}-\text{C}$	0	C^+-Cl
$\text{N}-\text{H}^+$	1.31	$\text{C}=\text{C}$	0	N^+-O
$\text{O}-\text{H}^+$	1.51	C^+-N	0.22	$\text{C}^+=\text{O}$
$\text{F}-\text{H}^+$	1.94	C^+-O	0.74	$\text{N}^+=\text{O}$
Group Moments				
C^+-CH_3	0.4	C^+-COOH	1.7	Adenine
C^+-OH	1.65	C^+-OCH_3	1.3	Thymine
C^+-NH_2	1.2–1.5	C^+-NO_2	3.1–3.8	Guanine
				Cytosine
				~3
				~4
				~7
				~8

Source: Intermolecular and Surface Forces, 3rd Ed., J.N. Israelachvili, Elsevier, Boston 2011

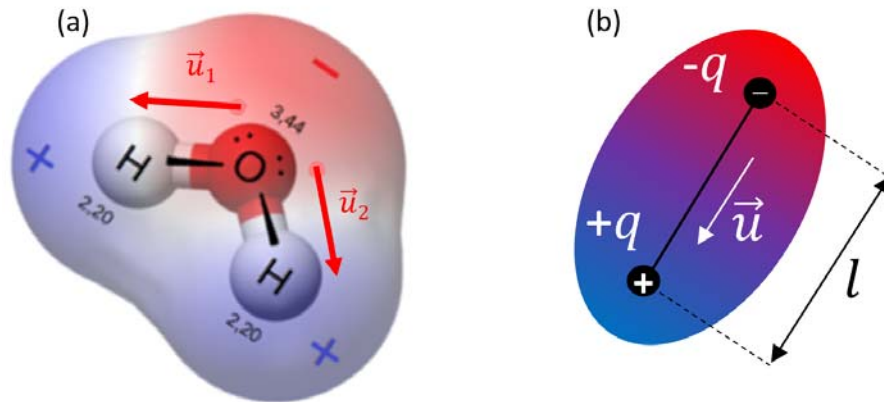


Figure 3.1: (a) Uneven electron distribution in polar water molecule. (b) Dipole residual model containing the resulting dipole moment \vec{u} composed of the partial charges $\pm q$ and charge displacement l .

A rough estimate of the resulting dipole of molecules can be obtained from adding up bond moments and/or group moments considering the relative orientations. As an example, we shall determine the dipole moment of water. Most generally, as we are dealing here with vector additions, we are using the parallelogram rule. The water molecule has two bond moments that point from each hydrogen atom to the oxygen atom. The chemistry definition of the dipole moment defines the direction as pointing from the positive to the negative atom. According to the parallelogram rule, the sum of these two vectors is a resultant vector pointing from the middle of the two hydrogen atoms to the oxygen (shown in red in Figure 3.2). The sum of the two vectors is $\mu \cong (u_1^2 + u_2^2 + 2u_1 u_2 \cos\theta)^{1/2}$. This simplifies to $\mu \cong 2u_1 \cos\frac{\theta}{2}$ when the two dipole moments u_1 and u_2 are the same magnitude.

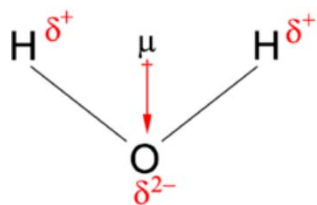


Figure 3.2: Direction of the dipole moment of a water molecule.

As mentioned above, the physicists define the direction of the dipole moment from negative to the positive charge, hence the dipole is aligned opposite to the direction of an electric field in a parallel plate capacitor that points from the positive electrode to the negative electrode. Considering now a dipole in the electric field of such a capacitor, it would rotate and align itself with the electric field to minimize its electrostatic free energy, as shown in Figure 3.3(a). The electric field generated by the dipole is illustrated in Figure 3.3(b), and determined in medium ϵ as

$$\vec{E}_{dipole} = \frac{1}{4\pi\epsilon_0\epsilon r^3} \frac{\vec{u}}{r} \quad (3.2)$$

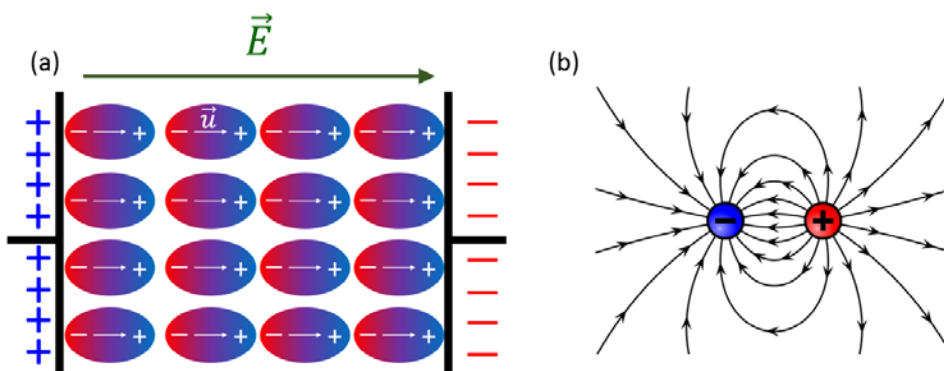


Figure 3.3: (a) Dipole alignment in electric field of a parallel plate capacitor. The original electric field of the capacitor in vacuum is reduced by the sum of the dipole fields. (b) Dipole electric field lines.

The dipole moments can be affected by the environment of the molecule. This is shown with glycine in Figure 3.4, where the amino group ($-\text{NH}_2$) acquires a proton and the hydroxyl group ($-\text{OH}$) loses a proton to the solution to produce a dipolar molecule.

Thus, in the case of the amino acid, glycine, the solvent is generating a solvent-induced **zwitterionic molecule**, i.e., a molecule with actual opposing net charges. A molecule with unequal positive and negative charges is called a **dipolar ion**.

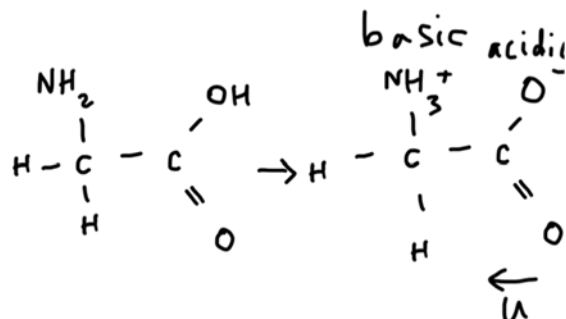


Figure 3.4: Water-induced charge induction of Glycine (conversion of a non-charged molecule into zwitterionic molecule)

3.2.2 Dipole Moment and Dipole Self-Energy

The dipole self-energy is the sum of the positive self-energies of the two partial charges $\pm q$ minus the Coulomb repulsion of the two opposing charges, i.e.,

$$\mu^i = \frac{1}{4\pi\epsilon_0\epsilon} \left(\frac{q^2}{2a} + \frac{q^2}{2a} - \frac{q^2}{2r} \right) = + \frac{q^2}{8\pi\epsilon_0\epsilon a} \text{ or } = + \frac{u^2}{4\pi\epsilon_0\epsilon l^3}. \quad (3.2)$$

where a is the ion radius and $r = l = 2a$, the dipolar charge separation. As for individual ions, the dipole self-energy depends on the electric permittivity ϵ of the medium. While the inverse dependence on ϵ for the self-energy, or more specifically the solubility, is valid for ions, as discussed in Chapter 2, it is a coarse estimate for dipoles (Eq. 3.2). This is because the dipole moment does not always correlate with the charge distribution of the molecule, since it depends on both factors, the magnitude of the two opposing charges q , and, the distance l of the charge separation. Different factors of q and l can yield the same dipole moment yet behave differently when the permittivity is changed. In addition, the dipole moment can vary depending on the solvent. Finally, unlike ions, molecules have additional large energy terms from non-electrostatic solute-solvent interactions that are not accounted for in the equation above.

3.3 Interactions involving Static and Rotating Dipoles

3.3.1 Static Ion-Dipole Interaction

Having discussed the dipoles in molecules, we will next explore dipolar interactions. First, we will focus on the interaction of dipoles with ions, as depicted in Figure 3.5 (a), which illustrates the interaction of sodium ions (Na^+) with water molecules. From a pair interaction perspective, Na^+ interacts attractively with the negative oxygen moiety, and, repulsively with the two positive hydrogen atoms of water. In Figure 3.5(b), we place the ion at location A, replace the water molecule with a dipole residual model discussed earlier, i.e., introduce the partial charges $\pm q$ at B and C with the charge separation $l = \overline{BC}$, and define the distance between the centers of mass of the ion and the dipole as r . The orientational angle of the resulting water dipole, θ , is measured in respect to the

direction of r . The ion-dipole interaction free energy $w(r)$ is determined from the sum of Coulombic interactions, as

$$w(r) = -\frac{Qq}{4\pi\epsilon_0\epsilon} \left[\frac{1}{AB} - \frac{1}{AC} \right] \quad (3.4)$$

\overline{AB} and \overline{AC} stand for the distances between the ion and the partial charges. It can be shown that \overline{AB} and \overline{AC} can be expressed in terms of r , l , and θ , as:

$$\begin{aligned} AB &= \left[\left(r - \frac{1}{2}l \cos \theta \right)^2 + \left(\frac{1}{2}l \sin \theta \right)^2 \right]^{1/2} \approx r - \frac{1}{2}l \cos \theta \\ AC &= \left[\left(r + \frac{1}{2}l \cos \theta \right)^2 + \left(\frac{1}{2}l \sin \theta \right)^2 \right]^{1/2} \approx r + \frac{1}{2}l \cos \theta \end{aligned} \quad (3.5)$$

The expressions simplified (see the right-hand side of Eqs (3.5), if we assume that $r \gg l$, i.e., at relative large ion-dipole distance in regards of the dipole size. Substituting Eqs (3.5) into Eq. (3.4) yields for the interaction free energy

$$\begin{aligned} w(r) = w(r, \theta) &= -\frac{Qq}{4\pi\epsilon_0\epsilon} \left[\frac{1}{r - \frac{1}{2}l \cos \theta} - \frac{1}{r + \frac{1}{2}l \cos \theta} \right] \\ &= -\frac{Qq}{4\pi\epsilon_0\epsilon} \left[\frac{l \cos \theta}{r^2 - \frac{1}{4}l^2 \cos^2 \theta} \right] \\ &= -\frac{Qu \cos \theta}{4\pi\epsilon_0\epsilon r^2} = -\frac{(ze)u \cos \theta}{4\pi\epsilon_0\epsilon r^2} \end{aligned} \quad (3.6)$$

In the equations above, we utilized that $u = ql$ and $r^2 - \frac{1}{4}l^2 \cos^2 \theta \approx r^2$ for $r \gg l$. Furthermore, if we consider that the electric field of the ion acting on the dipole is $E_{ion}(r) = Q/4\pi\epsilon_0\epsilon r^2$, we can relate the interaction free energy to the ion electric field, i.e.,

$$w(r, \theta) = -uE_{ion}(r) \cos \theta \quad (3.7)$$

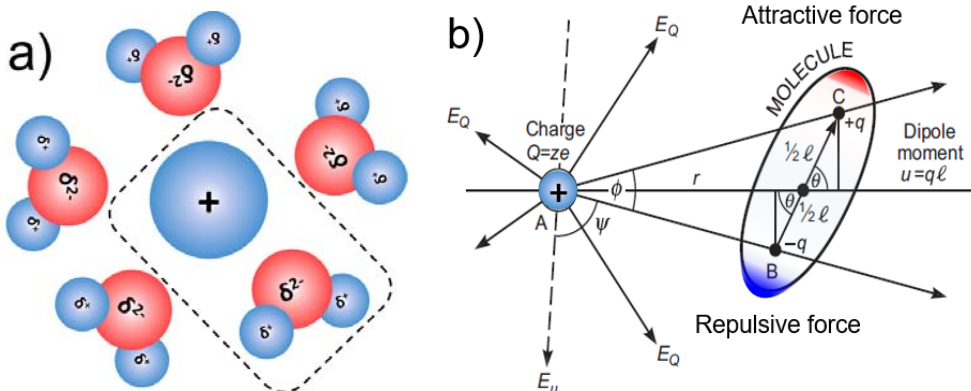


Figure 3.5: Electrostatic interactions between polar molecules and ions (or charged molecules); a) Na^+ ion in water, b) Na^+ ion with a single dipole residual model of the water molecule. The field of the ion (assumed positive) is E_Q , while that of the dipole (acting on the ion) is E_u .

To further discuss the equations derived above, the free energy for interaction between an ion of charge Q and a “point”-dipole u depends on the direction of the dipole, i.e., $\cos \theta$. For example, when a cation is close to a polar molecule, the maximum attraction will occur for $\theta = 0$ or $\cos \theta = 1$, and will be repulsive if the dipole points towards a cation, i.e., $\theta = 180^\circ$, or $\cos \theta = -1$, making the interaction energy positive. The electric field illustrations in Figure 3.6 visualize this situation. The illustration on the right in Figure 3.6 shows the direction of the force on a charge, which is not along r but along the line of the electric field joining their center.

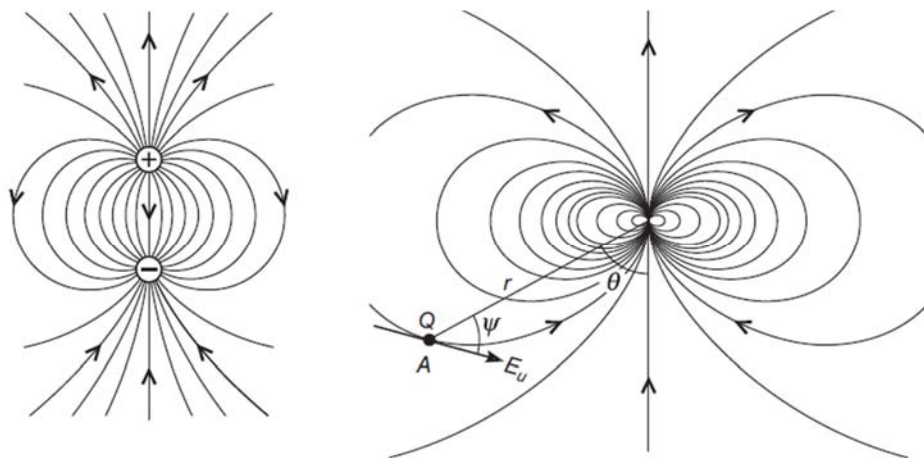


Figure 3.6: Ion-dipole interactions. The direction of an electrostatic dipole, as illustrated in the earlier figure, is from B to C— that is, along the direction of the field emanating from the dipole, as shown here, not the internal field. Source: Intermolecular and Surface Forces, 3rd Ed., J.N. Israelachvili, Elsevier, Boston 2011

In Figure 3.7, dipole-size dependent (from $l = 0$, $l = 0.02$ nm to $l = 0.1$ nm) ion-dipole pair-potentials $w(r)$ were plotted for a monovalent cation ($z = +1$) interacting with a dipolar molecule of $u = 1$ D in vacuum. Solid lines are exact solutions of Eqs (3.5) and (3.6) for finite sized dipoles, and, dashed lines are exact solutions for $l = 0$, which correspond to the approximate point-dipole formula, Eq. (3.7). The comparison shows that the point-dipole approximation is surprisingly accurate from large distances down to an ion-dipole distance of only $r \approx 0.2$ nm $\approx 2l$. Below that threshold the deviation is significant, i.e., quickly more than 10%. The comparison in Figure (3.7) suggests that if the dipole length is small, i.e., below 0.1 nm, the point-dipole approximation (Eq. 3.7) stays valid. The accuracy of the estimate is lost for large dipoles, as found, for instance for zwitterion molecules that require additional Coulombic considerations. The strong interaction ($> kT$) for $r \in \{0.2 - 0.4\}$ nm that can be inferred from the plots in Figure 3.7, manifests strong binding between ions and dipoles, which leads to mutual alignments.

We shall here briefly estimate the interaction in vacuum between a common ion and a water molecule, using our simplified model and attributing to the water molecule a molecular radius of 0.14 nm with a point of dipole moment of 1.85 D. Considering Na^+ ($z = +1$, $a = 0.095$ nm), the maximum electrostatic interaction free energy is

$$w(r, \theta = 0^\circ) = -\frac{(1.602 \times 10^{-10})(1.85 \times 3.336 \times 10^{-30})}{4\pi(8.854 \times 10^{-12})(0.235 \times 10^{-9})^2} = -1.6 \times 10^{-9}\text{J} \quad (3.8)$$

$$= -39 kT \text{ or } -96 \text{ kJ} \cdot \text{mol}^{-1} \text{ at } 300 \text{ K}$$

that manifests a strong attractive interaction at room temperature. This value is comparable to the experimental value of $100 \text{ kJ} \cdot \text{mol}^{-1}$. Considering other ions interacting with water, we find for the smallest monovalent ion, lithium (Li^+) of ionic radius $a = 0.068 \text{ nm}$, an interaction energy of roughly 50 kT , or $125 \text{ kJ} \cdot \text{mol}^{-1}$ (experimentally $142 \text{ kJ} \cdot \text{mol}^{-1}$) and, for the small divalent ions Mg^{2+} ($z = +2$, $a = 0.065 \text{ nm}$) and Be^{2+} ($z = +2$, $a = 0.03 \text{ nm}$) interaction energies of 100 kT and 150 kT , respectively. A practical consequence in nature of the strong ion-dipole interaction involving water is found in the nucleation of raindrops in thunderclouds.

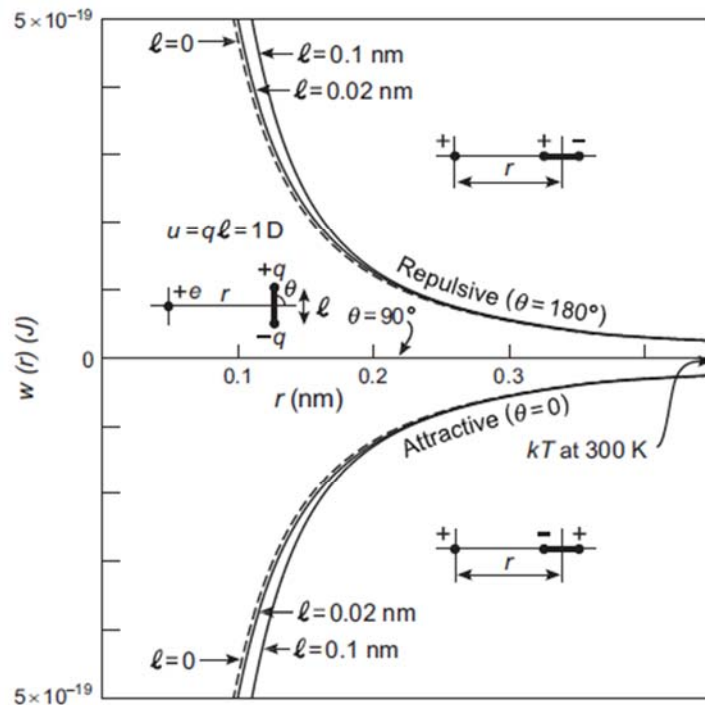


Figure 3.7: Charge-dipole interaction energy in vacuum ($\epsilon = 1$) between a unit elementary charge e and a dipole of moment $u = ql = 1 \text{ D}$ (1 Debye) oriented at different theta angles to the charge. Solid lines are exact solutions, Eqs (3.5) and (3.6), for finite sized dipoles with $l = 0.02 \text{ nm}$ and $l = 0.1 \text{ nm}$; dashed lines are exact solutions for $l = 0$, which correspond to the approximate point-dipole formula, Eq. (3.7). Note that for typical interatomic spacings ($r \approx 0.3 - 0.4 \text{ nm}$) the strength of the pair interaction greatly exceeds the thermal energy kT at 300 K. Source: Intermolecular and Surface Forces, 3rd Ed., J.N. Israelachvili, Elsevier, Boston 2011.

3.3.2 Dipole-Dipole Interaction

Apart from interactions between ions and polar molecules, the polar molecules themselves interact with each other as well. The interaction of two dipoles resemble that of two magnets. In the case of two point-dipoles of moments u_1 and u_2 at a distance of r , and angular relative positions θ_1, θ_2 and ϕ , the interaction energy can be calculated similar to ion-dipole interaction as,

$$w(r, \theta_1, \theta_2, \phi) = -\frac{u_1 u_2}{4\pi\epsilon_0\epsilon r^3} [2 \cos \theta_1 \cos \theta_2 - \sin \theta_1 \sin \theta_2 \cos \phi] \quad (3.9)$$

The maximum attraction will occur when the two dipoles are arranged in line, Figure 3.8, which simplify the interaction free energy to

$$w(r, 0, 0, \phi) = -\frac{2u_1 u_2}{4\pi\epsilon_0\epsilon r^3} \quad (3.10)$$

If the two dipoles align in parallel, the interaction energy $w(r, 90^\circ, 90^\circ, 180^\circ)$ is half of that shown in Eq. 3.10. Assuming that two point dipoles have equal dipole moment of 1 D, their interaction energy in vacuum will match kT at $r = 0.36$ nm, that is when the two point dipoles are in line, and, at $r = 0.29$ nm, when they are parallel or antiparallel. As these two distances are close to molecular separations in solids and liquids, only very polar molecules will have noticeable binding energy from dipolar interactions at room temperature. Figure 3.8 shows the variation of the pair interaction energy at different distances, r , for two dipoles with either as point dipole or dipoles with $l = 0$. The significant deviation is noticeable at $r < 3l$, where Eq. 3.9 becomes inaccurate.

As seen from the calculation above, it appears that an orientation where two dipoles point toward each other is always preferable. However, that was only if r is fixed. For some circumstances, dipolar molecules can longer have a better chance to align in parallel for shorter distance of r , which make it a favorable orientation.

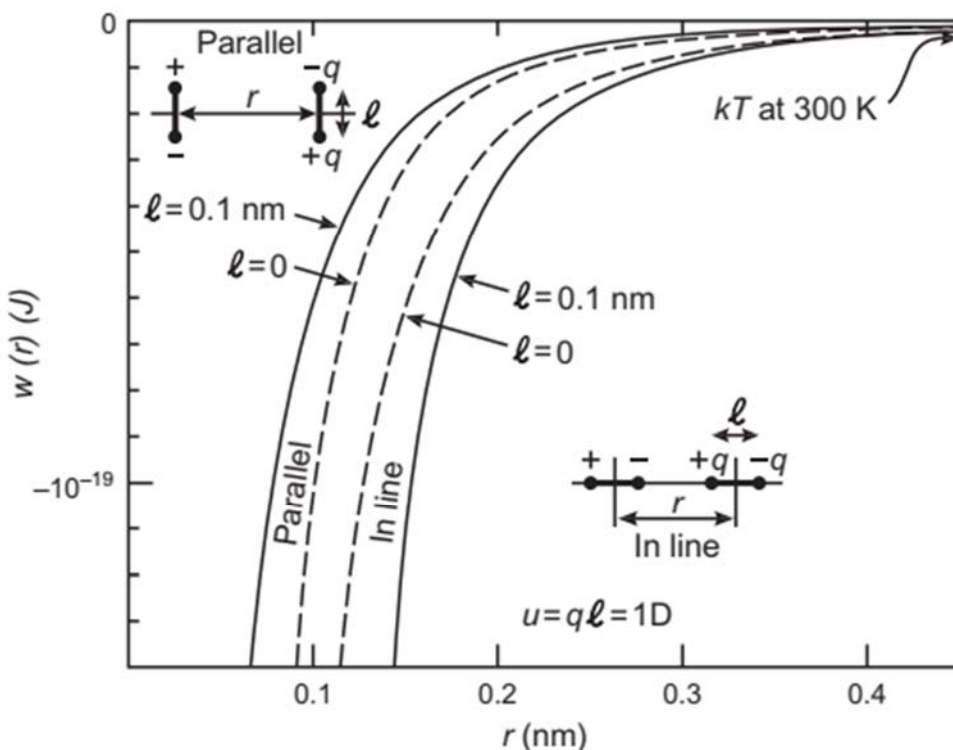


Figure 3.8: Dipole-dipole interaction energy in a vacuum between two dipoles each of moment 1 D. Note how much weaker this interaction is compared to the charge-dipole interaction and the large effect of finite dipole size. Source: Intermolecular and Surface Forces, 3rd Ed., J.N. Israelachvili, Elsevier, Boston 2011

3.3.3 Rotating Dipoles and Angle-Averaged Potentials

So far, the electrostatic interaction models involving dipoles were built on static circumstances, assuming the interacting polar molecules will not move or rotate during

the interaction process. This assumption is true when the thermal fluctuation such as Brownian motion can be neglected. However, the strong electrostatic constraints we discussed at the end of the prior section will begin to weaken dramatically when the two charged objects are moving apart or when the temperature is rising, which will lead to activations of translational, rotational and vibrational modes of the dipoles. As there are zero translational modes that can be activated in a monotonic increasing (or decreasing) potential (e.g., Coulomb potentials), and the activation of vibrational modes are much higher, we will restrict ourselves here to the activation of rotational modes. With the activation of rotational modes, the interaction energy becomes angle dependent. Rather than randomly moving and rotating (which is the case in Brownian motion), the interacting molecules will take certain favorable spatial orientations corresponding to their charge distributions, thus a set of weighting factors should also be introduced to calculate the potential over different angles.

Most appropriate is to consider a spherical (polar) coordination system with the coordinates r , θ and ϕ that substitutes the typical Cartesian system (x, y, z). The resulting (effective) potential $w(r)$ averaged over all possible angular dipolar orientations can be obtained from the Boltzmann averaging *potential distribution theorem*, that is:

$$\exp\left(-\frac{w(r)}{kT}\right) = \frac{\int \exp\left(\frac{-w(r, \Omega)}{kT}\right) d\Omega}{\int d\Omega} \equiv \left\langle \exp\left(-\frac{w(r, \Omega)}{kT}\right) \right\rangle \quad (3.11)$$

which relates the Boltzmann angle-averaged potential $w(r)$ to the static non-rotating potential $w(r, \Omega)$, where Ω is the solid angle and represents all rotational variables ($d\Omega = \sin\theta d\theta d\phi$). The bracket notation on the very right is a short hand writing of the angular Boltzmann average.

In the following discussion we will derive the asymptotic solution of the angle-averaged activation free energy $w(r)$ for *ion-dipole* interactions. First the dominator can be written as

$$\exp\left(-\frac{w(r)}{kT}\right) = \left\langle \exp\left(-\frac{w(r, \Omega)}{kT}\right) \right\rangle = w(r) \equiv \left\langle w(r, \Omega) \right\rangle = \frac{\int \exp\left(\frac{-w(r, \Omega)}{kT}\right) d\Omega}{\int d\Omega} \quad (3.12)$$

$$\int d\Omega = \int_0^{2\pi} d\phi \int_0^\pi \sin\theta d\theta = 4\pi \quad (3.13)$$

So, we can rewrite the potential equation, as

$$e^{-w(r)/kT} = \langle e^{-w(r, \theta, \phi)/kT} \rangle = \frac{1}{4\pi} \int_0^{2\pi} d\phi \int_0^\pi e^{-w(r, \theta, \phi)/kT} \sin\theta d\theta \quad (3.14)$$

We require for the asymptotic solution that the interaction potential is smaller than the thermal noise, i.e., $w(r, \theta) < kT$. This allows us to employ a Taylor expansion of the exponential function, i.e.,

$$\exp\left(-\frac{w(r)}{kT}\right) = 1 - \frac{w(r)}{kT} + \frac{1}{2} \left(\frac{w(r)}{kT} \right)^2 - \dots = \left\langle 1 - \frac{w(r, \Omega)}{kT} + \frac{1}{2} \left(\frac{w(r, \Omega)}{kT} \right)^2 - \dots \right\rangle \quad (3.15)$$

which leads to

$$\frac{\omega(r)}{kT} = \left\langle \frac{\omega(r, \Omega)}{kT} - \frac{1}{2} \left(\frac{\omega(r, \Omega)}{kT} \right)^2 + \dots \right\rangle \quad (3.16)$$

We can neglect approximately the terms after the square terms on the right side of the equation and will get

$$\omega(r) \approx \left\langle \omega(r, \Omega) - \frac{1}{2} \frac{\omega(r, \Omega)^2}{kT} \right\rangle \quad (3.17)$$

This expression is applicable to any potential involving rotating dipoles.

We consider next the ion-dipole interaction, for which we found earlier the following potential:

$$w(r, \theta) = -\frac{Qu \cos \theta}{4\pi\epsilon_0\epsilon r^2} = -\omega_{max} \cos \theta; \quad \omega_{max} \equiv \left| \frac{Qu}{4\pi\epsilon_0\epsilon r^2} \right| \quad (3.18)$$

which we substitute into Eq. (3.17). As every term in brackets involves solving the integral

$$\langle f(\varphi, \theta) \rangle = \frac{1}{4\pi} \int_0^{2\pi} d\varphi \int_0^\pi f(\varphi, \theta) \sin \theta d\theta$$

Eq. (3.18) substituted into Eq. (3.17) yields

$$\omega(r) = \left\langle -\frac{Qu}{4\pi\epsilon_0\epsilon r^2} \cos \theta - \left(\frac{Qu}{4\pi\epsilon_0\epsilon r^2} \right)^2 \frac{\cos^2 \theta}{2kT} \right\rangle \approx -\frac{Q^2 u^2}{6(4\pi\epsilon_0\epsilon)^2 kTr^4} \quad (3.19)$$

after having employed the integral solutions

$$\begin{aligned} \int_0^\pi \cos \theta \sin \theta d\theta &= 0 \\ \int_0^\pi \cos^2 \theta \sin \theta d\theta &= \frac{2}{3}. \end{aligned}$$

In the case of other interaction dipolar interaction, such as dipole-dipole interaction, we have to consider also other angular integrals, as provided below:

$$\begin{aligned} \langle \cos^2 \theta \rangle &= \frac{1}{4\pi} \int_0^{2\pi} d\varphi \int_0^\pi \cos^2 \theta \sin \theta d\theta = \frac{1}{3} \\ \langle \sin^2 \theta \rangle &= \frac{2}{3} \\ \langle \sin^2 \varphi \rangle &= \langle \cos^2 \varphi \rangle = \frac{1}{2} \\ \langle \sin \theta \rangle &= \langle \cos \theta \rangle = \langle \sin \theta \cos \theta \rangle = 0 \end{aligned}$$

We remember that the asymptotic solution of $w(r)$ required that $w(r) < kT$, i.e., for the ion-dipole interaction

$$kT > \frac{Qu}{4\pi\epsilon_0\epsilon r^2} \quad (3.30)$$

With this in mind we can estimate the “critical” ion-dipole distance r_{crit} that separates the regime of static (non-rotating dipoles) from freely rotating For ion-dipole interactions, $r = r_{crit}$ can be determined from the boundary condition, Eq. (3.20) setting $kT = w(r)$, yielding

$$r_{crit} = \sqrt{\frac{Qu}{4\pi\epsilon_0\epsilon kT}} \quad (3.21)$$

It follows that at close distance ($r < r_{crit}$) of a polar molecule from an ion, such as water, the polar molecules can be expected to align, i.e., result in an entropy reduction of the solvent in close vicinity of ions., or in other words, lose mobility to rotate. Information about the degree of dipolar rotational constraints in the vicinity of an ion is visualized in Figure 3.9 that compares the asymptotic solution to an analytical solution of the interaction equation before simplifying it with the Taylor expansion. It shows that the asymptotic solution holds even below r_{crit} , down to 0.4 r/r_{crit} .

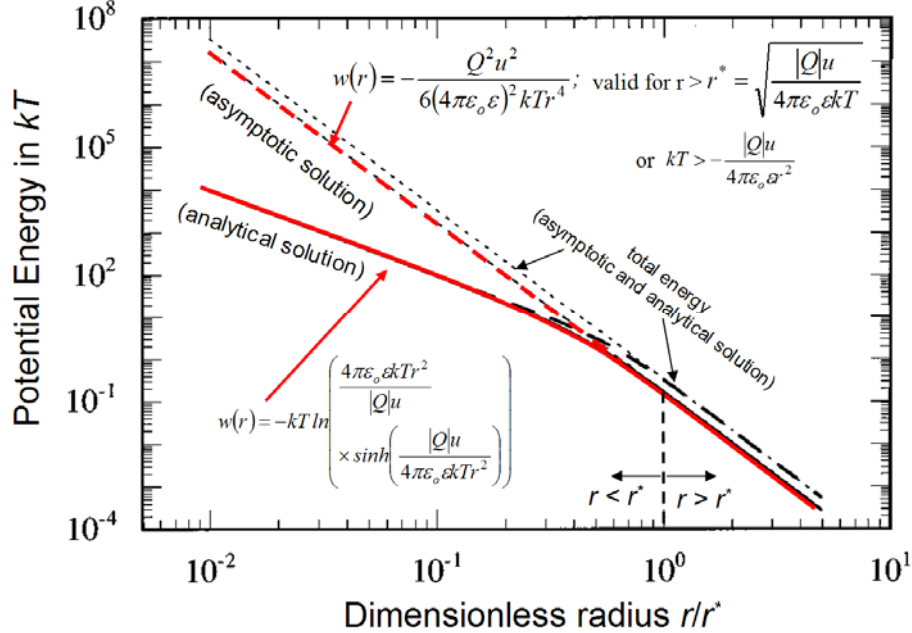


Figure 3.9: Interaction energy $w(r)$ between polar molecules and ions, whereby $r^* = r_{crit}$. The asymptotic solution is good down to 0.4 r/r^* .

For the rotating dipole-dipole interaction (which is also referred to as *Keesom* interaction), a similar angle averaging calculation of the interaction energy can be carried out, which leads to an angle-averaged free energy of

$$\omega(r) = -\frac{u_1^2 u_2^2}{3(4\pi\epsilon_0\epsilon)^2 kTr^6} \quad (3.22)$$

for $kT > \frac{u_1 u_2}{4\pi\epsilon_0\epsilon r^3}$. The Keesom interaction is the first of three polarization interactions, named as collective, *Van der Waals interaction*. As the Keesom interaction deals with the orientation of dipoles, it is known as *orientational polarization*. Its property, the *orientational polarizability* can be determined from the angular dependent polarizability $u\cos\theta$ and its corresponding energy $uE\cos\theta$ in an electric field E , where u is the magnitude of the dipole moment, via angle-averaging, i.e.,

$$u_{orient} = \langle u\cos\theta \exp\left(\frac{uE\cos\theta}{kT}\right) \rangle = \frac{u^2 E}{kT} \langle \cos^2(\theta) \rangle = \frac{u^2}{kT} E \quad (3.23)$$

under the condition that $uE < kT$. This defined the orientational polarizability

$$\alpha_{orient} = \frac{u^2}{kT} \quad (3.24)$$

3.4 Dipole Interactions involving Water

3.4.1 Dipole Interactions in Water, Solvation and Hydration Forces

Solute molecular interactions in polar solvents are affected by polarization effects between solvent and solutes, and solvation force. Solvation forces result from the result of displaced and spatially rearranged solvent molecules by the solutes. When the water is the solvent, molecular rearrangements in solvent unsettle the bulk hydrogen-bonding network, called icosahedral water cluster.

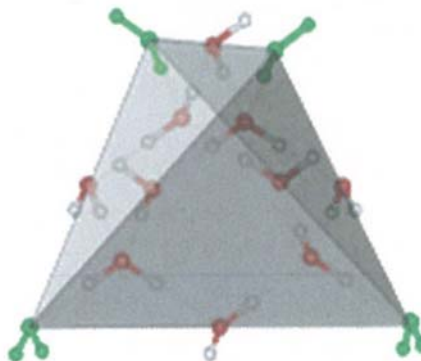


Fig 3.10: Hydrogen-bonding as an icosahedral water cluster

Water molecules rearrange themselves around solutes, an arrangement that is referred to as “hydration shells”. The first shell of water molecules around the solute molecule is called the primary or inner hydration shell. This inner hydration shell is highly structured and has positional and orientational order in their motion. Outer hydration shells are less ordered and water molecules in outer shells do not directly interact with the solute molecules but with other water molecules.

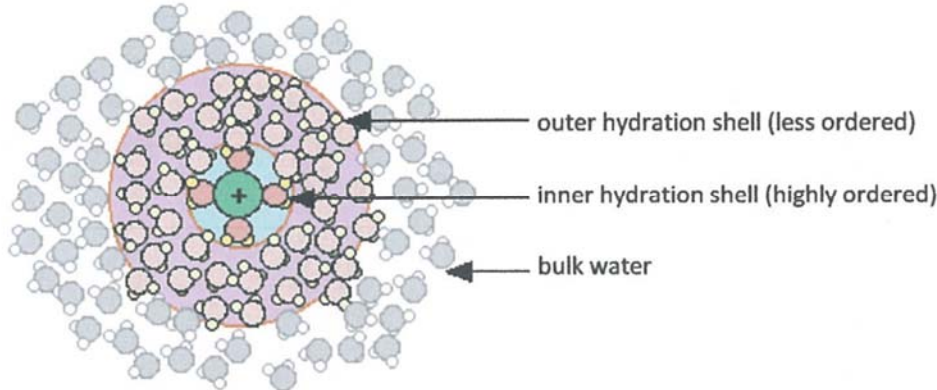


Fig 3.11: Clustering of water, as a solvent, around charged molecules

3.4.2 Hydrogen Bond

Hydrogen bonding is the strongest type of dipolar interactions. It exists between strong electronegative atoms (e.g., O, N, F, and Cl) and H atoms that are covalently bound to another electronegative atom. As the name suggests, hydrogen bonding involves hydrogen atoms. This is because hydrogen's small size and tendency to become positively polarized, which enables effective H-mediated bonding between two electronegative atoms, as illustrated in Fig 3.12.

The strength of hydrogen bonding ranges from 10 to 40 kJ mol⁻¹ or 5 to 10kT per bond at 298K, stronger than most Van der Waal bonds (\sim 1kJ mol⁻¹ or 1kT) but weaker than covalent or ionic bonds (\sim 500kJ mol⁻¹ or 100kT). The interaction potential of hydrogen bonds tend to follow the equation of ion-dipole interaction.

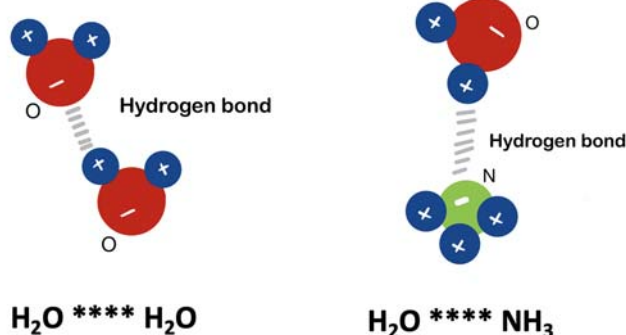


Figure 3.12: Hydrogen bonding involving electronegative atoms. (Left) oxygen, (right) nitrogen.

The empirical hydrogen-bonding equation

$$\omega(r) = \frac{-Q_{\text{H}+} u \cos\theta}{4\pi\epsilon_0\epsilon r^2} \quad (3.25)$$

resembles the ion-dipole interaction, because of the tiny size of the H atom that lets it be perceived as point dipole. While the interaction potential of hydrogen bond follows ion-dipole interaction equation, the magnitude of $Q_{\text{H}+}$ is experimentally found to be smaller than that of the elementary charge ($e+$).

The hydrogen bond is found to be fairly directional. Among different types of bonds, covalent bonds are the most directional with binding energies, followed by the moderately directional hydrogen bonds, and then non-directional Van der Waal interactions, Figure 3.13. The directionality of hydrogen bonds enables them to form weak three-dimensional structures in solids and significantly long range interactions in the liquid state. This gives rise to the term associated liquids. These associated liquids have somewhat ordered crystalline structures even in the liquid state over short distances.

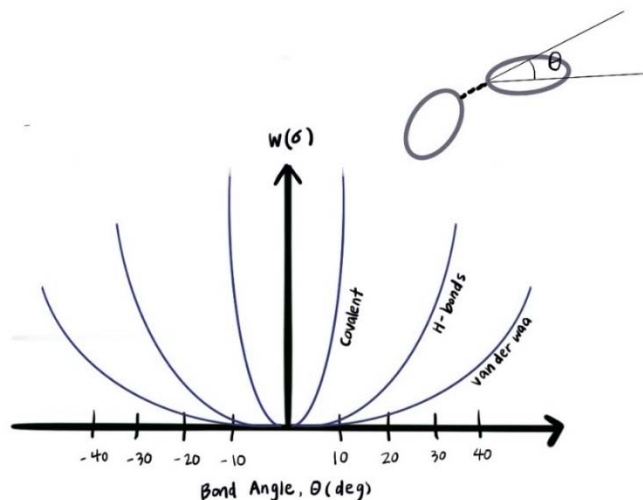


Figure 3.13: Bond-angle of different molecular interactions

Figure 3.14 illustrates how hydrogen bonding plays a significant role in water structuring with one water molecule forming four hydrogen bonds with neighboring water molecules. The oxygen atom forms two hydrogen bonds and each hydrogen atom forms one hydrogen bond. This tetrahedral structure accounts for most of the unusual properties of water, including high surface tension and high boiling point.

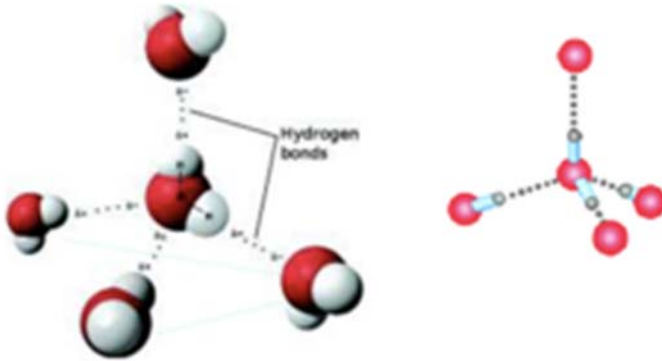


Figure 3.14: Three-dimensional structures of water.

3.5 Summary

In this chapter we extended our view from simple Coulombic interactions between ions and fixed polar molecules to orientational polarized (freely rotating) dipolar interactions that brought forward the first Van der Waals interaction term, the Keesom interaction. Figure 3.15 illustrates our accomplishments so far and what is coming regarding interactions. In the next chapter, we will discuss another form of polarization, namely the electronic polarization that deals with induced dipoles.

Also discussed in this chapter were the strongest dipolar interactions, namely, hydrogen bonding. We found that this particular interaction has a strong impact on how a solvent behaves, i.e., can structure a liquid. In the following chapter, we will extend our understanding involving hydrogen interaction, when we hear about hydrophobic interactions.

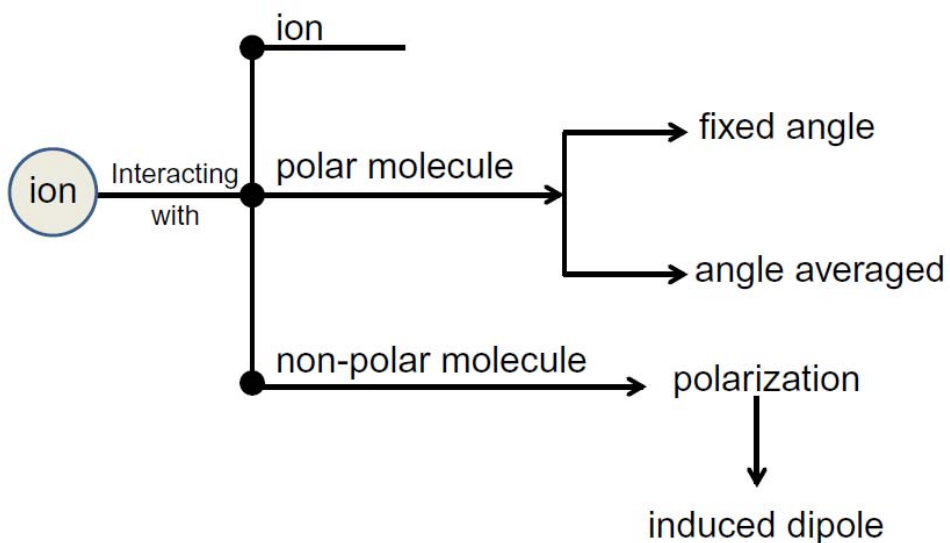


Figure 3.15: Schematics of our progress towards Van der Waals interactions.

3.6 Review

A polar molecule exhibits an asymmetric electron distribution around its core. This non-uniform distribution brings forward a partial charge separation l of charge q , and thus, a magnitude of the dipole moment of

$$u = ql \quad (3.1)$$

measured in Debye ($1 \text{ D} = 3.336 \times 10^{-30} \text{ C}\cdot\text{m}$). In Physics a dipole moment is oriented from negative to positive charge. In Chemistry, the direction of the dipole moment is from lower electronegative atom (partial positive charge) to higher electronegative atom (partial negative charge).

In analogy to the self-energy of an ion (see prior chapter), the dipole self-energy is the sum of the positive self-energies of the two partial charges subtracted by the Coulomb repulsion of the two opposing charges,

$$\mu^i = \frac{1}{4\pi\varepsilon_0\varepsilon} \left(\frac{q^2}{2a} + \frac{q^2}{2a} - \frac{q^2}{2r} \right) = +\frac{q^2}{8\pi\varepsilon_0\varepsilon a} = +\frac{u^2}{4\pi\varepsilon_0\varepsilon l^3} \quad (3.3)$$

where a is the ion radius, $r = l$ the charge separation, ε the electric permittivity of the medium, and ε_0 the permittivity of free space.

As ionic interactions, the electrostatic interaction of dipoles with other charged molecules, ions or dipoles, can be calculated based on Coulomb's law. The interaction between a dipole and a charged particle can be simplified as two combined interactions, attractive and repulsive, between a charged particle and each partial charge. The orientation θ of dipoles towards a point charge (ion) will affect the magnitude of interaction, i.e.,

$$w(r, \theta) = -\frac{(ze)u \cos \theta}{4\pi\varepsilon_0\varepsilon r^2} \quad (3.6)$$

where r represents the average distance between the ion and the dipole. It shall be noted that this equation is based on assumption, $r \gg l$, where l is the charge separation of the dipole. The maximum interaction is found for $\theta = 0$ or 180° , depending on the ion charge.

If a dipoles interacts with another dipole, we have to consider also the out-of-plane relative orientation ϕ , which leads to the following interaction free energy:

$$w(r, \theta_1, \theta_2, \phi) = -\frac{u_1 u_2}{4\pi\varepsilon_0\varepsilon r^3} [2 \cos \theta_1 \cos \theta_2 - \sin \theta_1 \sin \theta_2 \cos \phi] \quad (3.9)$$

If the dipoles are arranged in line end-to-end, a maximum interaction of

$$w_{max}(r, 0, 0, \phi) = -\frac{2u_1 u_2}{4\pi\varepsilon_0\varepsilon r^3} \quad (3.10)$$

is obtained. Note how the Coulomb pair interaction moved from a $1/r$ interaction between ions, to now a $1/r^3$ interaction between dipoles.

Up until now, the electrostatic interaction considered static dipoles. This is true when the thermal fluctuation (kT) is much smaller than the maximum interactions introduced above. However, the static assumption breaks down, when the thermal fluctuation exceeds the maximum interaction, which activates the rotational modes of the dipoles. With changing orientation, the interaction strength becomes statistically dependent on the angular distribution of the dipole(s). Based on Boltzmann averaging the interaction free energy between two dipoles in environment of permittivity ε is given, as

$$\omega(r) = -\frac{u_1^2 u_2^2}{3(4\pi\varepsilon_0\varepsilon)^2 k T r^6} \quad (3.22)$$

for $kT > w_{\max}(r)$, introduced in Eq. 3.10. This equation is known as the *Keesom interaction*, and represents the orientational polarization component of the Van der Waals interaction, and the first observation of the $1/r^6$ dependence.

For an ion-dipole interaction, the “critical” distance r_{crit} that separates the regime of static (non-rotating dipoles) from freely rotating dipoles is expressed by

$$r_{crit} = \sqrt{\frac{Qu}{4\pi\epsilon_0\epsilon kT}} \quad (3.21)$$

At close distances ($r < r_{crit}$) polar molecules are expected to align as a result of entropy reduction in the solvent. This has been addressed in Chapter 2 with water molecules aligning around ion solutes. Solute molecular interactions in polar solvents are affected by polarization effects between solvent and solutes, and solvation force. Solvation forces result from the displacement and spatial rearrangement of solvent molecules caused by the solutes. For water as the solvent, molecular rearrangements in the solvent unsettle the bulk hydrogen-bonding network, known as icosahedral water clusters. Water molecules rearrange themselves around solutes, an arrangement that is referred to as “hydration shells”. While inner hydration shells are highly structured outer shells are less ordered.

Water has the strongest type of dipolar interactions, namely hydrogen bonding, which is formed between a H atom and a highly electronegative atom (e.g. oxygen, nitrogen, fluorine, and chlorine). One of the simplest of water is the tetrahedral structure. It accounts for most of the unusual properties of water, including high surface tension and high boiling point.

The interaction potential of hydrogen bonding tends to follow the equation of the ion-dipole interaction, which is presented here adjusted, as

$$w(r) = \frac{-Q_{H+} u \cos\theta}{4\pi\epsilon_0\epsilon r^2} \quad (3.25)$$

Q_{H+} signifies the charge magnitude of the positive H atom, which is smaller than the elementary charge e. The permittivity ϵ is the one of bulk water. In contrast to Van der Waals interactions that show little directionality, the hydrogen bond is directional. The directionality of hydrogen bonds enables them to form weak, relatively structured, three-dimensional structures in solids and significantly long-range interactions in the liquid state, termed associated liquids.

Review Questions

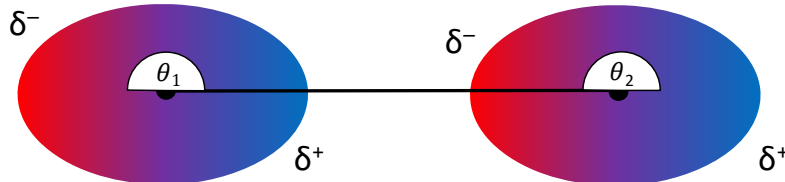
1. What is the direction of the dipole moment?
2. What is the definition of the magnitude of the dipole moment?
3. What is the unit of the dipole moment?
4. What assumptions are necessary to use $\frac{-(ze)\cos\theta}{4\pi\epsilon_0\epsilon r^2}$ to approximate the interaction of a dipole with a point charge?
5. Consider dipole-dipole interaction: When can you consider both angles θ_1 and θ_2 to be zero?
6. Under what conditions is it safe to assume that interacting polar molecules are not rotating?
7. Which equation is used to describe the orientational polarization component of the Van der Waals interaction?

8. Describe the different hydration shells of water molecules.
9. Why does the interaction potential of the hydrogen bond tend to follow the equation of ion-dipole interaction?
10. What characteristics of hydrogen bonding accounts for the tetrahedral shape of interacting water molecules?

Answer Key

1. In Physics a dipole moment is oriented from negative to positive charge. In Chemistry, the direction of the dipole moment is from lower electronegative atom (partial positive charge) to higher electronegative atom (partial negative charge).
2. $u = ql$ and in some occasions where the point-dipole is assumed ($l = 0$), this equation can be neglected as the dipole moment was already given
3. Debye (D), where $1 D = 3.336 \times 10^{-30} C \cdot m$
4. $r \gg l$. If the molecule is composed of extended conjugate system, this approximation will be less accurate since the length of dipole will be significantly larger.
5. When the dipoles are arranged in line end-to-end as shown in the figure below

$$\cos \theta_1 = \cos \theta_2 = 1$$



6. Interacting polar molecules are assumed to have no rotation or orientation when thermal fluctuation is trivial and can be neglected. As the temperature is usually fixed at room temperature, generally it is safe to assume the polar molecules are not rotating within the critical distance

$$r_{crit} = \sqrt{\frac{Qu}{4\pi\epsilon_0\epsilon kT}} \quad (3.21)$$

7. The Keesom interaction describes the orientation polarization component of the Van der Waals equation:

$$w(r) = -\frac{u_1^2 u_2^2}{3(4\pi\epsilon_0\epsilon)^2 k T r^6} \quad (3.22)$$

8. The first shell of water molecules around the solute molecule is called the primary or inner hydration shell. This inner hydration shell is highly structured and has positional and orientational order in their motion. Outer hydration shells are less ordered and water molecules in outer shells do not directly interact with the solute molecules but with other water molecules.
9. The empirical hydrogen-bonding equation resembles the ion-dipole interaction, because of the tiny size of the H atom that lets it be perceived as point dipole.
10. Directionality of the hydrogen bonding force the water molecule to arrange in tetrahedral structure where the interactions are optimal.

Literature – Sources and Further Reading

- (1) Intermolecular & Surface Forces, 3rd Ed., J.N. Israelachvili, Academic Press, Boston (2011), Ch. 4, 7.2-7.3, 8.1-8.5

Chapter 4: Polarization and Dispersion Interaction

In the prior chapter, we introduced one of the three $1/r^6$ Van der Waals interaction terms that was attributed to the *orientational polarization* of molecules, the *Keesom interaction*. Thereby, we restricted ourselves to polar molecules. If we consider now also systems composed of nonpolar molecules, i.e., molecules with zero dipole moment, we observe molecular interactions that originate from *electronic polarizations*, the so-called *Debye interaction*, and from *dispersion interactions* that originate from quantum fluctuations. We will in the following provide a discussion on polarizability and its unification, solvent effects and solvent polarization, and discuss dispersion interaction in its simplest form, namely, with the *London dispersion*.

4.1 Polarizability of Atoms and Molecules

So far, we examined polarization in terms of orientational polarization, where polar molecules interacted with each other within thermally perturbed electric fields. Here we will expand our view and also consider electronic polarization, i.e., the deformation (or shift) of electron distributions of a molecule caused by external electric fields. In many cases, the source of the external electric field is another molecule or an ion. As it turns out, all atoms and molecules can be polarized. In fact, whenever the dielectric constant of a solvent or medium has been previously invoked, we were merely modeling the effects of bulk polarization caused by solutes. Nearly all molecular interactions henceforth can be distilled to some form of an induced polarization.

4.1.1 A Simple Model for Induced Dipoles

The parametrization of an induced dipole moment u_{ind} is given by the electrical field E and the electronic polarizability α_o of the molecule in question, as

$$u_{ind} = \alpha_o E \quad (4.1)$$

The polarizability expresses the resistance of the molecule to be polarized. The induced dipole is due to the dynamic nature of the electron cloud of the atoms at play - when acted upon by an external electrical field, the electron density of a given molecule shifts with respect to the core nuclei of the molecule. The electronic polarizability, similar to the orientational polarizability u_{orient} , acts like a resistance to change, i.e., the higher the more difficult it is to polarize the molecule. The situation is illustrated in Figure 4.1 for a non-polar molecule that is experiencing the electric field of a cation.

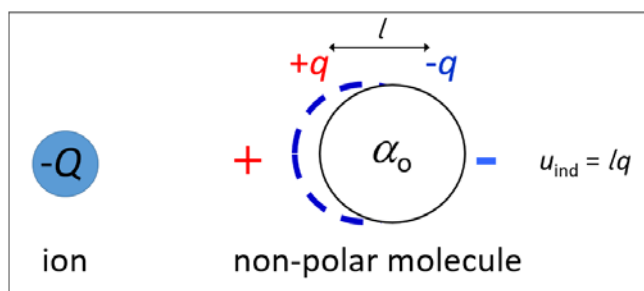


Figure 4.1: A positive ion (cation) shifts the charges in a nonpolar molecule defined by its electronic polarizability α_o and induces a dipole moment u_{ind} . The orientation of the induced dipole in vacuum is always so directed that the interaction is attractive. The situation can be different if a medium is involved. See later discussion below.

Table 4.1 below provides a list of selected molecules, as well as polarizability values of selected bonds and molecular groups. The units of polarizability is in

$(4\pi\epsilon_0)\text{\AA}^3 = 1.11 \times 10^{-10} \text{ C}^2\text{m}^2\text{J}^{-1}$, a “volumetric” size term that will be transparent in the next subsection.

Table 4.1: Electronic Polarizabilities α_0 of atoms, molecules, bonds and molecular groups

Atom/ Molecule	α_0 [(4 $\pi\epsilon_0$) \AA^3]	Chemical Bond	α_0 [(4 $\pi\epsilon_0$) \AA^3]	Molecular Group	α_0 [(4 $\pi\epsilon_0$) \AA^3]		
He	0.20	Aliphatic C-C	0.48	Ether C-O-C	1.13		
H ₂	0.81	C-O	0.60	Alcohol C-O-H	1.28		
H ₂ O	1.48	Aliphatic C-H	0.65	CH ₂	1.84		
Ar	1.63	Aliphatic O-H	0.73	Disilyl-ether Si- O-Si	1.39		
CO	1.95	N-H	0.74	Silanol S-O-H	1.60		
NH ₃	2.3	Partially Aromatic C=C	1.07	Amine C-NH ₂	2.03		
CH ₄	2.6	C=O	1.36				
HCl	2.6	Fully Aromatic C=C	1.65				
CO ₂	2.6	C-Cl	2.60				
CH ₃ OH	3.2	C-Br	3.75				
Xe	4.0						
CH ₂ =CH ₂	4.3						
C ₂ H ₆	4.5						
Cl ₂	4.6						
CHCl ₃	8.2						
C ₆ H ₆	10.3						
CCl ₄	10.5						

Consider now a non-polar ($u = 0$) molecule with polarizability α_0 at a distance r from and ion of charge Q . Recall that the ion's electrical field is

$$E_{ion} = \frac{Q}{4\pi\epsilon_0\epsilon r^2} \quad (4.2)$$

The ion field will cause, according to Eq. (4.1), a dipole moment of

$$u_{ind} = \frac{\alpha_o Q}{4\pi\epsilon_0\epsilon r^2} \quad (4.3)$$

Earlier we learned that the electric field from a dipole is given by

$$E_{dipole} = \frac{u(1 + 3\cos^2\theta)^{1/2}}{4\pi\epsilon_0\epsilon r^3} = \frac{2u}{4\pi\epsilon_0\epsilon r^3} |_{\theta=0}. \quad (4.4)$$

As the dipole electric field resulted from the polarization of a nonpolar molecule, we set for $u = -u_{ind} = -\alpha_o E_{ion}$, which yields for the resulting dipole field

$$E_{dipole,ind} = \frac{-2\alpha_o Q}{(4\pi\epsilon_0\epsilon)^2 r^5} \quad (4.5)$$

As the force between a charge and a dipole is given as $F = QE_{dipole}$ and the potential as the negative integral over the force, it follows for the interaction free energy,

$$w(r) = \frac{-Q^2 \alpha_o}{2(4\pi\epsilon_0\epsilon)^2 r^4} = -\frac{1}{2} \alpha_o E_{ion}^2 \quad (4.6)$$

Note the interaction free energy is half of what would be expected, if we replaced the non-polar molecule with a polar molecule with permanent dipole.

Eq. (4.6) can be extended to a polar molecule by replacing the electronic polarizability by the total polarizability, α , which also includes the orientational polarizability derived in chapter 3, and further discussed below, i.e.,

$$\alpha = \alpha_o + \alpha_{orient} = \alpha_o + \frac{u^2}{3kT} \quad (4.7)$$

which yields

$$w(r) = \frac{-Q^2 \alpha_o}{2(4\pi\epsilon_0\epsilon)^2 r^4} - \frac{-Q^2 u^2}{6(4\pi\epsilon_0\epsilon)^2 k T r^4} \quad (4.8)$$

This extended interaction potential between an ion and a polar molecule is composed of the electronic polarization interaction, and, the orientational polarization interaction, respectively.

4.1.1 The Polarizability of Nonpolar Molecules

To better familiarize us with the property of electronic polarizability and to relate it to molecular parameters that could be useful from a molecular design perspective, we discuss here an atom-like molecule, as depicted in Figure 4.2. A nucleus of elementary charge $+e$ shall be orbited as shown by an electron, Fig. 4.2(a). The electron circular trajectory shall be normal to an external electric field that we impose next, Fig. 4.2(b). Due to the electric field, forces will be acting on the electron as well as the positive core in the opposite direction. Due to the enormous mass difference, we will only consider an electron displacement opposite to the electric field over a distance l . The distance between the core and the electron shall be R that relates trigonometrically via the angle θ to l . The electron displacement l induces a dipole $u_{ind} = \alpha_o E$ in our simple molecular system.

We can identify two forces that are acting on the electron: A resultant external force F_{ext} felt by the electron due to the electric field E that is balanced by an internal restoring Coulombic force F_{int} , i.e.,

$$F_{ext.} = -eE = F_{int.} = \frac{-e^2}{4\pi\epsilon_0 R^2} \sin\theta \quad (4.9)$$

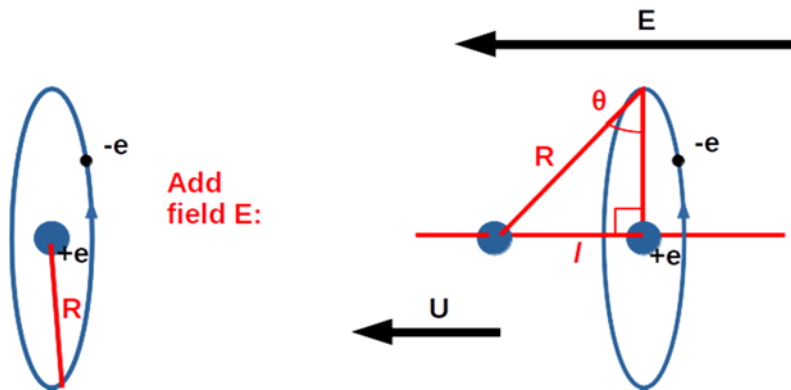


Figure 4.2: Simple molecular single electron model. (a) before and (b) after an electric E field is applied.

Substituting in Eq. (4.9) for $\sin\theta = l/R$ and $u_{ind} = e/l$ yields,

$$u_{ind} = 4\pi\epsilon_0 R^3 E = \alpha_o E \quad (4.10)$$

and thus, for the electronic polarizability

$$\frac{\alpha_o}{4\pi\epsilon_0} = R^3 \quad (4.11)$$

where R represents the molecular *polarizability radius*. If we consider the actual molecular radius, the polarizability radius is on the order 10 - 20% smaller than the molecular radius.

As an example, we can consider the water molecule, for which as per Table 4.1 above the polarizability in units of $4\pi\epsilon_0$ is $R^3 = 1.48 \times 10^{-30} \text{ m}^3 = (0.114 \text{ nm})^3$, which yields a polarization radius of $R = 0.114 \text{ nm}$ that is about 15 % off the radius of water (0.135 nm). Regardless of the small discrepancy, Eq. (4.11) provides an excellent molecular parameter for designing molecules of desired polarizability. This phenomenon can be observed in the literature, for example for adducts to large fullerene derivatives tabulated in Table 4.2.

Table 4.2: Calculated electronic polarizabilities α_{DFT} of hydrocarbons of increasing size.

Parent molecule	$N_{C=C}$	$\alpha_{DFT}, \text{Å}^3$			The polarizabilities were calculated using molecular simulation by the modern density functional theory (DFT) method. Source: Polarizability of C_{60} fullerene dimer and oligomers: the unexpected enhancement and its use for rational design of fullerene-based nanostructures with adjustable properties. D.S. Sabirov, RSC Adv., (2013), 3, 19430-19439.
		C_xH_y	$(C_xH_y)_2$	$C_{60}C_xH_y$	
$C_{21}H_{12}$	9	36.0	68.8	122.1	
$C_{30}H_{12}$	15	56.6	113.3	145.7	
$C_{36}H_{12}$	18	62.5	128.5	153.8	
$C_{42}H_{18}$	21	90.0	182.5	182.0	
$C_{50}H_{10}$	25	79.0	170.0	175.1	
C_{60}	30	82.7	180.0	180.0	

4.1.2 Total Polarizability

As mentioned already above, the electronic polarizability is joined by the orientational polarizability, if the molecule is polar. In Chapter 3, we derived via the Boltzmann distribution an expression for the angle averaged dipole moment, i.e.,

$$u_{orient} = \langle u \cos \theta \exp\left(\frac{uE \cos \theta}{kT}\right) \rangle = \frac{u^2 E}{kT} \langle \cos^2(\theta) \rangle = \frac{u^2}{kT} E \quad (4.12)$$

which, as per definition of the polarizability ($\alpha_{ind} = \alpha_o E$) yields for the orientational polarizability

$$\alpha_{orient} = \frac{u^2}{3kT} \quad (4.13)$$

We can now define the total polarizability of any given molecule by combining the electronic polarizability with the orientational polarizability, resulting in

$$\alpha = \alpha_o + \alpha_{orient} = \alpha_o + \frac{u^2}{3kT} \quad (4.14)$$

This equation is known as the *Debye-Langevin equation*. We can ask ourselves, what happens when $uE \gg kT$, i.e., when the external field is so strong that it completely biases the alignment of the dipolar molecule.

As it turns out, in this situation, there is no observed orientational polarization effect because all of the dipolar molecules will be in full alignment with the field.

4.2 Ion-Solvent Molecular Interactions

Up until now, we have expressed the medium solely by its bulk permittivity ϵ and ignored electric field effects on the medium caused by solutes. While we can overlook these interactions on a larger scale, they become important when considering interactions on short-length scales. This brings forward methods to analyze molecular systems, namely, a continuum description or molecular approaches. In a continuum analysis, at least one bulk property is assumed to hold throughout all length scales. Molecular approaches usually involve molecular dynamics or many-body integral calculations to model interactions at the molecular level and working up to macroscale properties.

To illustrate the two approaches, we will reinspect the Born energy from both a global as well as a microscopic perspective. But before that, we will briefly discuss the resulting electric field in medium towards a field imposed by an ion.

4.2.1 Polarization of a Medium

We shall consider an external electric field E that polarizes a liquid or solid medium. The medium, consisting of polarizable molecules, will counteract E with an opposing polarization field E_p , which will result in an effective field $E_{eff} = E - E_p$, whereby E_p depends on the nature of the medium molecules.

Let us assume the “external” field emanates from a solute with charge Q . We shall now relate the phenomenon of media polarizability to the dielectric constant ϵ of a given medium. To show this, we must first describe the net force F on the charge Q within the medium. The net force can be described two-fold, (i) the product of the charge and the effective field E_{eff} , and, (ii) the Coulomb force, i.e.,

$$F = \begin{cases} (E - E_p)Q = E_{eff}Q \\ \frac{Q^2}{4\pi\epsilon_0\epsilon r^2} \end{cases} \quad (4.15)$$

As we can relate the effective field to the ion electric field via the medium permittivity as $E_{eff} = E/\epsilon$, the opposing polarization field in the medium is

$$E_p = \left(\frac{\epsilon - 1}{\epsilon}\right)E \quad (4.16)$$

Eq. (4.16) confirms our intuition that in a vacuum or a sparse medium like a gas, where $\epsilon \approx 1$, there would not be any polarization field developed in the medium due to a lack of molecules to polarize, and thus, $E_p = 0$. Conversely, when ϵ is much greater than 1, E_p approaches in magnitude the ion electric field E . The takeaway here is that electrostatic effects are cloaked by a highly polarizable media, i.e. a media with a large permittivity ϵ . A material with high permittivity polarizes more in response to an applied electric field than a material with low permittivity, thereby storing more energy in the electric field. As we will see, the constant ϵ is helpful for our understanding of the medium of interest, because it connects the bulk material properties of the medium with the characteristics of its molecular components.

4.2.2 Using a Continuum Approach to Calculate Born Energy

In Chapter 2, the *self-energy* (μ^i) of an ion

$$\mu^i = \int_0^Q \frac{qdq}{4\pi\epsilon_0\epsilon a} = \frac{Q^2}{2(4\pi\epsilon_0)\epsilon a} \quad (4.17)$$

was described as the amount of energy that is required to bring a charge into a vacuum. This energy represents the electrostatic free energy of an ion in a medium with a constant permittivity (ϵ). The assumptions for this equation are: (i) the ions are unaffected by an electric field, (ii) it only represents the conditions in a vacuum, and (iii) it takes into consideration a single ion. If we consider ions in a medium with dielectric properties, the self-energy is renamed *Born energy* or *solvation energy*. The Born energy contains information about to what degree ions can dissolve and partition in different solvents. Considering now that ions affect the solvent, we extend the self-energy expression above towards the Born energy by taking into consideration the interactions of the ions with their surrounding solvent molecules. Given the interaction free energy between ion and dipole, Eq. (4.6), an ion radius a and the solvent number density ρ , the Born energy is

$$\mu^i = \int_a^\infty w(r)\rho 4\pi r^2 dr = \int_a^\infty \frac{\rho\alpha Q^2 4\pi r^2 dr}{2(4\pi\epsilon_0\epsilon)r^4} = \frac{-\rho\alpha Q^2}{8\pi\epsilon_0^2\epsilon^2 a} \quad (4.18)$$

whereby α is the total polarizability of the solvent molecule. In doing so, this equation takes into consideration the fact that there are numerous solvent molecules surrounding the ion and that the polarizability of polar molecules affects the overall net ion-induced dipole interaction. This is a continuum approach to calculating the Born energy, as the bulk permittivity of the solvent (ϵ) is used.

4.2.3 Using a Molecular Approach to Calculate Born Energy

In the case of an ion within a solvent, one can represent this system using a molecular approach as well. In order to do this, a connection must be made between the dielectric

constant (ϵ) and polarizability (α) of a solvent, such that the difference in permittivity between dissimilar solvents is taken into consideration. We consider now that the polarization density is

$$P = \epsilon_0 \chi E \quad (4.19a)$$

where χ is the electric susceptibility. The polarization density of the medium can also be expressed with the number density ρ and the molecular dipole moment μ as

$$P = \rho \mu \quad (4.19b)$$

If we further consider that the *electric susceptibility* can be expressed as $\chi = \epsilon - 1$, we have the following relationship between the molecular polarizability and permittivity of the solvent

$$\chi = \frac{\rho \alpha}{\epsilon_0} = \epsilon - 1 \quad (4.19c)$$

The electric susceptibility is the polarizability per unit volume of a medium. When considering an ion that is moving between two mediums with different permittivities ϵ_1 and ϵ_2 the Born equation, Eq.(4.18) needs to be integrated from χ_1 and χ_2 , i.e.,

$$\mu^i = \int_{\chi_1}^{\chi_2} \frac{-Q^2}{8\pi\epsilon_0^2 \epsilon^2 a} d\chi = \int_{\epsilon_1}^{\epsilon_2} \frac{-Q^2}{8\pi\epsilon_0^2 \epsilon^2 a} d\epsilon = -\frac{Q^2}{8\pi\epsilon_0 a} \left[\frac{1}{\epsilon_1} - \frac{1}{\epsilon_2} \right] \quad (4.20)$$

to yield an expression for the Born energy difference between two solvents.

It is important to note that the Born equation is valid as long as the polarization of molecules does not depend on the distance from the ion. In other words, as long as the polarizing field (E) and solvent dipole moment are not so large Fortunately, this condition is satisfied for ions in a polar solvent such as water.

4.3 Solvent Effects and Excess Polarizabilities

Earlier, we discussed the challenge of moving away from assuming that a solvent (or any medium) is a homogeneous continuum defined in terms of its bulk properties, such as the bulk solvent permittivity. There are several solvent effects that have to be considered when a pair of interacting molecules are introduced into a solvent:

- Solvents affect the magnitude of the interaction strength between solute molecules by affecting their intrinsic properties, i.e., their dipole moments and polarizabilities
- Solvents can change the polarity of interaction, i.e., make the interaction attractive, repulsive or even turn it off. And,
- Solvent molecules can change their entropy in the vicinity of solute molecules, and thus, introduce additional structural forces that have to be considered.

A dissolved molecule impinges on the space of the solvent and displaces it. From the perspective of the polarizability, the molecule overlays its polarizability over the one of the solvent, which is captured by the excess polarizability of a molecule over that of the solvent. This excess polarizability disappears if the molecule has the same polarizability as the solvent.

4.3.1 Excess Polarizability and Solvent Effect on Interaction Polarity

To account for the excess polarizability, a continuum approach is undertaken that treats the molecule as a dielectric medium of a given size and shape, and of permittivity

ε_i . For simplicity, we assume a spherical shape of the molecule of radius a_i . We shall consider that a molecule in a medium of permittivity ε is polarized by an external electric field E , as depicted in Fig. 4.3.

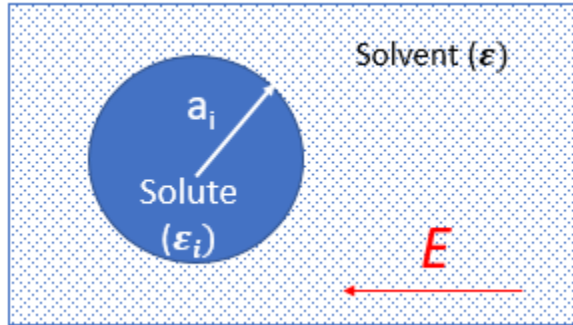


Figure 4.3: Spherical solute molecule in solvent exposed to external electric field.

The electric field will induce a dipole moment $u_{\text{ind}} = \alpha E$ in the solute, according to Eq. (4.1), whereby the polarizability α is not just only the electronic polarizability of the solute molecule in the vacuum or gas phase. We have also to consider the polarizability of the displaced solvent, which leads to the *excess polarizability* α_i found in classical Electrodynamics textbooks (e.g., Jackson or Landau-Lifshitz):

$$\alpha_i = 4\pi\varepsilon_0\varepsilon \left(\frac{\varepsilon_i - \varepsilon}{\varepsilon_i + 2\varepsilon} \right) a_i^3 \quad (4.21a)$$

Notice this expression resembles the polarizability Eq. (4.11), if we set

$$R^3 = \left(\frac{\varepsilon_i - \varepsilon}{\varepsilon_i + 2\varepsilon} \right) a_i^3 \quad (4.21b)$$

In other words, the solvent effect on the solute polarizability is reflective in a change of the polarization radius. If the solvent permittivity matches the solute permittivity, the polarization radius, and with it polarizability of the solute, vanishes. If the permittivity of the solute exceeds significantly the one of the solvent, i.e., $\varepsilon_i \gg \varepsilon$, the solvent effect on the solute polarizability is small. If the solvent permittivity of the solvent exceeds in magnitude the solute permittivity, i.e., $\varepsilon > \varepsilon_i$, the sign of the polarizability changes, which we will see yields to solvent induced repulsive polarization interaction.

The aspect of interaction polarity change (attractive vs. repulsive) is illustrated in Figure 4.4 between an ion (cation ($+Q$) and anion ($-Q$)) and a nonpolar molecule (ε). First the interaction is inspected in vacuum (Fig. 4.4 top). Both the cation as well as the anion induce dipoles in the non-polar molecule. As the induced dipoles are pointing according to the ion charge in the opposite direction, the induced interaction between the ion and the molecule stays attractive, regardless of the ion polarity. Second, we inspect the interaction in a medium with permittivity (ε). If the permittivity of the solute exceeds the permittivity of the solvent, i.e., $\varepsilon_i > \varepsilon$, the situation is the same as in vacuum. If however, as depicted in Figure 4.4 (bottom), the situation is reversed and the solvent permittivity is the larger one, i.e., $\varepsilon_i < \varepsilon$, the interaction polarity changes from repulsive to attractive, depending if the ion is positively or negatively charged, respectively. As discussed above, the reason for the polarity change in the interaction is the sign change of the excess polarizability given by the Eq. 4.21a.

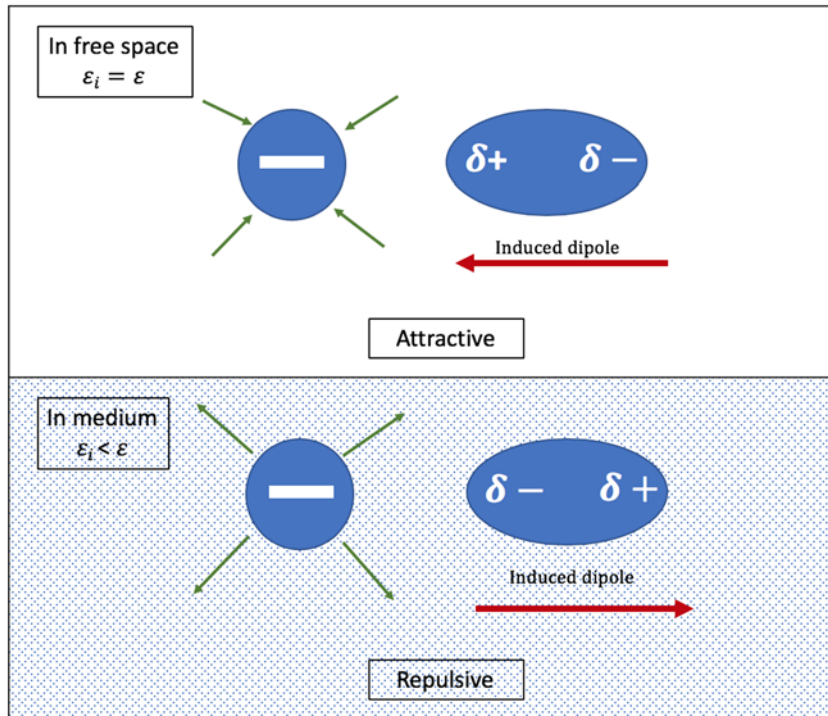


Figure 4.4: (Top) Illustration of the interaction between an ion and a non-polar molecule in vacuum. The ion (here an anion) induces a dipole in the non-polar molecule. The induced ion-dipole interaction between the ion and the molecule is attractive, regardless of the ion polarity (i.e., it could have been a cation, the induction polarity would have switch, but the interaction would still stay attractive. (Bottom) If the solvent permittivity is larger than the solute permittivity, the induced dipole is directed along the ion field, causing two negative charges to face each other (or two positive charges in the case of a cation) Consequently, the ion-dipole interaction switches from attractive to repulsive.

4.4 Dipole-Induced Dipole Interactions: Debye Interaction and Polarization interactions and Polarization Interactions

Previous chapters have introduced charge-induced dipole attraction between ions and polar and nonpolar molecules. Dipole-induced dipole interactions follow the same interaction characteristics as ion-induced dipole attraction. A dipole-induced dipole attraction is a weak attraction that results when a polar molecule with a permanent dipole interacts with polar or non-polar molecule by polarizing it. The induced dipole-dipole interaction is called *Debye interaction* if we restrict ourselves to non-polar molecules. . The Debye interaction energy, can be derived as,

$$w(r) = -\frac{\alpha_{o2}u_1^2 + \alpha_{o1}u_2^2}{(4\pi\epsilon_0\epsilon)^2r^6} \quad (4.22)$$

where α_{oi} ($i = 1,2$) are the corresponding electronic polarizabilities. Recall from earlier that the polarizability (α) of a molecule can consists of two parts, namely, the electronic and orientation polarizability. If we consider two polar molecules interacting with each other, we substitute in Eq. (4.22) for α_{oi} the total polarizabilities α_i ($i = 1,2$), which yields the *polarization interaction free energy* equation,

$$w_{pol}(r) = -\frac{\alpha_2 u_1^2 + \alpha_1 u_2^2}{(4\pi\epsilon_0\epsilon)^2 r^6}. \quad (4.23)$$

It is interesting to note that if we substitute α_0 with

$$\alpha_i = \alpha_{oi} + \frac{u_i^2}{3kT}; i = 1, 2 \quad (4.24)$$

the Debye-Langevin expression, the polarization interaction free energy falls into two components,

$$w_{pol}(r) = w_K(r) + w_D(r) = -\frac{u_1^2 u_2^2}{3(4\pi\epsilon_0\epsilon)^2 kTr^6} - \frac{\alpha_{o2} u_1^2 + \alpha_{o1} u_2^2}{(4\pi\epsilon_0\epsilon)^2 r^6} \quad (4.25)$$

namely, the Keesom $w_K(r)$ and Debye interaction $w_D(r)$, respectively.

The permanent polarizability values (α_1, α_2) and dipole moments (u_1, u_2) of the two interacting molecules are taken into consideration by the polarization equation Eq. (4.23). The Debye interaction, Eq. (4.23) is the second of the three energy contributions to the Van der Waals interaction between molecules.

As with any angle-averaged potential, also the polarization interaction does not fully align any dipoles but only affect the dipole orientation statistically, thus, the effective interaction is the average energy of both dipoles.

As atoms do not carry dipoles, Debye forces cannot occur between them. While the Keesom interactions are temperature dependent, the Debye interactions are not. For Debye interactions to exist between a pair of molecules at least one molecule has to be polar. The following special forms of the Debye interactions and polarization interactions exist:

(i) Debye interaction between similar non-polar molecules

$$w(r) = \frac{2\alpha_o u^2}{(4\pi\epsilon_0\epsilon)^2 r^6} \quad (4.26)$$

(ii) Polarization interaction between polar molecule (μ_i) and non-polar molecule (α_{o2})

$$w(r) = -\frac{\alpha_{o2} u_1^2}{(4\pi\epsilon_0\epsilon)^2 r^6} \quad (4.27)$$

4.4.1 Relationships between the Polarization of Isolated Molecules and Gas Molecular Properties and Condensed Phase Properties

With Eq. (4.22) we have introduced solute polarizability (excess polarizability) α_i for a spherical molecular geometry of radius a_i in a solvent of permittivity ϵ . With the spherical molecular volume $v_i = (4/3\pi)a_i^3$, we can rewrite the solute polarizability, Eq. (4.22) to

$$\alpha_i = 3\epsilon_0\epsilon \left(\frac{\epsilon_i - \epsilon}{\epsilon_i + 2\epsilon} \right) v_i^3 \quad (4.28)$$

which yields for isolated molecules (molecules in vacuum with $\epsilon = 1$) a total polarizability of

$$\frac{\alpha_i}{4\pi\epsilon_0} = \left(\frac{\epsilon_i - 1}{\epsilon_i + 2} \right) \frac{3v_i}{4\pi} = \left(\frac{\epsilon_i - 1}{\epsilon_i + 2} \right) \frac{3M}{4\pi N_A \rho^*} \quad (4.29)$$

where M is the molecular weight, N_A the Avogadro number and ρ^* the mass density. Eq. (4.28) is known as the *Clausius-Mossotti* equation. If we are only interested in the

electronic polarizability α_{oi} , we can extract from Eq. (4.29), with the Debye-Langevin expression, the following relationship:

$$\frac{\alpha_{oi}}{4\pi\epsilon_0} = \left(\frac{\epsilon_i - 1}{\epsilon_i + 2} \right) \frac{3v_i}{4\pi} \quad (4.30)$$

As the electronic polarizability can only be observed in the visible light regime, i.e., at frequency disturbances on the order of $v = v_{vis}$ of 10^{14} to 10^{15} s $^{-1}$, we can replace the static permittivity of the isolated molecule with the dynamic permittivity ϵ_{vis} at v_{vis} , i.e.,

$$\epsilon = \epsilon(v = 0) \rightarrow \epsilon_{vis} = \frac{n^2}{\mu} \quad (4.31)$$

where n is the refractive index of the “solute” medium, and, $\mu \approx 1$ is the relative magnetic permeability, which we will ignore in the further discussion. That said, the Clausius-Mossotti equation rewrites for the electronic polarizability to

$$\frac{\alpha_{oi}}{4\pi\epsilon_0} = \left(\frac{n_i^2 - 1}{n_i^2 + 2} \right) \frac{3v_i}{4\pi} \quad (4.32)$$

known as the *Lorenz-Lorentz* equation. The applicability of these two important equations, Eqs 4.29 and 4.32, towards the total polarizability and the electronic polarizability, respectively, of selected isolated molecules are provided on the next page in Table 4.3 and Table 4.4.

Tables 4.3 and 4.4 provide two venues to determine polarizabilities. One is from a gas molecular perspective, where the total polarizability is expressed by the Debye-Langevin equation with electronic and orientational polarization components. The other path is to determine the total polarizability with condensed phase (continuum) properties, i.e., the permittivity and the refractive index of the solute material. In this context it is interesting to look at the polarization response as a function of the probing frequency (Table 4.4).

Let us consider an electromagnetic oscillatory disturbance, $E(v)$, where v is the probing frequency. At static or low frequency both orientational as well as electronic polarization material responses occur. At frequencies above 10^{13} s $^{-1}$ the dipoles cannot follow anymore the alternating probing frequency, and hence, become invisible. This is illustrated in Figure 4.5. The total polarization reduces to the electronic polarization.

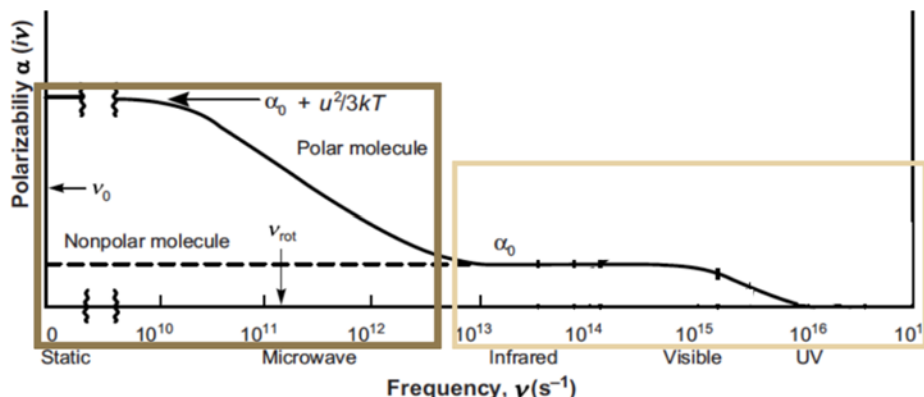


Figure 4.5: This plot shows the spectral analysis curve of polarizability in relation to the frequency applied to the electric field of the dipole. At low frequencies (brown square), both the electronic and orientation components of the dipole respond. At high frequencies (yellow square), only the electronic component responds to the changes in the electric field, so the polarizability of the dipole at high frequencies is driven only by the electronic component.

Table 4.3: Molecular Polarizabilities from Molecular and Bulk Properties

Molecular Approach: $\alpha_{total} = \alpha_0 + \frac{u^2}{3kT}$		
Molecule	Experimental Value (10^{-30} m3)	Polarizabilities Calculated Using Molecular Approach (10^{-30} m3)
CCl ₄	10.5	10.5
C ₆ H ₆	10.3	10.3
CHCl ₃	8.2	17.5 (20°C), 21.1 (-63°C)
H ₂ O	1.5	29.7
(CH ₃) ₂ OH	6.4	73.4
CH ₃ OH	3.2	26.8
C ₂ H ₅ OH	5.2	28.8
n-C ₆ H ₁₃ OH	12.5	36.1
C ₆ H ₅ OH	11.2	26.4

Table 4.4: Molecular Polarizabilities from Continuum Properties

Lorenz-Lorentz: $\frac{\alpha_{total}}{4\pi\epsilon_0} = \frac{(n-1)}{(n+2)} \frac{3v}{4\pi}$		Clausius-Mossotti: $\frac{\alpha_{total}}{4\pi\epsilon_0} = \frac{(\epsilon-1)}{(\epsilon+2)} \frac{3v}{4\pi}$
Molecule	Polarizabilities Calculated Using Lorenz-Lorentz (10^{-30} m3)	Polarizabilities Calculated Using Clausius-Mossotti (10^{-30} m3)
CCl ₄	10.5	11.2
C ₆ H ₆	10.4	10.5
CHCl ₃	8.5	17.9 (20°C), 21.1 (-63°C)
H ₂ O	1.5	6.9
(CH ₃) ₂ OH	6.4	23.5
CH ₃ OH	3.3	14.7
C ₂ H ₅ OH	5.1	20.7
n-C ₆ H ₁₃ OH	12.6	40.0
C ₆ H ₅ OH	11.1	26.1

4.4.2 Unified Polarization Equation

We have introduced two polarization interactions that contribute to the overall Van der Waals interaction energy – the Keesom interaction and the Debye interaction. These two interactions have involved polarization effects, for both nonpolar and polar molecules. The Keesom interaction describes orientational polarization, while the Debye interaction designate electronic polarization. We introduced with $w_{\text{pol}}(r)$, the sum of these two polarization interaction that entail two coupling terms of relevant interaction properties, namely, the coupling of the dipole moments ($\mu_i \mu_j$) and the coupling between dipole moments and the polarizabilities ($\alpha_i \alpha_j$). Missing is a third coupling component, and that is the polarization coupling ($\alpha_i \alpha_j$). The interaction free energy attributed to this third component is

$$w_{\alpha_1 \alpha_2}(r) = -\frac{\frac{\alpha_1 \alpha_2}{3kT}}{(4\pi \epsilon_0 \epsilon)^2 r^6} \quad (4.33)$$

and significantly smaller than the first two. Combining the polarization coupling, Eq. (4.33) with the polarization interaction, Eq. (4.25) yields the *unified polarization equation*

$$w(r)_{\text{up}} = -\frac{3kT \alpha_1 \alpha_2}{(4\pi \epsilon_0 \epsilon)^2 r^6} \quad (4.34)$$

Note that α_i ($i = 1, 2$) represent the total polarizabilities, as defined by Eq. (4.14). We substitute now the solute polarizability (excess polarizability), Eq. (4.28) for the total polarizations α_1 and α_2 , into Eq. (4.34), which yields for the unified polarization

$$w(r)_{\text{up}} = -\frac{3kT \left(\frac{\epsilon_1 - \epsilon}{\epsilon_1 + 2\epsilon}\right) \left(\frac{\epsilon_2 - \epsilon}{\epsilon_2 + 2\epsilon}\right) a_1^3 a_2^3}{r^6} \quad (4.35)$$

The unified polarization $w(r)_{\text{up}}$ has the expected $1/r^6$ dependence, as expected from the Van der Waals interaction. The last interaction component attributed to the polarization coupling provides an interesting feature, namely it also exists in a pair interaction of non-polar molecules for which the Keesom as well as the Debye interaction are zero. This brings us to discuss the interaction between non-polar interaction more closely.

4.5 Van der Waals-Dispersion Forces between Non-Polar Molecules

Molecular polarization interactions, in particular Keesom and Debye interactions, require at least one component to be polar. However, from experience we know that non-polar molecules such as alkanes can form condensed phase systems, i.e., must exhibit attractive interactions on the molecular scale. The question is where these forces come from and of what nature they are.

In our last discussion of polarization interactions, we recognized that not all molecules need to be polar to participate in electrostatic interactions. It only requires the induction of a dipole moment to allow them to interact in that nature. In order for induction to occur, we learned that an electric field is required, which a charged molecule, especially a molecule with permanent dipole can supply. Consider now that very similar to thermal fluctuations, there exist also *quantum fluctuations* that cause the electrons clouds to be

temporarily distorted. The origin for quantum fluctuations is *Pauli's uncertainty principle*. Any electronic distortion, regardless how long, brings forward a dipole moment. Hence, quantum fluctuations can cause temporary dipole moments in non-polar systems, and thus, lead to electrostatic interactions between all molecules. These charge-fluctuation forces are known as *dispersion forces*, and are, as said, like the polarization forces of electrodynamic nature. We will focus in this section on dispersion forces for isolated molecules, i.e., molecules in vacuum or gases. These particular dispersion forces are called *London dispersion forces*. The discussion of dispersion forces in media has to wait to the next chapter.

4.5.1 Properties of dispersion forces

Dispersion forces often provide the most important contribution to the van der Waals forces. They play an important role in numerous phenomena that are of practical importance, such as adhesion; physical adsorption; wetting; the properties of gases, liquids and thin films; and the structures of condensed macromolecules.

The key features of the dispersion forces can be summarized as follows:

- They show long range effects from interatomic spacings (0.2 nm) to 10 nm, distances,
- show both repulsive or attractive attributes,
- do not require any charges,
- not only bring molecules together but also align and orient them.
- are non-additive, as the force between two atoms is affected by the presence of other molecules nearby, and
- exist at $T = 0$ and are unaffected directly by temperature changes, in contrast to polarization interactions that depend on the existence and movements of dipoles. This is because in quantum mechanics, an electron even in its ground state and at zero temperature exhibits a zero-point motion, which corresponds to the fluctuations of the electron cloud, resulting in a propagating electromagnetic wave in the form of virtual photons.

4.5.2 The London Equation

We may analyze the dispersion forces in a semi-classic way. In a Bohr atom an electron is orbiting around a proton, as shown in Figure 4.6

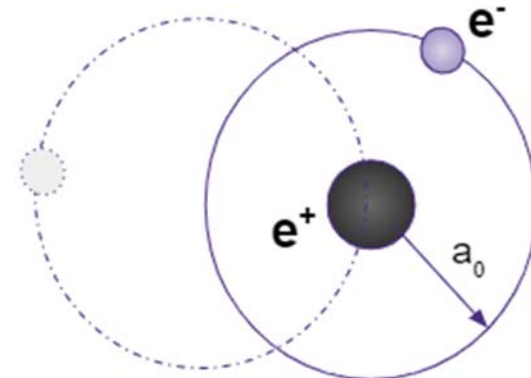


Figure 4.6: Electron fluctuation based on a Bohr Atom

The Bohr radius a_o defines the orbital radius of the electron in the ground state around the proton in the hydrogen atom. We can attribute an energy of interaction between the electron and proton that is given by the Coulomb Energy $e^2/4\pi\varepsilon_0 a_o$. Let us assume the electron fluctuates around its equilibrium position, as depicted in Fig. 4.6. The maximum fluctuation length, we can imagine without losing the electron, is on the order of a_o . The fluctuation is causing an instantaneous dipole moment, which will polarize any nearby neutral atom, giving rise to an interaction energy analogous to the Debye interaction between a polar molecule and a nonpolar molecule, Eq. 4.27, of

$$w(r) = -\frac{u_1^2 \alpha_{o2}}{(4\pi\varepsilon_0 \varepsilon)^2 r^6} = -\frac{(a_o e)^2 \alpha_o}{(4\pi\varepsilon_0 \varepsilon)^2 r^6} \quad (4.36)$$

where $\alpha_{o2} \equiv \alpha_o$ is the electronic polarizability of the second Bohr atom. Now, we consider that the quantum fluctuation energy $h\nu$, where $h = 6.626 \times 10^{-34}$ J/s and ν is the fluctuation frequency, is balanced by the Coulomb interaction, that is

$$\frac{e^2}{4\pi\varepsilon_0 a_o} = h\nu \quad (4.37)$$

As per Eq. (4.11) the polarizability can be expressed approximately as $\alpha_o \approx 4\pi\varepsilon_0 a_o^2$, equations (4.36) and (4.37) combined yield a quantum fluctuation induced attractive interaction free energy of

$$w(r) = -\frac{\alpha_o^2 h\nu}{(4\pi\varepsilon_0)^2 r^6} \quad (4.38)$$

This expression, which was derived here from a semi-classical physical model, compares well with the London derived expression based on quantum electrodynamic field perturbation theories. London's expression for the dispersion interaction energy between two identical atoms is

$$w_{disp,London}(r) = -\frac{3}{4} \frac{\alpha_o^2 h\nu_I}{(4\pi\varepsilon_0)^2} \frac{1}{r^6} = -\frac{3}{4} \frac{\alpha_o^2 I}{(4\pi\varepsilon_0)^2} \frac{1}{r^6} \quad (4.39)$$

that is, surprisingly only by a factor of $\frac{3}{4}$ off. As the fluctuation amplitude is comparable to the ionization of the atom (as per the semi-classical model and London's approximation), we have introduced in Eq. (4.38), the ionization frequency of the molecule ν_I , as well as the ionization energy $I = h\nu_I$. For two dissimilar non-polar molecules, London's equation expands to

$$w_{disp,London} = \frac{\alpha_{o1}\alpha_{o2}}{(4\pi\varepsilon_0)^2} \frac{h\nu_1\nu_2}{(\nu_1 + \nu_2)} \frac{1}{r^6} = -\frac{3}{2} \frac{\alpha_{o1}\alpha_{o2}}{(4\pi\varepsilon_0)^2} \frac{I_1 I_2}{(I_1 + I_2)} \frac{1}{r^6} \quad (4.40)$$

Most notable is that London's dispersion interaction yields again a $1/r^6$ distance dependence, and is the third and last component of the Van der Waals interaction, considering isolated non-polar molecules. Another aspect, which we addressed earlier is that the dispersion interaction reflects a coupling interaction between the polarizabilities of the molecules. This interaction is as expected independent of temperature and the molecule's charge properties. In other words, it is an interaction that cannot be turned off and always exists regardless of the molecule.

4.5.3 Polarization vs. Dispersion Contributions – The Frequency Range

If we compare the coupling interaction between the polarizabilities, Eq. (4.33), with the London expression, Eq. (4.39), for similar molecules in vacuum at room temperature, we find that the two expressions balance at a frequency of about $2.5 \times 10^{13} \text{ s}^{-1}$. This is within the infrared regime, about an order of magnitude outside the visible light regime ($4.3 \times 10^{14} - 7.7 \times 10^{14} \text{ s}^{-1}$). Dispersion interactions are known to reach down to

$$\nu_1 = \frac{2\pi kT}{h} n|_{n=1} = 4 \times 10^{13} \text{ s}^{-1} \quad (4.41)$$

at room temperature with vanishingly small contributions, while maximum contributions are achieved around

$$\nu_{40} = \frac{2\pi kT}{h} n|_{n=40} = 1.6 \times 10^{15} \text{ s}^{-1} \quad (4.42)$$

This shows that the dispersion interaction is not included in the polarization interaction, as most generally described by Eq. 4.23.

It is an opportune place to talk about the frequency range in regards of the discussed interactions, or polarization. Orientational polarization (Keesom interaction) is effective until damped in the microwave regime around $10^{11} - 10^{12} \text{ s}^{-1}$, while the electronic polarizations (Debye interaction) live on until the ultraviolet regime (10^{16} s^{-1}). The dispersion interaction ranges from the infrared regime (10^{13} s^{-1}) to deep into the ultraviolet regime (10^{16} s^{-1}). The distinct difference between the polarization interaction and the dispersion interaction is that the polarization interaction is defined by a single polarizability, e.g., the static polarizability at zero frequency, while the dispersion interaction is a sum of interactions corresponding to every frequency in the interval ν_1 to $\sim\nu_{1000} = 4 \times 10^{16} \text{ s}^{-1}$. It is the thousand-fold summation that makes the dispersion interaction generally the strongest Van der Waals component.

4.5.4 Strength of Dispersion Forces in Van der Waals Solids

While very small dispersion interacting non-polar atoms and molecules like argon remain gaseous at standard ambient temperature and pressure, larger molecules such as hexane condense to liquids or solids. The solids are referred to as *van der Waals solids*. To estimate the strength of the dispersion energy of van der Waals solids, we consider a crystal of spherical inert molecules at first. The system shall be a closely packed system with 12 nearest neighbors per atom (Fig 5.2), with a lattice cohesive energy per reference molecule of $6w(r)$ per molecule on first sight. If we also consider more distant neighbors, the factor of 6 turns to 7.22 (this lattice summation is analogous to obtaining the Madelung Constant of ionic solids). The *molar lattice energy* is therefore

$$U \approx 7.22 N_A \left(\frac{3\alpha_o^2 h \nu}{4(4\pi\epsilon_0)^2 \sigma^6} \right) \quad (4.43)$$

where $r \sigma$ is the equilibrium interatomic distance in the solid. For argon, the polarizability is $\alpha_0/4\pi\epsilon_0 = 1.63 \times 10^{-30} \text{ m}^3$, $h\nu = 2.52 \times 10^{-18} \text{ J}$, and $\sigma = 0.376 \text{ nm}$, we obtain $U \approx 7.7 \text{ kJ/mol}$, which is roughly equal to the latent heat of sublimation.

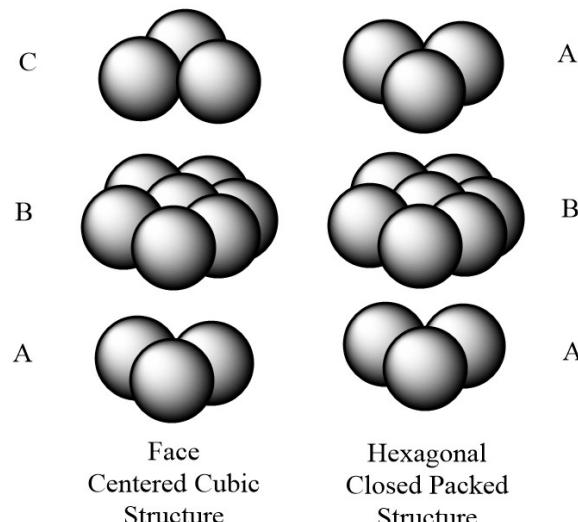


Figure 4.7: Close Packed Structures

4.5.5 Limitation of the Simple Van der Waals Model

From table 4.4, we can infer that when the diameter of a spherical molecule exceeds 0.5 nm, the London dispersion equation is inaccurate since the dispersion force does not act between the centers of the molecules but between the centers of electronic polarization within each molecule. Thus for large molecules like CCl_4 , the calculated value according to the simple model is too small.

Table 4.4: Strength of Dispersion interaction between Quasi-Spherical Nonpolar Molecules of Increasing Size

Interacting Molecules	Molecular Diameter σ (nm) (From Figure 7.1)	London Constant				Molar Cohesive Energy, U (kJ mol $^{-1}$)	Boiling Point, T_B (K)		
		Polarizability $\alpha_0/4\pi\epsilon_0$ (10^{-30} m^3)	Ionization Potential $I = h\nu_l$ (eV) ^b	Theoretical Eq. (6.3)	Measured from Gas Law Eq. (6.14) ^a				
Ne–Ne	0.308	0.39	21.6	3.9	3.8	2.0	2.1	22	
Ar–Ar	0.376	1.63	15.8	50	45	7.7	7.7	85	
CH_4 – CH_4	0.400	2.60	12.6	102 ^c	101 ^c	10.9	9.8	121	
Xe–Xe	0.432	4.01	12.1	233	225	15.6	14.9	173	
CCl_4 – CCl_4	0.550	10.5	11.5	1520	2960	23.9	32.6	265	
						$\frac{3\alpha_0^2 h\nu_l}{4(4\pi\epsilon_0)^2 \sigma^6 (1.5k)}$		350	

Source: Intermolecular and Surface Forces, 3rd Ed., J.N. Israelachvili, Elsevier, Boston 2011

Likewise, the simple London equation cannot be applied to asymmetric molecules such as alkanes, polymers, cyclic or planar molecules. To compute the binding energy within or between such complex molecules, we may first make some assumptions in order to build reasonable models for such molecules. Let us consider one such model for

normal alkanes, of general formula $\text{CH}_3\text{-}(\text{CH}_2)_n\text{-CH}_3$, where each molecule may be considered as a cylinder of diameter $\sigma = 0.40 \text{ nm}$ composed of CH_2 groups spaced linearly at intervals of $l = 0.127 \text{ nm}$, corresponding to the $\text{CH}_2\text{-CH}_2$ distance along an alkane chain. We can now consider one such molecule surrounded by six close-packed neighboring cylinders, Fig. 4.8, and sum up the dispersion energy of any one CH_2 group in the central molecule with all the CH_3 group in the six surrounding molecules. Thus, there will be 6 CH_2 group at $r=\sigma$, 12 at $\sqrt{\sigma^2 + l^2}$, and so on. The molar cohesive energy per CH_2 group will therefore be given by the following rapidly converging series:

$$U = \frac{3\alpha_0^2 h\nu}{4(4\pi\epsilon_0)^2} \left[\frac{6}{\sigma^6} + \frac{12}{[\sigma^2 + l^2]^3} + \frac{12}{[\sigma^2 + (2l)^2]^3} + \dots \right] \frac{N_o}{2} \quad (4.44)$$

Now each CH_2 group has the polarizability value $\alpha_0/4\pi\epsilon_0 = 1.84 \times 10^{-30} \text{ m}^3$, and $h\nu = 1.67 \times 10^{-18} \text{ J}$, so we obtain $U \approx 6.9 \text{ kJ/mol per } \text{CH}_2 \text{ group}$. This value compares well with data obtained from latent heat experiments, Table 4.5. Furthermore, the analysis shows that for straight-chain molecules one expects a direct proportionality between their latent heat, their molecular polarizability, their boiling point, their molecular length and their molecular weight. This linearity is not followed by spherical molecules. Also, for long, flexible chains, the molecules are no longer straight but coil up on themselves in the bulk solid or liquid.

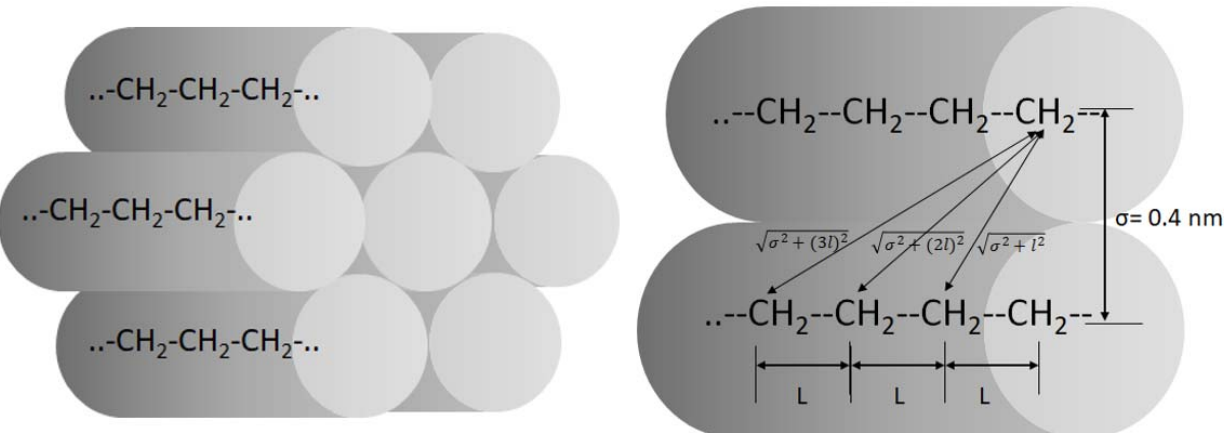


Figure 4.8: Modified model for alkanes

Table 4.5: Strength of Dispersion interaction between Linear Chain Alkane Molecules

Molecule	Number of C-C Bonds n	Molar Cohesive Energy (kJ mol^{-1})		
		Theoretical Eq. (6.7)	Measured $L_m + L_v$	Boiling Point T_B (K)
CH_4	0	9.8 (measured)	9.8	112
C_6H_{14}	5	44.3	45.0	342
$\text{C}_{12}\text{H}_{26}$	11	85.7	86.1	489
$\text{C}_{18}\text{H}_{38}$	17	127.1	125.9	590

Source: Intermolecular and Surface Forces, 3rd Ed., J.N. Israelachvili, Elsevier, Boston 2011

4.6 Van der Waals Forces between Polar Molecules

There are three distinct types of force contributions to the short-range Van der Waals interaction: The *induction*, *orientation*, and *dispersion* force. All three forces have an interaction free energy that varies with the inverse sixth power of the distance. Therefore, for two dissimilar polar molecules, we have

$$w_{VDW}(r) = \frac{-C_{VDW}}{r^6} \quad (4.45)$$

where the Van der Waals forces are made up of the three mentioned interaction contributions, i.e.,

$$\begin{aligned} w_{VdW}(r) &= -\frac{C_{induction} + C_{orientation} + C_{dispersion}}{r^6} \\ &= -\frac{(u_1^2 \alpha_{o2} + u_2^2 \alpha_{o1}) + \frac{u_1^2 u_2^2}{3kT} + \frac{3}{2} \frac{\alpha_{o1} \alpha_{o2} h v_1 v_2}{(v_1 + v_2)}}{(4\pi\epsilon_0)^2 r^6} \end{aligned} \quad (4.46)$$

Depending on the molecules, these three forces vary in their contributions. For instance, for methane, the methane-methane interaction has no contribution from induction and orientation forces. The Van der Waals force is given by dispersion forces only. The ratio of the Van der Waals partial coefficients is 0:0:102 with respect to C_{ind} : C_{orient} : $C_{dispersion}$. For the dissimilar molecular interaction between hydrogen molecule and neon, H₂O-Ne, the Wan der Waals coefficient ratio is 1 : 0 : 11. Table 4.6 lists more examples. The table also reveals some important properties of van der Waals interactions, namely,

1. *Dominance of dispersion forces.* Except for small polar molecules, dispersion forces contribute significantly more to the overall Van der Waals interaction than the dipole-dependent induction and orientation forces. It is also worth noting, that for Van der Waals interactions involving two dissimilar molecules with one non-polar, the dispersion forces still dominate the Van der Waals energy (e.g. H₂O - CH₄)
2. *Comparisons with experimental data.* The computed (theoretical) values for C_{VDW} and those obtained from the gas law coefficients a and b are very accurate, even for small polar molecules.
3. *Interactions of dissimilar molecules.* The van der Waals interaction energy between two dissimilar molecules, A and B , is usually an intermediate value between the interaction energy values for $A-A$ and $B-B$. The coefficient C_{VDW} for $A-B$ is close to the geometric mean of $A-A$ and $B-B$. This is very useful as it allows us to estimate the Van der Waals interactions between unlike molecules, for which experimental data are not available. This shall be briefly illustrated with the following example:

To find the Van der Waals interactions between Ne - CH₄, we know that Ne - Ne interacting molecules have an interaction energy of 4×10^{-79} J m⁶ (Table 4.6), while for CH₄ - CH₄, the value is 102. Now to find the VDW interactions between Ne - CH₄, we can take the geometric mean $\sqrt{4 * 102} = 20$, which is very close to the experimental value of 19.

However, this theoretical approach does not give accurate approximations for highly polar molecules such as water. For example, the net interaction of H₂O - CH₄ is much less than that of H₂O-H₂O or CH₄-CH₄. This suggests that water and methane are more strongly

attracted to themselves than to each other. This leads to *hydrophobicity* in nonpolar compounds, where they are immiscible with water. Their low water solubility and their propensity to separate into clusters is called the *hydrophobic effect*.

Table 4.6: Induction, Orientation and Dispersion free energy contributions to the total Van der Waals energy in a vacuum for various pairs of molecules at 293 K.

Similar Molecules	Van der Waals Energy Coefficients C (10^{-79} J m^6)						Total VDW Energy C_{VDW}	Dispersion Energy Contribution to Total (Theoretical) (%)	
	Electronic Polarizability $\frac{\alpha_0}{4\pi\epsilon_0} (10^{-30}\text{m}^3)$	Permanent Dipole Moment u (D) ^a	Ionization Potential $I = h\nu_i$ (eV) ^b	C_{ind} $\frac{2u^2\alpha_0}{(4\pi\epsilon_0)^2}$	C_{orient} $\frac{u^4}{3kT(4\pi\epsilon_0)^2}$	C_{disp} $\frac{3\alpha_0^2h\nu_i}{4(4\pi\epsilon_0)^2}$			
Ne–Ne	0.39	0	21.6	0	0	4	4	4	
CH ₄ –CH ₄	2.60	0	12.6	0	0	102	102	100	
HCl–HCl	2.63	1.08	12.7	6	11	106	123	157	
HBr–HBr	3.61	0.78	11.6	4	3	182	189	207	
HI–HI	5.44	0.38	10.4	2	0.2	370	372	350	
CH ₃ Cl–CH ₃ Cl	4.56	1.87	11.3	32	101	282	415	509	
NH ₃ –NH ₃	2.26	1.47	10.2	10	38	63	111	162	
H ₂ O–H ₂ O	1.48	1.85	12.6	10	96	33	139	175	
<hr/>									
Dissimilar Molecules				$\frac{u_1^2\alpha_{02} + u_2^2\alpha_{01}}{(4\pi\epsilon_0)^2}$	$\frac{u_1^2u_2^2}{3kT(4\pi\epsilon_0)^2}$	$\frac{3\alpha_{01}\alpha_{02}h\nu_1\nu_2}{2(4\pi\epsilon_0)^2(\nu_1 + \nu_2)}$			
Ne–CH ₄				0	0	19	19 ^c	—	100
HCl–HI				7	1	197	205	—	96
H ₂ O–Ne				1	0	11	12	—	92
H ₂ O–CH ₄				9	0	58	67	—	87

^a1 D = 3.336×10^{-30} Cm.

^b1 eV = 1.602×10^{-19} J.

^cThis approximate value may be compared with the ab initio calculation by Fowler et al., (1989) that gives $23 \times 10^{-79} \text{ J m}^6$.

Source: *Intermolecular and Surface Forces*, 3rd Ed., J.N. Israelachvili, Elsevier, Boston 2011

4.7 Retardation Effects

It is possible that the $1/r^6$ Van der Waals potential is distorted due to time effects. When two atoms are quite far apart, the time taken for the electric field of the first atom to reach the second atom and return can be comparable with the period of the fluctuating dipole itself. At distances beyond about 5 nm, the van der Waals force begins to decrease more rapidly, and at 100 nm separation, the retarded van der Waals force is about one order smaller than the original, approaching a dependence of $1/r^7$. This is called the *retardation effect*, and the dispersion forces between molecules and particles at large separation are called *retarded forces*. Only the dispersion energy suffers retardation.

4.8 Summary

This Chapter discusses polarization and dispersion interactions, the two key Van der Waals (VdW) interactions. All atoms and molecules can be polarized, and the degree of the so-called electronic polarization is known as *electronic polarizability*, α_0 . The electronic polarizability reflects the proportionality constant that relates the induced dipole moment u_{ind} by an external electric field, i.e., $u_{ind} = -\alpha_0 E$. Based on the definition of the

electronic polarizability, the force between an ion charge Q and a non-polar molecule with polarizability α_o can be determined, as

$$w(r) = \frac{-Q^2 \alpha_o}{2(4\pi\epsilon_0\epsilon)^2 r^4} = -\frac{1}{2} \alpha_o E_{ion}^2 \quad (4.6)$$

where ϵ is the permittivity of the surrounding media and $E_{ion} = Q/4\pi\epsilon_0\epsilon r^2$ is the electric field of the ion. While the polarizability of non-polar molecules is described solely by α_o , polar molecules can also be orientationally polarized, which yields the total polarizability α described by the *Debye-Langevin equation*,

$$\alpha = \alpha_o + \alpha_{orient} = \alpha_o + \frac{u^2}{3kT} \quad (4.14)$$

With the total polarizability, Eq. 4.6 can be extended to the interaction between ions and polar molecules:

$$w(r) = \frac{-Q^2 \alpha_o}{2(4\pi\epsilon_0\epsilon)^2 r^4} - \frac{-Q^2 u^2}{6(4\pi\epsilon_0\epsilon)^2 kTr^4} \quad (4.8)$$

To describe the solubility of an ion solute in a solvent, we introduce the *Born energy*, which is equivalent to the self-energy of the solute molecule in a medium. The Born energy of an ion (with radius a) and number density ρ is given by:

$$\mu^i = \int_a^\infty w(r) \rho 4\pi r^2 dr = \int_a^\infty \frac{\rho \alpha Q^2 4\pi r^2 dr}{2(4\pi\epsilon_0\epsilon)r^4} = \frac{-\rho \alpha Q^2}{8\pi\epsilon_0^2 \epsilon^2 a} \quad (4.18)$$

where α represents the total polarizability of the solvent molecules. Considering a solute moving from one solvent of permittivity ϵ_1 to another of ϵ_2 , yields for the change in Born energy,

$$\Delta\mu^i = \int_{\epsilon_1}^{\epsilon_2} \frac{-Q^2}{8\pi\epsilon_0^2 \epsilon^2 a} d\epsilon = \int_{\epsilon_1}^{\epsilon_2} \frac{-Q^2}{8\pi\epsilon_0^2 \epsilon^2 a} d\epsilon = -\frac{Q^2}{8\pi\epsilon_0 a} \left[\frac{1}{\epsilon_1} - \frac{1}{\epsilon_2} \right] \quad (4.20)$$

Extending our scope from ion-induced dipole interaction to dipole-induced dipole interaction, involving two polar molecules with permanent dipoles u_i ($i = 1, 2$), the interaction free energy attributed to the electronic polarizability is expressed by

$$w(r) = -\frac{\alpha_{o2} u_1^2 + \alpha_{o1} u_2^2}{(4\pi\epsilon_0\epsilon)^2 r^6} \quad (4.22)$$

known as the *Debye interaction*, where α_{oi} ($i = 1, 2$) stands for the two electronic polarizabilities. If we consider also the interaction attributed to the orientational polarization, we replace the electronic polarizability α_{oi} with the total polarizability α_i , which yields the polarization interaction free energy

$$w_{pol}(r) = -\frac{\alpha_2 u_1^2 + \alpha_1 u_2^2}{(4\pi\epsilon_0\epsilon)^2 r^6} \quad (4.23)$$

that is equivalent to the sum of the Debye and Keesom interaction, using the Debye-Langevin expression above.

We consider next that when a molecule is in a medium, it overlays its polarizability over that of the solvent. This results in known as the *excess polarizability*. The excess polarizability will no longer exist, if the molecule and solvent have the same polarizability. For a spherical molecule of radial size a_i polarizability ϵ_i in a solvent of polarizability ϵ , the excess polarizability is:

$$\alpha_i = 4\pi\epsilon_0\epsilon \left(\frac{\epsilon_i - \epsilon}{\epsilon_i + 2\epsilon} \right) a_i^3 = 3\epsilon_0\epsilon \left(\frac{\epsilon_i - \epsilon}{\epsilon_i + 2\epsilon} \right) v_i^3 \quad (4.21a)$$

where $v_i = (4/3\pi)a_i^3$ is the molecular volume. We find for the gas phase ($\epsilon = 1$) a total polarizability of

$$\frac{\alpha_i}{4\pi\epsilon_0} = \left(\frac{\epsilon_i - 1}{\epsilon_i + 2} \right) \frac{3v_i}{4\pi} = \left(\frac{\epsilon_i - 1}{\epsilon_i + 2} \right) \frac{3M}{4\pi N_A \rho^*} \quad (4.29)$$

known as the Clausius-Mossotti equation. (M is the molecular weight, N_A the Avogadro number and ρ^* the mass density.) If we are interested in the electronic polarizability only, we consider the Lorentz-Lorentz equation

$$\frac{\alpha_{oi}}{4\pi\epsilon_0} = \left(\frac{n_i^2 - 1}{n_i^2 + 2} \right) \frac{3v_i}{4\pi}. \quad (4.32)$$

The Lorentz-Lorentz equation is based on the fact that the electronic polarization is occurring at frequencies in the visible light regime, which allows us to substitute, approximately, the permittivity of the solvent by its squared refractive index, n^2 .

As mentioned earlier with the polarization interaction free energy, Eq. 4.23, it is the Debye and Keesom interactions with the two coupling terms of dipole moments ($\mu_i\mu_j$) and dipole moments and polarizabilities ($\mu_i\alpha_{oj}$) that make up the polarization interaction. There is a missing third coupling component, which is the polarization coupling ($\alpha_{oi}\alpha_{oj}$). Considering this third component and combining the orientation component with electronic polarizability component, we obtain a *unified polarization* interaction

$$w(r)_{up} = - \frac{3kT \left(\frac{\epsilon_1 - \epsilon}{\epsilon_1 + 2\epsilon} \right) \left(\frac{\epsilon_2 - \epsilon}{\epsilon_2 + 2\epsilon} \right) a_1^3 a_2^3}{r^6} \quad (4.34)$$

So far, we summarized the material in this chapter that is concerned with electronic and orientational polarization, two important contributions to the Van der Waals interaction free energy. The most important VdW contribution, however, originate from dispersion forces. Dispersion forces, also called *London dispersion forces*, if we restrict ourselves to the gas phase, consider quantum electrodynamic fluctuations. They do not require any charges or permanent charge displacement, and, show both repulsive and attractive attributes. London dispersion interactions can be expressed as

$$w_{disp, London} = \frac{\alpha_{o1}\alpha_{o1}}{(4\pi\epsilon_0)^2} \frac{h\nu_1\nu_2}{(\nu_1 + \nu_2)} \frac{1}{r^6} = - \frac{3}{2} \frac{\alpha_{o1}\alpha_{o1}}{(4\pi\epsilon_0)^2} \frac{I_1 I_2}{(I_1 + I_2)} \frac{1}{r^6} \quad (4.40)$$

with the ionization energies $I_i = h\nu_i$ ($i = 1, 2$). An example, that illustrates only dispersion interactions is the liquid condensation of alkanes, which are non to be non-polar VdW binding molecules. Limitations of using the London equation include that (i) it cannot be applied to asymmetric molecules such as alkanes or cyclic molecules, and (ii) it is inaccurate when the diameter of a spherical molecule is larger than 0.5 nm. Modified models must be used in these cases to estimate the dispersion energy.

We can conclude that short range VdW interactions consist of three types of interactions related to *induction*, *orientation*, and *dispersion*. For two dissimilar polar molecules, we have the following sum of interaction free energy to consider for VdW binding molecules in the gas phase:

$$\begin{aligned}
 w_{VdW}(r) &= -\frac{C_{induction} + C_{orientation} + C_{dispersion}}{r^6} \\
 &= -\frac{(u_1^2 \alpha_{o2} + u_2^2 \alpha_{o1}) + \frac{u_1^2 u_2^2}{3kT} + \frac{3 \alpha_{o1} \alpha_{o2} h v_1 v_2}{(v_1 + v_2)}}{(4\pi\epsilon_0)^2 r^6}
 \end{aligned} \tag{4.46}$$

The individual strengths of the three energy contributions depend on the molecules. For small polar molecules the dispersion forces typically contribute significantly more to VdW forces. Retardation effects describe the distortion of the VdW potential, when two atoms are far apart and must be considered at distances greater 5 nm.

Review Questions

1. Describe the difference between orientational and electronic polarization.
2. Given the Debye-Langevin equation, what happens when $uE \gg kT$? (When the external field is so strong that it completely biases the alignment of the dipolar molecule)
3. Provide an expression for the Debye interaction between similar polar molecules.
4. Provide polarization interaction between polar molecule (μ_i) and non-polar molecule (α_{o2})
5. Why do we need to consider the solvent effects when a pair of molecules are interacting in a solvent?
6. Write three key features of dispersion forces.
7. Cl_2 (chlorine) and Br_2 (bromine) have approximately the same shape and they are nonpolar.
 - a) Both Cl_2 and Br_2 form solids upon cooling. Explain the reason behind the phenomena by relating London dispersion forces.
 - b) At 25°C , Cl_2 is a gas although Br_2 is a liquid. Explain the reason. (*Hint:* You may shape your answer according to the figure given below)



8. What is the difference between *Clausius-Mossotti* and *Lorenz-Lorentz* relations?
9. At what frequency, or range of frequencies, is the polarization interaction calculated at?
10. What is the retardation effect and at what distance does it begin to take effect?
11. How do we estimate the VDW interaction energy between two dissimilar atoms?
12. Why is the dispersion interaction generally the strongest of the VDW forces?

Answer Key

1. Orientational polarization originates for polar molecules at thermally energies large enough to perturbed electric field interactions. Electronic polarization involves the deformation (or shift) of electron distributions of a molecule caused by external electric fields.

2. There is no observed orientational polarization effect because all of the dipolar molecules will be in full alignment with the field.
3. $w(r) = \frac{2\alpha_0 u^2}{(4\pi\epsilon_0\epsilon)^2 r^6}$
4. $w(r) = -\frac{\alpha_{o2} u_i^2}{(4\pi\epsilon_0\epsilon)^2 r^6}$
5.
 - Solvents affect the magnitude of the interaction strength between solute molecules by affecting their intrinsic properties, i.e., their dipole moments and polarizabilities
 - Solvents can change the polarity of interaction, i.e., make the interaction attractive, repulsive or even turn it off. And,
 - Solvent molecules can change their entropy in the vicinity of solute molecules, and thus, introduce additional structural forces that have to be considered.
6. They
 - show both repulsive and attractive attributes
 - do not require any charges
 - bring molecules together and align/orient them
7. a) When elements are cooled, the kinetic energy of the Cl_2 and Br_2 molecules decreases and the London forces are strong enough to overcome the kinetic energy and hold the molecules in a solid. Therefore, we can say London dispersion forces are responsible for the solid formation.
- b) Because the Br_2 molecules are larger and London dispersion forces are sufficient to cause them to form a liquid at 25°C while not for Cl_2 since they are smaller.
8. The Lorenz-Lorentz equation relates the refractive index rather than the dielectric constant as in the *Clausius-Mossotti* relation.
9. Zero, or static frequency.
10. The retardation effect refers to the rapid decrease in VDW interaction energy that takes place beyond a distance of 5 nm.
11. The VDW interaction energy between two dissimilar atoms is typically estimated as the average between the calculated VDW interaction energies between each of the two atoms with themselves.
12. Because the dispersion interaction is composed of a thousand-fold summation, from frequencies 1- 1000.

Literature – Sources and Further Reading

1. Intermolecular & Surface Forces, 3rd Ed., J.N. Israelachvili, Academic Press, Boston (2011), Ch. 5 pp 91-106.
2. Polarizability of C60 fullerene dimer and oligomers: the unexpected enhancement and its use for rational design of fullerene-based nanostructures with adjustable properties. D.S. Sabirov, RSC Adv., (2013), 3, 19430-19439.

Chapter 5: Molecular Interactions in Solvent

5.1 Overview

In this chapter, we expand our view of molecular interactions by considering the frequency dependent responses of solutes and solvents, and, discuss solvent entropic phenomena that lead to apparent molecular pair interactions that differ substantially from gas phase interactions. More specifically, we will introduce with *McLachlan* a formalism that extends our view of dispersion interaction, introduce the concept of dispersion self-energy, and assess collective interaction phenomena, i.e., the hydrophobic effect that leads to the technologically highly relevant hydrophobic and hydrophilic interactions.

5.2 The General Theory of Van der Waals Forces between Molecules and Van der Waals Forces in a Medium

In the previous chapters, we learned about the three specific Van der Waals interaction contributions that include with, the *Keesom interaction* and *Debye interaction*, the *polarization interaction*, and with the *London theory*, a simplified version of the *dispersion interaction*. In our effort of unification, we extended the polarization interaction from gas phase systems to condensed liquid systems by including the solvent effect on the polarizability. However, solvent effects have been so far not included in the dispersion interaction. Furthermore, most of our understanding on molecular interactions has been based on static properties of permittivity and polarizability, with the exception of the London dispersion, where we considered single frequency property responses in the visible light regime (10^{-15} s^{-1}). Neglected has been the matter that any system, that includes also single molecules, have the tendency to respond depending on the frequencies of testing (perturbation). In fact, any physical system has an intrinsic response (relaxation) time, and if perturbed faster, will act time delayed. Consequently, the properties become frequency dependent. To remedy the shortcoming of (i) a single frequency probing of the polarization and dispersion properties, and, (ii) the general desire to obtain a unified theory of Van der Waals interaction that includes also condensed phase systems (i.e., liquid solutions), we will treat in the following the solute polarizabilities and the solvent permittivities as time dependent properties, and, include the excess polarizabilities.

5.2.1 General Theory of Van der Waals Interactions: McLachlan Equation

As mentioned, there are two issues with the London theory of dispersion: (i) It is assumed that atoms and molecules have only a single ionization frequency (or absorption frequency), and, (ii) the theory does not take into account the interactions of molecules in a solvent. Motivated by the *unified polarization (up)* equation involving static material properties, that is (from Chapter 4)

$$w(r)_{up} = -\frac{3kT\alpha_1\alpha_2}{(4\pi\epsilon_0\epsilon)^2 r^6} \quad (5.1a)$$

with the static permittivity of the solvent, ϵ , and the static permittivity of the solutes α_i ($i = 1, 2$) given by

$$\alpha_i = \alpha_{oi} + \alpha_{orient,i} = \alpha_i + \frac{u_i^2}{3kT} \quad \text{for isolated molecules in the gas phase, or} \quad (5.1b)$$

$$\alpha_i = 4\pi\epsilon_0 \left(\frac{\epsilon_i - \epsilon}{\epsilon_i + 2\epsilon} \right) a_i^3 \quad \text{for molecules in the medium, } \epsilon \quad (5.1c)$$

McLachlan came out with a generalized theory of Van der Waals forces. He created an equation that considers the polarization (induction, orientation) and dispersion. We will later see that this equation can be easily extended with Eq. (4.1c) to interactions in a solvent medium. McLachlan followed Eq. (5.1a) to express the Van der Waals (VdW) free energy as:

$$w_{VdW}(r) = \left\{ -\frac{3kT}{(4\pi\epsilon_0)^2 r^6} \frac{\alpha_1(0)\alpha_2(0)}{\epsilon_3^2(0)} - \frac{6kT}{(4\pi\epsilon_0)^2 r^6} \sum_{n=1,2,\dots}^{\infty} \frac{\alpha_1(iv_n)\alpha_2(iv_n)}{\epsilon_3^2(iv_n)} \right\} \quad (5.2a)$$

where the first zero-frequency term on the right $w(r)_{v=0}$ expresses the polarization interaction, and the second term the non-zero frequency dispersion interaction, $w(r)_{v>0}$. This can be expressed as

$$w_{VdW}(r) = -\frac{6kT}{(4\pi\epsilon_0)^2 r^6} \sum_{n=0,1,\dots}' \frac{\alpha_1(iv_n)\alpha_2(iv_n)}{\epsilon_3^2(iv_n)} \quad (5.2b)$$

where the prime over the summation Σ' indicates that the zero-frequency $n = 0$ term is multiplied by $\frac{1}{2}$. Singled out in Eq. (5.2a) before the sum is the polarization term that only contains the static ($v_{n=0} = 0$) parameters $\alpha_{i=1,2}(0)$ and $\epsilon_3(0)$. $\alpha_1(iv_n)$ and $\alpha_2(iv_n)$ are the polarizabilities of molecules 1 and 2, and $\epsilon_3(iv_n)$ is the dielectric permittivity of medium 3. iv_n represent the imaginary frequencies (explained in more detail later), that are chosen as arguments for the frequency, to obtain a real number property value for $\alpha_{i=1,2}(iv_n)$. The McLachlan formula is useful for computing the dispersion forces between molecules that have many different ionization potentials or absorption frequencies.

Practically it is very challenging to obtain the frequency dependent properties of the McLachlan equation. As an estimate we can consider a damped harmonic oscillator with a well-defined system frequency of relaxation. In the case of the electronic polarizability, it is the ionization frequency ν_i (or absorption frequency), and for the rotational polarizability, we consider the rotational relaxation frequency ν_{rot} . As pointed out earlier, the relaxation frequency manifests a critical frequency beyond which, the system response amplitude is damped, as it lags behind. At the relaxation frequency the system is very susceptible to oscillation (high amplitude).

The damped harmonic oscillator applied to the electronic polarizability is named the Classical Electron Oscillator (CEO) model in the literature (also known as Lorentz Oscillator model), and is depicted in Figure 5.1.

The energy balance of the CEO model is described by the differential equation

$$m \frac{\partial^2 x(t)}{\partial t^2} + b \frac{\partial x(t)}{\partial t} + kx(t) = -qE(t) \quad (5.3)$$

where m is the mass of the electron, $x(t)$ the displacement in the direction of the harmonic electric field disturbance $E(t)$, t the time, b the damping factor, k the spring constant (second derivative of the electron binding potential) and q the charge displacement.

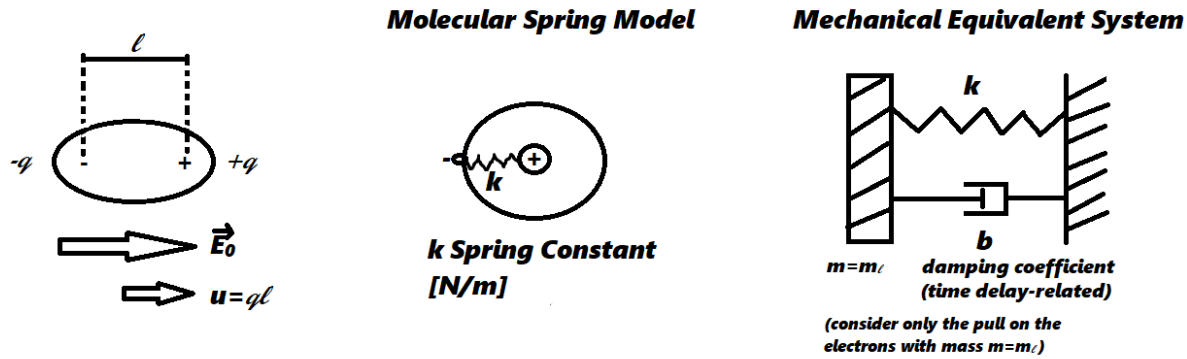


Figure 5.1 Classical Electron Oscillator, a damped simple harmonic oscillator model for dipole induction, used to determine the electronic polarizability in terms of the frequency. The direction of the dipole moment u is from negative to positive. Only the electron is moving (much lighter than the ion atom/molecule ion core) in the electric field.

At the resonance peak we find the frequency $\omega_0 = 2\pi\nu_0 = \sqrt{k/m}$, which yields for the electronic polarizability (and our assumption of a single adsorption frequency), the ionization frequency $\nu_0 = \nu_I$. We can solve this second order time-dependent differential equation for an harmonic oscillating electric field $E^*(t) = E(\omega) e^{-i\omega t}$ (expressed in complex notations, where * identifies complex quantities), which yields for the complex displacement,

$$x^*(\omega) = -\frac{q}{m} \frac{E(\omega)}{\omega_0^2 - \omega^2 - i\omega b/m} \quad (5.4)$$

The time varying charge displacement results in a frequency-dependent complex dipole moment $u^*(\omega) = -qx^*(\omega)$ (negative sign, as we consider the electron distortion to be opposite to the electric field and the dipole moment). We can now introduce the frequency dependent (apparent) electronic polarizability via the induced dipole moment as $u^*(\omega) = \alpha^*(\omega)E(\omega)$, which yields for the complex polarizability

$$\alpha^*(\omega) = \frac{q^2}{m} \frac{1}{\omega_0^2 - \omega^2 - i\omega b/m} \quad (5.5)$$

If we neglect the dampening term, we find an expression of the static electronic polarizability in terms of the resonance frequency, i.e., $\alpha_0 \equiv \alpha(\omega)|_{\nu \rightarrow 0} = q^2/m\omega_0^2$. Next we substitute this expression for α_0 into Eq. (5.5), and consider only the real part $\alpha(\nu) \equiv \text{Re}[\alpha^*(\omega)]$ of the complex solution $\alpha^*(\omega)$, which gives us to the Lorentz expression of the frequency dependent polarizability,

$$\alpha(\omega) = \frac{\alpha_0}{1 - \left(\frac{\omega}{\omega_0}\right)^2} \quad (5.6)$$

We replace now ω and ω_0 with ν and ν_I , respectively, which brings us to the final expression of the frequency dependent polarizability in terms of the ionization frequency, i.e.,

$$\alpha(\nu) = \frac{\alpha_0}{1 - \left(\frac{\nu}{\nu_I}\right)^2} \quad (5.7)$$

Most absorption frequencies are within the ultraviolet region, where $\nu_I \approx 3 \times 10^{15} \text{ s}^{-1}$, thus the value of $\alpha(\nu)$ at the visible frequency range ($\nu = 5 \times 10^{15} \text{ s}^{-1}$) is, based on Eq. (5.7), approximately equivalent to the static electronic polarizability α_o

Molecules with permanent dipole moments (u) have an additional dipolar polarizability contribution, namely the orientational polarizability, $\alpha_{\text{orient}} = u^2 / 3kT$, as previously discussed in Chapter 4 for a static (zero-frequency) electric field disturbance. At non-zero dynamic frequencies, the complex orientational polarizability is

$$\alpha_{\text{orient}}^*(\nu) = \frac{u^2}{3kT \left(1 - \frac{i\nu}{\nu_{\text{rot}}}\right)} \quad (5.8)$$

where ν_{rot} is an average rotational relaxation frequency of the molecule (found usually in the far infrared or microwave region of frequencies, $\nu_{\text{rot}} \approx 10^{11} \text{ s}^{-1}$). Combining now Equations 5.7 and 5.8 yields for the total complex polarizability,

$$\alpha^*(\nu) = \frac{u^2}{3kT \left(1 - \frac{i\nu}{\nu_{\text{rot}}}\right)} + \frac{\alpha_o}{1 - \left(\frac{\nu}{\nu_I}\right)^2} \quad (5.9)$$

It turns out that the real part, i.e., $\alpha(\nu) \equiv \text{Re}[\alpha^*(\nu)]$ is obtained by replacing the real frequency ν with the imaginary frequency $i\nu$, i.e.,

$$\alpha(i\nu) = \alpha^*(\nu \rightarrow i\nu) = \frac{u^2}{3kT \left(1 + \frac{\nu}{\nu_{\text{rot}}}\right)} + \frac{\alpha_o}{1 + \left(\frac{\nu}{\nu_I}\right)^2} \quad (5.10)$$

As we are dealing with quantized fluctuations, the relevant frequencies are also quantized, i.e., we set

$$\nu_n = \frac{2\pi kT}{h} n \approx 4 \times 10^{13} n \text{ s}^{-1} \text{ at } 300 \text{ K} \quad (5.11)$$

where $h = 6.626 \times 10^{-34} \text{ J/s}$ is the Planck constant. This is perceived by equating the quantum fluctuation energy with the thermal fluctuation, that is,

$$E_n = h\nu_n = (2\pi kT)n \quad (5.12)$$

and solving for n . Substituting ν by ν_n in Eq. (5.12) brings forward

$$\alpha(i\nu_n) = \frac{u^2}{3kT \left(1 + \frac{\nu_n}{\nu_{\text{rot}}}\right)} + \frac{\alpha_o}{1 + \left(\frac{\nu_n}{\nu_I}\right)^2} \quad (5.13)$$

the final form of our harmonic oscillator estimates for the time dependent total polarizability. Eq. (5.13) reduces to the Debye-Langevin equation for $\nu = 0$, that is

$$\alpha(0) = \alpha_o + \frac{u^2}{3kT} \quad (5.14)$$

Using once more the CEO model for the permittivity of the solvent in the McLachlan expression, leads to

$$\epsilon(i\nu_n) = 1 + \frac{n^2 - 1}{1 + \left(\frac{\nu_n}{\nu_e}\right)^2} \quad (5.15)$$

where n is the refractive index, roughly defined as $n \approx \sqrt{\epsilon(\nu_{\text{vis}})}$. Thus, with Equations (5.13) and (5.15) we have derived expressions based on a oscillator model for both property parameters, the polarizability and the permittivity in the McLachlan expressions, Equations (5.2a,b).

Figure 5.2 provides a sketch of the polarizability as function of the frequency imposed by an external electric field for similar polar and non-polar molecules in the gas phase ($\epsilon = 1$). In the static case $\alpha(v_0 = 0)$ the polarizability is equivalent to the Debye-Langevin term. At $v = v_{\text{rot}}$ the orientational polarizability is damped by approximately one half. Around $v \approx 10^{13} \text{ s}^{-1}$ the orientational polarizability is “frozen”, i.e., not fast enough to follow the electric field. From here on, only the electronic structure can be polarized until about $v \approx 10^{16} \text{ s}^{-1}$ when the electric field frequency exceeds even the electronic response.

At $v = v_1$ dispersion interactions start to become effective. This is illustrated with the superimposed dashed line in Figure 5.2 that represents the McLachlan term $\alpha_0^2(iv_n)v$ (the multiplier v becomes clear further below, when the summation is replaced by an integral). At $v \approx v_{40}$ the dispersion contribution reaches a maximum, and vanishes around $v \approx v_{1000}$. The non-zero McLachlan summation starting at $n = 1$ is proportional to the integral $\int \alpha_0^2(iv_n) dv$.

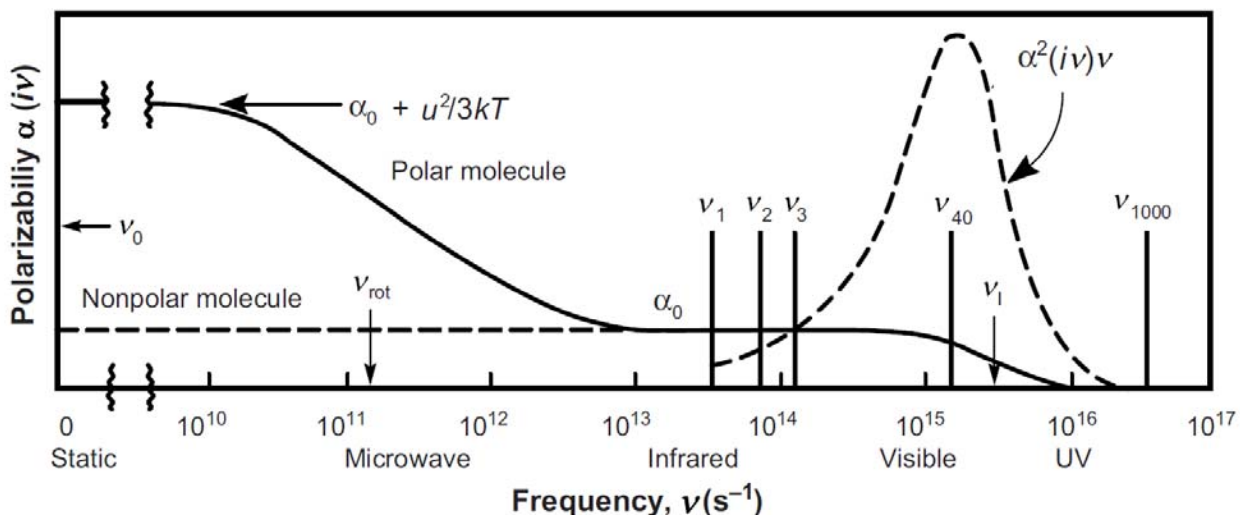


Figure 5.2 Total gas polarizability $\alpha(iv)$ for similar polar and non-polar molecules as a function of frequency. The superimposed dashed function $\alpha^2(iv)v$ reflects the respective magnitude of the dispersion energy per frequency interval. Source: Intermolecular and Surface Forces, 3rd Ed., J.N. Israelachvili, Elsevier 2011

To show that the McLachlan expression is confirmed by the more sophisticated but restricted quantum electromechanically derived London equation, we replace the sum over n by an integration over v , with $dn = (h/2\pi kT)dv$, which let us substitute

$$kT \sum_{n=1,2,\dots}^{\infty} \rightarrow \frac{h}{2\pi} \int_{v=v_1}^{\infty} dv \quad (5.16)$$

Replacing accordingly the sum in the time dependent dispersion contribution in the McLachlan equation (Eq. 5.2a) by the integral, yields to

$$w(r)_{v>0} = - \frac{6kT}{(4\pi\epsilon_0)^2 r^6} \sum_{n=1,2,\dots}^{\infty} \frac{\alpha_1(iv_n)\alpha_2(iv_n)}{\epsilon_3^2(iv_n)} = - \frac{3h}{(4\pi\epsilon_0)^2 \pi r^6} \int_0^{\infty} \alpha_1(iv_n)\alpha_2(iv_n)dv$$

where we replaced the lower integration limit ν_1 with zero, as it is much smaller than the ionization frequency ν_I . Next, we substitute the electronic polarizability expressed in Eq. 5.10 into the integral and integrate using the definite integral,

$$\int_0^\infty \frac{dx}{(a^2+x^2)(b^2+x^2)} = \frac{\pi}{2ab(a+b)}$$

and thus, obtain after some more calculation the London equation

$$w_L(r) = -\frac{3}{2} \frac{\alpha_{o1}\alpha_{o2}}{(4\pi\epsilon_0)^2 r^6} \frac{h\nu_1\nu_2}{(\nu_1 + \nu_2)} = -\frac{3}{2} \frac{\alpha_{o1}\alpha_{o2}}{(4\pi\epsilon_0)^2 r^6} \frac{I_1 I_2}{(I_1 + I_2)} \quad (5.17)$$

which confirms the validity of the McLachlan approach.

5.2.2 McLachlan Equation Expanded with the Excess Polarizability to Solvents

In the previous section we introduced with the McLachlan equation a unified model for the Van der Waals interaction that considers the frequency dependence of the material properties, namely, the polarizabilities of small molecules and the solvent permittivity. To make it truly applicable to solvents, we also have to consider the displaced solvent polarizability.

When it comes to the interactions of molecules in a medium, then the polarizabilities $\alpha(iv)$ in the McLachlan expressions, Eqs (5.2 a,b) are replaced by the effective or excess polarizabilities of the molecules. The excess polarizability based on an earlier Chapter is

$$\alpha_i = 4\pi\epsilon_0\epsilon \left(\frac{\epsilon_i - \epsilon}{\epsilon_i + 2\epsilon} \right) a_i^3 \quad (5.18)$$

As we are dealing now with three permittivities for the two solvent molecules and the solvent, we must be specific with our indices, as pointed out earlier. We will index the solute permittivities and molecular radii, a_i (assuming spherical shapes), with 1 and 2, and the solvent with 3, as depicted in Figure 5.3.

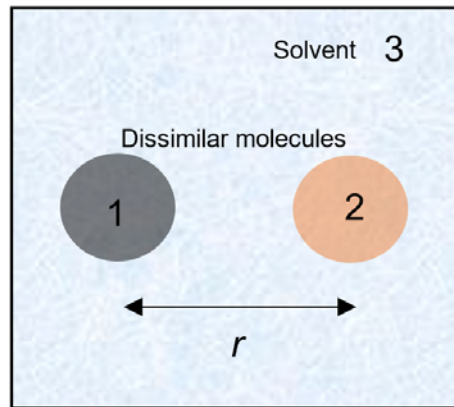


Figure 5.3 Dissimilar solvent molecules interacting in a solvent medium.

Considering now that all properties are time dependent, we write the excess polarizabilities for our solutes as

$$\alpha_i(\nu) = 4\pi\epsilon_0\epsilon_3(\nu) \left(\frac{\epsilon_i - \epsilon_3(\nu)}{\epsilon_i(\nu) + 2\epsilon_3(\nu)} \right) a_i^3 \quad (5.19)$$

with $i = 1,2$. Substituting these new expression for our solute permittivities into the McLachlan equations (Eq. 5.2(a,b)), yields for the time-independent polarization contribution

$$w(r)_{v=0} = -\frac{3kTa_1^3a_2^3}{r^6} \left(\frac{\varepsilon_1(0) - \varepsilon_3(0)}{\varepsilon_1(0) + 2\varepsilon_3(0)} \right) \left(\frac{\varepsilon_2(0) - \varepsilon_3(0)}{\varepsilon_2(0) + 2\varepsilon_3(0)} \right) \quad (5.20)$$

where $\varepsilon_1(0)$, $\varepsilon_2(0)$ and $\varepsilon_3(0)$ stand for the static permittivities of the solutes and solvent medium. Similarly, the time-dependent dispersion contribution to McLachlan, produces

$$w(r)_{v>0} = -\frac{3ha_1^3a_2^3}{\pi r^6} \int_0^\infty \left(\frac{\varepsilon_1(iv) - \varepsilon_3(iv)}{\varepsilon_1(iv) + 2\varepsilon_3(iv)} \right) \left(\frac{\varepsilon_2(iv) - \varepsilon_3(iv)}{\varepsilon_2(iv) + 2\varepsilon_3(iv)} \right) dv \quad (5.21)$$

having converted the sum to an integral according to Eq. (5.16). Considering now that it is very difficult to come by sufficient experimental data to deduce the property functions in Eq. (5.21), we can substitute the permittivity with the damped oscillator model expression introduced earlier with Eq. (5.15). If we furthermore assume that all three media possess the same absorption frequency ν_e , the dispersion interaction can be approximated, as

$$w(r)_{v>0} \approx -\frac{\sqrt{3}h\nu_e a_1^3 a_2^3}{2r^6} \frac{(n_1^2 - n_3^2)(n_2^2 - n_3^2)}{(n_1^2 + 2n_3^2)^{1/2}(n_2^2 + 2n_3^2)^{1/2} \left[(n_1^2 + 2n_3^2)^{1/2} + (n_2^2 + 2n_3^2)^{1/2} \right]} \quad (5.22)$$

for which we again introduced the refractive index as $n \approx \sqrt{\varepsilon(\nu_{vis})}$.

If we combine now this simplified version of the McLachlan dispersion with the static polarization expression, Eq. 5.20, we obtain an estimated version of the McLachlan's unifying Van der Waals theory in solvents for similar solute molecules, namely,

$$w_{VdW}(r) \approx \begin{cases} w(r)_{v=0} + w(r)_{v>0} \\ - \left[3kT \left(\frac{\varepsilon_1(0) - \varepsilon_3(0)}{\varepsilon_1(0) + 2\varepsilon_3(0)} \right)^2 + \frac{\sqrt{3}h\nu_e}{4} \frac{(n_1^2 - n_3^2)^2}{(n_1^2 + 2n_3^2)^{3/2}} \right] \frac{a_1^6}{r^6} \end{cases} \quad (5.23)$$

This simplified expression of the solvent extended McLachlan equation provides us now with the means of discussing the two Van der Waals forces contributions (static and dynamic) and the involved material properties in greater detail.

To begin with, the total van der Waals interaction free energy equation, (Eq. 5.23) consists of two parts, a polarization term ($v = 0$) followed by a dispersion term ($v > 0$). Typically (but not always), the energetic prefactor $h\nu_e$ exceeds significantly kT around room temperature, and thus, the dispersion forces dominate the dipolar contribution. Moreover, based on the equations above that neglect cooperative solvent effects such as the hydrophobic effect (discussed below), the Van der Waals forces become smaller in a solvent medium in comparison with that in the free space since the solvent, medium possesses a larger refractive index than the free space. A simple number example is provided in the Worked Problem 5.1.

Worked problem 5.1

Determine the interaction free energy of two acetone molecules in (a) the gas phase and (b) water, using McLachlan's solvent extended approximation (Eq. 5.23).

Hint: The refractive index of water is 1.33, the refractive index of acetone is 1.36. The permittivities are: $\epsilon_{\text{acetone}} = 21$, $\epsilon_{\text{water}} = 80$. Assume that the distance between two molecules remains the same and temperature is 300 K. Absorption frequency is $3 \times 10^{15} \text{ s}^{-1}$.

Solution:

Due to the same distance between the two acetone molecules and diameter, according to the equation 5.23, we only need to calculate the pre-factors in equation 5.23.

For two acetone molecules in the gas phase:

$$3kT \left(\frac{\epsilon_1(0) - \epsilon_3(0)}{\epsilon_1(0) + 2\epsilon_3(0)} \right)^2 + \frac{\sqrt{3}h\nu_e}{4} \frac{(n_1^2 - n_3^2)^2}{(n_1^2 + 2n_3^2)^{3/2}} = 3kT \left(\frac{21 - 1}{21 + 2} \right)^2 + \frac{\sqrt{3}h\nu_e}{4} \frac{(1.36^2 - 1)^2}{(1.36^2 + 2)^{3/2}}$$

$$= 1.77 \times 10^{-21}$$

For two acetone molecules in the water phase:

$$3kT \left(\frac{\epsilon_1(0) - \epsilon_3(0)}{\epsilon_1(0) + 2\epsilon_3(0)} \right)^2 + \frac{\sqrt{3}h\nu_e}{4} \frac{(n_1^2 - n_3^2)^2}{(n_1^2 + 2n_3^2)^{3/2}} = 3kT \left(\frac{21 - 80}{21 + 2 \times 80} \right)^2 + \frac{\sqrt{3}h\nu_e}{4} \frac{(1.36^2 - 1.33^2)^2}{(1.36^2 + 2 \times 1.33^2)^{3/2}}$$

$$= 9.2 \times 10^{-20}$$

From the above results, van der Waals interaction in the free space is about 52 times larger than that in the water. Now you can have clear understanding that Van der Waals interaction is much reduced in the solvent in comparison with that in the free space.

On closer inspection, if we compare the dispersion contribution (for $\nu > 0$) of the solvent extended McLachlan equation, Eq. 5.23, for similar molecules in the gas phase

$$w(r)_{\nu>0} = - \frac{\sqrt{3}h\nu_e a_1^6}{4r^6} \frac{(n_1^2 - 1)^2}{(n_1^2 + 2)^{3/2}} \quad (5.24)$$

with London's equation, Eq. (5.17),

$$w_L(r) = - \frac{3h\nu_I \alpha_0^2}{(4\pi\epsilon_0)^2 r^6} = - \frac{3h\nu_I a_1^6}{4r^6} \frac{(n_1^2 - 1)^2}{(n_1^2 + 2)^2}$$

(note, we substituted α_0 with $4\pi\epsilon_0 a_1^3$), we find the ratio

$$\frac{w_L(r)}{w(r)_{\nu>0}} = \sqrt{3} \frac{\nu_I}{\nu_e}$$

instead of unity. The discrepancy between the two equations originates from the absorption frequency of the isolated molecule ν_I , which is different from the condensed phase ν_e . We can relate the two frequency via the Clausius-Mossotti-Lorenz equations, discussed earlier, and find the following relationship:

$$\nu_e = \nu_I \sqrt{3/(n_1^2 + 2)} \quad (5.25)$$

Substituting Eq. (5.25) into Eq. (5.24) yields the London's equation, and thus, resolves the discrepancy.

Furthermore, when analyzing the polarity (attractive vs. repulsive) of dispersion forces between molecules with Eq. (5.24), we find that the forces are negative (attractive) for similar molecules, and the forces can be either (attractive or repulsive) for dissimilar molecules, depending on the refractive indices of the solutes and solvent. Naturally,

everything said about the refractive indices, lead back to the permittivity, as per the inclusion of the refractive index, i.e., $n \approx \sqrt{\varepsilon(\nu_{vis})}$.

It is worth mentioning that the McLachlan Eq. 5.23 (and earlier versions) are useful in determining if solutes are miscible in particular solvents. For any small refractive index difference between n_1 and n_3 , there would be small attraction between them, which means that they tend not to associate.

Finally, the zero-frequency contribution will have significant impact on the free energy when the non-zero-frequency contribution becomes small. This will occur when the refractive indices are close to each other. For example, the refractive indices of lower molecular weight alkanes ($n_{CH_4} \approx 1.3$, $n_{C_4H_{16}} \approx 1.33$, $n_{C_5H_{12}} \approx 1.36$) are close to that of water ($n_{H_2O} \approx 1.33$). Therefore, when they interact with water molecules, the dispersion forces no longer dominate the VdW force. While $\varepsilon_{H_2O}(0) \approx 80$ and $\varepsilon_{alkane}(0) \approx 2$, the overall Waals force reduces to

$$w(r) \approx w(r)_{v=0} \approx \frac{-kTa_1^6}{r^6} \quad (5.26)$$

which is totally entropic. The above equation (5.26) indicates that the entropy will increase when two alkane molecules get close to each other in water, which further indicates the increase in the freedom of water molecules. However, the measured values indicate a much stronger interaction than the value from the equation (5.26). For example, a free energy of dimerization of order $kT\left(\frac{a}{2a}\right)^6 \approx \frac{kT}{64}$, almost equal to 0.04 kJ/mol for two small molecules with radius of a. While the experiment values are 100 times larger: for CH₄, C₆H₆ and C₆H₁₂, the values are approaching 10 kJ/mol. The disagreement between the calculated values and the experiment values is associated with the breakdown in the simple model of excess polarizability that involves highly polar solvent or solute molecules, similar to the discussion in Section 5.8 (shown in textbook). The unique role of water as both a solvent and a medium for solute-solute interactions will be discussed in the following section.

5.2.3 Molecular Dispersion Self-Energy

In analogy to the Born self-energy of an ion discussed in an earlier chapter, we will introduce next the dispersion self-energy. It provides a deeper understanding of the solubility and partitioning of molecules in solvent media.

As depicted in Figure 5.4(a), we consider molecule 1 of diameter $\sigma=2a$ to be transferred from free space into a solvent medium 2. Assuming a closed packed system, i.e., a system in which we assume 12 nearest neighbors around a reference molecule with an equilibrium molecular distance σ , six solvent-solvent bonds have to be broken first to form an empty space (cavity) to accommodate molecule 1. Then 12 new solute-solvent bonds are formed with molecule 1. To estimate the energy involved in these two processes, we will use the London dispersion equation (with this we assume very small non-polar isotopically shaped molecules). It has been shown in a prior chapter that the molar cohesive energy using London's equation is given as

$$U = 7.22N_A \left[\frac{3\alpha_o^2 h\nu_I}{4(4\pi\varepsilon_o)^2 \sigma^6} \right] \propto \left[\frac{3\alpha_o^2 h\nu_I}{4(4\pi\varepsilon_o)^2 \sigma^6} \right] \quad (5.27)$$

Thus, the interaction involved in forming the cavity and placing molecule 1 into media 1, yields an approximate net free energy change of

$$\Delta\mu_{disp}^i \approx \frac{3h\nu_I}{4(4\pi\varepsilon_0)^2\sigma^6} [6\alpha_{o2}^2 - 12\alpha_{o1}\alpha_{o2}] \quad (5.28a)$$

where we assumed ν_I to be the same for both the solute and solvent molecules.

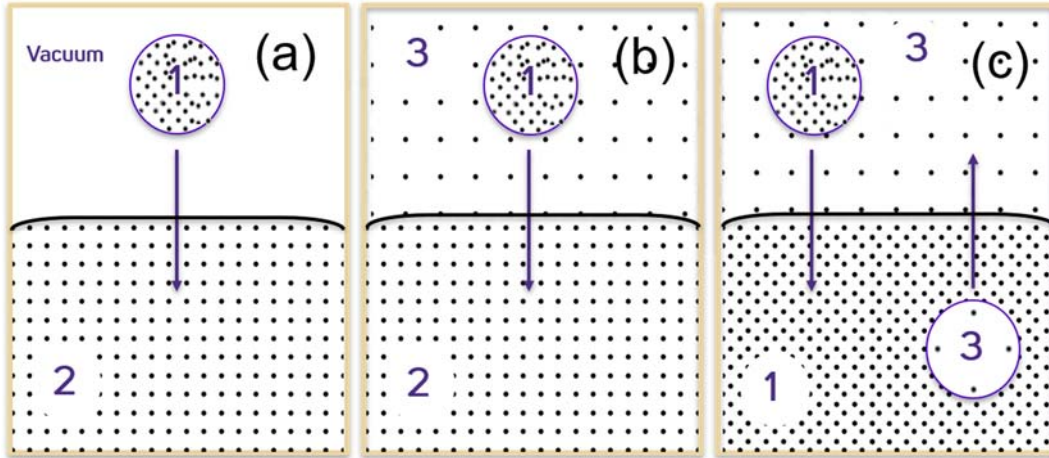


Figure 5.4 Molecules of radius a (diameter σ) interacting in a solvent medium. Molecules transferring from one medium to another.

Next, we assume molecule 1 to be transferred from solvent 3 to solvent 2, Fig. 5.4(b). This leads according to what we discussed, to the following interaction free energy change:

$$\Delta\mu_{disp}^i \approx \frac{3h\nu_I}{4(4\pi\varepsilon_0)^2\sigma^6} [(6\alpha_{o2}^2 - 12\alpha_{o1}\alpha_{o2}) - (6\alpha_{o3}^2 - 12\alpha_{o1}\alpha_{o3})] \quad (5.28b)$$

which is roughly proportional to

$$\Delta\mu_{disp}^i \propto [-(\alpha_{o2} - \alpha_{o1})(2\alpha_{o1} - \alpha_{o2} - \alpha_{o3})] \propto [-(n_2^2 - n_3^2)(2n_1^2 - n_2^2 - n_3^2)] \quad (5.28c)$$

Note, Eq. (5.28c) can be either positive or negative. If we assume that medium 1 is equal to medium 2, Eq. (5.28c) reduces to

$$\Delta\mu_{disp}^i \approx -\frac{6(3h\nu_I)}{4(4\pi\varepsilon_0)^2\sigma^6} [\alpha_{o1} - \alpha_{o3}]^2 \propto -(\sqrt{U_1} - \sqrt{U_3})^2 \propto -(n_1^2 - n_3^2)^2 \quad (5.28d)$$

which will be always negative. U_1 and U_3 are the cohesive energies (or latent heats of vaporization) of the two solvents given by Eq. (5.27). According to these equations above, we can say that transferring a molecule into its own environment is always negative and energetically favorable as shown in Figure 5.4(c).

5.3 Cooperative Interactions involving the Solvent

In the prior discussion, we heavily focused on solute molecule interactions in a homogenous structureless solvent. Only in our brief discussion involving Eq. 5.26, we entertained the notion that the solvent itself can be structured, and as such, lead to entropic changes within. Structural changes and preferences of the solvent explain in greater detail, the solvent's strong influence on the solute interaction strength, as well as, the solute-solute interaction polarity. We will in the following consider water as our solvent

and question, and solutes that are either non-polar, i.e., do not interact with water, or polar, and thus, interact with water. The first situation leads to hydrophobic ("water disliking") interactions, and the second to hydrophilic ("water loving") interactions.

5.3.1 The Hydrophobic Effect

The *hydrophobic effect* is an entropic solvent effect, which leads to the insolubility of nonpolar molecules in water. It is (a) the tendency of nonpolar molecules to aggregate in an aqueous solution, and (b), the energy minimal approach of the solvent that lets it happen. In other words, the solvent does not want to come in-between the solutes, but rather phase separates from them. An understanding of this so-called underlying hydrophobic effect is crucial because it plays a key role in defining the concepts of micelle formation, protein folding, ligand-protein and protein-protein binding, nucleic acid interactions, metabolites, partitioning of drugs etc. We can say the hydrophobic effect is the fundamental essence to life.

The hydrophobic effect is responsible for increased heat capacities compared to regular solutions that lack the strong coordination of water, and, is affected by the exposed surface area and with it shape of the solute molecule. In this light, let us consider a mixture of oil and water as depicted in Figure 5.5. When an oil drop (a carbon rich nonpolar compound) is dispensed into water, the water molecules have the choice of dissolving the hydrocarbons in the oil drop or, cage them up in the drop and structure around. It all depends on the sign of the Gibbs free energy transfer ΔG for this process, as discussed earlier.

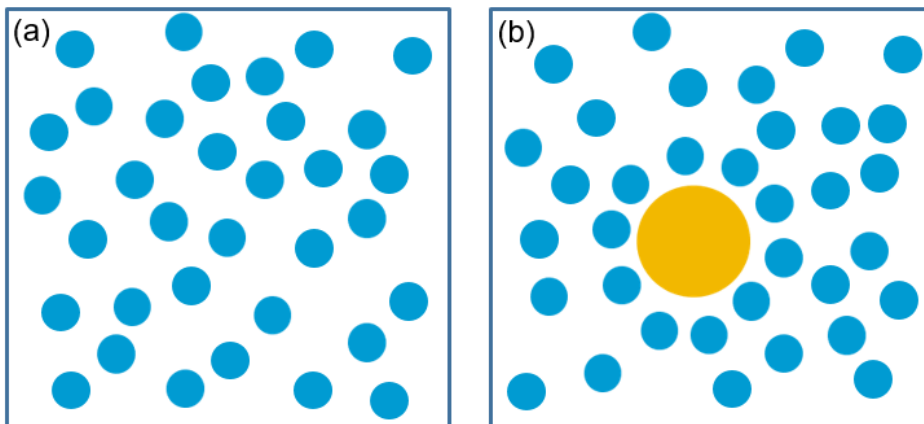


Figure 5.5 Illustration of (a) water, and a water-oil solution.

The energy transfer equation that governs the hydrophobic effect is

$$\Delta G = \Delta H - T\Delta S \quad (5.29)$$

where ΔH is the enthalpy of interaction that be attributed to the electronic polarization energy and the dispersion interaction, and, ΔS is the orientational entropy, we can attribute to packing interactions and structure within the solvent and the solute phases, typically given by permanent dipole-dipole interactions and hydrogen interactions. We already discussed with Figure 5.5, the different entropic terms, and also the fact that for a spontaneous process $\Delta G < 0$, and thus, the water encapsulation (Fig. 5.5(b)) around the oil droplet is statistically the most likely outcome.

In contrast to many liquid substances, water is known in its liquid phase to possess an icosahedral-like network structure, as the minimum energetic state. If water now structures around an inert solute molecule (such as a hydrocarbon molecule), the entropy is generally lowered, and thus, work is involved. This is shown here with one of the least expensive (from an energy perspective) ordering model, the “Iceberg” model in Figure 5.6(a). Sizes and shapes of nonpolar solute molecules are critical in determining the water structure; therefore, water molecules can form additional different structures around the solute as shown in Figure 5.6(b). Still, the model leads to an entropy decrease and thus would not run spontaneously.

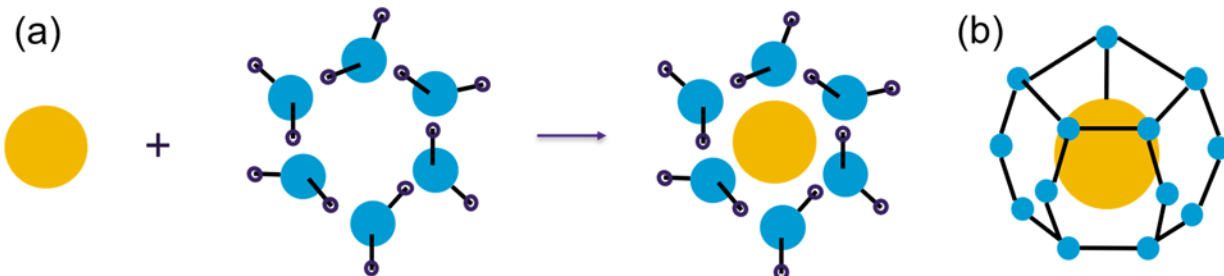


Figure 5.6 “Iceberg” model of nonpolar solutes into water. (A) At room temperature the water molecules surrounding a nonpolar solute adopt only a few orientations (low entropy).

Placing now an entire droplet with a non-polar surface into water would disturb the hydrogen-bonding network of bulk water. The water molecules closest to the hydrocarbon surface reorient so that fewer but stronger water-water hydrogen bonds come into existence close to the nonpolar molecule. This forming exhibit much greater oriental ordering and hence lower entropy than bulk water.

The hydrophobic effect has also great importance in protein folding. Protein folding is a process in which a protein will fold into its native 3-dimensional structure, a conformation that is usually biologically functional. As seen in Figure 5.7(a), when protein is in its unfolded state, there will be more interfacial area which causes more water molecule to be ordered. Because of this more hydrocarbon-water interfacial area, ΔS will be smaller than zero which means lead to a more unfavorable solvent entropy. In contrast, when it is in a folded state as depicted in Figure 5.7(b), there will be less entropic water ordering at the interface compared to Figure 5.7(a), since there are less unfavorable solvent-water bonds needed to cage the interface.

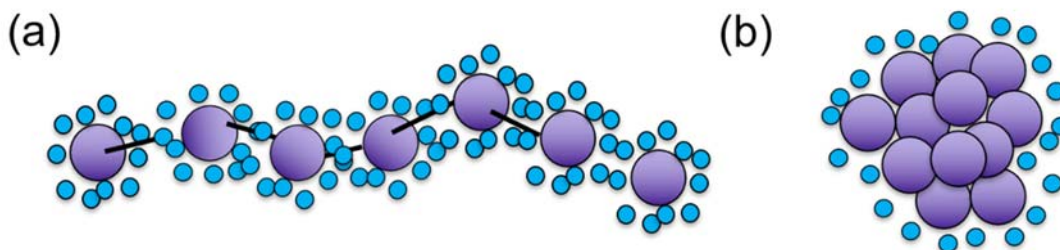


Figure 5.7 Illustration of protein in an unfolded state (a) and folded state (b) with surrounding water molecules.

5.3.2 Hydrophobic Interaction

Hydrophobic molecules exhibit strong Van der Waals (VdW) attractions to each other in water, stronger than in free space. For example, the VdW energy between two methane molecules in water is almost six times larger than its counterpart in free space (-14 x 10⁻²¹ J vs. -2.5 x 10⁻²¹ J, respectively.) The methane gas phase value was obtained using Eq. (5.30) at T = 300 K.

$$w_{VdW}(r) = w_{induction}(r) + w_{orientation}(r) + w_{dispersion}(r)$$

$$= \frac{(u_1^2 a_{02} + u_2^2 a_{01}) + \left(\frac{u_1^2 u_2^2}{3kT}\right) + \left(\frac{3a_{01}a_{02}h\nu_1\nu_2}{2(\nu_1 + \nu_2)}\right)}{(4\pi\epsilon_0)^2 r^6} \quad (5.30)$$

If we employ the simplified expression of the solvent extended McLachlan equation Eq. (5.23) for methane in water at T = 300 K using for the static permittivities of methane $\epsilon_1(0) \approx 1$, and of water $\epsilon_3(0) = 78$, absorption frequency $\nu_e \approx 3.0 \times 10^{15}$ s⁻¹, and the refractive indices of methane ($n_1 \approx 1$) and water ($n_3 = 1.3$), and a methane diameter of 3.8 nm (= 2a_i), the interaction energy is -1.92 x 10⁻²¹ J. It is smaller than the interaction in vacuum, due to the presence of the solvent. Thus, the experimentally observed difference in methane attraction in vacuum vs. water cannot be attributed to van der Waals forces alone. Historically, an additional attraction was attributed to the existence of a "hydrophobic bond" between molecules in water. However, we know now that such a bond does not exist.

Instead, the unusually strong attraction between hydrophobic molecules in water can be attributed to a significant increase in solvent entropy (discussed earlier and depicted in Fig. 5.5) that occurs when two hydrophobic molecules come together. This entropic effect is due to the rearrangements of the H-bonding network that tries to minimize the interaction with the solute and maximize hydrogen bonding between the water molecules. Figure 5.8 shows the effect of minimizing the number of water molecules interacting with the hydrophobic (e.g., alkane) moiety. The cage-like structure imposes a compressing force on the hydrophobic molecules within, leading to apparent higher interaction forces between the nonpolar molecules.

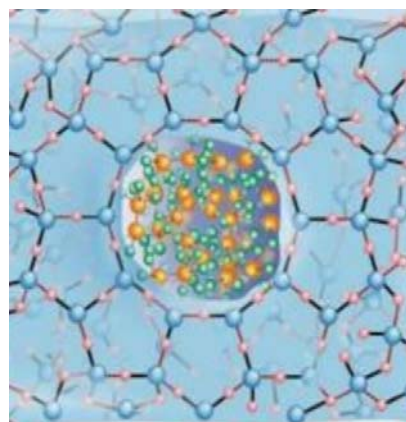


Figure 5.8 Disturbed water network forming hydrogen-bonded cage-like structures around hydrophobic molecules.

While there is now a deeper understanding of the hydrophobic interactions between nonpolar molecules in water, there are very few measurements of this interaction due to the inherent insolubility of nonpolar molecules in water. Deriving an equation for the hydrophobic interaction between two molecules is even more difficult because the interactions exist over a much longer range than typical VdW interactions of additive pair-potential. Any theory of the hydrophobic interactions between solute molecules in water must also depend on the complex H-bonding network and the role of proton hopping and how they affect the local polarizability of water. Theoretical approaches have been proposed, but the sheer number of molecules involved in these interactions make deriving a universal equation for the interactions between hydrophobic molecules and water nearly impossible.

To overcome these challenges, Israelachvili and Pashley sought to derive an empirical equation for the hydrophobic pair-potential of hydrophobic molecules in water. They explored the hydrophobic force law between two hydrophobic surfaces in water and found that the interaction force decreases exponentially as a function of distance within a range of 4-10 nm. From these findings, they proposed that the hydrophobic pair-potential $w_H(r)$ for small solute molecules is exponential and proportional to the diameter σ of the molecules or molecular groups. Therefore, the hydrophobic pair potential may be expressed as

$$w_H(r) \approx -20 \sigma e^{-\frac{r-\sigma}{D_H}} \text{ kJ/mol} \quad (5.31)$$

$$\approx -8\sigma e^{-(r-\sigma)/D_H} \text{ kT at 298K}$$

where σ is in nm, r is the distance between two hydrophobic molecules, and D_H is the empirical hydrophobic decay length. The empirical decay length, or the exponentially distance-dependence for the hydrophobic interaction, explored by Israelachvili and Pashley was approximately 1 nm.

We shall in the following explore the energy involved in a molecular dimer. In order to find the free energy of dimerization of two hydrophobic molecules in water, we substitute for the pair distance, r , the molecular diameter σ . This leads to be based on Eq. (5.31):

$$\Delta G_{\text{dimer}} = w_H(\sigma) \approx -20 \sigma \text{ kJ mol}^{-1} \approx -8\sigma kT \text{ at 298 K} \quad (5.32)$$

For example, for cyclohexane ($\sigma = 0.57 \text{ nm}$), this gives $\Delta G_{\text{dimer}} \approx -11.4 \text{ kJ/mol} (\sim 5 \text{ kT})$. We recall that the experimentally measured value is equal to -11.3 kJ/mol . Therefore, this proposed equation adequately represents the free energy of dimerization of cyclohexane in water. The hydrophobic force needed to separate two molecules that are in contact is given by

$$F_H(\sigma) = -\left(\frac{dw_H}{dr}\right)_{r=\sigma} \approx -3 \times 10^{-11} \sigma (\text{nm}) \text{ N at 298 K} \quad (5.33)$$

As for cyclohexane $\sigma = 0.57 \text{ nm}$, the adhesion force between the two molecules is about 17 pN.

5.3.3 Hydrophilic Interaction

Having discussed inert solvent molecules regarding hydrogen bonding, we will finish our discussion on cooperative solvent effects with polar solutes that engage in hydrogen bonding interaction in water, dubbed hydrophilic interactions. Hydrophilic interactions

refer to the characteristics of specific molecules to strongly repel each other in water in favor of water-solubility. As one may expect, most charged molecules, including zwitterions, are hydrophilic. Interestingly, nonpolar and uncharged molecules can be hydrophilic depending on their geometry. The true concept of hydrophilicity relies on the ability for a molecule to H-bond with water. Therefore, a molecule that has a polar group may not be hydrophilic, and a molecule with a nonpolar group may not be hydrophobic. Table 5.1. lists common hydrophilic groups and molecules, as well as polar groups that are not hydrophilic when attached to a long carbon chain.

Table 5.1. Hydrophilic and hydrophobic groups and molecules.

Hydrophilic Molecules and Ions	Molecular Groups (Ionic)	Nonionic Polar Groups	Solid Surfaces	Polar Groups (not always hydrophilic)
Alcohols	Carboxylate –CO ⁻	Amine –NH ₂	Hydroxylate silica (below 600°C)	Alcohol --OH
Sugars	Sulfonate –SO ₃ ⁻	Amine oxide –NO(CH ₃) ₂	Swelling clays	Ether –OCH ₃
Chaotropes	Sulfate –SO ₄ ⁻	Sulfoxide –SOCH ₃	Chromium	Mercaptan –SH
Soluble proteins	Phosphate ester –PO ₂ ⁻ O–	Phosphine oxide –PO(CH ₃) ₂	Gold	Amide –CONH ₂
Nucleic Acids DNA & RNA	Trimethyl ammonium –N ⁺ (CH ₃) ₃			Nitroalkanes –NO, --NO ₂
Polyelectrolytes	Dimethyl ammonium >N ⁺ (CH ₃) ₂			Ketone –COCH ₃

At least three different levels of ordering and order parameters are responsible for the predicted structuring of water on a hydrophilic surface, which is shown in Figure 5.10. *Orientational ordering* affects electrostatic and entropic charge-transfer interactions of the molecules, while *positional ordering* of the molecules into layers affects the oscillatory forces. Finally, density variations near surfaces can cause additional steric repulsion between surfaces and a reduced attraction between hydrophobic surfaces. These three order parameters cause the binding of water to a hydrophilic surface or solute to be directional, therefore leading to an additional steric barrier. This orientational ordering restricts proton-hopping, indicating one of the main differences between the structure of water on hydrophilic and hydrophobic surfaces. The steric and directional barriers also restrict the rotation of water molecules, preventing interactions with the bulk solvent. In addition to the effect of surfaces on the structuring of water molecules, certain molecules known as *chaotropic agents* are capable of fully disrupting the local water structure. An example of a chaotropic agent is urea, which can cause proteins to unfold when dissolved in water. Therefore, it is clear that hydrophilic and hydrophobic interactions are unique in that they are interdependent on all local molecules. They are

highly dependent on the orientation and structure of H-bonds with water and solute and therefore are not additive.

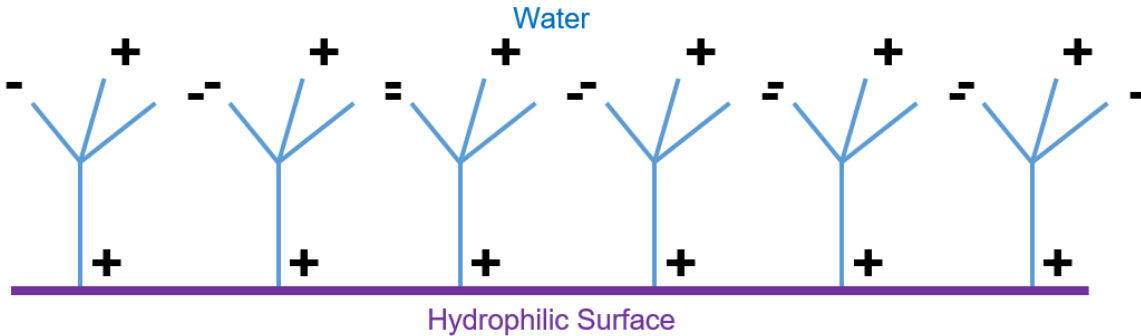


Figure 5.9 The hydrophilic-water interface. The charge of a hydrophilic surface dictates the orientation of water molecules on the surface. In this figure, the molecule is oriented with a partially positive hydrogen atom facing towards the surface. This restricts the water molecule orientation on the first layer, and therefore the orientation of following layers. This orientation restriction does not exist with hydrophobic surfaces.

5.4 Summary

This chapter covers the *McLachlan expression* of the Van der Waals (VdW) interactions, *dispersion self-energy*, and the *hydrophobic effect*. Included are in the Van der Waals (VdW) interactions the (static) polarization interactions and the (dynamic) dispersion interactions. With McLachlan, a unified description of VdW interactions is provided, in terms of the static and dynamic contributions, as described in the following expression:

$$w_{VdW}(r) = \begin{cases} w(r)_{v=0} + w(r)_{v>0} & (5.2a) \\ -\frac{3kT}{(4\pi\epsilon_0)^2 r^6} \frac{\alpha_1(0)\alpha_2(0)}{\epsilon_s^2(0)} - \frac{6kT}{(4\pi\epsilon_0)^2 r^6} \sum_{n=1,2,\dots}^{\infty} \frac{\alpha_1(iv_n)\alpha_2(iv_n)}{\epsilon_s^2(iv_n)} & (5.2b) \end{cases}$$

Included in the McLachlan's expression, Eq. 5.2b, are the static polarizabilities $\alpha_i(0)$ ($i = 1, 2$, representing the two solutes), the static permittivity of the solvent $\epsilon_s(0)$, and, the frequency-dependent (dynamic) counterparts $\alpha_i(iv_n)$ and $\epsilon_s(iv_n)$, where $v_n \equiv (2\pi kT/h)n$, and i is the imaginary unit. The frequency dependent properties can be either obtained from experiments, or, approximately from models, such as the *damped harmonic oscillator model*.

Restricting ourselves to simple rotational and electronic relaxations of the solutes with the corresponding relaxation frequencies v_{rot} and v_I (ionization frequency), the frequency-dependent polarizability can be expressed as,

$$\alpha(iv_n) = \frac{u^2}{3kT \left(1 + \frac{v_n}{v_{rot}}\right)} + \frac{\alpha_o}{1 + \left(\frac{v_n}{v_I}\right)^2} \quad (5.13)$$

and the dynamic permittivity of the solvent, as

$$\epsilon(iv_n) = 1 + \frac{n^2 - 1}{1 + \left(\frac{v_n}{v_e}\right)^2} \quad (5.15)$$

where ν_e represents the electronic relaxation frequency, and, n is the solvent refractive index, roughly defined as $n \approx \sqrt{\epsilon(\nu_{vis})}$ in the visible frequency regime. It can be shown that the McLachlan expression corresponds to the London expression of the VdW dispersion, i.e.,

$$w_L(r) = -\frac{3}{2} \frac{\alpha_{o1}\alpha_{o2}}{(4\pi\epsilon_0)^2 r^6} \frac{h\nu_1\nu_2}{(\nu_1 + \nu_2)} = -\frac{3}{2} \frac{\alpha_{o1}\alpha_{o2}}{(4\pi\epsilon_0)^2 r^6} \frac{I_1 I_2}{(I_1 + I_2)} \quad (5.17)$$

for gas phase system.

To extend the McLachlan expression to solute-solute interactions in solvents, the solvent excess polarizability is included, which yields the following two expressions in the McLachlan equation Eq. 5.2a, for the static and dynamic interactions:

$$w(r)_{v=0} = -\frac{3kTa_1^3a_2^3}{r^6} \left(\frac{\epsilon_1(0) - \epsilon_3(0)}{\epsilon_1(0) + 2\epsilon_3(0)} \right) \left(\frac{\epsilon_2(0) - \epsilon_3(0)}{\epsilon_2(0) + 2\epsilon_3(0)} \right) \quad (5.20)$$

$$w(r)_{v>0} \approx -\frac{\sqrt{3}h\nu_e a_1^3 a_2^3}{2r^6} \frac{(n_1^2 - n_3^2)(n_2^2 - n_3^2)}{(n_1^2 + 2n_3^2)^{\frac{1}{2}}(n_2^2 + 2n_3^2)^{\frac{1}{2}} \left[(n_1^2 + 2n_3^2)^{\frac{1}{2}} + (n_2^2 + 2n_3^2)^{\frac{1}{2}} \right]} \quad (5.22)$$

Having discussed the solute-solute VdW interactions in solvents, the self-energy of dispersion is considered, as it is an important property in solution problems. The self-energy of solutes in solvents entails the inclusion of the energy involved to make space for the solute in the solvent, and thus, produces a two terms expression for the dispersion self-energy, i.e.,

$$\Delta\mu_{disp}^i \approx \frac{3h\nu_I}{4(4\pi\epsilon_0)^2\sigma^6} [6\alpha_{o2}^2 - 12\alpha_{o1}\alpha_{o2}] \quad (5.28a)$$

where the positive first term results from the cavity formation, and the negative second term from the solute-solvent bonding. For a solute molecule moving from one solvent to another, one must subtract the final dispersion self-energy from the initial dispersion self-energy, yielding:

$$\Delta\mu_{disp}^i \approx \frac{3h\nu_I}{4(4\pi\epsilon_0)^2\sigma^6} [(6\alpha_{o2}^2 - 12\alpha_{o1}\alpha_{o2}) - (6\alpha_{o3}^2 - 12\alpha_{o1}\alpha_{o3})] \quad (5.28b)$$

Assuming that the solute molecule is made of the same material as the solvent it is entering, this equation can be further reduced to:

$$\Delta\mu_{disp}^i \approx -\frac{6(3h\nu_I)}{4(4\pi\epsilon_0)^2\sigma^6} [\alpha_{o1} - \alpha_{o3}]^2 \propto -(\sqrt{U_1} - \sqrt{U_3})^2 \propto -(n_1^2 - n_3^2)^2 \quad (5.28d)$$

Since above equation is always negative, the dispersion self-energy of a solute molecule entering a solvent of the same composition is always energetically favorable.

Finally, an apparent force attributed to the *hydrophobic effect* is discussed that non-polar solute molecules experience when interacting with each other in water. The hydrophobic effect is an entropic solvent effect that leads to spontaneous non-polar molecular aggregation in aqueous solutions. It results in increased heat capacities of the solutions, because of the coordination of water and exposure to solute molecules. The hydrophobic effect is governed by the Gibbs free energy transfer equation,

$$\Delta G = \Delta H - T\Delta S \quad (5.29)$$

where ΔH is the change in enthalpy, T is the temperature, and ΔS is change in entropy. Enthalpy of the interaction is dependent on electronic polarization energy and dispersion interaction. For a process to be spontaneous it is required that $\Delta G < 0$. The entropic contribution entails both the solute entropy, as well as, the solvent conformational entropy, which is dependent on the solvent molecular orientation.

Considering that the solvent in aqueous solutions is water, the water structure is important. Water exhibits an icosahedral structure that is maintained around hydrophobic molecules, and thus, imposing a compressing force leading to apparent higher interaction forces between the solutes, compared to vacuum. The interaction force decreases exponentially as a function of distance within a 4 to 10 nm range. This can approximately modelled approximately by the hydrophobic pair potential $w_H(r)$, which is given as,

$$w_H(r) \approx -20 \sigma e^{-(r-\sigma)/D_H} \text{ kJ mol}^{-1} \quad (5.31)$$

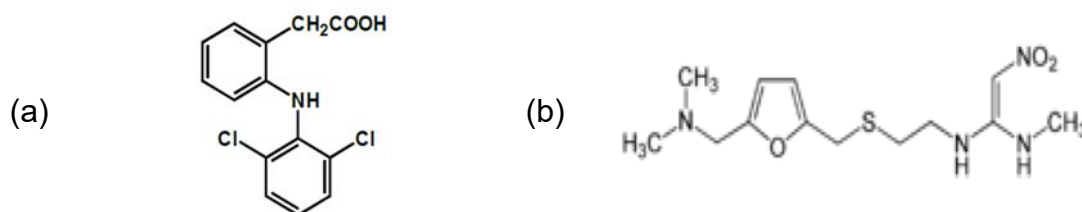
where r is the distance between two hydrophobic molecules, D_H is the empirical hydrophobic decay length, and σ is the diameter of the molecule. The hydrophobic force needed to separate two molecules is given by

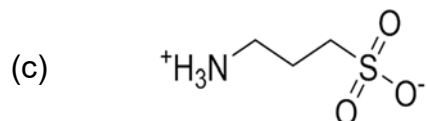
$$F_H(\sigma) = -\left(\frac{dw_H}{dr}\right)_{r=\sigma} \approx -3 \times 10^{-11} \sigma \text{ (nm)} \text{ N at 298 K} \quad (5.33)$$

In contrast to hydrophobic interactions that involves non-polar (water inert) molecules, hydrophilic interactions consider polar molecules, many of them capable of hydrogen bonding. Hydrophilic interactions lead to water solubility of the solute molecules. Most small, charged molecules are hydrophilic, while nonpolar and uncharged molecules may also be hydrophilic depending on whether their geometry allows for hydrogen bonding. The orientation of water on surfaces changes depending if the surface is hydrophobic or hydrophilic. Three order parameters determine this: orientational ordering, positional ordering and density variations. Orientational ordering affects electrostatics, positional ordering affects oscillatory forces, and density variations cause steric repulsions. An orientation restriction occurs on charged hydrophilic surfaces and does not occur on hydrophobic surfaces. Chaotropic agents, such as urea, disrupt local water structure causing proteins to denature. Hydrophilic and hydrophobic interactions are therefore interdependent and not additive.

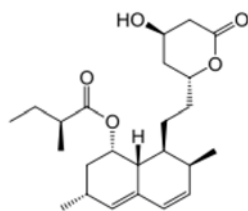
5.5 Review Questions

1. What is the Hydrophobic Effect? How is responsible for increased heat capacities?
2. Assume that a reaction has ΔH of -28 kJ and ΔS of -60 J/K. At what temperature will it change from spontaneous to non-spontaneous? (What sign for Gibbs free energy will a reaction happen spontaneously?)
3. Label the following molecules as hydrophobic or hydrophilic.





(d)



4. For the equation:

$$\Delta\mu_{disp}^i \approx \frac{3hv_I}{4(4\pi\epsilon_0)^2\sigma^6} [(6\alpha_{02}^2 - 12\alpha_{01}\alpha_{02}) - (6\alpha_{03}^2 - 12\alpha_{01}\alpha_{03})]$$

- a. Define all the parameters.
- b. Provide a physical description of each term.
- 5. TRUE/FALSE: A solute dissolving into a solvent with the same material composition ALWAYS has a favorable dispersion self-energy.
- 6. For the equation:

$$\Delta\mu_{disp}^i \approx -\frac{6(3hv_I)}{4(4\pi\epsilon_0)^2\sigma^6} [\alpha_{01} - \alpha_{03}]^2 \propto -(\sqrt{U_1} - \sqrt{U_3})^2 \propto -(n_1^2 - n_3^2)^2$$

Alkanes have a similar refractive index to water, so the equation above suggests that the joining of alkanes together in an aqueous solvent should only be weakly favorable. However, alkanes are mostly insoluble in water, which indicates that the joining of alkanes together in aqueous solvent is highly favorable. Why is the theoretical energy calculated in this equation different from the measured cohesion energy?

- 7. When does the zero-frequency contribution have significant impact on the free energy?
- 8. Why there is a discrepancy between London's dispersion equation and dispersion contribution in McLachlan equation?
- 9. Why the Van der Waals forces become smaller in a solvent medium in comparison with that in the free space?
- 10. In which region is the relationship $n = \sqrt{\epsilon}$ valid?
- 11. What should be considered with interactions in a medium, not in vacuum?

Answer key

1. a) The hydrophobic effect is the free energy that drives reduction in apolar surface area across a reaction equilibrium – the energy gained is dominated by the solvent entropy gained in going from a higher number of lower entropy waters ordered on apolar surfaces to a higher number of higher entropy bulk water molecules upon reduction in apolar surface area exposed to water, it is dominated by this solvent entropy gain but has a small enthalpy associated with it as well, depending on T.

- b) Heat capacity, ΔC_p , is related to the solvent entropy term that represents changes in accessible apolar/polar surface areas across a reaction equilibrium that is driving the hydrophobic effect.
2. A reaction proceeds spontaneously when $\Delta G < 0$, and it is nonspontaneous when it is bigger than zero. We need to set $\Delta G = 0$ and solve the equation for T. Therefore, using equation 5.29, the answer is going to be 467 K. (Negative)
 3. a) hydrophobic b) hydrophobic c) hydrophilic d) hydrophobic.
 4. a) $\Delta\mu_{disp}^i$ = self-energy from dispersion, h = Planck's constant, ν_I = ionization frequency, ϵ_0 = vacuum permittivity, σ = interatomic radius, α_{0x} = electronic polarizability of medium x
 b) $(6\alpha_{02}^2 - 12\alpha_{01}\alpha_{02})$ is the self-energy of solute 1 in medium 2. $6\alpha_{02}^2$ is from the six solvent-solvent bonds that must be broken to create a cavity in solvent 2, while $12\alpha_{01}\alpha_{02}$ is from the twelve solute-solvent bonds that form when the solute enters the cavity. $(6\alpha_{03}^2 - 12\alpha_{01}\alpha_{03})$ is the self-energy of solute 1 in medium 3. $6\alpha_{03}^2$ is from the six solvent-solvent bonds that must be broken to create a cavity in solvent 3, while $12\alpha_{01}\alpha_{03}$ is from the twelve solute-solvent bonds that form when the solute enters the cavity.
 5. TRUE
 6. This equation only gives dispersion self-energy and does not account for other driving forces. In this case, entropy is the main driver of alkanes to self-associate in aqueous solvent, not dispersion forces.
 7. When the refractive indices of solute and solvent molecules are close to each other, the non-zero-frequency contribution becomes small and zero-frequency contribution will be dominant.
 8. Because the absorption frequency of the isolated molecule ν_I is different from the condensed phase ν_e . However, two frequencies can be related via the Clausius-Mossotti-Lorenz equations.
 9. Medium possesses a larger refractive index than the free space.
 10. In visible frequency region.
 11. The displaced solvent polarizability.

Literature – Sources and Further Reading

- (1) Intermolecular & Surface Forces, 3rd Ed., J.N. Israelachvili, Academic Press, Boston (2011), Ch. 6 (6.6-6.8 7) and Ch. 8 (8.5-8.7)

Chapter 6: Van der Waals Forces between Macroscopic Systems and Surface

Van der Waals (VdW) forces are central for our understanding of molecular interactions. Although the magnitude of VdW forces are not as strong as ionic interactions or hydrogen bonding, they are always present regardless the environmental conditions or the degree of separation. In previous chapters, we limited our discussion of VdW forces to pairwise interactions (point-point interactions) of molecular entities. In this chapter, we will expand that view and discuss VdW forces involving macroscopic bodies and surfaces. In particular, we will introduce a macroscopic version of the VdW interaction parameter known as Hamaker constant, and introduce an integrated form of the McLachlan equation, namely, the Lifshitz equations. In our exploration of macroscopic VdW interactions, we will discuss adhesion, molecular adsorption, wetting and electrostatic screening.

6.1 Van der Waals Forces in Macroscopic Molecular Systems

To appreciate the strength, as well as, the length scale over which intermolecular forces between macroscopic bodies can act, we will have to expand our point particle view and contemplate multi-particle interactions that are involved in a body-body interaction, Fig. 6.1. We also have to consider the geometries involved. In a first simplified approach, we consider to sum the pair interactions, point by point. In that sense we impose on the Van der Waals interactions to be additive. In a second, more sophisticated step, we drop the requirement of additivity, which is unsuitable for dispersion forces, and employ a mean-field theory, the Lifshitz theory with bulk properties, the permittivities.

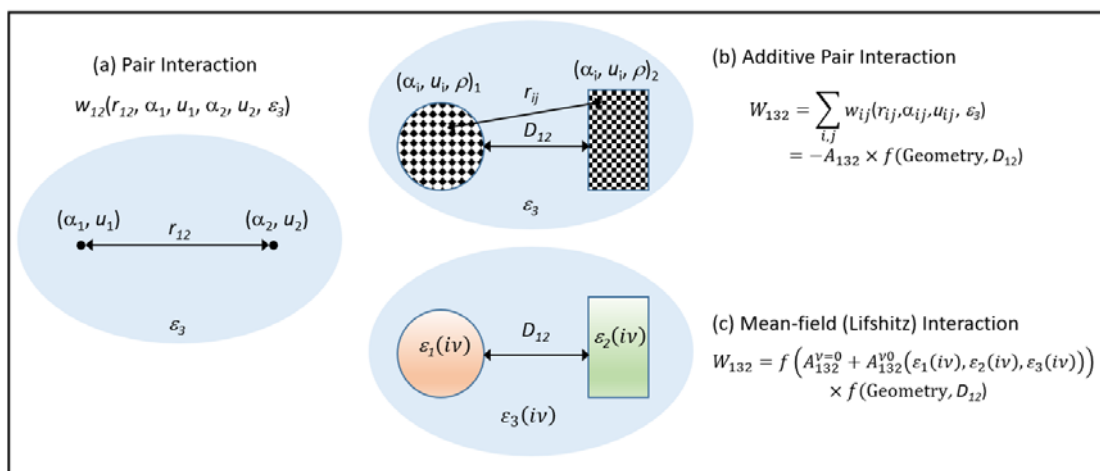


Fig. 6.1: Van der Waals interaction, (a) pair interaction based on molecular properties, (b) summation of pair interactions comprised by the macroscopic VdW interaction parameter A , Mean-field (Lifshitz) interaction based on the permittivity of macroscopic material.

6.1.1 Pairwise Van der Waals Interaction Potential between Macroscopic Bodies

Let us assume that the pair potential between two molecules is attractive and of the form $w(r) = -C/r^n$, where C is the interaction parameter and r is distance between a pair. We consider now the interaction of a molecule at distance D from an infinite half space

("planar surface") of a macroscopic body, as depicted in Figure 6.2. For integration purposes, we assume an infinitesimal circular ring of radius x with cross-sectional area $dxdz$. The ring volume is then given as $2\pi x dxdz$. The number of molecules in the ring is provided by $2\pi\rho dxdz$, where ρ is the number density of the molecules in the solid. Based on this, the net interaction energy between the molecule at distance D and the planar surface is obtained by the following integral

$$\begin{aligned} w(D) &= -2\pi C\rho \int_{z=D}^{z=\infty} dz \int_{x=0}^{x=\infty} \frac{x dx}{(z^2 + x^2)^{n/2}} \\ &= -\frac{2\pi C\rho}{(n-2)} \int_D^\infty \frac{dz}{z^{n-2}} = -\frac{2\pi C\rho}{(n-2)(n-3)D^{n-3}} \end{aligned} \quad (6.1)$$

requiring $n > 3$. If we now consider VdW interactions, we set $n = 6$, which yields an interaction free energy

$$w(D) = -\frac{\pi C\rho}{6D^3} \quad (6.2a)$$

The corresponding force is

$$F(D) = -\frac{dw(D)}{dD} = -\frac{\pi C\rho}{2D^4} \quad (6.2b)$$

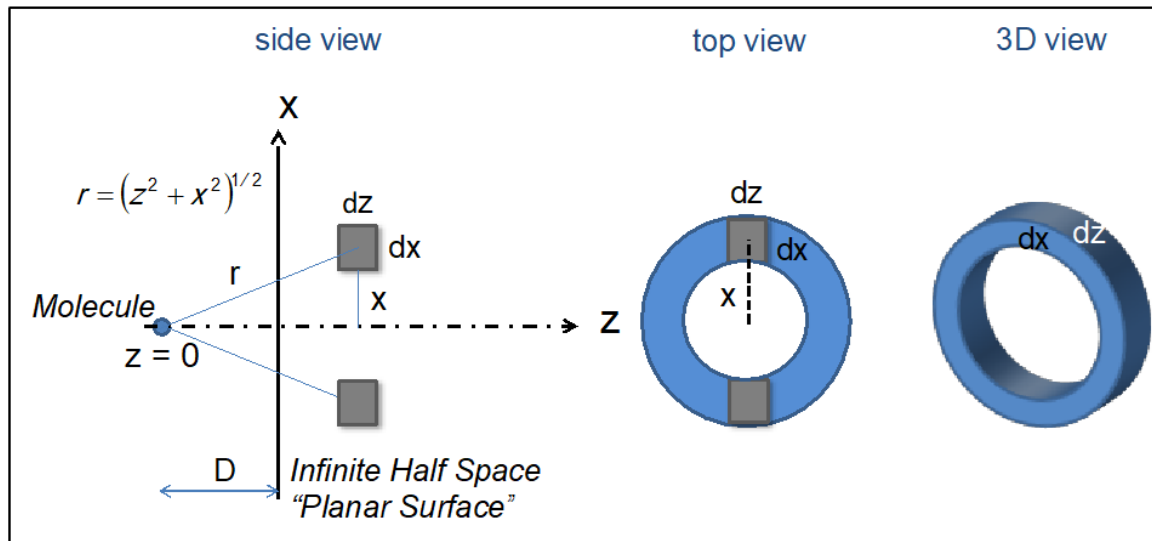


Figure 6.1: Pairwise additivity of a single molecule (at $z = 0$) interacting with a half space (of molecules of number density) at closest distance D . The infinitesimal construct for integration is a ring of radius x with cross-sectional infinitesimal area $dxdz$.

6.1.2 Van der Waals Force-Laws for Bodies of Different Geometries: The Hamaker Constant

Similarly, we can derive the pairwise integrated Van der Waals interaction for different geometries of interacting bodies, such as sphere-sphere, Sphere-plane, and plane-plane interactions, as shown in Figure 6, with their respective VdW interaction free energies $W(D)$, where D represent the shortest distance. In all the energetic expressions, we find the constant $\pi^2 \rho_1 \rho_2 C_{VdW}$, which brings us to define a macroscopic VdW interaction parameter, namely, the Hamaker constant A , i.e.

$$A = \pi^2 \rho_1 \rho_2 C_{VdW} \quad (6.3)$$

Note that based on this definition, the Hamaker constant has the same sign as the Van der Waals interaction parameter C_{VdW} . It follows that for attractive interactions, the Hamaker constant is positive.

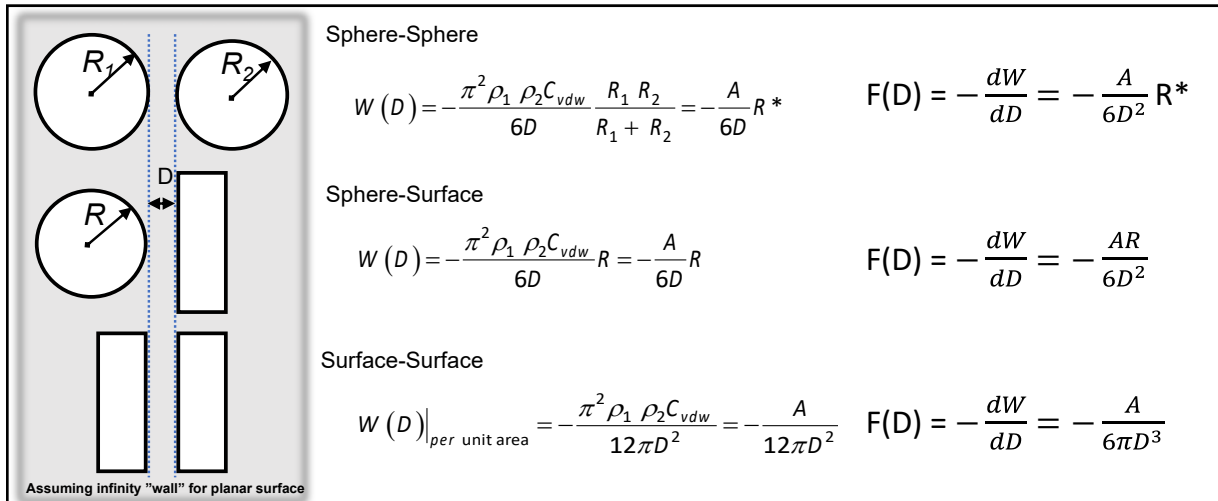


Figure 6.3: Net VdW interaction free energy and force for various geometries employing pairwise additivity. The Hamaker representation (Eq. 6.3) is substituted for each interaction. The convoluted radius $R^* = R_1 R_2 / (R_1 + R_2)$ is used where appropriate. The surface-surface interaction is per unit area and assumes infinite planes.

The following example shall illustrate the strength of adhesion forces assuming a contact distance of 0.2 nm due Pauli repulsive forces.

Worked Problem 6.1

Determine the interaction force between two spheres of radii $R = 1$ cm in contact ($D = 0.2$ nm) for a Hamaker constant $A = 10^{-19}$ J

Solution:

We use the first geometric representation in Figure 6.3, which yields for the force

$$\begin{aligned} W(D) &= \frac{-A}{6D} \left(\frac{R_1 R_2}{R_1 + R_2} \right) \\ &= \frac{10^{-19} \text{ J}}{6 \times 0.2 \times 10^{-9} \text{ m}} \left(\frac{0.01 \text{ m} \times 0.01 \text{ m}}{0.01 \text{ m} + 0.01 \text{ m}} \right) = 4.16666667 \times 10^{-13} \text{ J} \end{aligned}$$

Note that these forces can be measured by conventional means.

Using the Hamaker constant, we can explore the interaction energies (W) and the forces (F) of geometries but also sizes, as further shown in Figure 6.4. For instance, the interaction force between nanoparticles at very close distance (i.e., <1 % of the particle size) still follows the $1/D^6$ power law behavior. In general, the Hamaker constants are on the order of 10^{-19} J for interactions in vacuum. As per the definition of the Hamaker constant, Eq. (6.3), we need the pair interaction parameter C and the number densities in the two solids to calculate it. An example is provided below. Table 6.1 provides three

Hamaker constant values for hydrocarbons, carbon tetrachloride and water. Hamaker constants for Hydrocarbon, CCl_4 , and H_2O are similar although they are vastly different in their size and polarizability. Although this is an oversimplification, the Hamaker constants of condensed matter are usually found in the range $(0.4\text{-}4) \times 10^{-19} \text{ J}$.

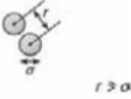
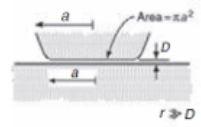
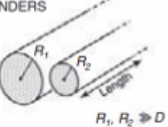
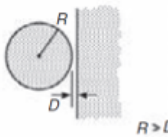
Geometry of bodies with surfaces D apart ($D \ll R$)	Van der Waals Interaction*		
	Energy, W	Force, $F = -dW/dD$	
Two atoms or small molecules	TWO ATOMS or SMALL MOLECULES  $r \gg \sigma$	$-C/r^6$	$-6C/r^7$
Two flat surfaces (per unit area)	TWO FLAT SURFACES  $r \gg D$	$W_{\text{flat}} = -A/12\pi D^2$	$-A/6\pi D^3$
Two parallel cylinders or rods of radii R_1 and R_2 (per unit length)	TWO PARALLEL CYLINDERS  $R_1, R_2 \gg D$	$\frac{-A}{12\sqrt{2}D^{3/2}} \left(\frac{R_1 R_2}{R_1 + R_2} \right)^{1/2}$	$\frac{-A}{8\sqrt{2}D^{5/2}} \left(\frac{R_1 R_2}{R_1 + R_2} \right)^{1/2}$
Cylinder of radius R near a flat surface (per unit length)	CYLINDER ON FLAT  $R \gg D$	$\frac{-A\sqrt{R}}{12\sqrt{2}D^{3/2}}$	$\frac{-A\sqrt{R}}{8\sqrt{2}D^{5/2}}$
Two Nanoparticles with radii R_1 and R_2	 $D \ll R_1, R_2$	$-\frac{16}{9} \frac{AR_1^3 R_2^3}{D^6} = -\frac{n_1 n_2 C}{D^6}$ $n_i = \frac{4}{3} \pi R_i^3 \rho_i; i = 1, 2$	$-\frac{n_1 n_2 6C}{D^7}$

Figure 6.4: Net VdW interaction free energy for various geometries and body sizes. (Modified from Source: Intermolecular and Surface Forces, J.N. Israelachvili, Academic Press)

Worked Problem 6.2

Determine the Hamaker constant for a VdW interaction parameter $C = 10^{-77} \text{ J} \cdot \text{m}^6$ and a number density $\rho = 3 \times 10^{28} \text{ m}^{-3}$ in both bodies

Solution:

We use equation 6.3 for calculation of Hamaker constant.

$$\begin{aligned}
 A &= \pi^2 \rho_1 \rho_2 C_{VdW} \\
 &= (3.14159)^2 \times (3 \times 10^{28} \text{ m}^{-3})^2 \times 10^{-77} \text{ J} \cdot \text{m}^6 \\
 &= 8.88 \times 10^{-20} \text{ J}
 \end{aligned}$$

Table 6.1: Van der Waals parameters, number densities and Hamaker Constants.

Medium	$C [10^{-79} \text{ Jm}^6]$	$\rho [10^{28} \text{ m}^{-3}]$	$A [10^{-19} \text{ J}]$
Hydrocarbon	50	3.3	0.5
CCl ₄	1500	0.6	0.5
Water	140	3.3	1.5

6.1.3 Hamaker Constants – Combining Relations

Considering the vast different materials in the world interacting through various fluids, it is often impossible to find data regarding the Hamaker constant for a specific material situation. Frequently, we have to divert to approximate solutions for unknown Hamaker constants that involve *combining relations* of known quantities. One of these combining relationships approximates the Hamaker constant of dissimilar material 1 and 2 through medium 3, by identical material interactions through the same media, i.e.,

$$A_{132} = \pm \sqrt{A_{131}A_{232}} \quad (6.4)$$

In vacuum, this equation simplifies to

$$A_{12} = \pm \sqrt{A_{11}A_{22}} \quad (6.5)$$

Note the nomenclature. We use for the material that interact through the medium, the number 1 and 2, while the medium in-between always carries the number 3. In the case of vacuum (or gas) we drop the medium (i.e., the number 3).

We can also find the following relationships of Hamaker constant for identical material within media 3:

$$A_{131} \approx A_{313} \approx A_{11} + A_{33} - 2A_{13} \approx (\sqrt{A_{11}} - \sqrt{A_{33}})^2 \quad (6.6)$$

Alternatively, Hamaker constant for different material within media can be expressed as

$$A_{132} \approx (\sqrt{A_{11}} - \sqrt{A_{33}})(\sqrt{A_{22}} - \sqrt{A_{33}}) \quad (6.7)$$

We shall illustrate above relations with the next example.

Worked Problem 6.3

Calculate the Hamaker constant for Quartz-Octane-Air.

Quartz: $A_{11} = 6.3 \times 10^{-20} \text{ J}$; Octane: $A_{33} = 4.5 \times 10^{-20} \text{ J}$

Solution:

Using equation 6.7:

$$A_{132} = (\sqrt{A_{11}} - \sqrt{A_{33}})(\sqrt{A_{22}} - \sqrt{A_{33}})$$

1 and 2 interact across medium 3. We treat air as vacuum, i.e., $A_{22} \approx 0$.

$$A(\text{quartz-octane-air}) = (\sqrt{6.3} - \sqrt{4.5})(\sqrt{0} - \sqrt{4.5}) 10^{-20} \text{ J} = -0.82 \times 10^{-20} \text{ J}$$

This result compares well to the more rigorously computed value of $-0.71 \times 10^{-20} \text{ J}$.

As described earlier, the Hamaker constant of molecules in the vacuum state is usually positive, which implies attraction between the identical molecules. However, using above Hamaker constant relations, we can find molecular interactions with negative Hamaker constant, which reflects the repulsive interactions between bodies interacting in specific media. We remember from earlier chapters that the interaction between solutes can turn repulsive, when the permittivity of the solvent exceeds the permittivity of one of the solutes. Returning to the Hamaker constant and Eq. (6.7), we can see that A_{132} turns negative, if the following inequality applies

$$A_{11} < A_{33} < A_{22} \quad (6.8)$$

Thus, repulsion between two dissimilar materials is obtained if the solvent's Hamaker constant is in between the Hamaker constants of the solute materials. Using Eq. 6.6 for identical particles in a medium, that is

$$A_{131} \approx (\sqrt{A_{11}} - \sqrt{A_{33}})^2 \geq 0 \quad (6.9)$$

we find that the solvent can only neutralize attraction forces between two identical molecules.

6.1.4 Derjaguin Approximation

The *Derjaguin Approximation* relates the force law, $F(D)$, between two curved surfaces to the interaction free energy per unit area, $W(D)$, between two planar surfaces. This makes this approximation a very useful tool, since it is usually easier to derive the interaction energy for two planar surfaces rather than for curved surfaces. The *Derjaguin Approximation* reads as follows:

$$F(D)_{\text{curved}} \cong 2\pi R^* W''(D)_{\text{planar}} \quad (6.10)$$

where D is the separation distance, and R^* is the combined curvature of the two surfaces, i.e., $1/R^* = 1/R_1 + 1/R_2$.

The *Derjaguin Approximation* is valid not only for additive inverse power law potentials (such as Van der Waals interactions) but for any type of force law, whether attractive, repulsive or oscillatory, as long as the range of the interaction and the separation distance D is much smaller than the curvature.

To illustrate the power of the *Derjaguin Approximation* we will provide a derivation based on the inverse power law potential. We start with the pair potential

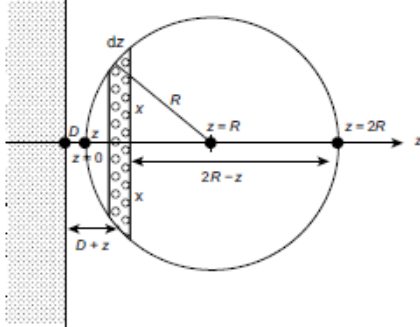
$$w(r) = \frac{-C}{r^n} \quad (6.11)$$

with the interaction parameter C . The interaction distance, r , is provided in Figure (6.5) by

$$r = \sqrt{z^2 + x^2} \quad (6.12)$$

Now we let a single molecule of the sphere at distance D interact with the planar surface in Figure (6.5) which yields the following interaction potential:

$$w(D) = -2\pi C \rho \int_{z=D}^{\infty} dz \int_{x=0}^{\infty} \frac{xdx}{(z^2 + x^2)^{n/2}} = \frac{2\pi C \rho}{(n-2)} \int_D^{\infty} \frac{dz}{z^{n-2}} = \frac{-2\pi C \rho}{(n-2)(n-3)D^{n-3}}; n > 3 \quad (6.13)$$

**Figure 6.5:** Sphere-plane parameters.

If we consider the differential volume $dV = x^2 dz = (2R - z)z dz$ provided by a thin circular section of the sphere of area x^2 and thickness dz , the net interaction energy is

$$W(D) = \frac{-2\pi^2 C\rho^2}{(n-2)(n-3)} \int_{z=0}^{z=2R} \frac{(2R-z)z dz}{(D+z)^{n-3}} \quad (6.14)$$

based on equation (3), a molecule-plane distance of $D+z$, and unchanged number density in the sphere and the plane. For very small distances (i.e., $D \ll R$) only small values of z contribute which simplifies the integral as follows

$$W(D) = \frac{-2\pi^2 C\rho^2}{(n-2)(n-3)} \int_{z=0}^{\infty} \frac{2Rz dz}{(D+z)^{n-3}} \quad (6.15)$$

and yields the following final solution for the interaction energy between curved surfaces

$$W(D) = \frac{4\pi^2 C\rho^2 R}{(n-2)(n-3)(n-4)(n-5)D^{n-5}} \quad (6.16)$$

Note that the radius, R , in Figure (6.5) represents the combined radius, R^* , in the case of two curved surfaces. In the case of Van der Waals forces, i.e., $n = 6$, the interaction energy becomes

$$W(D)_{curved} = \frac{\pi^2 C\rho^2 R}{6D} \text{ (curved surfaces)} \quad (6.17)$$

The force for curved surface interaction will therefore be

$$F(D)_{curved} = -\frac{\partial W(D)}{\partial D} = \frac{-\pi^2 C\rho^2 R}{6D^2} \text{ (curved surfaces).} \quad (6.18)$$

Analogously, one finds for planar surface interactions that

$$W''(D)_{planar} = \frac{-\pi C\rho^2}{12D^2} \text{ (planar surfaces),} \quad (6.19)$$

which leads to the relationship

$$F(D)_{curved} \cong 2\pi R^* W''(D)_{planar} \quad (6.20)$$

confirming the *Derjaguin Approximation*. Consider last, two spheres in contact (D , the interaction distance). The interaction energy W can be replaced by two times the surface energy, which yields a contact interaction force for curved surfaces of

$$F(D)_{\text{curved}} = 4\pi\gamma R^* \quad (6.21)$$

6.2 The Lifshitz Theory of Van der Waals Forces

So far, we assumed simple pairwise additivity and ignored the indirect contribution of neighboring atoms to the interaction energy in the interaction. In rarefied media like gases this effect is negligible, and we can still assume the additivity, but this straightforward additivity breaks down in condensed matters like solids or liquids. This is a huge limitation of the pairwise additivity-based approach of the molecular interaction energy, especially in efforts to compare particles with multiple atomic structures. In the Lifshitz theory, the atomic structure is ignored and the forces based on continuous media, as earlier the McLachlan equation applied to solutions. The Lifshitz theory leaves most of the equations above intact, except that we determine the Hamaker constant based on a mean-field theory using bulk permittivity properties of the materials involved. Based on Lifshitz, the Hamaker constant is determined from

$$\left(A_{132} = \frac{3}{4} kT \left(\frac{\varepsilon_1 - \varepsilon_3}{\varepsilon_1 + \varepsilon_3} \right) \left(\frac{\varepsilon_2 - \varepsilon_3}{\varepsilon_2 + \varepsilon_3} \right) + \frac{3h}{4\pi} \int_{v_1}^{\infty} \left(\frac{\varepsilon_1(iv) - \varepsilon_3(iv)}{\varepsilon_1(iv) + \varepsilon_3(iv)} \right) \left(\frac{\varepsilon_2(iv) - \varepsilon_3(iv)}{\varepsilon_2(iv) + \varepsilon_3(iv)} \right) dv \right) \quad (6.22)$$

where k is the Boltzmann constant, T the absolute temperature, h the Planck constant, $\varepsilon_i = \varepsilon_i(0)$ the zero frequency (static) permittivity of media, $i = 1, 2, 3$, and, $\varepsilon_i(iv)$ the dynamic permittivity. In Eq. (6.10), first term on the right accounts for the polarization interactions that includes the Keesom and Debye contributions. The second term accounts for the dispersion interaction. As with McLachlan, $\varepsilon(iv)$ are “real” values of ε at imaginary frequencies that can be experimentally determined.

The Lifshitz expression of the macroscopic Van der Waals interaction parameter - the Hamaker constant, exhibits, with the polarization and the dispersion, two energy contributions that have distinct features. For one thing, the static polarization cannot exceed $\frac{3}{4}kT$. Furthermore, the dispersion interaction can dominate the overall interaction, if one solute phase or particle phase has a large refractive index. Conversely, the dispersion contribution can vanish, if the refractive index of any solute/particle phase is close to the one of the environmental mediums.

6.2.1 Hamaker Constants for Dielectric media

If we consider two non-conducting(dielectric) material phases or particles (media 1 and 2) defined by the property set $(\varepsilon_1, n_1, \varepsilon_2, n_2)$ in an environmental condensed phase (medium 3) given by (ε_3, n_3) , the time-dependent dispersive component of the dielectric permittivity can be expressed via the damped oscillator model as,

$$\varepsilon(iv) = 1 + \frac{\varepsilon - n^2}{1 + \frac{v}{v_{rot}}} + \frac{n^2 - 1}{1 + \left(\frac{v}{v_e}\right)^2} \approx 1 + \frac{n^2 - 1}{1 + \left(\frac{v}{v_e}\right)^2} \quad (6.11)$$

The approximation on the right-hand side neglects the rotational contribution due to the fact that already the onset (lowest) frequency for dispersion, $\nu_1 = 4 \times 10^{13} \text{ s}^{-1}$ exceeds the rotational relaxation frequency $v_{rot} \sim < 10^{13} \text{ s}^{-1}$, by good an order of magnitude. Let us determine in the following worked example the refractive index of water.

Worked Problem 6.4

Determine the dynamic refractive index $n_w, \varepsilon_w(iv)$ of water at $\varepsilon = 3.0 \times 10^{15} \text{ s}^{-1}$ for a measured dynamic permittivity of 0.2318 at room temperature.

Solution:

We use the approximation of Eq. (6.11)

$$\varepsilon(iv) \approx 1 + \frac{n^2 - 1}{1 + \left(\frac{v}{v_e}\right)^2}$$

and substitute for v and $\varepsilon_w(iv)$ the values $3.0 \times 10^{15} \text{ s}^{-1}$ and 0.2318, respectively. Forming around for the refractive index yields $n_w = 1.333$.

If we now substitute the expression of dynamic dielectric permittivity, Eq. (6.11), into the Lifshitz Eq. (6.10) and integrate, whereby we assume for the three media the same electron absorption frequency ν_e , the Lifshitz representation of the Hamaker constant simplifies to,

$$A_{132} \approx \frac{3}{4} kT \left(\frac{\varepsilon_1 - \varepsilon_3}{\varepsilon_1 + \varepsilon_3} \right) \left(\frac{\varepsilon_2 - \varepsilon_3}{\varepsilon_2 + \varepsilon_3} \right) + \frac{3hv_e}{8\sqrt{2}} \frac{(n_1^2 - n_3^2)(n_2^2 - n_3^2)}{\sqrt{(n_1^2 + n_3^2)} \sqrt{(n_2^2 + n_3^2)} \left\{ \sqrt{(n_1^2 + n_3^2)} + \sqrt{(n_2^2 + n_3^2)} \right\}} \quad (6.12)$$

Let us further assume two identical materials that interact through medium 3, the Lifshitz equation simplifies to

$$A_{131} \approx \begin{cases} \frac{3}{4} kT \left(\frac{\varepsilon_1 - \varepsilon_3}{\varepsilon_1 + \varepsilon_3} \right)^2 + \frac{3hv_e}{16\sqrt{2}} \frac{(n_1^2 - n_3^2)^2}{(n_1^2 + n_3^2)^{3/2}} \\ A_{131}^{(\nu=0)} \quad + \quad A_{131}^{(\nu>0)} \end{cases} \quad (6.13)$$

where the first term on the right-hand side reflects the static Hamaker constant, and the second term, the dynamic Hamaker constant contribution.

If we set $\varepsilon_3 = 1$ and $n_3 = 1$, the Lifshitz equations (6.12-13) yields the non-retarded Hamaker constant for dielectric material phases in “vacuum”. Selected identical material examples, employing Eq. (6.13), are provided in Table 6.2 and compared to exact computed solutions involving to part Eqs (6.10) and (6.11) and experimentally determined functions of the dielectric permittivity. We illustrate in the worked example below how to obtain the Hamaker constant of water-water interaction through inert air at 300 K

Table 6.2: Hamaker Constants for Two Identical Media Interacting in inert air at 300 K

Medium	Dielectric Constant	Refractive Index	Absorption Frequency $\nu_e (10^{15} \text{ s}^{-1})$	Hamaker Constant $A (10^{-20} \text{ J})$			
				Lifshitz Theory	Exact solutions	Pairwise Additivity	Experiment
Liquid He	1.057	1.028	5.9	0.057			
Water	80	1.333	3.0	3.7	3.7-5.5	15	
n-Pentane	1.84	1.349	3.0	3.8	3.75		
n-Dedecane	2.01	1.411	3.0	5.0	5.0		
Hydrocarbon	2.25	1.50	3.0	7.1		5.0	
Polystyrene	2.55	1.557	2.3	6.5	6.6-7.9		
PTFE	2.1	1.359	2.9	3.8	3.8		
Silica	3.8	1.448	3.2	6.3	6.5		5-6
Metals (Au,Ag,Cu)	∞	—	3-5	25-40	20-50		

Worked Problem 6.5

Determine the Hamaker constant between water-water (identical media) interacting in inert air at 300 K.

Solution:

The static permittivity of water ε_w is approximately 80 at room temperature. Its static refractive index n_w and absorption frequency ν_e are 1.333 and $3.0 \times 10^{15} \text{ s}^{-1}$, respectively. The dynamic refractive index ε_w (i.e.) is 1.33 (see Worked Example 1). We utilize Eq. (6.13) to determine the Hamaker constant, i.e.,

$$A_{131} \approx \frac{3}{4} kT \left(\frac{\varepsilon_w - 1}{\varepsilon_w + 1} \right)^2 + \frac{3h\nu_e}{16\sqrt{2}} \frac{(n_w^2 - 1)^2}{(n_w^2 + 1)^{3/2}}$$

in which we replaced ε_w for ε_1 and for the surrounding medium $\varepsilon_3 = n_3 = 1$. Substituting the value for the Boltzmann constant k , the Planck constant h and property values above, yields

$$\begin{aligned} A_{ww} &= \frac{3}{4} \left(1.38 \times 10^{-23} \frac{\text{J}}{\text{K}} \right) (300 \text{ K}) \left(\frac{80 - 1}{80 + 1} \right)^2 + \\ &\quad + \frac{3(6.63 \times 10^{-34} \text{ J} \cdot \text{s})(3.0 \times 10^{15} \text{ s}^{-1}) (1.33^2 - 1)^2}{16\sqrt{2}} \frac{1}{(1.33^2 + 1)^{3/2}} \\ &= 3 \times 10^{-21} \text{ J} + 3.4 \times 10^{-20} \text{ J} \\ &= 3.7 \times 10^{-20} \text{ J} \end{aligned}$$

which compares well to the exact solution of $3.7-5.5 \times 10^{-20} \text{ J}$

In Figure 6.6, we illustrate the dielectric permittivity of a two phase (symmetric case) system, namely water and the hydrocarbon, dodecane. We can consider the continuous medium (ε_3, n_3) to be water and the two identical phases to be dodecane (ε_1, n_1). Superimposed (dashed line) is the non-retarded dispersion expressed in terms of the permittivities involved at given frequencies. The area underneath that curve is

proportional to the non-retarded dispersion energy $A_{\nu>0}$, as expressed by Eq. (6.13), involving both the water and hydrocarbon phase. In the following worked example, we determine the total Hamaker constant between two dodecane phases across water, and its static and dynamic contributions.

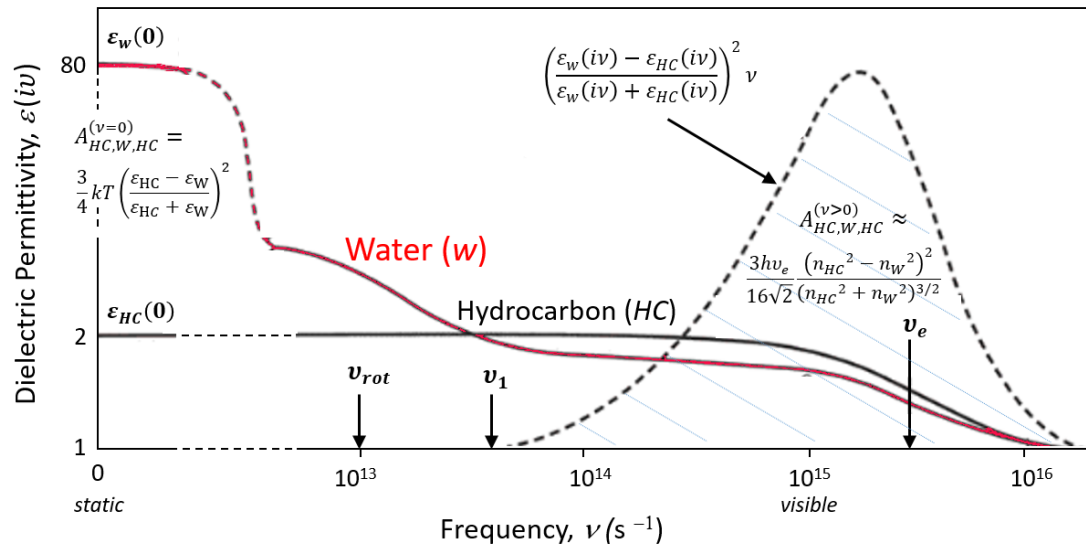


Figure 6.6: Dielectric permittivity $\epsilon(i\nu)$ as a function of frequency ν for water and hydrocarbon.

Worked Problem 6.6

Determine (a) static Hamaker contribution, (b) the dynamic Hamaker constant to (c) the total Hamaker constant between two dodecane phases across water. The necessary property value can be obtained from Table 6.2.

Solution:

$$(a) A_{131}^{(\nu=0)} = \frac{3}{4} kT \left(\frac{\epsilon_1 - \epsilon_3}{\epsilon_1 + \epsilon_3} \right)^2 = \frac{3}{4} \left(1.38 \times 10^{-23} \frac{\text{J}}{\text{K}} \right) (300 \text{ K}) \left(\frac{2.01 - 1}{2.01 + 1} \right)^2 = 3.5 \times 10^{-22} \text{ J}$$

$$(b) A_{131}^{(\nu>0)} = \frac{3hv_e}{16\sqrt{2}} \frac{(n_1^2 - n_3^2)^2}{(n_1^2 + n_3^2)^{3/2}} = \frac{3(6.63 \times 10^{-34} \text{ J·s})(3.0 \times 10^{15} \text{ s}^{-1})}{16\sqrt{2}} \frac{(1.411^2 - 1)^2}{(1.411^2 + 1)^{3/2}} = 5 \times 10^{-20} \text{ J}$$

$$(c) A_{total} = A_{131}^{(\nu=0)} + A_{131}^{(\nu>0)} \approx 5 \times 10^{-20} \text{ J}$$

6.2.2 Hamaker Constant for Conducting media

Moving on from dielectric (or non-conducting) media to conducting materials (e.g., metals) and aqueous solutions, we have to anticipate very high refractive indices, leading (if we would employ the Lifshitz approximation above) to unreasonably high Hamaker

constants. This is due to free flow of charges. This brings us back to the functional expression of the permittivity in terms of frequency. It was found that the most appropriate expression for metals is approximately given by

$$\varepsilon(v) \approx 1 - \frac{v_e^2}{v^2}$$

so that, if expressed for imaginary frequencies,

$$\varepsilon(iv) \approx 1 - \frac{v_e^2}{v^2} \quad (6.14)$$

It follows for two identical metals within vacuum, the Lifshitz approximation of the Hamaker constant for metals is

$$A_{11} \approx \frac{3}{4} kT \left(\frac{\varepsilon_1 - 1}{\varepsilon_1 + 1} \right)^2 + \frac{3hv_e}{16\sqrt{2}} \frac{(n_1^2 - 1)^2}{(n_1^2 + 1)^{3/2}} \quad (6.15)$$

This equation can be further simplified by considering that the dielectric permittivities and refractive indices are large for metals, to

$$A_{11} \approx \frac{3}{4} kT + \frac{3hv_e}{16\sqrt{2}} \approx 4 \times 10^{-19} \text{ J} \quad (6.16)$$

if we assumed for $v_e = 4 \times 10^{15} \text{ s}^{-1}$. Notice that the value obtained for the Hamaker constant is on order of one magnitude higher than those of non-conducting media. In addition, we can see that the first term, the static polarization, with only $3 \times 10^{-21} \text{ J}$, contributes little to the total Hamaker constant. Hence, the non-zero frequency dispersion energy dominates the Van der Waals interaction for metals.

Finally, we address the Van der Waals interaction between a metal and a dielectric media through a medium. It was shown that the following approximate equation

$$A_{132} \approx \frac{3}{8\sqrt{2}} \left(\frac{n_1^2 - n_3^2}{n_1^2 + n_3^2} \right) \frac{h\sqrt{v_1 v_3} \cdot v_2}{(\sqrt{v_1 v_3} + \frac{v_2}{\sqrt{n_1^2 - n_3^2}})} \quad (6.17a)$$

provides a good estimate of interactions between dielectric/ceramic materials (n_1, ε_1) and metals (n_2, ε_2) through an intervening liquid (ε_3). In the case of a vacuum environment, the equation simplifies to

$$A_{12} \approx \frac{3}{8\sqrt{2}} \left(\frac{n_1^2 - 1}{n_1^2 + 1} \right) \frac{hv_1 v_2}{(v_1 + v_2 / \sqrt{n_1^2 - 1})} \quad (6.17b)$$

Also, in the metal-dielectric interaction the dispersion term dictates the overall Van der Waals interaction, which is consistent with our earlier statement that the dispersion energy dominates, when one material possesses a large refractive index.

6.2.3 Theoretical and Experimental Hamaker Constants Comparison

To conclude, we compare theoretical and experiment Hamaker constants to see how the calculated values obtained from approximation equations match the exact computed solutions and experimental results. Table 6.2 already showed good correspondences between our approximations and the full Lifshitz equation. If we compared the calculated Hamaker constants in Table 6.2 with the results determined earlier from pairwise

additivity, we find differences for materials with high permittivity, because pairwise additivity overestimates the contribution of the zero-frequency contributions.

From Table 6.3, we can infer that there is a good agreement between calculated and experimental Hamaker constants across different media. In general, for non-conducting (dielectric) materials, the Hamaker constant across various media is much smaller than that across vacuum or air. We notice that the third medium influence of conducting material interaction is negligible due to the metals high permittivity and refractive index.

Table 6.3: Hamaker Constants for Media 1 and 2 Interacting across Medium 3 at Room Temperature

<i>Interacting Media</i>			<i>Hamaker Constant A (10⁻²⁰J)</i>		
1	3	2	<i>Lifshitz Theory</i>	<i>Exact solution</i>	<i>Experiment</i>
Air	Water	Air	3.7	3.7	
Octane	Water	Octane	0.36	0.4	
Dodecane	Water	Dodecane	0.44	0.4-0.5	0.5
Water	Hydrocarbon	Water	0.3-0.5	0.34-0.54	0.3-0.9
Ag, Cu, Au	Water	Ag, Cu, Au	—	10-40	40 (gold)
Water	Pentane	Air	0.08	0.11	
Water	Octane	Air	0.51	0.53	
Mica	Water	Mica	2.0	1.3-2.9	2.2

6.3 Effect of Wetting Films and Disjoining Films

As pointed out earlier, the Hamaker function is positive when van der Waals interactions are attractive. However, there are situations where the Hamaker function is negative and the van der Waals interactions are repulsive. We saw this in the previous section on the Lifshitz theory applied to the intervening medium that exhibit a permittivity between that of the two interacting media. We will apply this concept to explain the wetting properties of liquid helium.

6.3.1 Superfluid Helium – A Wetting Film

As illustrated in Figure (6.7), liquid helium shall exist at -270 °C (around 3 K). At this point the molecules exhibit a unique property of being able to climb up and over the sides of a beaker as well as being able to seep through quantum sized imperfections in the bottom of a beaker. There is no friction between the molecules due to a coordinated action between the atoms. This unique effect of the liquid state of helium can be explained by its low permittivity of $\epsilon \approx n^2 = 1.057$, which is lower than for most materials as it nears that of vacuum.

In the container that holds helium, there is helium vapor that sits at the surface of the liquid. The permittivity of the helium vapor phase is greater than that of the liquid phase. Due to this difference in ϵ , there is a repulsive van der Waals force occurring at the

interface between the vapor phase and the liquid phase. The repulsive force causes the energy of the liquid to decrease and the liquid will climb the walls of the container in order to recover VdW energy. (You could also say the vapor pushes the liquid up at the vessel wall.)

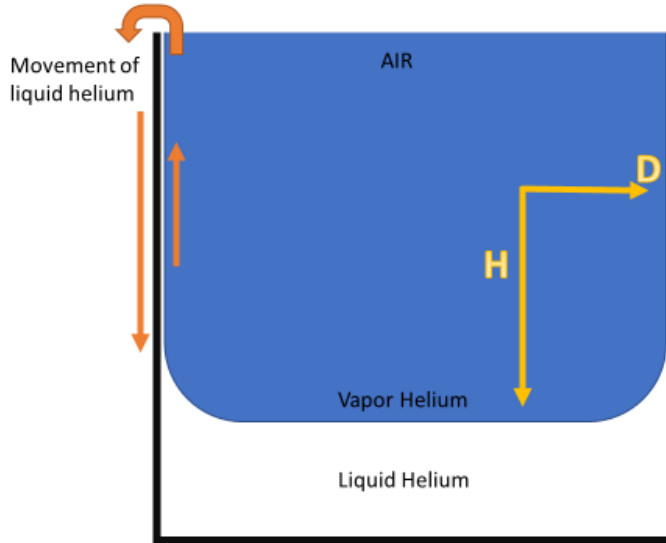


Figure 6.7: Illustration of liquid helium crawling up sides of container.

However, there is also gravitation energy that comes into play when the liquid changes height. As the height increases, gravitational energy will decrease the driving force for liquid helium to climb up. The net energetic effect per unit area (J/m^2) is given as:

$$G(D) = -\frac{A}{12\pi D^2} + mgH \quad (6.30)$$

where A is the Hamaker constant, m is the mass, D is the thickness at height H , and g is the gravitational acceleration ($9.81 m/s^2$). As long as $G(D)$ is negative, liquid helium will keep climbing up. We relate the mass to the density ρ per unit length, i.e., $m = \rho D$, which yields for Eq. 6.30,

$$G(D) = -\frac{A}{12\pi D^2} + \rho g H D \quad (6.31)$$

At steady state, we can assume for any film thickness H , the film of liquid helium is at equilibrium, that is $dG/dD = 0$. Hence, we solve for the pressure (force per unit area)

$$G(D)' = \frac{2A}{12\pi D^3} + \rho g H = \frac{A}{6\pi D^3} + \rho g H = 0 \quad (6.32)$$

Rearrangement of Eq. (6.32) yields for the film thickness D at height H :

$$D = \left(-\frac{A}{6\pi\rho g H} \right)^{1/3} \quad (6.32)$$

As $D > 0$, this equation requires for A , the Hamaker value, to be negative, and therefore implies that the repulsive VdW pressure force is maintained across the film.

Returning to the equilibrium condition, Eq. 6.32, we find with $A/6\pi D^3 < 0$ a repulsive VdW pressure across the entire film. If we replace $A/6\pi D^3$ by $P(D)$, we can write Eq. 6.32 as

$$P(D) = +\rho g H \quad (6.33)$$

This repulsive pressure is known as the *disjoining pressure*. It can arise from any type of interaction. Considering the figure earlier in this section, it is important to note that the thickness and height that the liquid reaches, as it crawls up the container wall, is not dependent on the amount of the liquid in the entire container. The equilibrium height is dependent upon the vapor pressure at the flat liquid surface.

With the barometric distribution law of the relative vapor pressure p/p_o ,

$$p/p_o = e^{-\rho v g H / kT} \quad (6.34)$$

where v is the molecular volume, we can express under equilibrium condition, $G(D)' = 0$, the disjoining pressure as,

$$P(D) = -(kT/v)\ln(p/p_o) = -(RT/V)\ln(p/p_o) \quad (6.35)$$

where V represents the molar volume. This equation is useful because it shows how the equilibrium thickness can be changed based on the relative vapor pressure, p/p_o . This allows for vapor pressure control instead of gravitational control.

6.4 Retardation: Separation Effect on Van der Waals Interaction

When comparing experimental values of VdW dispersion interactions with values derived based on the various VdW equations above, we find strong discrepancies for distances exceeding ~ 10 nm. This is due to the *retardation effect*, which is a manifestation of the time-delayed response to dispersion interactions. The effect is most noticeable in macroscopic interactions, where forces are still significant at larger distances. As a consequence, it is to note that the VdW interaction parameter, the Hamaker constant, is not actually constant. It slowly decreases as the distance between the interacting objects increases. It is manifested in the measured forces over distance in Fig. 6.8.

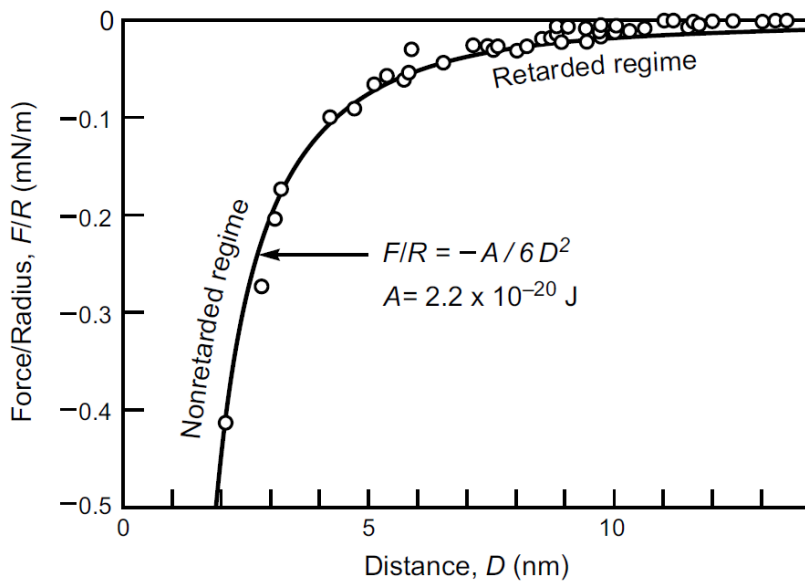
The Lifshitz equations do not include effects of time delays of responses to interactions. As there is no simple fix to account for time induced retardation effect on the VdW formulism, the here empirically derived equation shall serve as an approximation for the (dispersion) Hamaker constant in the transition region from the non-retarded to retarded regime. It is

$$A = \frac{A_{\text{non-ret}}}{\left(1 + \frac{pDv_e}{c}\right)} = \frac{A_{\text{non-ret}}}{\left(1 + \frac{pD}{100 \text{ nm}}\right)} \quad (6.36)$$

where p is the dimensionless interaction density, $A_{\text{non-ret}}$ is the non-retarded Hamaker constant, we used throughout this chapter so far, and D is the distance between the two interacting materials. The interaction density depends on the geometries involved and is provided for some geometries in Table 6.4, and further discussed below.

Table 6.4: Density Compilation of Different Interacting Geometries

First Surface	Second Surface	Interaction Density (ρ) [...]
Plane	Plane	5.3
Sphere	Sphere	11
Plane	Sphere	14

**Figure 6.8:** Attractive VDW force F between two curved mica surfaces of radius R measured in water and aqueous electrolyte solutions. (Israelachvili)

6.4.1 Retardations Considering Two Spheres

When considering two spheres, the non-retarded force, F_{disp} , is proportional to the negative inverse of the thickness, while F_{disp} of the retarded force between two spheres is proportional to $-1/D^2$. The transition between the non-retarded regime and the retarded regime occurs around a 10 nm distance. Approaching the retarded regime, the inverse power law dependence of the dispersion force increases the exponent by 1 while the zero-frequency temperature dependent contribution does not change since it is not affected by retardation.

6.4.2 Metals

When considering metals, the dispersion forces are very high and dominate the zero-frequency polarization contribution. This leads to high retarded dispersion forces noticeable over large separations ($\sim 10 \mu\text{m}$).

6.4.3 Hydrocarbons Interacting Across Water

In considering the interaction of hydrocarbons across water, the short distance non-retarded dispersion is small in comparison to the zero-frequency contribution. The long

range VdW force is dominated by the non retarded temperature dependent contribution even though this is a slightly weaker force overall.

6.4.4 Two Surfaces in a Vacuum

The fully retarded interaction between two surfaces in a vacuum can be represented by the equation below:

$$F(D) = \frac{kT}{16\pi D^2} \left(\frac{\varepsilon - 1}{\varepsilon + 1} \right)^2 - \frac{\pi hc}{1440 D^2} \left(\frac{\varepsilon - 1}{\varepsilon + 1} \right)^2 f(\varepsilon) \quad (6.37)$$

The first term represents the normal non-retarded contribution, which decays at $1/D^2$. The second term of the equation represents the decay depending on $1/D^3$. The final function is roughly constant when ε is less than 4 and increases asymptotically towards 1 at higher ε .

6.4.5 Casimir Equation

The equation below represents the force per unit area of metals and other conducting media when the dielectric constant is approaching infinity.

$$\begin{aligned} F(D) &= -\frac{\partial W}{\partial D} = -\left(\frac{kT}{8\pi D^3} + \frac{\pi hc}{480 D^4} \right) \\ &= -\frac{1.64 \times 10^{-22}}{D^3} \left(1 + \frac{7.95 \times 10^{-6}}{D} \right) Nm^{-2} \end{aligned} \quad (6.38)$$

The second term in the equation above is the well-known as the Casimir equation, which is found in the Lifshitz theory. The retarded dispersion force dominates the interaction of distances at and above 10nm. Below this distance the regime becomes non-retarded.

6.4.6 Wetting films – Hydrocarbon Films on Water

The non-retarded Hamaker constant of hydrocarbon, pentane film on water is very small (c.f. Table 6.2), $A \approx 10^{-21}$ J, which is from the negative zero frequency contribution of $A_{v=0} = 0.8 \times 10^{-21}$ J and the positive dispersion contribution $A_{v>0} = 1.6 \times 10^{-21}$ J. The positive dispersion will dominate at small distances. At large distances, retardation effects take hold of the positive dispersion forces and its value will decrease. This causes A to change sign at a particular separation distance. This is why pentane spreads on water while dodecane does not. The higher molecular weight alkane's positive dispersion force contributes more and prevents spreading on water.

6.5 The Electrolyte Screening Effect

Recall in earlier chapters the Debye screening length is the length at which the electric field is screened dependent on distance. The decay is represented by k^{-1} and is also known as the Fermi screening length. This electric screening only affects the zero frequency contribution, $A_{v=0}$. The dispersion contribution, $A_{v>v_1}$ remains unaffected because the electrolyte ions cannot respond at high frequencies. The screened non retarded Hamaker constant is below:

$$A = A_{v=0}(e^{-kD}) + A_{v>v_1} \quad (6.39)$$

The screening of $A_{v=0}$ is analogous to the retardation of $A_{v>v_1}$, but only occurs at small separations. For interparticle interactions across such a solution at more than 2 nm, the attraction is determined solely by the dispersion force.

6.6 Work of Adhesion

The *work of adhesion* (W_{adh}), also called *adhesion energy*, is defined as the energy required to separate two bodies from contact to infinity. Attributing half of the work of adhesion to each surface, we introduce the so-called *interfacial energy* (γ). Interfacial and adhesion energy are both opposite in sign to the stored energy between the two surfaces, so they are positive when the surfaces and bodies have a net attraction and negative when the surfaces and bodies have a net repulsion.

6.6.1 Adhesion Energy Between Two Planar Surfaces

The energy between two planar surfaces at a separating distance D , excluding bulk cohesive interactions, is:

$$\Delta W = W(D_o) - W(D) = -\frac{A}{12\pi} \left(\frac{1}{D_o^2} - \frac{1}{D^2} \right) = -\frac{A}{12\pi D_o^2} \left(1 - \left(\frac{D_o}{D} \right)^2 \right) \quad (6.40)$$

in which A is the Hamaker constant, W is the interaction free energy between the two surfaces per unit area, and D_o is the closest the two surfaces can get to each other due to Pauli repulsion. D_o is known as the “cutoff” distance. If $D = D_o$, the two planes are in contact, and $\Delta W = 0$. If D approaches infinity, the planes are far apart, the subtracted quotient $(D_o/D)^2$ approaches 0, and the energy between the two planes per unit area becomes:

$$\Delta W = -\frac{A}{12\pi D_o^2} \quad (6.41)$$

Because W_{adh} and γ are defined in terms of the energy change when the surfaces are separated by an infinite distance, rather than the energy change when the surfaces come together from an infinite distance, the work of adhesion and the interfacial energy per unit area are

$$W_{adh} = \frac{A}{12\pi D_o^2} \quad \text{and} \quad \gamma = \frac{1}{2} W_{adh} = \frac{A}{24\pi D_o^2} \quad (6.42)$$

respectively.

6.6.2 Adhesion Energy Between Surfaces with Different Geometries

A similar process can be used to calculate the work of adhesion between two surfaces with other geometries by using the van der Waals energies. For instance, to calculate the work of adhesion between a surface composed of spheres and a planar surface (Figure 6.9), one would multiply the energy between each sphere and the plane by the surface density of the spheres.

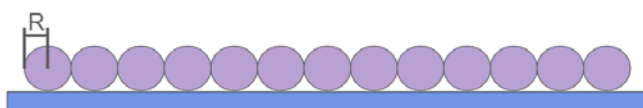


Figure 6.9: A surface composed of spheres of radii R contacting a planar surface.

Based on Figure 6.3, when the separation distance D between the two surfaces approaches infinity, the individual energy between a sphere and the plane per unit area is

$$\Delta W_{ind.} = \frac{-AR}{6D_0} \quad (6.43)$$

Assuming compact packing, the surface density of the spheres is $\rho_{surf} = \frac{1}{2\sqrt{3}R^2}$. Therefore, the total energy per unit area between the two surfaces is

$$\Delta W_{total} = \Delta W_{ind.} \rho_{surf} = -\frac{A}{12\sqrt{3}D_0R} \quad (6.44)$$

The adhesion energy and interfacial energies per unit area are

$$W_{adh} = \frac{A}{12\sqrt{3}D_0R} \quad \text{and} \quad \gamma = \frac{A}{24\sqrt{3}D_0R} \quad (6.45)$$

If R approaches D_o , then the work of adhesion is similar between two planes and a plane with a surface of close-packed spheres. If $R \gg D_o$, however, as is true for large structures like C_{60} , the adhesion energy between the two planes is significantly higher. Intuitively, this makes sense because the larger the spheres, the fewer close, high-energy interactions can form between the sphere's surface and the contacting plane. The smaller the spheres, the more the sphere-covered surface resembles a smooth plane, and the more similar the adhesion energy is to the adhesion energy between two smooth planes.

6.6.3 Estimating the Cutoff Distance

Counterintuitively, the cutoff distance D_o is *not* the same as the interatomic radius σ . However, D_o can be estimated using σ , as seen by calculating the interfacial energy γ of an individual atom or molecule. In a close-packed lattice with a planar surface, each surface molecule has only 9 nearest-neighbor interactions, compared to the 12 that bulk molecules can have. Each interaction provides an energy contribution of $w = -C/\sigma^6$. The Hamaker constant is as per definition $A = \pi^2 C \rho^2$ for two surfaces of the same composition. The surface and bulk densities for a close-packed structure are $\rho_{surf} = \frac{1}{\sigma^2 \sin(60^\circ)}$ and $\rho_{bulk} = \frac{\sqrt{2}}{\sigma^3}$. Therefore, the interfacial energy per unit area is

$$\begin{aligned} \gamma &\approx -\frac{1}{2}(3w)\rho_{surf} \approx \frac{3C}{2\sigma^6 \sigma^2 \sin(60^\circ)} \approx \frac{3C}{\sigma^8 \sqrt{3}} \approx \frac{\sqrt{3}C\rho_{bulk}^2}{2\sigma^2} \approx \frac{\sqrt{3}A}{2\pi^2 \sigma^2} \\ &\approx \frac{A}{3.63\pi\sigma^2} \approx \frac{A}{24\pi \left(\frac{\sigma}{2.5}\right)^2} \end{aligned} \quad (6.46)$$

It follows that for the contact distance,

$$D_o \approx \frac{\sigma}{2.5} \quad (6.47)$$

Using $D_o = 0.165$ nm, Eq. (6.46) can be rearranged to yield an alternative way to estimate the Hamaker constant, this time based on the interfacial energy,

$$A = 2.1 * 10^{-24} \gamma \text{ Joules} \quad (6.48)$$

Remarkably, using an interatomic distance of $\sigma = 0.4 \text{ nm}$ ($D_o = 0.165 \text{ nm}$), the theoretical interfacial energy is within 10-20% of the measured interfacial energy for a large variety of solids and liquids. Table 6.5 provides calculated surface energies based on Hamaker constants obtained from the Lifshitz theory and Eq. (6.46) with $D_o = 0.165 \text{ nm}$. Since this 10-20% error in magnitude is comparable to the error in computing Hamaker constant values, the rough approximations performed above do not seem to have significantly increased the overall error. Because Hamaker constant approximations are notoriously poor if metals or hydrogen and electronegative atoms are involved, Eq. (6.46) is inaccurate when the interaction includes metal or significant hydrogen-bonding. Poor agreement between theoretical and measured adhesion energies when strong hydrogen bonds are involved can be seen in the bottom panel of Table 6.5.

Table 6.5: Calculated Surface Energies based on Lifshitz Theory.

Material (ϵ) in Order of Increasing ϵ	Theoretical A (10^{-20} J)	Surface Energy, γ (mJ m^{-2})	
		Simple Theory $\gamma = A/24\pi D_0^2$ ($D_o = 0.165 \text{ nm}$)	Experiment (20°C)
Liquid helium (1.057)	0.057	0.28	0.12–0.35
<i>n</i> -Perfluoro-pentane (1.72)	2.59	12.6	10.3
<i>n</i> -Pentane (1.8)	3.75	18.3	16.1
<i>n</i> -Octane (1.9)	4.5	21.9	21.8
Cyclohexane (2.0)	5.2	25.3	25.5
<i>n</i> -Dodecane (2.0)	5.0	24.4	25.4
<i>n</i> -Hexadecane (2.1)	5.2	25.3	27.5
PTFE (2.1)	3.8	18.5	18.3
CCl ₄ (2.2)	5.5	26.8	29.7
Benzene (2.3)	5.0	24.4	28.8
Rubber (2.35)	5.7	27.8	35
Polystyrene (2.6)	6.6	32.1	33
Polydimethyl-siloxane, PDMS (2.75)	4.4	21.4	21.8
Polyvinyl chloride (3.2)	7.8	38.0	39
Acetone (21)	4.1	20.0	23.7
Ethanol (26)	4.2	20.5	22.8
<hr/>			
Methanol (33)	3.6	18	23
Glycol (37)	5.6	28	48
Glycerol (43)	6.7	33	63
Water (80)	3.7	18	73
Hydrogen peroxide H ₂ O ₂ (84)	5.4	26	76
Formamide (109)	6.1	30	58
<hr/>			
Adhesion energy in a medium ^b $W = -2\gamma_i = -A/12\pi D_0^2$ (mJ m^{-2})			
Mica in water and dilute NaCl and KCl solutions	2.0	19	~10

Adapted from Israelachvili, *Intermolecular and Surface Forces*, Third Edition [1].

6.7 Interfacial Energy Involving Metals

6.7.1 Limitations of Previous Interfacial Energy Equations

One problem with using Eq. (6.46) for determining interaction parameters involving metal surfaces is that metallic interfaces have smaller effective cutoff distances than the interfaces between VdW solids and liquids listed in Table 6.5. Smaller D_o lead to larger measured interfacial energies γ than the interfacial energies calculated using Eq. (6.46) with $D_o = .165 \text{ nm}$. Lattice incommensurability, which is when the two adjacent lattices of each surface are not aligned, is another source of error. Incommensurate lattices occur when the two lattices have differently spaced nodes, as between most dielectrics (such as ceramic) and metals, or when two lattices with equal lattice spacing are offset or rotated relative to each other (see Figure 6.10). Since most systems involving a dielectric and a metal have differently spaced nodes, there is larger variation in the interfacial energy between such asymmetric systems than would be ill-predicted with Eq. (6.46), depending on how far nodes are from each other. Therefore, a more material sensitive interfacial energy cutoff-distance must be used for such systems.

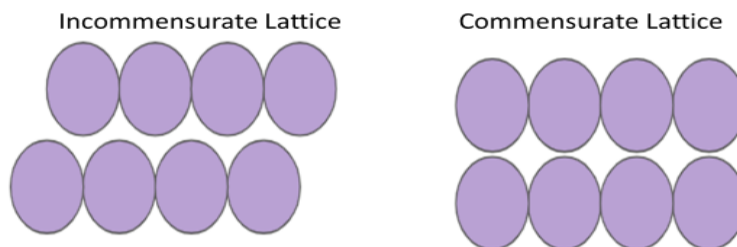


Figure 6.10: Simple diagram of commensurate and incommensurate lattices, in which the nodes are represented by spheres. In this case, the incommensurate lattices are misaligned because they are offset by some fraction of the interatomic distance.

The most serious limitation of Eq (6.46) for metal-metal interfaces, however, are metal bonds. These interactions are strong when the surfaces are close enough to exchange electrons (less than 0.5 nm), and decay rapidly as the metals get further apart. The presence of metal bonds makes interfacial energy between metals about one order of magnitude larger than predicted by the VdW-based Eq. (6.46).

6.7.2 Metal-Metal Interfacial Energy

Interfacial energies for various metals are displayed in Table 6.6.

Table 6.6: Interfacial Energies Between Two Identical Metal Surfaces at 300 K

Substance	Interfacial Energy (γ) [mJ/m ²]
Aluminum	1100
Silver	1500
Copper	2000
Iron	2400
Tungsten	4400

As we would expect from the presence of metal bonds in addition to VdW forces, metals have significantly higher interfacial energy than VDW solids and liquids (compare Table 6.5 with Table 6.6). This was captured by Banerjee et. al. for two similar metal surfaces by

$$W(D) = -2\gamma \left(1 - \frac{D - D_0}{\lambda_M}\right) e^{-(D-D_0)/\lambda_M} \quad (6.49)$$

where λ_M is the characteristic decay length of a particular metal [2]. Minimum energy occurs at $D = D_0$, at which point $W(D_0) = -2\gamma$. Lattice incommensurability from rotation or offset lattice spacing can also lower interfacial energy relative to theoretical values for interactions between similar metals. Table 6.6 compares the interfacial energies for commensurate and incommensurate lattices.

Table 6.6: Interfacial Energy Between Like and Unlike Metals with Commensurate and Incommensurate Lattices [2,3]

Type of Metal-Metal Interfaces	Commensurate Lattice [mJ/m ²]	Incommensurate Lattice [mJ/m ²]
Al(111) - Al(111)	715	490
Zn(0001) - Zn(0001)	545	505
Mg(0001) - Mg(0001)	550	460
Al(111) - Zn(0001)	N/A	520
Zn(0001) - Mg(0001)	N/A	490
Al(111) - Mg(0001)	N/A	505

Incommensurate lattices have lower interfacial energy for a similar reason that spheres contacting a plane have lower interfacial energy than two planes contacting each other. Commensurate lattices have closer (higher magnitude energy) contacts with each other, since each node on one surface aligns with each corresponding node on the other surface with minimal separation distance D_0 . On the other hand, incommensurate lattices experience an effective separation distance of $D > D_0$, since each node has horizontal, in addition to vertical, separation from each interacting node in the other surface (see Figure 6.10).

6.8 Surfaces with Adsorbed Layers

The force between two surfaces with adsorbed layers interacting through a medium (Figure 6.11) is given by

$$F(D) = -\frac{1}{6\pi} \left(\frac{A_{232'}}{D^3} - \frac{\sqrt{A_{121}A_{32'3}}}{(D+T)^3} - \frac{\sqrt{A_{1'2'1'}A_{323}}}{(D+T')^3} + \frac{\sqrt{A_{1'2'1'}A_{121}}}{(D+T+T')^3} \right) \quad (6.50)$$

in which T and T' are the thicknesses of adsorbed layer 2 and 2', D is the distance separating adsorbed layer 2 and 2', and A_{ijk} is the Hamaker constant for media i and k interacting through medium j .

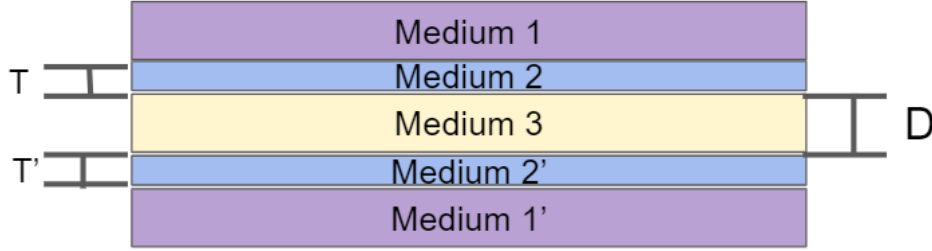


Figure 6.11: Diagram showing Medium 1 and 1' coated with Medium 2 and 2', respectively, with separating Medium 3. The separation distance between Medium 2 and 2' is D , while the thickness of Medium 2 and 2' are T and T' , respectively

If Medium 1 = Medium 1', Medium 2 = Medium 2', and $T = T'$, equation. (6.50) can be reduced to:

$$F(D) = -\frac{1}{6\pi} \left(\frac{A_{232}}{D^3} - \frac{2\sqrt{A_{121}A_{323}}}{(D+T)^3} + \frac{A_{121}}{(D+2T)^3} \right) \quad (6.51)$$

By employing the combining relation $A_{ijk} = \sqrt{A_{iji}A_{kkj}}$, equation (6.51) can be further simplified to

$$F(D) = -\frac{1}{6\pi} \left(\frac{A_{232}}{D^3} - \frac{2A_{123}}{(D+T)^3} + \frac{A_{121}}{(D+2T)^3} \right) \quad (6.52)$$

At small separations ($D \ll 2T$), the second and third term are small relative to the first term, so equation (6.52) can be reduced to

$$F(D) = -\frac{A_{232}}{6\pi D^3} \quad (6.53)$$

At large separations ($D \gg 2T$), the thickness terms drop out and equation (6.52) can be rewritten, as

$$F(D) = -\frac{1}{6\pi} \left(\frac{A_{232} - 2A_{123} + A_{121}}{D^3} \right) \quad (6.54)$$

Once again, using the combining relations $A_{iji} = A_{ii} + A_{jj} - A_{ij}$ and $A_{ijk} = (\sqrt{A_{ii}} - \sqrt{A_{jj}})(\sqrt{A_{kk}} - \sqrt{A_{jj}})$ yields

$$\begin{aligned} A_{232} &= A_{22} + A_{33} - 2A_{23} & A_{122} &= A_{11} + A_{22} - 2A_{12} \\ A_{123} &= (\sqrt{A_{11}} - \sqrt{A_{22}})(\sqrt{A_{33}} - \sqrt{A_{22}}) \end{aligned} \quad (6.55)$$

and thus from Eq. (6.54),

$$F(D) = -\frac{A_{131}}{6\pi D^3} \quad (6.56)$$

Equations (6.53) and (6.56) show that at small separations, the interaction between the adsorbed layers dominates, while at large separations, the interactions between the bulk materials dominate. Consequently, if present, the properties of the adsorbed layer or coating mostly determines the adhesion energy between two bodies.

6.9 Summary

Previous chapters have discussed the Van der Waals (VdW) interaction free energy from the perspective of point particle (pair) interactions. Chapter 6 details the interaction energy between macroscopic bodies, first from a summation perspective, which is then extended with *Lifshitz*' mean-field theory to account for the non-additivity of dispersion interactions. Included in the scope of this discussion on macroscopic interactions, adhesion, adsorption, wetting and electrostatic screening are illuminated.

The integration of point particle interactions yields a new VdW interaction parameter, known as Hamaker constant that extends the pair interaction parameter C_{VdW} to include the molecular number densities ρ_i ($i = 1, 2$) of the two macroscopic bodies, i.e.,

$$A = \pi^2 \rho_1 \rho_2 C_{VdW} \quad (6.3)$$

The total interaction free energy is furthermore dependent on the geometry of the surfaces, which is excluded from the Hamaker constant. In the case of two spheres or two planar objects interacting over a distance D , the VdW free energy is given by

$$W(D) = \frac{-A}{6D} \frac{R_1 R_2}{R_1 + R_2} \text{ and } W''(D)|_{\text{unit area}} = \frac{-A}{12\pi D^2},$$

respectively, as provided in Ch. 6 in Figure 6.3 with more geometrical examples. More generally, Hamaker constants are indexed considering the three media involved, that is A_{132} in which 1 and 2 represent the two interacting media (bodies) through medium 3. There are multiple combining equations available that are used to estimate Hamaker constants from others. An example is

$$A_{132} \approx \pm \sqrt{A_{131} A_{232}} \quad (6.4)$$

where the Hamaker constant between media 1 and 2 through medium 3 is obtained from the Hamaker constants of the similar materials interacting through the same medium.

As geometric curvatures can be challenging in determining interaction forces, the Derjaguin approximation provides a convenient way out, by relating the interaction forces between curved geometries to planar interactions, i.e.,

$$F(D)|_{\text{curved}} \cong 2\pi \left(\frac{R_1 R_2}{R_1 + R_2} \right) W''(D)|_{\text{planar}} \quad (6.20)$$

where R_i ($i = 1, 2$), represent the local or global curvatures of the two adjacent surfaces at distance D .

At the macroscopic level, not only the sum of participating pairwise interactions but also the contribution of neighboring atoms, and, the response interactions must be considered. This is accomplished with a mean-field approach embedded in the *Lifshitz Theory* of VdW forces. The Hamaker constant in terms of Lifshitz,

$$A_{132} = \frac{3}{4} kT \left(\frac{\epsilon_1 - \epsilon_3}{\epsilon_1 + \epsilon_3} \right) \left(\frac{\epsilon_2 - \epsilon_3}{\epsilon_2 + \epsilon_3} \right) + \frac{3h}{4\pi} \int_{v_1}^{\infty} \left(\frac{\epsilon_1(iv) - \epsilon_3(iv)}{\epsilon_1(iv) + \epsilon_3(iv)} \right) \left(\frac{\epsilon_2(iv) - \epsilon_3(iv)}{\epsilon_2(iv) + \epsilon_3(iv)} \right) dv \quad (6.22)$$

entails the permittivities of the interacting bodies (1, 2) and the medium (3) within which they interact. The first term in Eq. (6.22) represents the *Keesom* and *Debye polarization* contributions, and the second term represents the *dispersion* interaction. While the

polarization interactions are only dependent on the static permittivities, the dispersion interactions are frequency ν dependent (more specifically dependent on the imaginary frequencies) Considering that the dispersion forces are mostly active at frequencies in the visible regime, the Hamaker constant can be approximated for dielectric media by,

$$A_{132} \approx \frac{3}{4} kT \left(\frac{\epsilon_1 - \epsilon_3}{\epsilon_1 + \epsilon_3} \right) \left(\frac{\epsilon_2 - \epsilon_3}{\epsilon_2 + \epsilon_3} \right) + \frac{3h\nu_e}{8\sqrt{2}} \frac{(n_1^2 - n_3^2)(n_2^2 - n_3^2)}{\sqrt{(n_1^2 + n_3^2)}\sqrt{(n_2^2 + n_3^2)} \left\{ \sqrt{(n_1^2 + n_3^2)} + \sqrt{(n_2^2 + n_3^2)} \right\}} \quad (6.24)$$

where n_i ($i = 1, 2, 3$) represent the refractive indices of the materials involved. Eq. (6.24) is in good correspondence with rigorous calculations and experimental observations, as documented in Ch. 6 in Tables 6.2 and 6.3. Different approximations are found for conductive material. For metal-metal interactions, the dispersion interaction becomes dominant, as seen here for similar materials through vacuum:

$$A_{11} \approx \frac{3}{4} kT + \frac{3h\nu_e}{16\sqrt{2}} \approx 4 \times 10^{-19} \text{ J} \quad (6.28)$$

Generally, the third medium effect on the interaction between metals (conductors) is negligible due to high permittivities and refractive indices.

Beyond a 10 nm distance, the experimental VdW interaction begins to deviate from that predicted by the previous equations above. The reason is the *retardation effect*, i.e., the time-delayed response of the VdW dispersion interaction. Mathematically, the retardation effect implies that the Hamaker constant is not constant but decreases with distance. The VdW power law $1/r^6$ tends to shift to a $1/r^7$ interaction at an interaction distance that goes beyond tens of nanometers for dielectric materials. In metals on the otherhand, the high dispersion forces are able to overcome the retardation effect up to distances of 10 μm and beyond. The dispersion force in metals can be modeled by the Casimir Equation:

$$F(D) = -\frac{\partial W}{\partial D} = -\left(\frac{kT}{8\pi D^3} + \frac{\pi hc}{480D^4} \right) = -\frac{1.64 \times 10^{-22}}{D^3} \left(1 + \frac{7.95 \times 10^{-6}}{D} \right) \text{ Nm}^{-2} \quad (6.38)$$

where $F(D)$ is the force per unit area of the metal and the dielectric constant is assumed to approach infinity.

Having discussed with metals, aspects of high permittivity materials, another permittivity consequence on the Van der Waals interaction is discussed next. Superfluid helium is known to have a lower permittivity in its liquid condensed phase than in its vapor phase. When liquid helium is contained in a vessel, the difference in the permittivity of the vapor resting above the liquid causes a repulsive VdW force to occur at the liquid/vapor interface, as molecular diffusion at an interface is directed from the high permittivity phase to the low permittivity phase. This repulsive force can cause the net energy $\Delta G(D)$,

$$\Delta G(D) = -\frac{A}{12\pi D^2} + mgH \quad (6.30)$$

composed of the planar interaction energy that is compressing the film and the gravitational energy that is acting on liquid film at the vessel wall, to turn negative, and thus, the liquid to climb the container wall. The maximum height the liquid helium can climb is given by gravity and the vapor pressure. The equilibrium condition, $\Delta G(D) = 0$,

defines the disjoining pressure, $P(D) = +\rho gH$, which can be used to calculate the relative vapor pressure using the barometric distribution law, i.e.,

$$p/p_o = e^{-P(D)v/kT} = e^{-\rho vgH/kT} \quad (6.34)$$

where ρ is the mass density of the liquid phase of helium, v is the molecular volume, and H is the height of the wall wetting liquid in the vessel.

In the first part of this chapter we focused on the VdW interaction forces at a given separation distance D . This last part of this chapter deals with two objects in contact. It introduces a new energy term, namely, the *work of adhesion* (W_{adh}), which is the energy required to separate two bodies from contact to infinity. By attributing half the work to each surface, we define the interfacial energy, γ . W_{adh} depends on the Hamaker constant and the *contact distance*, D_o , between the two object-surfaces, as well as, the interfacial geometry. For two planar surfaces,

$$W_{adh} = \frac{A}{12\sqrt{3}D_o R} \quad \text{and} \quad \gamma = \frac{A}{24\sqrt{3}D_o R} \quad (6.45)$$

For non-metal, non-H-bonding materials, the cutoff distance is universal, i.e., $D_o = 0.165$ nm. Metal interfaces have smaller cutoff distances, due to lattice alignment effects such as incommensurability, and metal bonds, which dominate at distances less than 0.5 nm. These factors make the interfacial energy between metals approximately one order of magnitude larger than predicted based on VdW interactions. The interaction energy between two similar metal surfaces can be obtained from

$$W(D) = -2\gamma \left(1 - \frac{D - D_o}{\lambda_M}\right) e^{-(D-D_o)/\lambda_M} \quad (6.49)$$

where λ_M is the characteristic decay length particular to the metal. In contact, $D = D_o$, the work of similar metal adhesion is twice the interfacial energy γ , as defined.

A final consideration to contact forces is to consider a composite system, as depicted here,

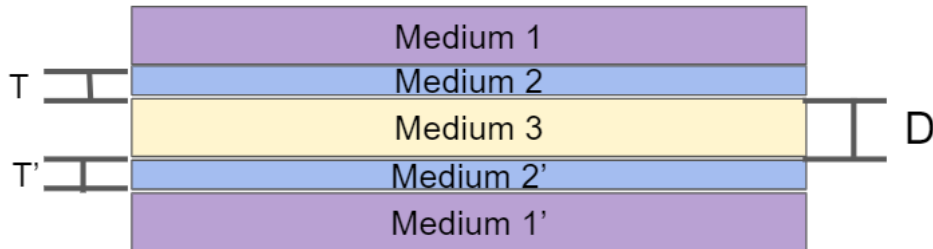


Figure 6.11: Diagram showing Medium 1 and 1' coated with Medium 2 and 2', respectively, with separating Medium 3. The separation distance between Medium 2 and 2' is D , while the thickness of Medium 2 and 2' are T and T' , respectively

in which the interaction between the top and bottom material (1 and 1') is tuned by the thickness $2T$ of adsorbate layers (medium 2 and 2'), introduced by a third media (3) of thickness D . It turns out that for $D \ll 2T$, the adhesive force reduces to the properties of medium 2 and 3, ignoring the properties of the outside material 1, while for $D \gg 2T$, all material properties matter. This invites many practical applications, and this not only related to adhesives, but also optics and electronics.

6.10 Review Questions

1. What does the sign of the Hamaker constant indicate about the interaction (attractive vs. repulsive)? Explain why this makes sense.
2. In what case does the dispersion term (second term) in the Lifshitz equation disappear?
3. Why does pairwise additivity hold for gases, but not condensed matter?
4. In what case is the Derjaguin approximation useful?
5. Describe how retardation effects alter the Hamaker constant between two bodies. How does this effect change over different separating distances?
6. What causes the retardation effect?
7. How does the amount of liquid helium present impact the height the liquid climbs up the vessel walls and the thickness of the liquid as it climbs?
8. Why are the signs of adhesion and interfacial energy negative between surfaces with a net repulsion?
9. When is it acceptable to use the universal cutoff distance? Why is it acceptable?
10. How do incommensurate lattices impact the adhesion and interfacial energy of metals?
11. For conducting materials, how Keesom and Debye polarization and dispersion interaction contributes to the Hamaker constant and Why?

ANSWER KEY

1. A positive Hamaker constant indicates an attractive interaction. This stands to reason as the interaction potential $w(r)$ is only negative(attractive) with a positive Hamaker constant.
2. The dispersion term disappears if the refractive index of either material is similar to that of the medium between them.
3. In condensed matter, atoms neighboring a pairwise interaction are much closer, and therefore have larger contributions to interaction energy.
4. The Derjaguin approximation is useful when determining the interaction free energy of two curved surfaces, as the interaction free energy is much easier to determine for a planar surface than a curved one.
5. The retardation effect implies that the Hamaker constant decreases with distance.
6. The retardation effect is due to a time-delayed response in the vdW dispersion interaction.
7. It doesn't. The height climbed and thickness are independent of the volume of liquid helium present. These factors are controlled by the vapor pressure at the flat vapor/liquid interface.
8. Because the work of adhesion (and interfacial energy) are defined as the work to separate two surfaces in contact to infinity (versus bring them together from infinity), a net repulsion would mean that there is no attraction between the surfaces. This means that there would be work required to bring the two surfaces together, rather than to separate them.
9. It is acceptable for non-metals that don't have strong H-bonds. It is acceptable because it does not add more error to calculations than already exists in the estimated Hamaker constants.

10. Incommensurate lattices lower the adhesion and interfacial energy of metals By definition, incommensurate lattices have misaligned nodes, which means that the distance between each surface's molecules (nodes) is larger, lowering the interaction energy magnitude between these molecules and thus the overall interfacial energy.
11. For conduction material, the contribution of Keesom and Debye polarization is negligible. The contribution of dispersion energy is dominant because the refractive index and dielectric permittivity is much large for conduction material.

Literature – Sources and Further Reading

3. Intermolecular & Surface Forces, 3rd Ed., J.N. Israelachvili, Academic Press, Boston (2011), Ch. 2 pp 23-43, Ch. 7 pp 147-148, Ch. 15 pp 342-344.
4. Banerjee, A., Ferrante, J., & Smith, J. R. (1991). Adhesion at Metal Interfaces. In L. H. Lee (Ed.), *Fundamentals of adhesion* (pp.325-348). New York: Plenum.
5. Ferrante, J., & Smith, J. R. (1985). Theory of the bimetallic interface. *Physical Review B*, 31(6), 4327-3434.

Chapter 7: Self-Assembly

7.1 Overview

To illustrate the importance of interactions and other critical parameters, such as solution concentration, let us consider the spontaneous non-covalent molecular assembling route, referred to as self-assembly process, which is illustrated in Figure 1 for systems that condense in a two-dimensional crystalline form on a liquid interface (Fig. 1(a)) and a solid interface (Fig. 1(b)). Self-assembly refers to the reversible and cooperative assembly of molecular building blocks into an ordered structure. For self-assembly, in the classical sense, to take place without intervention of external forces, the process must lead to a lower Gibbs free energy, thus self-assembled structures are thermodynamically more stable than the single, unassembled components.

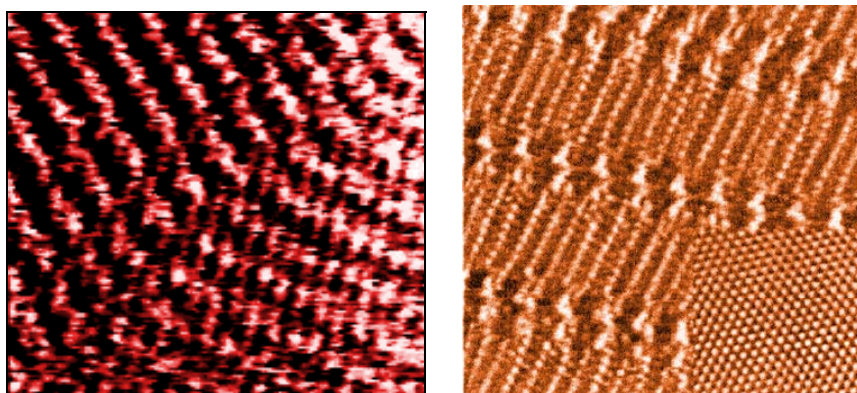


Figure 1: (a) Lipid film originally self-assembled on the liquid phase of water and then transferred to a solid surface by Langmuir Blodgett technique,¹ (b) liquid crystal molecules self-assembled on graphite (C18ISA/HOPG)².

Typically for molecular self-assembly one distinguishes between:

- **static self-assembly** (Ex: lyotropic liquid crystal phases, Fig. 2), and
- **dynamic self-assembly** (Ex. peptide aggregation from buffer solution, Fig. 3), which extends self-assembly to pattern formation of pre-existing components (known as non-equilibrium self-organized systems)

Static self-assembly, which refers to the classical self-assembled aggregate, describes systems at equilibrium that do not dissipate energy once formed. The formation itself, however, might have required energy. **Dynamic self-assembly** is an ever-present process in non-equilibrium physical and biological systems. It is the basis in nature for spawning hierarchical structures, and used in synthetic approaches, as illustrated in the example in Figure 3. The formation of patterns in dynamic self-assembly is directly linked to energy dissipation.

¹ R.M. Overney et al., Phys. Rev. Lett. **72**, 3546 (1994)

² S. De Feyter et al., Org. Mesoscopic Chem., Blackwell Science (1999)

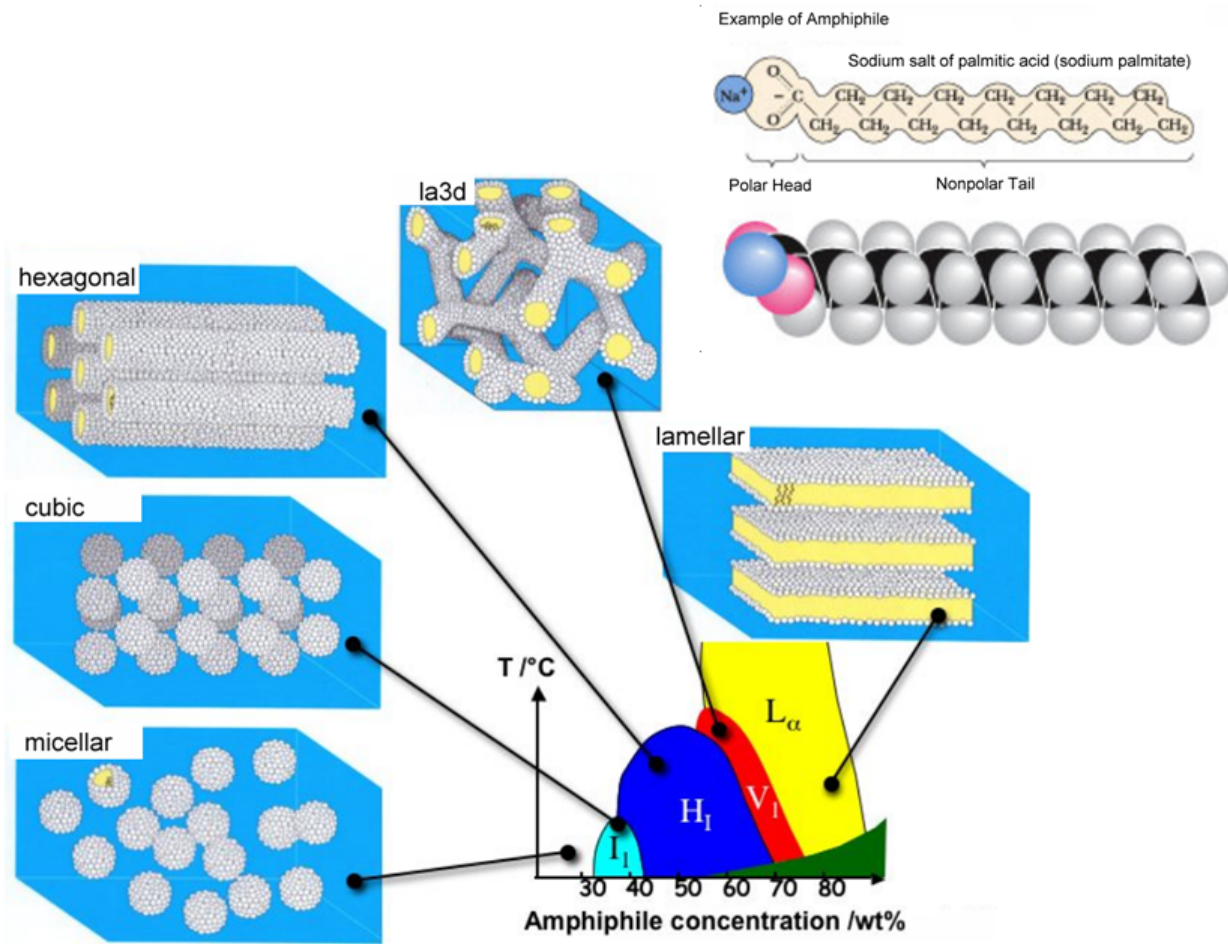


Figure 2: Schematics³ showing the aggregation (self-assembling) of amphiphiles into micelles (bottom left), and then, under appropriate conditions into lyotropic liquid crystalline phases⁴ (cubic, hexagonal, la3d, lamellar) as a function of amphiphile concentration and of temperature.

Self-assembly of materials relies on the fluctuations in the position and the orientation of the molecules (particles) due to Brownian motion. The interaction strength between the molecules and the environment (e.g., surface, solvent) play an important role. Self-assembly interaction strengths are on the order of 3-10 kJ/mol, and comparable to the thermal energy responsible for Brownian motion (e.g., 2.4 kJ/mol at room temperature).⁶

³ Extracted and modified from R.G. Laughlin (1996), "The Aqueous Phase Behaviour of Surfactants", Academic Press, London, and D.F. Evans and H. Wennerström (1999), "The Colloidal Domain, Wiley VCH, New York.

⁴ Lyotropic liquid crystalline phases are liquid crystalline phases involving a solvent.

⁵ J. Wang et al., *Soft Matter*, **5**, 3870-3878 (2009)

⁶ 1 kcal/mol = 0.04336 eV = 6.948e⁻¹⁴ erg = 4.184 kJ/mol

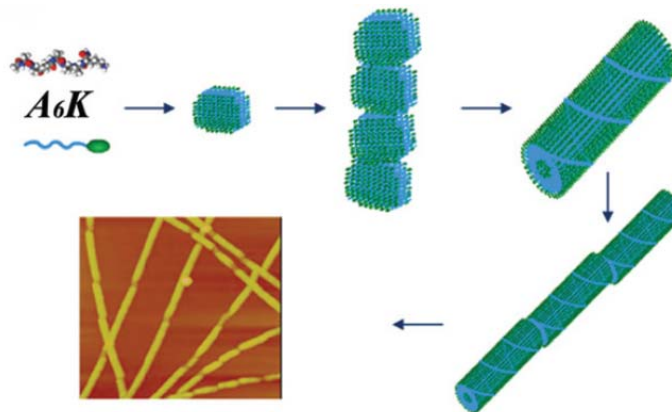


Figure 3: Schematic illustration of the dynamic self-assembly process and nanostructures formed of surfactant-like peptides (A6K) in aqueous buffer.⁵

Weak or soft interactions needed for molecular ordering of more complex systems include:

- hydrogen interactions
- coordination bonds in ligands and complexes,
- polar interactions
- dipolar interactions
- Van der Waals interactions, and
- hydrophobic interactions.

7.2 Thermodynamics of Self-Assembly

The literature on self-assembly is colossal and often confusing, in particular regarding definitions but also regarding theoretical treatments. We briefly discuss here self-assembly for small molecules based on thermodynamic fundamentals. If we consider an equilibrium situation, containing amphiphilic molecules, in form of monomers, dimers, trimers and larger aggregates in solution, the chemical potentials of the different aggregates have to be equivalent, i.e.,

$$\mu = \mu_1^o + kT \log X_1 = \mu_2^o + \frac{1}{2}kT \log \frac{1}{2}X_2 = \mu_3^o + \frac{1}{3}kT \log \frac{1}{3}X_3 = \dots = \mu_N^o + \frac{1}{N}kT \log \left(\frac{X_N}{N} \right) = \text{constant}$$

<i>monomers</i>	<i>dimers</i>	<i>trimers</i>
-----------------	---------------	----------------

with

- equilibrium chemical potential μ ,
- the aggregation number N ,
- the standard chemical potential contribution μ_N^o in aggregates of number N , which is also known as the *interaction free energy per molecule*, and
- the concentration X_N (or activity – see later) of molecules in aggregates of number N .

The second term in the chemical potential is the entropic term of the potential and expresses the energy associated to structure (cooperativity). An equivalent equilibrium description in terms of the concentration X_N is

$$X_N = N \left\{ X_1 \exp \left[\frac{\mu_1^o - \mu_N^o}{kT} \right] \right\}^N.$$

For large aggregates, i.e., $N \gg 1$, the aggregated concentration can be approximated, as

$$X_N \approx N \{X_1 e^\alpha\}^N,$$

where α reflects the interaction strength, discussed further below.⁷ Under the assumption of sufficiently low monomer concentrations, such that the two expressions for X_N above are smaller than unity, it follows $X_1 > X_2 > X_3 > \dots$ for all α . In other words, at low monomer concentration most molecules will exist in monomer form in the solution, while the concentration of aggregates is close to zero. Hence, in terms of the *total concentration* $C \equiv \sum_i X_i (i = 1, 2, 3, \dots)$, $X_1 \approx C$ for sufficiently low X_1 .

As aggregation depends on the cohesive energies between the molecules in the aggregated and the dispersed (monomer) states, we require

$$\mu_N^o < \mu_1^o \text{ or } \mu_N^o - \mu_1^o < 0$$

for the formation of large stable aggregates. While as stated above, the monomer concentration plays a role in the aggregate concentration, the functional variation of μ_N^o with N plays an important role in the physical properties of the aggregates, such as their size and polydispersity.

Let us consider the simplest aggregate namely a one-dimensional (1D) rod, which shall be in equilibrium with monomers in solution, as depicted in Figure 4.

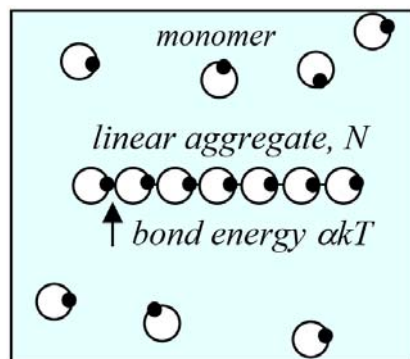


Figure 4: 1D Assembly

The total free energy $N\mu_N^o$ of the rod composed of N monomers is

$$N\mu_N^o = -(N-1)\alpha kT$$

⁷ This approximation involving dilute monomer solutions with large aggregates required the substitution

$\mu_N^o = \frac{-(N-1)\alpha kT}{N}$, as derived further down in the text.

where αkT represent the monomer-monomer bond energy.⁸ $\alpha \equiv (\mu_1^o - \mu_\infty^o)/kT$ is a positive constant that depends on the strength of the intermolecular interactions. Thus, we have an expression of the interaction free energy per molecule μ_N^o in an aggregate in terms of the aggregation number N , i.e.,

$$\mu_N^o = -\left(1 - \frac{1}{N}\right)\alpha kT \equiv \mu_\infty^o + \frac{\alpha kT}{N} \quad (\text{rod-shaped micelles})$$

whereby, we have introduced the bulk energy μ_∞^o of a molecule in an infinite aggregate. A similar expression is obtained for any type of rod-like structure, such as closed looped micelles, or cylindrical micelles.

For two dimensional (disc-shaped) and three-dimensional (sphere-shaped) aggregates the following expressions for $\mu_N^o(N)$ can be derived:

$$\mu_N^o = \mu_\infty^o + \frac{\alpha kT}{N^{1/2}} \quad (\text{disc-shaped micelles})$$

$$\mu_N^o = \mu_\infty^o + \frac{\alpha kT}{N^{1/3}} \quad (\text{sphere-shaped micelles})$$

Note that for all shapes the interaction free energy per molecule μ_N^o decreases progressively with N . The interaction free energy per molecule in an aggregate can be expressed in more general terms, as

$$\boxed{\mu_N^o = \mu_\infty^o + \frac{\alpha kT}{N^p}},$$

where p is a number that reflects the shape or the dimensionality of the aggregates.

7.3 Critical Monomer concentration

As discussed above, at sufficiently low monomer concentration, the likelihood for aggregation is close to zero. This invites the definition of a *critical micelle concentration* (CAC),⁹ above which the monomer concentration does stagnate while the aggregate concentration takes off, as illustrated in the sketch of Figure 5. The reason for the concentration stagnation of the monomer is due to the fact that X_N , expressed by

$$X_N \approx N \{X_1 e^\alpha\}^N \quad \text{or} \quad X_N = N \left\{ X_1 \exp \left[\frac{\mu_1^o - \mu_N^o}{kT} \right] \right\}^N$$

cannot exceed unity, and thus once X_1 approaches $e^{-\alpha}$ or $\exp \left[-\frac{\mu_1^o - \mu_N^o}{kT} \right]$,

the concentration of monomers in the solution stagnates and the monomers aggregate.

⁸ Note we deducted the terminal monomer bond to the right in Figure 4.

⁹ More appropriately, CAC should be named *critical monomer concentration* as X_1 is the critical concentration parameter for aggregation.

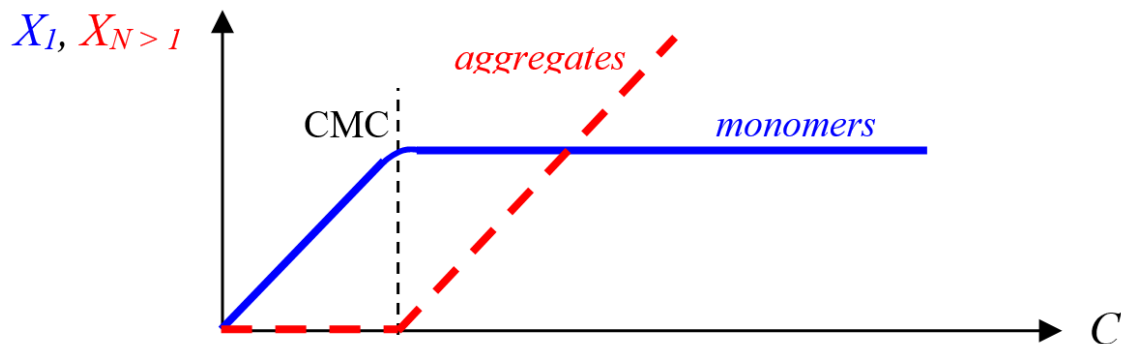


Figure 5: Monomer and aggregate concentrations as function of the total concentration.

For a spherically shaped aggregate of radius r , the interaction parameter α , which is typically larger than 1, can be expressed in terms of the surface tension γ as

$$\alpha = \frac{4\pi r^2 \gamma}{kT}$$

Thus, at CMC for large aggregates, the critical monomer concentration can be expressed in terms of the aggregate surface tension, as

$$(X_1)_{CMC} \approx e^{-\alpha} = e^{-\frac{4\pi r^2 \gamma}{kT}}.$$

Table 2 that provides CMC values of some common surfactants and lipids.

Table 2: CMC values of some common surfactants.¹⁰

Surfactant (R _n =C _n H _{2n+1})	CMC [mM]	ΔG[kJ/mol] (per CH ₂ group)*	Number of carbon atoms in chain
<i>Cationic</i>	66	1.8	10
Alkyl trimethylammopnium bromides R ₁₀ -N(CH ₃) ₃ ⁺ Br ⁻	63	1.7	
<i>Anionic</i>			
Sodium alkyl sulphates R ₁₀ -SO ₄ ⁻ Na ⁺	130	1.7	

$$\Delta G = RT \ln(f); f = \text{increment of CMC per } CH_2 \text{ group}$$

¹⁰ Source: Intermolecular & Surface Forces, J. Israelachvili, Academic Press

7.4 Ostwald Ripening

A consequence of the size-dependence of the solubility is the *Ostwald-Ripening* process that is illustrated in Figure 4.

Consider a supersaturated solution $\mu_l - \mu_s > 0$, i.e., a solution in which the chemical potential of the solute in the solution is higher than the equilibrium solution. The solute will precipitate out of solution. Let us assume we have already solid particles of equal size in the solution. As long as the chemical potential of solution exceeds the chemical potential of the solids, solutes will deposit on the particles. Consequently, the chemical potential of the solution will decrease due to loss of solute to the solid phase. At some point, the solution will be in equilibrium with the solid particles.

Now, let us consider a distribution of solid particles in the solution. The same precipitation process will occur, as just described, until the chemical potential of the solution μ_l equals the chemical potential of the smallest particle μ_s^{small} . As the driving force for precipitation for larger particles is still positive, i.e., $\Delta\mu = \mu_l - \mu_s > 0$, precipitation will locally continue around the larger particles. At the same time, the chemical potential of the solution decreases below the limit of the smaller particles, which changes the sign of $\Delta\mu = \mu_l - \mu_s < 0$. This causes the smaller particles to dissolve. The smaller they get, the faster they dissolve, until, they disappear. This process of local growth of larger particles at the expense of smaller ones is called Ostwald ripening. It is a slow process, and has recently found entrance in controlling the size during the growth of quantum dots.

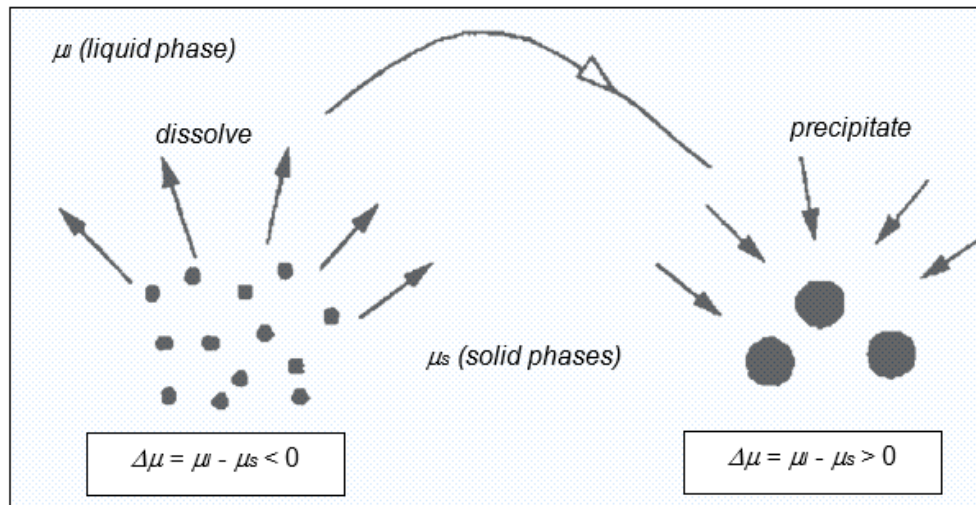


Fig. 4: Illustration of the Ostwald Ripening process.

Literature – Sources and Further Reading

Intermolecular & Surface Forces, 3rd Ed., J.N. Israelachvili, Academic Press, Boston (2011), Ch. 19 pp 503-513.

Chapter 8: Statistical Mechanics of Pair Interactions in Gases

8.1 Overview

To understand how a molecular system behaves, a system specific language is needed that is based on terms such as *energy*, *entropy*, *enthalpy* and *free energy*, as well as, identifies the driving forces. The microscopic laws, or more specifically the laws that are based on classical mechanics applied to the microscopic world, deal with a large number of particles that are the constituent of matter. We know that based on classical theories, the initial state of a system gradually evolves into future states. But how can this be described, if we take a microscopic view?

On the molecular scale, we deal with particle distributions, while on the macroscale we have macroscopic properties, such as temperature, heat and entropy, if we look at a thermodynamic system. It was Boltzmann's law that provided a link between the two scales, relating the macroscopic property of entropy, S , in gases to the multiplicity of the microscopic degree of freedom W , i.e.,

$$S = k \ln W \quad (8.1)$$

for a macrostate of given energy E_i , of $i = 1, 2, 3, \dots, t$ possible energy states. Thereby, the multiplicity of the macrostate (a macroscopic observable) reflects the number of distinct microstates yielding the same macrostate. Boltzmann introduced with his law a constant k (or $k_B = 1.38 \times 10^{-23} \text{ J/K}$), which is known as the Boltzmann constant. With Boltzmann's law a statistical approach was introduced that successfully connects the microscale to the macroscale using a statistical (probabilistic) approach, known as *Statistical Mechanics*, Fig. 8.1.

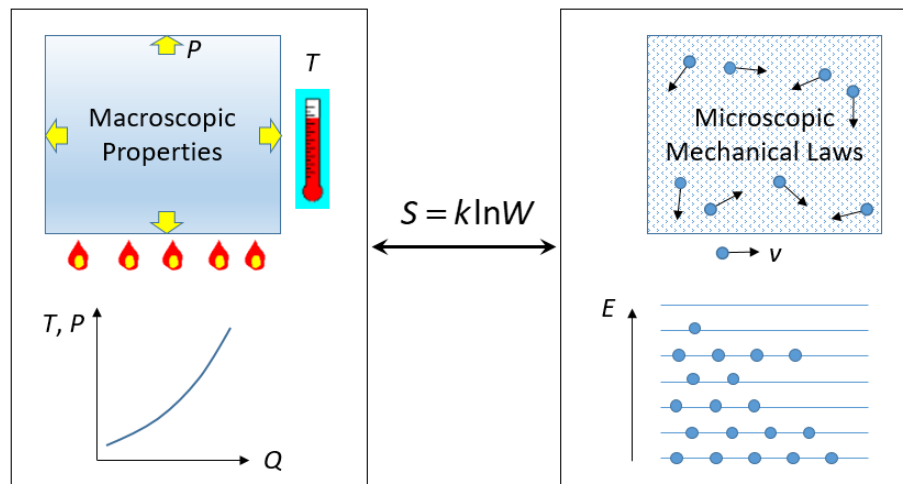


Figure 8.1: (Left) The macroscopic properties of temperature T , pressure P as a function of supplied heat Q of a system are depicted. (Right) The microscopic properties (molecular velocity) and mechanical laws distribute the molecules energetically on energy levels. Boltzmann's law provides a link between the two scales.

In the prior chapter, we developed and introduced a wide variety of pair interaction potentials between molecules (particles). For the Van der Waals interaction alone, we have seen a wide variety of potential. In the course of this chapter we will use Boltzmann's law to connect microscopic pair potentials between molecules in the gas phase to

macroscopic properties, such as the internal energy. But before we get there, we have to develop a better understanding on how to distribute molecules of different configurations into energy state that are observables on the macroscopic scale.

8.2 Boltzmann's Law, Factor and Distribution Law

8.2.1 Multiplicity - Examples

As the multiplicity is key to understand Statistical Mechanics, we will use two examples to illustrate its value, as well as utilize Boltzmann's law. In the first example, we will discuss the critical temperature between two phase states that although simplified, find application in investigating protein denaturation. The second example will provide a theoretical description of why gases have a tendency of expanding into larger volumes.

8.2.1.1 Example 1: Molecular Chain Denaturation

We shall consider a protein or polymer in solution and determine the critical temperature T_c that discriminates the molecule to be in a folded or collapsed state versus denatured or extended state. The molecular model we are employing for simplicity is a four-bead linear molecule with five possible microstates distributed on two macrostates that can be experimentally observed. The configurations are depicted in Figure 8.2. In the collapsed state, the endpoints of the polymer chain are non-covalently bound with the stabilization energy $-\varepsilon$. The remaining four microstates represent denatured configurations.

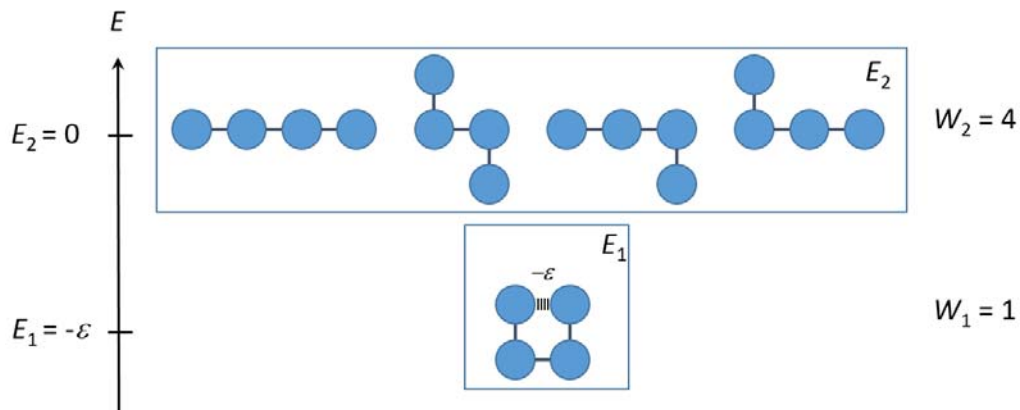


Figure 8.2: Four-bead linear molecular configurations, exhibiting with a collapsed and an extended state, two macrostates with only one microscopic configuration in the collapsed state, W_1 , and four microscopic configurations in the extended state, W_2 .

Assuming constant temperature and volume, we describe the useful energy that can be obtained from the system, i.e., the interaction free energy, with the Helmholtz free energy \mathcal{F} , i.e.,

$$\mathcal{F} = U - TS \quad (8.2)$$

where U is the internal energy, T the absolute temperature and S the entropy. Thereby, we distinguish between the free energy of the collapsed state \mathcal{F}_C and the extended state \mathcal{F}_E with corresponding subscripts for the internal energy and entropy. For the two macrostates, the internal energy is given by the stabilization energy, i.e., $U_C = -\varepsilon = E_1$ for the collapsed state, or zero for the extended state, i.e., $U_E = 0 = E_2$.

Employing now for the entropy Boltzmann's law, Eq. (8.1), and substitute the values 1 and 4 for the respective multiplicities of the collapsed and extended state, respectively, yields the following free energies:

$$\mathcal{F}_C = -\varepsilon - kT \ln(W_1) = -\varepsilon - kT \ln(1) = -\varepsilon$$

$$\mathcal{F}_E = 0 - kT \ln(W_2) = -kT \ln(4)$$

If equated, these two equations yield the critical temperature

$$T_o = \frac{\varepsilon}{k \ln\left(\frac{W_2}{W_1}\right)} \quad (8.4)$$

or with the given multiplicities, it follows $T_o = \varepsilon / (k \ln(4))$. The situation is depicted for the free energy in Figure 8.3.

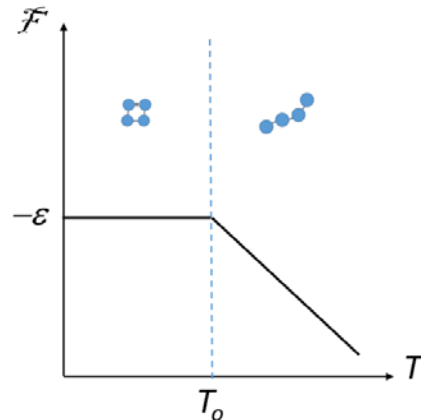


Figure 8.3: Free energy as function of the system temperature. For $T < T_o$, the collapsed states are more prominent. Above T_o the extended states are more prevalent.

8.2.1.2 Example 2: Gas Expansion

One of the key principles of Statistical Mechanics is the *Extremum Principles*. It states: “*The maximum multiplicity predicts the most probable outcome*”. It is the principle that we employ here to show why a gas spreads out into a larger volume.

In this example, we consider three indistinguishable gas molecules in three volumes A, B and C, as depicted in Figure 8.4. The smallest volume C (with volume 3) allows for just one configuration.

	Configurations	Volume
Macrostates		
A	[Diagram: 5 boxes, 2 red, 3 white]	5
B	[Diagram: 4 boxes, 3 red, 1 white]	4
C	[Diagram: 3 boxes, all red]	3

Figure 8.4: Molecule distributions in three volumes A, B, C.

To determine the number of configuration for larger volumes, i.e., their multiplicity, we have to employ the combination formula

$$W(N, M) = \binom{N}{M} \equiv \frac{M!}{N!(M-N)!} \text{ with } M! \equiv 1 \times 2 \times 3 \times \dots \times M \quad (8.5)$$

where M represents the volume size (number of places the molecule can be placed in a given volume) and N the number of particles. For instance, for volume A, $M = 5$, and thus, $W_A(3,5) = 5!/(3! \times 2!) = 10$. We find that

$$W_A(3,5) = 10$$

$$W_B(3,4) = 4$$

$$W_C(3,3) = 1$$

that the multiplicity increases with volume size. Considering now the Extremum Principle introduced above that predicts the most probable outcome, W_A is the most probable result. As in the macroscopic system “equilibrium” is equivalent to the statistically most probable outcome, the gas molecules will spread into increased volume, and hence, exert a pressure on the pressure wall.

	Configurations	Volume
Macrostates		
A		5
		4
		3

Figure 8.4: Molecule distributions in three volumes A, B, C.

8.2.2 Multiplicity and Probability

The probability P_i of a given macrostate is simply defined as the normalized multiplicity of that state, whereby the normalization factor represents the sum of all multiplicities, i.e.,

$$p_i = \frac{W_i(N, M_i)}{\sum_j W_j(N, M_j)} \quad (8.6)$$

For our gas expansion example above, we find the following probabilities to fill the three volumes:

$$p_A = \frac{W_A(3,5)}{\sum_{j=A,B,C} W_j(3, M_j)} = \frac{10}{10 + 4 + 1} = \frac{2}{3}$$

$$p_B = \frac{W_i(3,4)}{\sum_{j=A,B,C} W_j(3,M_j)} = \frac{4}{10+4+1} = \frac{4}{15}$$

$$p_C = \frac{W_i(3,3)}{\sum_{j=A,B,C} W_j(3,M_j)} = \frac{1}{10+4+1} = \frac{1}{15}$$

Note that the sum of all probabilities $\sum P_j = 1$ has to sum up to 1.

8.2.3 Boltzmann Factor and Boltzmann Distribution Law

We discuss with Boltzmann's law the starting point for modeling and predicting macroscopic properties or phenomena from a molecular perspective using different forms of distributions. Averages over these distributions are what experiments measure. For instance,

- The properties of gases are obtained from energy distributions that originate from translational energies and interaction energies.
- Chemical reaction equilibria are connected to "atom and molecular energies" of the reactants and products.
- Biomolecular processes, such as ligand binding to DNA are related to the distribution of energies of all ligation states.

In previous chapters, we introduced and utilized the *Boltzmann factor* as the relative population n_i/n_j of two macrostates with energy E_i and E_j , as

$$\frac{n_i}{n_j} = \exp\left(-\frac{E_i - E_j}{kT}\right) \quad (8.7)$$

In terms of the probabilities of the two states, it is

$$\frac{p_i}{p_j} = \exp\left(-\frac{E_i - E_j}{kT}\right) \quad (8.8)$$

For a given system of energy states E_1, E_2, \dots, E_t , the sum of all probabilities is

$$\sum_{i=1}^t p_i = 1 \quad (8.9)$$

and the average energy expectation value is

$$\langle E \rangle = \sum_{i=1}^t p_i E_i \quad (8.10)$$

It can be shown with the method of Lagrange multipliers (see sources for further reading at the end of this chapter) that with what was said above, the equilibrium probability brings forward the following exponential distribution law,

$$p_i = \frac{\exp\left(-\frac{E_i}{kT}\right)}{\sum_{j=1}^t \exp\left(-\frac{E_j}{kT}\right)} \quad (8.11)$$

the *Boltzmann distribution law*, for state E_i relative to the ground state $E_0 = 0$. The denominator (a normalization factor) is known as the *Partition Function*, Q :

$$Q = \sum_{j=1}^t \exp\left(-\frac{E_j}{kT}\right) \quad (8.12)$$

8.3 Partition Function

More generally, we can express the Boltzmann distribution law and the partition function in respect to the lowest energy level E_1 (above we assumed $E_0 = 0$), i.e.,

$$p_i = \frac{\exp(-(E_i - E_1)/kT)}{Q}, \text{ and } Q = \sum_{j=1}^t \exp\left(-\frac{E_j - E_1}{kT}\right),$$

which yields the macroscopic partition function

$$Q = \sum_{j=1}^t \exp\left(-\frac{E_j - E_1}{kT}\right) = 1 + e^{-(E_2 - E_1)/kT} + e^{-(E_3 - E_1)/kT} + \dots + e^{-(E_t - E_1)/kT}.$$

The partition function, because of its temperature dependence is the bridge between the microscopic world and the macroscopic thermodynamic properties. As the sum over the system Boltzmann factors $\exp(-E_j/kT)$, it specifies how the molecules (particles) are partitioned throughout the accessible states E_1, E_2, \dots, E_t . An intuitive way of thinking about the partition function is as the number of states that are effectively accessible to a system.

Let us look at the following examples with $t = 6$ states, $N = 7$ particles, and $T_1 < T_2 < T_3$, as depicted in Figure 8.5.

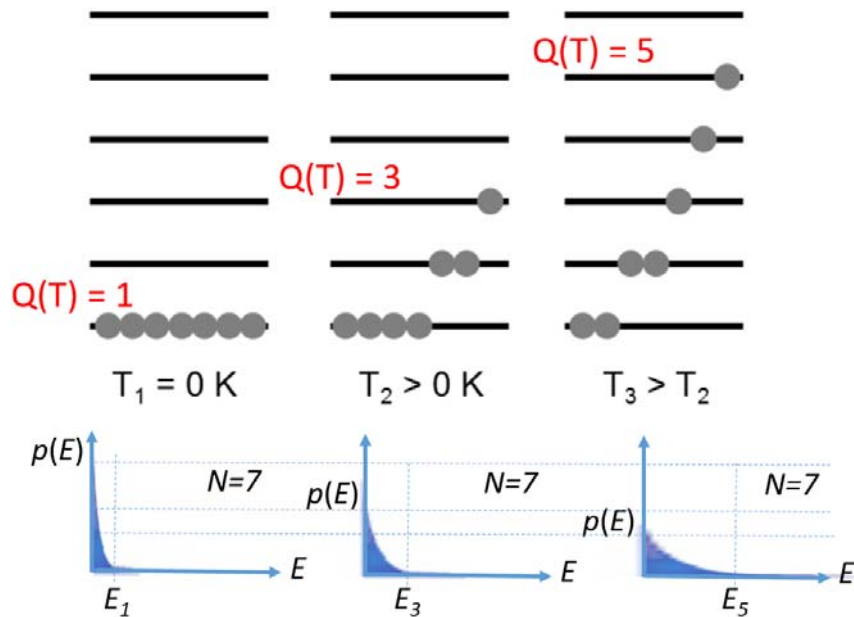


Figure 8.5: Distribution of $N = 7$ particles on accessible energy states E_i for three different temperatures with specific macroscopic partition functions.

Extreme values for the distribution function describing how many energy levels are occupied is $Q = 1$ for $T \rightarrow 0$, and, $Q = t$ for $T \rightarrow \infty$.

8.4 Independent Distinguishable and Indistinguishable particles

Gas molecules are independent *indistinguishable particles*, while atoms or molecules in a “lattice structure” are *distinguishable* based on their position label.

We focus first on distinguishable particles. Let us consider a system with energy levels E_j and $N=2$ distinguishable particles with label A (surface atoms) and B (bulk atoms). We assign to each particle energy levels ε_i^A and ε_k^B with $i = 1, 2, \dots, t_A$ and $k = 1, 2, \dots, t_B$. The system energy is $E = \varepsilon_i^A + \varepsilon_i^B$. Because the subsystems are independent, we can write the partition function of the subsystems as:

$$q_A = \sum_{i=1}^{t_A} \exp\left(-\frac{\varepsilon_i^A}{k_B T}\right) \text{ and } q_B = \sum_{k=1}^{t_B} \exp\left(-\frac{\varepsilon_k^B}{k_B T}\right)$$

for surface and bulk particles, respectively. It follows for the partition function of the entire system:

$$Q = \sum_{j=1}^t \exp\left(-\frac{E_j^A}{k_B T}\right) = \sum_{i=1}^{t_A} \sum_{k=1}^{t_B} \exp\left(-\frac{\varepsilon_i^A}{k_B T}\right) \exp\left(-\frac{\varepsilon_k^B}{k_B T}\right) = q_A q_B$$

More generally, for a system having N independent and **distinguishable particles**, each with the same microscopic (molecular) partition function q , the macroscopic partition function is

$$Q = q^N \quad (8.13a)$$

It can be shown that for **indistinguishable particles** (i.e., gases), we overcounted the possibilities by $N!$, which yields for the macroscopic partition function:

$$Q = \frac{q^N}{N!} \quad (8.13b)$$

8.5 Partition Function and Thermodynamic Properties

Consider a canonical ensemble system having fixed (T, V, N) (temperature, volume, particle number). We describe the *macroscopic internal energy* by a thermodynamic Boltzmann average of microscopic energy states as

$$U = \langle E \rangle = \sum_{j=1}^t p_j E_j$$

It is the weighted average of the energy levels with the probability for each state to be populated. Substituting $p_j = \frac{e^{-E_j/kT}}{Q}$ yields,

$$U = \frac{\sum_{j=1}^t E_j e^{-E_j/kT}}{Q} \quad (8.14)$$

If we define $\beta = 1/kT$, we notice that

$$\sum_{j=1}^t E_j e^{-E_j/kT} = \frac{dQ}{d\beta}$$

and hence,

$$U = -\frac{1}{Q} \left(\frac{dQ}{d\beta} \right) = -\left(\frac{d \ln Q}{d\beta} \right)$$

If we now substitute for $d\beta/dT = d(1/kT)/dT = -1/kT^2$, it follows for the macroscopic internal energy,

$$U = kT^2 \left(\frac{d \ln Q}{dT} \right) \quad (8.15)$$

where Q is the macroscopic partition function. From a microscopic perspective, we substitute for Q equations 8.13(a) and 8.13(b); i.e.,

$$Q = \frac{q^N}{N!} \text{ and}$$

$Q = q^N$ with the specific averaged microscopic energy values,

$$\langle \varepsilon \rangle = kT^2 \left(\frac{d \ln q}{dT} \right) \quad (8.16)$$

Table 8.1 below provides many of the important thermodynamic quantities in terms of the partition function for constant (T, V, N).

8.5.1 Stirling Approximation

It can be shown that for $N \gg 1$

$$\ln(N!) \approx \left(\frac{N}{e} \right)^N \quad (8.17)$$

where $e = 2.718\dots$ is the Euler's number. Based on the Stirling Approximation, we can write for the internal energy of indistinguishable particles

$$\begin{aligned} U &= kT^2 \left(\frac{\partial}{\partial T} \ln Q \right) \text{ with } Q = \frac{q^N}{N!} \approx \left(\frac{eq}{N} \right)^N \Rightarrow \ln Q \approx N \ln \left(\frac{eq}{N} \right) \\ &= kT^2 \left(\frac{\partial}{\partial T} N \ln \left(\frac{eq}{N} \right) \right) \\ &= NkT^2 \left(\frac{\partial}{\partial T} \ln \left(\frac{eq}{N} \right) \right) \end{aligned}$$

With $\frac{d}{dT} [\ln(a f(T))] = \frac{1}{f(T)} \frac{df}{dT}$ follows

$$U = NkT^2 \frac{\left(\frac{\partial q}{\partial T} \right)_{N,V}}{q} \quad (8.18)$$

Table 8.1: Thermodynamic quantities derived from the partition function

Internal Energy, U	$U = kT^2 \left(\frac{\partial \ln Q}{\partial T} \right)_{V,N}.$
Entropy, S	$S = k \ln Q + \frac{U}{T}.$
Helmholtz Free Energy, F	$F = U - TS = -kT \ln Q.$
Chemical Potential, μ	$\mu = \left(\frac{\partial F}{\partial N} \right)_{T,V} = -kT \left(\frac{\partial \ln Q}{\partial N} \right)_{T,V}.$
Pressure, p	$p = - \left(\frac{\partial F}{\partial V} \right)_{T,N} = kT \left(\frac{\partial \ln Q}{\partial V} \right)_{T,N}.$

Source: Molecular Driving Forces" by Dill

8.6 Molecular Partition Function from the Standard Chemical Potential

If we assume z nearest neighbors as the only interacting particles around a molecule in the gas phase, then the internal energy attributed to the interaction free energy per molecule is

$$\mu^o = \frac{z}{2} w(r, T)$$

where r is the equilibrated molecular mean distance at temperature T . (The factor $1/2$ is to correct for double counting the interactions) μ^o is known as self-energy or *Standard Chemical Potential*.

The standard chemical potential is part of the chemical potential defined as

$$\mu = \left(\frac{\partial \mathcal{F}}{\partial N} \right)_{T,V} \quad (8.19)$$

where \mathcal{F} is the Helmholtz free energy for constant T, V . The Helmholtz free energy can be expressed in terms of the macroscopic partition function (see Table 8.1 above) as

$$\mathcal{F} = -kT \ln Q$$

If we substitute for Q the molecular partition function expression for indistinguishable particles, i.e., $Q = q^N/N!$ (Eq. 8.13b), and, apply the Stirling approximation $q^N/N! \approx (eq/N)^N$, the free energy can be expressed as

$$\mathcal{F} = -NkT \ln \left(\frac{eq}{N} \right) \quad (8.20)$$

Substituting Eq. (8.20) into Eq. (8.19) yields

$$\mu = -kT \ln \left(\frac{eq}{N} \right) + kT = -kT \ln \left(\frac{q}{N} \right) \quad (8.21)$$

To obtain the form of the chemical potential for gases involving the gas pressure P , i.e.,

$$\mu = \mu^\circ + kT \ln(P) \quad (8.22)$$

we single out the volume V dependence (pressure dependence) from the partition function in Eq. (8.20) by defining

$$q \equiv q_o V$$

(Note the unit of q_o is m^{-3}). We introduce now the ideal gas law

$$V = \frac{NkT}{P}$$

and rewrite Eq. (8.20):

$$\mu = -kT \ln(q_o kT) + kT \ln(P) \quad (8.23)$$

Comparing the chemical potential expressions in Eqs (8.22) and (8.23) provides an expression of the standard chemical potential in terms of the volume deprived molecular partition function,

$$\mu^\circ = -kT \ln(q_o kT) \quad (8.24)$$

Thus, as the standard chemical potential can be expressed both in terms of the partition function $q_o = q/V$ and the pair interaction free energy $w(r, T)$, i.e.,

$$\mu^\circ = \begin{cases} -kT \ln(q_o kT) \\ \left(\frac{z}{2} \right) w(r, T) \end{cases} \quad (8.25)$$

we can express the molecular partition function in terms of the pair interaction:

$$q = q_o V = \frac{1}{kT} \left[\exp \left(-\frac{z w(r, T)}{2 kT} \right) \right] V \quad (8.26)$$

(Note this expression was not corrected for its units that are expected to be dimensionless. The reason for the discrepancy is the resolved logarithm. The units will be resolved further below by considering a ratio of partition functions)

8.7 Internal Energy of a Gas System

We consider next the internal energy U of N indistinguishable particles ($N \gg 1$) that originates from the short-range pair interaction free energy $w(r, T)$ between single particles. The Van der Waals interaction between gas molecules are an appropriate example here. Having established above (Eq. 8.18), the internal energy can be expressed as

$$U = NkT^2 \frac{\left(\frac{\partial q}{\partial T}\right)_{N,V}}{q}$$

"Short-ranged" implies that the pair interaction is limited to the nearest neighbors.

As per the equation for the internal energy, we need to determine the derivative of the partition function, Eq. (8.26),

$$\begin{aligned} \left(\frac{\partial q}{\partial T}\right)_{N,V} &= -\frac{V}{kT^2} \exp\left[-\left(\frac{z}{2}\right)\frac{w(r,T)}{kT}\right] - \frac{V}{kT} \exp\left[-\left(\frac{z}{2}\right)\frac{w(r,T)}{kT}\right] \left(\frac{z}{2}\right) \left(-\frac{1}{kT^2} w(r,T) + \frac{1}{kT} \frac{dw}{dT}\right) \\ &= -\frac{V}{kT^2} \left(1 - \left(\frac{z}{2}\right) \left(\frac{1}{k} \frac{dw}{dT} - \frac{w(r,T)}{kT}\right)\right) \exp\left[-\left(\frac{z}{2}\right)\frac{w(r,T)}{kT}\right] \end{aligned} \quad (8.27)$$

Substituting Eqs (8.26,8.27) into Eq. (8.18) yields for the internal energy of indistinguishable particle system based on the interaction free energy

$$U = NkT^2 \frac{-\frac{V}{kT^2} \left(1 - \left(\frac{z}{2}\right) \left(\frac{1}{k} \frac{dw}{dT} - \frac{w(r,T)}{kT}\right)\right) \exp\left[-\left(\frac{z}{2}\right)\frac{w(r,T)}{kT}\right]}{\frac{V}{kT} \exp\left[-\left(\frac{z}{2}\right)\frac{w(r,T)}{kT}\right]}$$

Further simplified, the internal energy is

$$U = -NkT \left(1 - \left(\frac{z}{2}\right) \left(\frac{1}{k} \frac{dw}{dT} - \frac{w(r,T)}{kT}\right)\right) \quad (8.28)$$

This equation is limited to independent and indistinguishable particle systems with short pair interactions.

Literature – Sources and Further Reading

Molecular Driving Forces – Statistical Thermodynamics in Chemistry and Biology, Dill and Bromberg, Garland Science, New York (2002).

